

The University of Michigan Research Institute  
Electron Physics Laboratory

Errata

MODULATION CHARACTERISTICS OF O-TYPE ELECTRON-STREAM DEVICES

Harold Sobol

Technical Report No. 33, AF 30(602)-1845

(The corrections have been underlined.)

Page 4, line 17, delete the hyphen between beam and modulations.

Page 4, line 24, insert hyphen between gridded and gun.

Page 11, line 20 should read "... the interaction equations."

Page 49, Eq. 2.68 should read

$$\Delta a_{db} = M \left( 1 + \frac{\Delta I_1}{I_{01}} \right) A(y, \Delta I, \Delta V) - A(y, 0, 0)$$

Page 93, line 22 should read  $\gamma a'$  = 2.12.

Page 128, line 22 should read "Nonlinear analyses..."

Page 128, line 25 should read "...interaction equations".

Page 136, line 17 should read

$$t_2 = \left( \frac{1 + \frac{\Delta I}{I_{01}}}{M^3} \right)^{1/2}$$

Page 149, line 1 should read "... is presently"

Page 236, last term of Eq. H.4 should read

$$\dots + \frac{\exp - j\beta_e Cbz}{1 - \frac{4QC}{b^2}}$$



THE UNIVERSITY OF MICHIGAN RESEARCH INSTITUTE  
ANN ARBOR, MICHIGAN

MODULATION CHARACTERISTICS OF O-TYPE ELECTRON-STREAM DEVICES


TECHNICAL REPORT NO. 33

Electron Physics Laboratory  
Department of Electrical Engineering

By

Harold Sobol

Approved by:

  
\_\_\_\_\_  
J. E. Rowe, Head  
Electron Physics Laboratory

Project 2750

CONTRACT NO. AF30(602)-1845  
DEPARTMENT OF THE AIR FORCE  
PROJECT NO. 4506, TASK NO. 45152  
PLACED BY: THE ROME AIR DEVELOPMENT CENTER  
GRIFFISS AIR FORCE BASE, NEW YORK

October, 1959

This report has also been submitted as a dissertation in partial fulfillment of the requirements for the degree of Doctor of Philosophy in The University of Michigan, 1959.

## ABSTRACT

The purpose of this dissertation is to present a general study of the modulated O-type electron-stream device. The modulations are classified according to the frequency of the modulating signal. Low modulation frequencies are very much less than the carrier frequency, while high modulation frequencies are comparable in rate to the carrier frequency. In order to simplify the analysis, the low- and high-frequency cases are investigated separately.

The O-type device undergoing a low-frequency beam modulation is described by a set of quasi-static functions. These functions are found by standard linear methods when the carrier is a low-level signal. The analysis includes modulation effects on  $C$ ,  $QC$ ,  $b$ , and  $d$ , as well as the initial wave amplitudes, and is valid for large modulation amplitudes. The device with a large-signal carrier is investigated using the nonlinear Lagrangian formulation. The modulation characteristics are used to calculate the output spectra when modulating signals having specific wave shapes are applied.

The significant results of the low-frequency study for the traveling-wave amplifier and the crestatron are:

### A. Traveling-wave amplifier

1. An approximately linear phase modulation with a large accompanying amplitude modulation can be produced by varying the beam potential. The phase linearity and phase-modulation index are almost independent of the carrier level and in some cases tend to improve as the carrier signal is increased to the saturation level.
2. Amplitude modulation with a small degree of accompanying phase modulation can be produced by varying the beam current. The amplitude-modulation index decreases as the carrier signal is increased from the small- to the large-signal levels.
3. It is important to consider modulation effects on the initial loss parameter  $A$  in the voltage-modulated, high-C amplifier.
4. Space charge decreases the phase modulation and increases the amplitude modulation in the voltage-modulated amplifier, while it decreases the amplitude modulation and increases the phase modulation in the current-modulated amplifier.
5. Loss increases the phase modulation and decreases the amplitude modulation for both voltage and current modulations.

## B. Crestatron

Current or voltage modulation produces a linear (in db) amplitude variation with a small accompanying phase modulation.

An analysis of the high-frequency case is also given. The nonlinearities are introduced through the ballistic equations; however, an Eulerian analysis is used. The longitudinal-beam parametric amplifier is studied as a special case of the high-frequency problem. The first upper and lower sidebands around the pump signal are included, whereas in previous theories only the lower sideband was considered.

It is found that the gain in db for this "multifrequency" model is approximately one-half of the value obtained using the earlier model. The upper sideband is very heavily excited, indicating that noise will be carried at this frequency. The threshold pump signal required to produce gain with a finite diameter beam is greater than the signal required in the single-sideband case. The results obtained by using this model are more closely correlated with experimental data than the results obtained from previous theories. Therefore it can be concluded that it is necessary to consider at least two sidebands and probably more when analyzing the longitudinal-beam parametric amplifier.

## ACKNOWLEDGMENTS

The author wishes to express his gratitude to the members of his doctoral committee for their assistance, and especially to Professor J. E. Rowe, chairman of the committee for his encouragement and guidance. The author is also grateful to those who assisted in the preparation of the text and to Y. C. Lim and L. Flanigan for their valuable aid in programming the computer.

## TABLE OF CONTENTS

	<u>Page</u>
ABSTRACT	iii
ACKNOWLEDGMENTS	v
LIST OF TABLES	ix
LIST OF ILLUSTRATIONS	x
CHAPTER I. STATEMENT OF THE PROBLEM AND LITERATURE SURVEY	1
1.1 Introduction	1
1.2 Beam Modulation	2
1.2.1 Low Modulation Frequencies	2
1.2.2 High Modulation Frequencies	3
1.3 Literature Survey on Previous Modulation Studies	3
1.3.1 Low Modulation Frequencies	3
1.3.2 High Modulation Frequencies	5
1.4 Purposes of This Study	6
CHAPTER II. DERIVATION OF THE LOW MODULATION FREQUENCY DEVICE FUNCTIONS FOR THE TRAVELING-WAVE AMPLIFIER	7
2.1 Introduction	7
2.2 Modulation Device Functions for the Linearized TWA	14
2.3 Taylor Series Form for the Modulation Device Functions of the Linear TWA	27
2.4 Modulation Device Functions for the Large- Signal TWA	29
CHAPTER III. NUMERICAL RESULTS FOR THE MODULATION DEVICE FUNCTIONS	50
3.1 Small-Signal Modulation Device Functions	50
3.1.1 Propagation Constants as Functions of the Modulation-Signal Amplitudes	50
3.1.2 The Effect of Low-Frequency Beam Modulation on the Initial Loss Parameter A	58
3.1.3 Linear Modulation Device Functions	68
3.1.4 Taylor Series Approximations to the Device Functions	73
3.2 Results for the Modulation Device Functions of Large-Signal Amplifiers	78
3.3 Experimental Modulation Device Functions	87
3.3.1 Measurement Technique	87
3.3.2 Results	87
3.3.3 Comparison between Experimental and Theoretical Results	93
3.4 Summary of Results and Remarks on Traveling-Wave Amplifiers for Modulation Applications	102



TABLE OF CONTENTS (cont.)

	<u>Page</u>
CHAPTER IV. FREQUENCY SPECTRUM OF THE TRAVELING-WAVE AMPLIFIER WITH A LOW-FREQUENCY BEAM MODULATION	105
4.1 General Modulation Theory	105
4.2 Sinusoidal Modulation	110
4.3 Pulse Modulation	113
4.4 Sawtooth Modulation	115
4.5 Physical Description of Frequency Translation by Sawtooth Modulation	118
4.6 Differences in Spectrum for TTM and PM	122
CHAPTER V. LOW FREQUENCY BEAM MODULATION OF OTHER O-TYPE DEVICES	124
5.1 Low-Frequency Beam Modulations of a Crestatron	125
5.2 Low-Frequency Beam Modulations of a Backward-Wave Oscillator	128
5.2.1 The Effect of Modulation on the Start- Oscillation Conditions	133
5.2.2 Modulation of the BWO with Currents Higher than Start-Oscillation Current	143
CHAPTER VI. HIGH-FREQUENCY BEAM MODULATIONS	148
6.1 Introduction	148
6.2 General Formulation of the Two-Frequency Problem	150
6.3 Longitudinal-Beam Parametric Amplifier	158
6.3.1 Mathematical Description	158
6.3.2 A Description of the Mechanics of Parametric Amplification in a Longitudinal Beam	181
CHAPTER VII. SUMMARY, CONCLUSIONS, AND SUGGESTIONS FOR FURTHER STUDY	187
7.1 Low-Frequency Modulation Study	187
7.2 High-Frequency Analysis	189
7.3 Suggestions for Further Study	190
7.3.1 Experiments on the Low-Frequency Beam- Modulated TWA	190
7.3.2 Modulation Study of the Large-Signal BWO	190
7.3.3 High-Frequency Modulations	190
APPENDIX A. OTHER METHODS FOR MODULATING A TRAVELING-WAVE AMPLIFIER AT LOW FREQUENCIES	192
A.I Phase Modulation by Variations in Signal Level	192
A.II Phase Modulation by Modulation of Cold Circuit Velocity	192

TABLE OF CONTENTS (concl.)

	<u>Page</u>
APPENDIX B. WAVE AMPLITUDES FOR THE LOW-FREQUENCY BEAM-MODULATED TRAVELING-WAVE TUBE WITH A BUNCHED BEAM ENTERING THE INTERACTION REGION	197
APPENDIX C. TAYLOR SERIES EXPANSIONS FOR THE MODULATION DEVICE FUNCTIONS	200
APPENDIX D. EXTENSION OF THE CAUCHY PRODUCT TO SERIES WITH INDICES RUNNING FROM $-\infty$ TO $\infty$	210
APPENDIX E. SOLUTION OF THE BWO MODULATION EQUATIONS ON AN ANALOG COMPUTER	213
APPENDIX F. CHARACTERISTIC EQUATION FOR THE LONGITUDINAL-BEAM PARAMETRIC AMPLIFIER	223
APPENDIX G. ALTERNATE DERIVATION OF THE CHARACTERISTIC EQUATION FOR THE LONGITUDINAL-BEAM PARAMETRIC AMPLIFIER	229
APPENDIX H. METHODS OF COUPLING TO INDIVIDUAL SPACE-CHARGE WAVE MODES	233
APPENDIX I. EVALUATION OF MATRIX ELEMENTS FOR DETERMINING WAVE AMPLITUDES IN THE LONGITUDINAL-BEAM PARAMETRIC AMPLIFIER	237
BIBLIOGRAPHY	239
LIST OF SYMBOLS	243

LIST OF TABLES

<u>Table</u>		<u>Page</u>
6.1	Matrix Elements $\epsilon, \eta, \tau, \pi$ $m = 0.10 \exp j\theta, a' = b' = 1.0, v_1(0) = 1.0$	178
6.2	Complex Wave Amplitude Coefficients $m = 0.10 \exp j\theta, a' = b' = 1.0, v_1(0) = 1.0$	179
C.1	TWA Parameters and their Derivatives	202
E.1	Potentiometer Settings Modulated BWO Start Oscillation Conditions, $C_o = 0.05$	220

LIST OF ILLUSTRATIONS

<u>Figure</u>		<u>Page</u>
2.1	Model for Analysis of Modulated TWA.	10
2.2	Initial Effects of Beam-Potential Modulation. (No r-f signal, space-charge debunching neglected)	33
2.3	Applegate Diagram of Modulated TWA, Illustration of Angle Relations.	34
2.4	Expanded View of Flight Lines.	36
2.5	Space-Charge Model	42
2.6	Flight Lines Showing Electron Distribution in Space and Time.	46
3.1	Small-Signal Propagation Constants for TWA with Modulated Beam Potential. ( $C_0 = 0.10$ , $QC_0 = 0$ , $b_0 = 0.1525$ , $d_0 = 0$ , $\Delta I = 0$ )	52
3.2	Small-Signal Propagation Constants for TWA with Modulated Beam Current. ( $C_0 = 0.10$ , $QC_0 = 0$ , $b_0 = 0.1525$ , $d_0 = 0$ , $\Delta V = 0$ )	53
3.3	Small-Signal Propagation Constants for TWA with Modulated Beam Potential. ( $C_0 = 0.10$ , $QC_0 = 0.250$ , $b_0 = 1.0$ , $d_0 = 0$ , $\Delta I = 0$ )	54
3.4	Small-Signal Propagation Constants for TWA with Modulated Beam Current. ( $C_0 = 0.10$ , $QC_0 = 0.250$ , $b_0 = 1.0$ , $d_0 = 0$ , $\Delta V = 0$ )	55
3.5	Small-Signal Propagation Constants for TWA with Modulated Beam Potential. ( $C_0 = 0.10$ , $QC_0 = 0.250$ , $b_0 = 1.0$ , $d_0 = 0.50$ , $\Delta I = 0$ )	56
3.6	Small-Signal Propagation Constant for TWA with Modulated Beam Current. ( $C_0 = 0.10$ , $QC_0 = 0.250$ , $b_0 = 1.0$ , $d_0 = 0.50$ , $\Delta V = 0$ )	57
3.7	Phase Variation in the Main Interaction Region during Beam-Potential Modulation. ( $C_0 = 0.10$ , $\Delta I = 0$ , $b_0$ adjusted for maximum gain)	59
3.8	Amplitude Variation in the Main Interaction Region during Beam-Potential Modulation. ( $C_0 = 0.10$ , $\Delta I = 0$ , $b_0$ adjusted for maximum gain)	60

LIST OF ILLUSTRATIONS (cont.)

<u>Figure</u>		<u>Page</u>
3.9	Amplitude Variation in the Main Interaction Region during Beam-Current Modulation. ( $C_0 = 0.10$ , $\Delta V = 0$ , $b_0$ adjusted for maximum gain)	61
3.10	Phase Variation in the Main Interaction Region during Beam-Current Modulation. ( $C_0 = 0.10$ , $\Delta V = 0$ , $b_0$ adjusted for maximum gain)	62
3.11	Variation of the Phase of A during Beam-Potential Modulation. ( $C_0 = 0.10$ , $\Delta I = 0$ , $b_0$ adjusted for maximum gain)	64
3.12	Variation of the Magnitude of A during Beam-Potential Modulation. ( $C_0 = 0.10$ , $\Delta I = 0$ , $b_0$ adjusted for maximum gain)	65
3.13	Variation of the Phase of A during Beam-Current Modulation. ( $C_0 = 0.10$ , $\Delta V = 0$ , $b_0$ adjusted for maximum gain)	66
3.14	Variation of the Magnitude of A during Beam-Current Modulation. ( $C_0 = 0.10$ , $\Delta V = 0$ , $b_0$ adjusted for maximum gain)	67
3.15	Phase Modulation Device Functions for Beam-Potential Modulation. ( $C_0 = 0.10$ , $\Delta I = 0$ , $b_0$ adjusted for maximum gain)	69
3.16	Amplitude-Modulation Device Functions for Beam-Potential Modulation. ( $C_0 = 0.10$ , $\Delta I = 0$ , $b_0$ adjusted for maximum gain)	70
3.17	Phase-Modulation Device Functions for Beam-Current Modulation. ( $C_0 = 0.10$ , $\Delta V = 0$ , $b_0$ adjusted for maximum gain)	71
3.18	Amplitude-Modulation Device Functions for Beam-Current Modulation. ( $C_0 = 0.10$ , $\Delta V = 0$ , $b_0$ adjusted for maximum gain)	72
3.19	Variation of Phase during Beam-Potential Modulation. ( $C_0 = 0.10$ , $QC_0 = 0$ , $d_0 = 0$ , $b_0 = 0.1525$ , $\Delta I = 0$ , $y = 3.4$ )	74
3.20	Variation of Amplitude during Beam-Potential Modulation. ( $C_0 = 0.10$ , $QC_0 = 0$ , $d_0 = 0$ , $b_0 = 0.1525$ , $\Delta I = 0$ , $y = 3.4$ )	75

LIST OF ILLUSTRATIONS (cont.)

<u>Figure</u>		<u>Page</u>
3.21	Comparison of Phase Variations during Beam-Potential Modulation. ( $C_0 = 0.10$ , $QC_0 = 0.250$ , $b_0 = 1.0$ , $d_0 = 0.50$ , $\Delta I = 0$ )	77
3.22	Phase-Modulation Device Functions during Beam-Potential Modulation, Large-Signal Calculation. ( $C_0 = 0.10$ , $QC_0 = 0$ , $d_0 = 0$ , $b_0 = 0.1525$ , $\Delta I = 0$ )	79
3.23	Amplitude-Modulation Device Function during Beam-Potential Modulation, Large-Signal Calculation. ( $C_0 = 0.10$ , $QC_0 = 0$ , $d_0 = 0$ , $b_0 = 0.1525$ , $\Delta I = 0$ )	80
3.24	Amplitude-Modulation Device Function during Beam-Current Modulation, Large-Signal Calculation. ( $C_0 = 0.10$ , $QC_0 = 0$ , $d_0 = 0$ , $b_0 = 0.1525$ , $\Delta V = 0$ )	81
3.25	Phase-Modulation Device Function during Beam-Current Modulation, Large-Signal Calculation. ( $C_0 = 0.10$ , $QC_0 = 0$ , $d_0 = 0$ , $b_0 = 0.1525$ , $\Delta V = 0$ )	82
3.26	Phase-Modulation Device Function during Beam-Potential Modulation, Large-Signal Calculation. ( $C_0 = 0.10$ , $QC_0 = 0.125$ , $d_0 = 0$ , $b_0 = 0.65$ , $B = 1.0$ , $a'/b' = 2.0$ )	83
3.27	Amplitude-Modulation Device Function during Beam-Potential Modulation, Large-Signal Calculation. ( $C_0 = 0.10$ , $QC_0 = 0.125$ , $d_0 = 0$ , $b_0 = 0.65$ , $B = 1.0$ , $a'/b' = 2.0$ )	84
3.28	Phase-Modulation Device Function during Beam-Potential Modulation, Large-Signal Calculation. ( $C_0 = 0.10$ , $QC_0 = 0.250$ , $d_0 = 0$ , $b_0 = 1.0$ , $B = 1.0$ , $a'/b' = 2.0$ )	85
3.29	Amplitude-Modulation Device Function during Beam-Potential Modulation, Large-Signal Calculation. ( $C_0 = 0.10$ , $QC_0 = 0.250$ , $d_0 = 0$ , $b_0 = 1.0$ , $B = 1.0$ , $a'/b' = 2.0$ )	86
3.30	Block Diagram of Equipment Set up for Measurement of Modulation Device Functions.	88
3.31	Measured Phase-Modulation Device Functions during Beam-Potential Modulation, Small-Signal Operation. (Hewlett-Packard TWA 490-B, $I_0 = 3\text{ma}$ , $P_{in} = -35\text{ dbm}$ )	89
3.32	Measured Amplitude-Modulation Device Functions during Beam-Potential Modulation, Small-Signal Operation. (Hewlett-Packard TWA 490-B, $I_0 = 3\text{ma}$ , $P_{in} = -35\text{ dbm}$ )	90

LIST OF ILLUSTRATIONS (cont.)

<u>Figure</u>		<u>Page</u>
3.33	Measured Phase-Modulation Device Functions during Beam-Potential Modulation, Large-Signal Operation. (Hewlett-Packard TWA 490-B, $I_0 = 3\text{ma}$ , $P_{in} = 0\text{ dbm}$ )	91
3.34	Measured Amplitude-Modulation during Beam-Potential Modulation, Large-Signal Operation. (Hewlett-Packard TWA 490-B, $I_0 = 3\text{ma}$ , $P_{in} = 0\text{ dbm}$ )	92
3.35	Measured Amplitude-Modulation Device Functions during Beam-Current Modulation. (Hewlett-Packard TWA 490-B, $I_0 = 3\text{ma}$ )	94
3.36	Measured Phase-Modulation Device Functions during Beam-Current Modulation, Large-Signal Operation. (Hewlett-Packard TWA 490-B, $I_0 = 3\text{ma}$ , $P_{in} = 0\text{ dbm}$ )	95
3.37	Schematic Drawing of TWT. (Huggins HAL-HP) Used in Hewlett-Packard TWA 490-B	96
3.38	Phase Modulation-Device Function during Beam-Potential Modulation, Small-Signal Operation. (Hewlett-Packard TWA 490-B, 2KMC, $I_0 = 3\text{ma}$ )	98
3.39	Amplitude-Modulation Device Function during Beam-Potential Modulation, Small-Signal Operation. (Hewlett-Packard TWA 490-B, 2KMC, $I_0 = 3\text{ma}$ )	99
3.40	Amplitude-Modulation Device Function during Beam-Current Modulation, Small-Signal Operation. (Hewlett-Packard TWA 490-B, 2KMC, $I_0 = 3\text{ma}$ )	100
3.41	Phase-Modulation Device Function during Beam-Current Modulation, Small-Signal Operation. (Hewlett-Packard TWA 490-B, 2KMC, $I_0 = 3\text{ma}$ )	101
4.1	Modulating Wave Forms, (a) Sinusoidal, (b) Pulse, (c) Ideal Sawtooth, (d) Sawtooth with Finite Flyback Time.	114
4.2	Ideal Phase Conditions for Serrodyne.	120
4.3	Flight Line Diagram of Serrodyne.	121
5.1	Propagation Constants for a Crestatron with Modulated Beam Potential. ( $C_0 = 0.10$ , $d_0 = 0$ , $QC_0 = 0$ , $b_0 = 2.4$ )	126

LIST OF ILLUSTRATIONS (cont.)

<u>Figure</u>		<u>Page</u>
5.2	Propagation Constants for a Crestatron with Modulated Beam Current. ( $C_0 = 0.10$ , $d_0 = 0$ , $QC_0 = 0$ , $b_0 = 2.4$ )	127
5.3	Variation of Crestatron Wave Amplitudes during Beam-Potential Modulation. ( $C_0 = 0.10$ , $d_0 = 0$ , $QC_0 = 0$ , $b_0 = 2.4$ )	129
5.4	Variation of Crestatron Wave Amplitudes during Beam-Current Modulation. ( $C_0 = 0.10$ , $d_0 = 0$ , $QC_0 = 0$ , $b_0 = 2.4$ )	130
5.5	Modulation Device Functions for Crestatron with Beam-Potential Modulation. ( $C_0 = 0.10$ , $d_0 = 0$ , $QC_0 = 0$ , $b_0 = 2.4$ )	131
5.6	Modulation Device Functions for Crestatron with Beam-Current Modulation. ( $C_0 = 0.10$ , $d_0 = 0$ , $QC_0 = 0$ , $b_0 = 2.4$ )	132
5.7	Model for Analysis of Modulated BWO.	135
5.8	Impedance <sup>1</sup> and Phase Velocity <sup>2</sup> Characteristics of (-1) Mode of Bifilar Helix.	139
5.9	First Estimate of Normalized Frequency, $\zeta_3$ , Obtained from $\omega$ - $\beta$ Diagram. (Bifilar Helix; at $\Delta V = 0$ , $ka = 0.30$ )	140
5.10	BWO Modulation Parameters $\zeta_1$ and $\zeta_2$ as Functions of Frequency, $\zeta_3$ . (Bifilar Helix; at $\Delta V = 0$ , $ka = 0.30$ )	141
5.11	BWO Modulation Parameter F as Function of Frequency, $\zeta_3$ . (Bifilar Helix; at $\Delta V = 0$ , $ka = 0.30$ ; Annular Beam $H = 0.6$ , $R = 1.2$ )	142
5.12	Variation of Start-Oscillation Frequency of BWO as Function of Beam-Potential Modulation. ( $C_0 = 0.05$ , $QC_0 = 0$ , $d_0 = 0$ , $b_0 = 1.56$ ; Bifilar Helix; Annular Beam, $H = 0.60$ , $R = 1.2$ ; at $\Delta V = 0$ , $ka = 0.30$ )	144
5.13	Variation of Start-Oscillation Length of BWO as Function of Beam-Potential Modulation. ( $C_0 = 0.05$ , $QC_0 = 0$ , $d_0 = 0$ , $b_0 = 1.56$ ; Bifilar Helix; Annular Beam, $H = 0.60$ , $R = 1.2$ ; at $\Delta V = 0$ , $ka = 0.30$ )	145



LIST OF ILLUSTRATIONS (concl.)

<u>Figure</u>		<u>Page</u>
5.14	Variation of Start-Oscillation Frequency of BWO as Function of Beam-Potential Modulation. ( $C_0 = 0.05$ , $QC_0 = 0.20$ , $d_0 = 0$ , $b_0 = 1.59$ ; Bifilar Helix; Annular Beam, $H = 0.60$ , $R = 1.2$ ; at $\Delta V = 0$ , $ka = 0.30$ )	146
5.15	Variation of Start-Oscillation Length of BWO as Function of Beam-Potential Modulation. ( $C_0 = 0.05$ , $QC_0 = 0.02$ , $d_0 = 0$ , $b_0 = 1.59$ ; Bifilar Helix; Annular Beam, $H = 0.60$ , $R = 1.2$ ; at $\Delta V = 0$ , $ka = 0.30$ )	147
6.1	Longitudinal-Beam Parametric-Amplifier Propagation Constants ( $\mu_1 \dots \mu_4$ ) as Functions of the Pump Amplitude ( $a' = b' = 1.0$ ) .	173
6.2	Longitudinal-Beam Parametric-Amplifier Propagation Constants ( $\mu_5 \dots \mu_8$ ) as Functions of the Pump Amplitude ( $a' = b' = 1.0$ ) .	174
6.3	Longitudinal-Beam Parametric-Amplifier Propagation Constants ( $\mu_1 \dots \mu_4$ ) as Functions of the Pump Amplitude ( $a' = 0.697$ , $b' = 0.513$ ).	175
6.4	Longitudinal-Beam Parametric-Amplifier Propagation Constants ( $\mu_5 \dots \mu_8$ ) as Functions of the Pump Amplitude ( $a' = 0.697$ , $b' = 0.513$ ).	176
6.5	Multimode Coupling in the Longitudinal-Beam Parametric Amplifier.	186
A.1	Change in Phase Shift vs. Input Power. ( $C = 0.10$ , $d = 0$ , $N_g = 5.75$ , $B = 1$ )	193
A.2	Change in Phase Shift vs. Input Power. ( $C = 0.05$ , $d = 0$ , $N_g = 13$ , $B = 1$ )	194
E.1	Approximate Maximum Values of $ v $ and $ \rho $ Based on Unit $V_c$ .	216
E.2	"Roadmap" of Analog Computer Equipment for Finding Start-Oscillation Conditions of a Modulated BWO.	219
E.3	Trial and Error Procedure for Finding Start-Oscillation Conditions with Beam-Potential Modulation.	222
H.1	Doubly Gridded Cavity Resonator for Exciting Single Space-Charge Wave.	234



## CHAPTER I. STATEMENT OF THE PROBLEM AND LITERATURE SURVEY

### 1.1 Introduction

The O-type electron-stream tube is a transit-time device which amplifies or generates a radio-frequency signal by either a beating or an exponential growth of electromagnetic or space-charge waves, and in which there are no transverse static fields that significantly affect the interaction mechanism. The stability of the electron stream is maintained by a longitudinal static field, parallel to the axis of the electron flow. The traveling-wave amplifier<sup>1</sup> (TWA) and the electron-wave<sup>2</sup> amplifier are examples of growing-wave interaction, while the backward-wave oscillator<sup>3</sup> (BWO) and the crestatron<sup>4</sup> are examples of beating-wave interaction. The analyses of these devices are well covered in the literature.

With the advent of improved techniques for noise reduction, the applicability of the O-type tube for systems has been greatly enhanced. The traveling-wave tube which is inherently a broadband amplifier has certain narrow band features that make it very appealing as a modulator\*, whereas its broadband capabilities contribute toward its usefulness as a mixer. The traveling-wave amplifier thereby makes it possible to accomplish modulation and mixing at high power levels.

---

\* Modulation is the process of impressing intelligence variations on a physical quantity such as on an electromagnetic wave amplitude or frequency<sup>5</sup>. A device in which the modulation process takes place is known as a modulator.

The type-0 backward-wave oscillator was designed to satisfy the systems' needs for a power source that could be continuously frequency-tuned or modulated at fast rates by electronic methods.

## 1.2 Beam Modulation

The term modulation\* as used in this dissertation is a coherent periodic disturbance in the form of a signal placed on an electron beam at some frequency differing from the carrier or main signal frequency. The disturbance will in general produce sidebands around each harmonic of the carrier frequency and will alter the phase and amplitude of the carrier at the output of the device. Two distinct classes of modulation frequency rates are to be discussed.

1.2.1 Low Modulation Frequencies. A low-frequency beam modulation occurs when the beam velocity and current density are varied at rates sufficiently slow so that the time of one modulation cycle is much greater than the transit time for an electron through the tube. A phase modulation (PM) or transit-time modulation (TTM) is produced by variations of the velocity of electrons entering the interaction region. An amplitude modulation (AM) is produced by variation of the electron current density at the entrance to the interaction region. It is to be noted that AM is inherent in the production of PM or TTM, and similarly either PM or TTM is inherent in the production of AM. The sideband frequencies around each harmonic of the carrier frequency will be assumed to occur sufficiently close to that carrier harmonic so that

---

\* These beam modulations are not to be confused with the r-f velocity or density modulations in which an r-f signal "modulates" an electron stream and causes bunching. In this dissertation, to avoid confusion, the word modulation will not be associated with the bunching phenomena but will only be used in reference to the beam modulations as defined above.

its circuit properties (phase velocity, group velocity and impedance) are identical to those of the carrier harmonic. The foregoing statements concerning the output spectrum do not necessarily apply to the voltage-tunable oscillator since in this case the modulation changes the carrier frequency.

1.2.2. High Modulation Frequencies. A beam modulation where the period of the modulation signal is comparable to the transit time of the device is called a high-modulation frequency disturbance. In this case the sideband components see different circuit properties than the carrier. For high modulation frequencies there are differences between the output spectra resulting from PM and TTM for the same applied modulation. It has been shown<sup>6</sup> that these differences occur in the amplitude of spectral components; the frequency location of the components however remain unchanged.

### 1.3 Literature Survey on Previous Modulation Studies

1.3.1 Low Modulation Frequencies. Learned<sup>7</sup> recognized the advantage of mixing at high power levels and utilized the effects of modulating the transit time of a klystron to produce frequency shifting for use in television relay systems. This modulated klystron was called a Synchrodyne. The transit time was varied sinusoidally and the output resonator was tuned to the desired sideband.

In recent years the traveling-wave amplifier has been used in similar applications. There have been several modulation studies of the TWA, however none of these were very complete and some were based on rather drastic assumptions. Bray<sup>8</sup> introduced the TWA as a modulator and proposed using it in the same manner as Learned had used the klystron. He demonstrated by a very simple small-C analysis, which neglected

space-charge forces, loss, nonsynchronism and nonlinear effects that the "hot" circuit phase velocity can be made to vary almost linearly as a function of the average beam potential in the interaction region. By sinusoidally varying the beam potential and using a filter to select the desired side frequency, the TWA was made to perform the same function as the Synchrodyne.

Steele<sup>9</sup> repeated Bray's analysis for phase modulation using the same simplifications, and also included a discussion of inherent AM. Furthermore these analyses were limited to small excursions of the beam potential.

Cumming<sup>6</sup> advanced the art by introducing the Serrodyne, which is a saw-tooth modulated transit-time device. This method of modulation is vastly superior to sinusoidal modulation for frequency shifting applications, since by using it almost all of the energy at the carrier frequency can be translated to one of the sidebands, while a very low-level output is produced at each of the other sidebands and the carrier. Cumming presented an analysis for the TWA with low-frequency beam-modulations, in which he considered most of the variables neglected in the preceding papers, but neglected modulation effects of the initial loss parameter  $A$  and nonlinear effects. His work was also limited to those excursions of the beam current and voltage for which the gain and transit time could be described by a Taylor series approximation accurate to two terms.

Mendel<sup>10</sup> proposed the use of a gridded gun traveling-wave tube for the amplification of narrow pulses. A cw r-f signal was applied to the circuit and the beam was pulsed. The envelope of the amplified signal was detected and an amplified pulse obtained. A simplified small-signal analysis was used for the theoretical study of this amplifier.

Beam and Blattner<sup>11</sup> investigated the variations in the phase of the r-f output caused by power supply and signal-level fluctuations. The effect of applying a modulated signal to the various gun elements was considered. They also demonstrated experimentally that the phase of the output signal could be made to vary with changes in the magnetic focusing field. A small-C linear theory was used in their analytical study and the propagation constants were approximated by fitting curves to Pierce's<sup>1</sup> data.

1.3.2 High Modulation Frequencies. Putz<sup>12</sup> presented a nonlinear theory for the TWA in which he did not consider crossings of trajectories, space-charge forces, loss and finite C values. He then used his results to investigate the cross modulation between two signals placed on the circuit. Experiments by Nation and Harrison<sup>13</sup> verified some of Putz's work.

Wade and DeGrasse<sup>14,15</sup> built and analyzed a traveling-wave tube mixer constructed with two helix sections. The first helix was adjusted to amplify both the signal and the local-oscillator frequencies while the second helix was operated in its dispersive region and adjusted so that it passed the desired i-f frequency. The analytical study included an investigation of several beam-type mixers. The analyses were made using a hydrodynamic beam to describe the nonlinearities necessary for mixing.

Louisell and Quate<sup>16</sup> recently suggested that a longitudinal-beam tube used as a fast- or slow-wave amplifier can produce parametric amplification of space-charge waves. This particular analysis considered only one sideband.

In summary, the literature contains several analyses of modulated traveling-wave tubes. However, each of the above analyses has certain limitations. It appears that a comprehensive study of the modulated

TWA, taking into account all of the Pierce parameters, nonlinear effects and large excursion modulations, has not been presented. A study of this type would be desirable if the full modulation capabilities of traveling-wave amplifiers and other O-type devices are to be utilized in communication and radar systems.

#### 1.4 Purposes of This Study

The purposes of this study are:

1. To develop a general method of determining the low-frequency beam-modulation characteristics of O-type tubes operated under varied conditions. The effect of beam modulations on the gain parameter, the loss, space-charge forces, the initial wave amplitudes, trajectory crossings and nonlinearities, as well as large modulation amplitudes will be considered. The results of this study will provide information for the design of O-type tubes for modulation applications.
2. To study high-frequency beam modulations and to use the results in an analysis of the longitudinal-beam parametric amplifier.



## 2.1 Introduction

The first problem of this dissertation will be to describe the variation of the characteristics of a TWA when a low-frequency signal is used to modulate the beam.

A low-frequency modulating signal can be used to phase or amplitude modulate the carrier or to do both simultaneously. In general a phase modulation is inherent in the production of AM and vice versa. It is possible to apply several low-frequency modulations simultaneously. The modulation signal can be applied by one or by a combination of several of the methods listed below.

1. The beam velocity at the entrance to the interaction region may be varied by changing the average potential of the circuit at the modulation frequency.
2. The beam velocity may be varied by changing the average potential of the electron gun anode at the modulation frequency. This method will result in a current modulation for space-charge limited operation. (Therefore to produce PM with little AM, it is preferable to modulate the circuit d-c potential rather than the anode potential, since the beam current is relatively independent of circuit potential.)
3. The average beam current can be varied by modulating the bias on a grid used near the cathode. This method results in an AM with little inherent PM.
4. The phase shift through the tube can be made to vary slightly by changing the magnetic focusing fields<sup>11</sup>. This suggests

another possible modulation scheme in which the electric focusing field in an electrostatically focused tube can be modulated to produce PM, although a study of such a scheme might be directed toward the detrimental effects of focusing-supply ripple, rather than the purposeful effects of modulation.

5. The collector potential can be varied to produce amplitude variations. This is feasible since the efficiency of the tube is a function of the collector potential. This method would appear to produce little PM since the modulation takes place over a short distance.

The above methods involve the application of a modulation voltage to directly perturb the beam. There are other modulation methods in which the signal is not applied directly to the beam.

6. It has been shown<sup>17,11</sup> that variations of the r-f input signal level can produce variations in the phase of the r-f output signal. Therefore an amplitude-modulated r-f input can be converted to an r-f output that is phase and amplitude modulated.
7. In method 1, the useful sidebands are generated by varying the beam velocity with respect to a fixed cold-circuit velocity, which in turn produces a variation of the phase velocity of the growing wave. A similar effect may be produced by varying the cold velocity of the circuit with respect to the fixed beam velocity. This can be done by modulating the bias on a ferrite or dielectric material surrounding the circuit.

A further discussion of methods 6 and 7 is given in Appendix A. The remainder of this chapter will be devoted to a discussion of methods 1-3.

Before proceeding it will be necessary to make further distinction between low- and high-frequency beam modulations than that given previously

in Section 1.2. A low modulation frequency must have a period which is much greater than the transit time of an electron through the tube, and also must satisfy the condition that the time and space derivatives of any function at that frequency are negligibly small compared to derivatives of the same function at the carrier frequency. Therefore, all functions of the modulation frequency are treated as constants in the interaction equations. Under these assumptions the operation of a TWA undergoing a low-frequency beam-modulation can be described by a set of quasi-stationary (for modulation frequencies) equations, based on the unmodulated operation.

The steady state fundamental r-f output signal of an electron tube is fully described when the gain and phase shift are specified with respect to the input signal. The functions describing the dependence of gain and phase shift on the modulation are called the "Modulation Device Functions". The Modulation Device Functions are derived from the quasi-stationary set mentioned above.

A direct but cumbersome method of finding the device functions would be to recalculate the various stationary Pierce parameters for instantaneous values of the modulation signal and then to determine the gain and phase shift with this new set of parameters as though the tube were unmodulated. There is a more elegant method of finding the device functions which requires only one set of stationary parameters, given for unmodulated operation. The device functions may then be found for any modulation condition without having to recalculate a new set of parameters.

The general model used for the analyses in this chapter is shown in Fig. 2.1. An electron beam emanates from a gun which has a grid to control the flow of current. A low-frequency signal  $V_g$  applied between

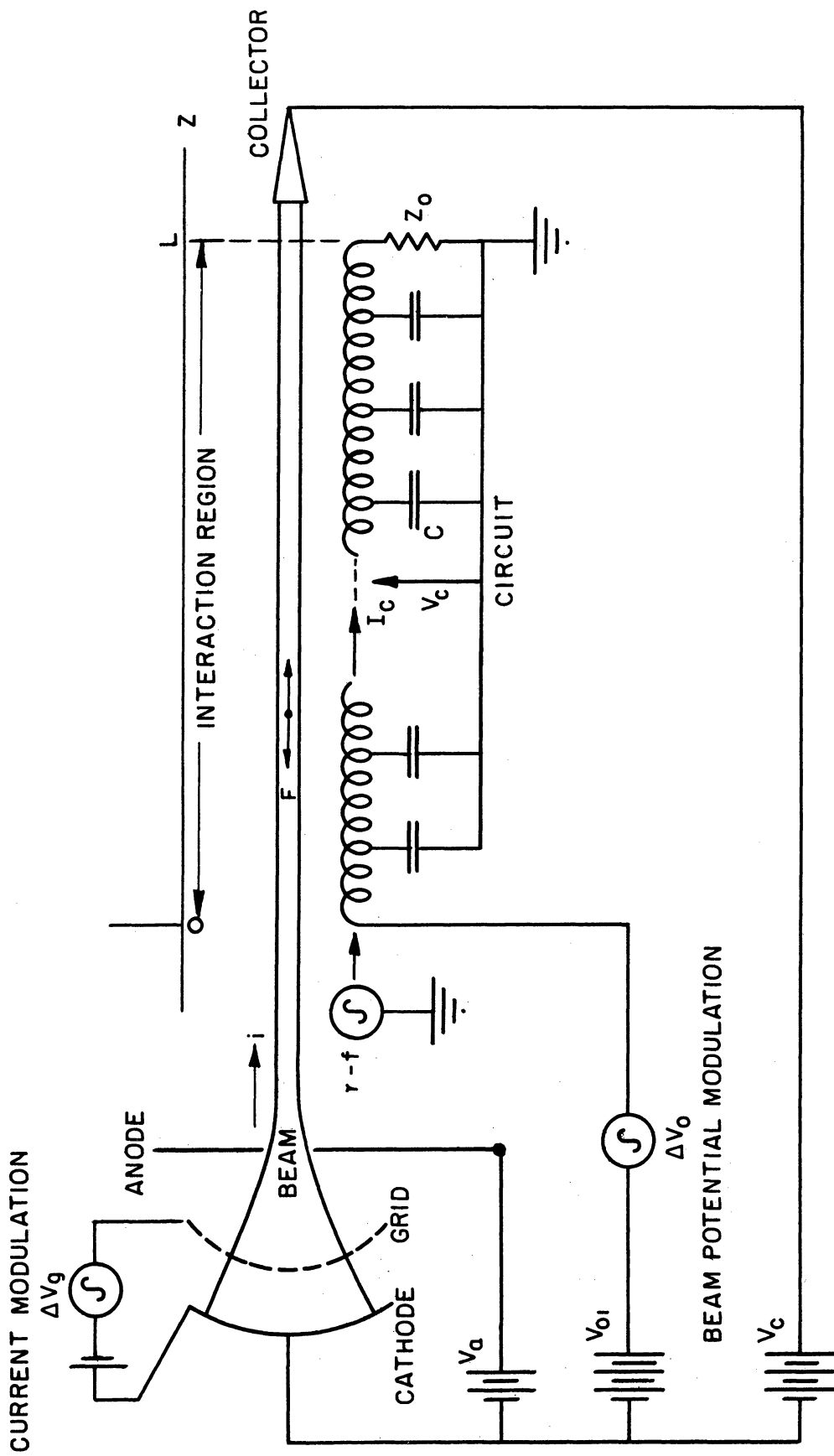


FIG. 2.1 MODEL FOR ANALYSIS OF MODULATED TWA.

the cathode and grid causes the beam current to vary by an amount  $\Delta I$ . The beam flows close to a slow-wave circuit represented by the terminated transmission line. The cold-propagation phase constant of the transmission line is  $\beta$  and the characteristic impedance is given by

$$Z_0 = \frac{E^2}{2\beta^2 P} = \sqrt{\frac{L}{C}},$$

where  $E$  is the amplitude of the axially directed field at the beam radius without the beam present, and  $P$  is the cold power flow associated with the field  $E$ . An r-f signal  $V_c e^{j\omega t - \Gamma z}$  is applied at the input to the circuit and propagates toward the load  $Z_0$ . The circuit is at a potential  $V_{01} + \Delta V$ , where  $\Delta V$  is the low frequency voltage modulating the beam velocity. The current modulation  $\Delta I$  may contain some modulation due to  $\Delta V$ , as in the case of applying the signal to the anode.

Only longitudinal fields are considered so that this problem reduces to a one-dimensional analysis. There exists a space-charge debunching force  $F$ , which results from the bunched beam. The debunching force is again only a longitudinal force. The major assumptions made in using this model are listed below.

1. This is a one-dimensional model. There are no transverse variations of fields, therefore the beam is, in effect, a line charge and is so considered in the interreaction equations. The one-dimensional theory further assumes that the beam is constrained only to axial motion (which implies an infinite axial magnetic field).
2. Relativistic effects are not considered.
3. The average space charge in the beam is neutralized by a sufficient number of positive ions.

4. The sideband frequencies propagate at the same rate as the carrier and see the same impedance.

Further assumptions are listed as the analysis is carried on.

The device functions will be found by rederiving the equations of motion for the beam and the circuit equation for the particular device under consideration in such a manner as to allow variations in the d-c beam parameters. The boundary conditions must be similarly reconsidered in light of the aforementioned variations. Once a set of equations and the necessary boundary conditions have been found, the equations can be integrated and the device functions determined.

The transmission-line equations for a terminated slow-wave structure driven by an axial beam flowing close to the circuit, and supporting a wave with its group and phase velocities in the positive z-direction are given by

$$\frac{\partial V_c}{\partial z} = - \frac{Z_o}{v_o} \frac{\partial I_c}{\partial t}$$
$$\frac{\partial I_c}{\partial z} = - \frac{1}{Z_o v_o} \frac{\partial V_c}{\partial t} + \frac{\partial \rho}{\partial t} \quad , \quad (2.1)$$

where  $V_c$  = r-f potential of the wave on the circuit in volts,

$I_c$  = r-f current in the circuit in amperes,

$v_o$  = phase velocity of the carrier on the circuit in meters/sec,

$\rho$  = charge density of the beam exciting the circuit in coulombs/meter, and

$t$  = time in seconds.

The equations of motion for the one-dimensional O-type device are found from the Newtonian Force equation and the law of continuity of charge. These two equations are nonlinear.

The force equation for the one-dimensional problem is given as

$$\frac{du(t,z)}{dt} = \frac{\partial u}{\partial t} + u \frac{\partial u}{\partial z} = -\eta E = \eta \frac{\partial V}{\partial z} \quad , \quad (2.2)$$

where  $u$  = total velocity of an electron

$\eta$  = magnitude of the charge-to-mass ratio of an electron,

$E$  = total electric field acting on the beam and it is derived from the potential  $V$  which is the sum of the potential due to the circuit wave  $V_c$  and that due to the space-charge potential  $V_{sc}$ . The force  $F$  in Fig. 2.1 is derivable from the potential  $V_{sc}$ .

The continuity of charge law demands the total charge must be conserved.

The boundary conditions to be imposed for the low modulation frequencies are that the velocity and charge density of the electron flow entering the interaction region contain only the average values plus the low-frequency modulations. An r-f input signal is placed on the circuit at the beginning of the interaction region.

The solution of the above system will now be considered for two levels of the applied carrier signal. In one case a low-level signal is applied and a linearized perturbation method is used. For the second case larger signals are considered and the nonlinear equations must be used. The two methods of solution must be consistent as the r-f signal level is reduced from the high to the low level.

Pierce's techniques will be modified and applied to find the device functions for the linearized amplifier while Rowe's<sup>17</sup> methods will be used for the large-signal amplifier.

In order to avoid repetition, many of the generally accepted results of these two authors will be used in the analyses which follow.

Those points which have caused controversy will be more fully discussed.

## 2.2 Modulation Device Functions for the Linearized TWA

The Modulation Device Functions for the small-signal TWA will now be derived. In order to use the linearized equations, it is necessary to introduce the following assumptions in addition to those already made in Section 2.1.

1. All functions varying at the carrier frequency are assumed to have an exponential variation with time and distance,  $e^{j\omega t - \Gamma z}$ ; therefore the distance derivatives are replaced by the operator  $\partial/\partial z = -\Gamma$ . Similarly the time derivatives are replaced by  $\partial/\partial t = j\omega$ .
2. The total velocity, current, and charge density are each considered to be composed of a sum of a fixed average value, a slowly varying component at the modulation frequency, and a rapidly varying r-f component. The r-f component is assumed small compared to the other two. The above assumption may be written in mathematical form as,

$$f = f_{01} + f_1(z, \omega_1 t, \omega_2 t \dots \omega_n t) + f_2(z, \omega t)$$

where  $f$  = total function,

$f_{01}$  = unmodulated average value,

$f_1$  = component at the modulating frequencies,

$f_2$  = r-f component,

$\omega_1 \dots \omega_n$  = various modulation frequencies that are applied or generated, and

$\omega$  = carrier frequency.

Also

$$f_2 \ll f_{01}, f_1$$



and

$$\frac{\partial f}{\partial t} \approx \frac{\partial f_2}{\partial t} , \quad \frac{\partial f}{\partial z} \approx \frac{\partial f_2}{\partial z}$$

3. The space-charge debunching force  $F$  is derivable from a potential  $V_{sc}$ , where  $V_{sc}$  represents the effect of the energy going into the slow passive and noninteracting modes and the fast noninteracting modes. The potential  $V_{sc}$  is directly proportional to the r-f charge density. A capacitor  $C_1$  can be defined as a proportionality constant such that

$$q = C_1 V_{sc} ,$$

where

$q$  is in coulombs/m

$C_1$  is in farads per m

and

$$F = |q| \frac{\partial V_{sc}}{\partial z} .$$

4. The electron stream is assumed to have the properties of hydrodynamical flow.

Allow the average beam potential over an r-f cycle to be varied in accordance with

$$V_o = V_{o1} + \Delta V(t, t_A) , \quad (2.3)$$

and the average beam current to vary as

$$I_o = I_{o1} + \Delta I(t, t_B) , \quad (2.4)$$

where  $\Delta V$  and  $\Delta I$  may each be periodic functions of different modulation frequencies, however both frequencies are much lower

than the carrier frequency.  $t_A$  and  $t_B$  are used to describe coherence and phase difference between  $\Delta V$ ,  $\Delta I$  and the r-f signal.  $I_{O1}$  and  $V_{O1}$  are the unmodulated beam current and potential respectively. It is assumed that any average values introduced by  $\Delta I$  and  $\Delta V$  are negligible when compared to the unmodulated values.

The following modulation parameters are introduced:

$$M^3 = M^3(t, t_A, t_B) = \frac{1 + \frac{\Delta V}{V_{O1}}}{1 + \frac{\Delta I}{I_{O1}}}, \quad (2.5a)$$

$$\xi_1 = \left(1 + \frac{\Delta V}{V_{O1}}\right)^{1/2}, \quad (2.5b)$$

and

$$\xi_2 = \left(\frac{1 + \frac{\Delta I}{I_{O1}}}{M^3}\right)^{1/2} = \frac{1 + \frac{\Delta I}{I_{O1}}}{\xi_1} \quad (2.5c)$$

The circuit equation is independent of the average beam parameters.

Pierce's<sup>1\*</sup> normal-mode theory gives the circuit equation as

$$V = \left[ \frac{\Gamma \Gamma_1 \left(\frac{E^2}{\beta^2 P}\right)}{2(\Gamma_1^2 - \Gamma^2)} - j \frac{\Gamma}{\omega C_1} \right] i, \quad (2.6)$$

where  $V$  = total potential seen by the beam

$\Gamma_1$  = unforced or normal-mode propagation constant for the particular mode which becomes the interaction mode,

$\Gamma$  = perturbed propagation constant,

$i$  = forcing term or beam current.

---

\* Equation 7.8.

The force equation, Eq. 2.2, may be linearized using assumption 2 of this section. After substituting the exponential variations given in assumption 1, the linearized form of Eq. 2.2 becomes

$$\left\{ j\omega - u_{01} \left( 1 + \frac{\Delta V}{V_{01}} \right)^{1/2} \Gamma \right\} v = -\eta \Gamma V, \quad (2.7)$$

where  $v$  = r-f velocity amplitude, and

$$u_{01} = \sqrt{2\eta V_{01}}.$$

Equations 2.5 and 2.6 can be combined to give

$$v = \frac{-\eta \Gamma V}{j\omega - u_{01} \xi_1 \Gamma}. \quad (2.8)$$

The linearized r-f current is given as the sum of the product of the d-c charge density and the r-f velocity and the product of the d-c velocity and the r-f charge density, hence

$$i = \rho_{01} \left( \frac{1 + \frac{\Delta I}{I_{01}}}{M^3} \right)^{1/2} v + u_{01} \left( 1 + \frac{\Delta V}{V_{01}} \right)^{1/2} \rho \quad (2.9)$$

where

$$-I_{01} = \rho_{01} u_{01}.$$

Again using Eq. 2.5, Eq. 2.9 becomes

$$i = \frac{\rho_{01} \xi_2 v}{1 + j \frac{\Gamma u_{01} \xi_1}{\omega}}. \quad (2.10)$$

The continuity of charge conditions for this one-dimensional fluid stream is given as

$$\nabla \cdot (\rho v) = \frac{\partial i}{\partial z} = - \frac{\partial \rho}{\partial t}$$

which, after introducing the operator forms, becomes

$$\rho = -j \frac{\Gamma i}{\omega} \quad (2.11)$$

Equations 2.6, 2.8, 2.10 and 2.11 are combined to give the secular equation for determining the propagation constant  $\Gamma$ .

$$1 = \frac{j\Gamma^2 \Gamma_1 \left( \frac{E^2}{\beta^2 P} \right) \beta_{eo} \xi_2}{4(\Gamma_1^2 - \Gamma^2) V_{o1} (j\beta_{eo} - \Gamma \xi_1)^2} + \frac{\beta_{eo} \Gamma^2 I_{o1} \xi_2}{2V_{o1} \omega C_1 (j\beta_{eo} - \Gamma \xi_1)^2} \quad (2.12)$$

where  $\beta_{eo}$  is defined as

$$\beta_{eo} = \frac{\omega}{u_{o1}}$$

Pierce's small-signal parameters are used in the modulation problem to define the unmodulated tube. The parameters are defined as:

$$C_o^s = \frac{E^2}{\beta^2 P} \frac{I_{o1}}{8V_{o1}}, \text{ the gain parameter} \quad (2.13a)$$

$$QC_o = \frac{\beta_{eo} C_o}{\omega C_1 \frac{E^2}{\beta^2 P}}, \text{ the space-charge parameter} \quad (2.13b)$$

$$d_o = \frac{0.0183 \frac{\text{Loss in db}}{\text{wavelength}}}{C_o}, \text{ the loss factor} \quad (2.13c)$$

$$b_o = \frac{1}{C_o} \left\{ \frac{u_{o1}}{v_o} - 1 \right\}, \text{ the injection velocity parameter} \quad (2.13d)$$

$v_o$  = the cold phase velocity of the circuit.

Following Pierce, the normal mode unforced propagation constant is assumed to be,

$$-\Gamma_1 = -j\beta_{eo} - j\beta_{eo} C_o b_o - \beta_{eo} d_o, \quad (2.14)$$

and the interaction propagation constant is assumed to be

$$-\Gamma = -j\beta_{eo} + \beta_{eo} C_o \delta(\xi_1, \xi_2) \quad (2.15)$$

Note that the perturbation of the propagation constant is defined as being a perturbation from the unmodulated beam wave number.

Equations 2.13, 2.14 and 2.15 give the normalized form of the secular equation as

$$\frac{1}{\xi_2} \left[ j \frac{1-\xi_1}{C_o} + \xi_1 \delta \right]^2 = \frac{[1 + C_o(b_o - jd_o)][1 + C_o(2j\delta - C_o\delta^2)]}{-b_o + jd_o + j\delta + C_o \left[ j b_o d_o + \frac{d_o^2}{2} - \frac{b_o^2}{2} - \frac{\delta^2}{2} \right]} - 4QC_o [1 + C_o(2j\delta - C_o\delta^2)] \quad (2.16)$$

The roots of this equation describe the waves that will propagate, in terms of the unmodulated parameters and the modulation. For no modulation, both  $\xi_1$  and  $\xi_2$  become unity and Eq. 2.16 becomes the secular equation for the unmodulated TWA.

It can be seen from Eq. 2.16 that there will be four waves propagating in this device. As is well known, one of the roots represents a backward traveling-wave which is far from synchronism and thus may be neglected. The remaining three roots represent forward waves. They are a slow and increasing wave, a slow and decaying wave, and a fast and unchanging wave (in the absence of loss). The general solution therefore is given as the linear sum of the three forward waves. The total potential

at the beam is

$$V(z) = \sum_{i=1}^3 V_i \exp(-j\beta_{e0}z + \beta_{e0}\delta_i C_0 z) \quad (2.17)$$

The initial amplitudes  $V_i$ , are found from the input boundary conditions.

Equation 2.8 can be written as

$$v(z) = \frac{-j\eta}{u_{01} C_0} \sum_{i=1}^3 \frac{1 + j C_0 \delta_i}{\xi_1 \delta_i + j \frac{1 - \xi_1}{C_0}} V_i \exp(-j\beta_{e0}z + \delta_i \beta_{e0} C_0 z), \quad (2.18)$$

and Eq. 2.10 can be written as

$$\frac{-2V_{01} C_0^2}{I_{01} \xi_2} i(z) = \sum_{i=1}^3 \frac{1 + j C_0 \delta_i}{\left(\xi_1 \delta_i + j \frac{1 - \xi_1}{C_0}\right)^2} V_i \exp(-j\beta_{e0}z + \delta_i \beta_{e0} C_0 z). \quad (2.19)$$

At a specific position,  $z = z_0$ , Eqs. 2.17, 2.18, and 2.19 represent three linear equations for unknown amplitudes  $V_i$ . The system of linear equations can be written in matrix form as

$$\begin{bmatrix} V(z_o) \\ \frac{-u_{o1} C_o V(z_o)}{j\eta} \\ \frac{-2V_{o1} C_o^2 i(z_o)}{I_{o1} \xi_2} \end{bmatrix} =$$

$$\begin{bmatrix} 1 & 1 & 1 \\ \frac{1+jC_o \delta'_1}{\xi_1 \delta'_1} & \frac{1+jC_o \delta'_2}{\xi_1 \delta'_2} & \frac{1+jC_o \delta'_3}{\xi_1 \delta'_3} \\ \frac{1+jC_o \delta'_1}{\xi_1 \delta'^2_1} & \frac{1+jC_o \delta'_2}{\xi_1 \delta'^2_2} & \frac{1+jC_o \delta'_3}{\xi_1 \delta'^2_3} \end{bmatrix} \times \begin{bmatrix} V_1 e^{-\beta_{eo} z_o (j-\delta_1 C_o)} \\ V_2 e^{-\beta_{eo} z_o (j-\delta_2 C_o)} \\ V_3 e^{-\beta_{eo} z_o (j-\delta_3 C_o)} \end{bmatrix} \quad (2.20)$$

where

$$\delta'_1 \triangleq j \frac{1-\xi_1}{C_o} + \delta_i \xi_1 \quad ,$$

therefore

$$1 + jC_o \delta_i = \frac{1}{\xi_1} (1+jC_o \delta'_i) \quad .$$

If  $z_o$  is chosen as  $z_o = 0$  the r-f current and velocity vanish since the beam carries no r-f information at the input other than noise. The matrix is then given as

$$\begin{bmatrix} V(0) \\ 0 \\ 0 \end{bmatrix} = \begin{bmatrix} \\ \\ \\ \end{bmatrix} A \begin{bmatrix} V_1 \\ V_2 \\ V_3 \end{bmatrix} \quad (2.21)$$

where A is the same matrix of the coefficients as given in Eq. 2.20. This matrix equation has the same form as the unmodulated TWA with the exception that  $\delta$  is replaced by  $\delta'$ .

It is more useful to express Eq. 2.21 in terms of the potentials on the circuit rather than those at the beam. Therefore rewrite Eq. 2.21 as

$$\begin{bmatrix} V(z_0) \\ 0 \\ 0 \end{bmatrix} = \begin{bmatrix} \\ \\ \\ \end{bmatrix} A \begin{bmatrix} V_{c1} \frac{V_1}{V_{c1}} \\ V_{c2} \frac{V_2}{V_{c2}} \\ V_{c3} \frac{V_3}{V_{c3}} \end{bmatrix}, \quad (2.22)$$

where  $V_{c_i}$  is the initial amplitude of the  $i$ th component of the circuit potential.

The ratio  $V_i/V_{c_i}$  may be determined from the circuit equation. Since  $C_1$  is a capacitance relating the space-charge potential,  $V_{sc}$ , and charge, Eq. 2.6 may be written as

$$V = V_c + V_{sc} \quad ;$$



hence

$$\frac{V}{V_c} = 1 + \frac{V_{sc}}{V_c} \quad (2.23)$$

The space-charge potential  $V_c$  is

$$V_{sc} = -j \frac{i\Gamma}{\omega C_1} ,$$

and the circuit potential  $V_c$  is

$$V_c = \frac{\Gamma \Gamma_1 \frac{E^2}{\beta^2 P}}{2(\Gamma_1^2 - \Gamma^2)} i .$$

Equation 2.23 can now be evaluated for the  $i$ th component. Using the secular equation, 2.16, after some algebraic manipulation, Eq. 2.23 becomes

$$\frac{V_i}{V_{ci}} = \left[ 1 + \frac{4QC_0 \xi_1^2}{\xi_1^2 \delta_i'^2} (1 + jC_0 \delta_i')^2 \right]^{-1} \quad (2.24)$$

Equation 2.24 can now be used in Eq. 2.22 and the resulting system inverted to find the amplitudes of the circuit waves. The result is

$$\begin{bmatrix} V(z_0) \\ 0 \\ 0 \end{bmatrix} = \begin{bmatrix} a_1 & a_2 & a_3 \\ b_1 & b_2 & b_3 \\ c_1 & c_2 & c_3 \end{bmatrix} \times \begin{bmatrix} V_{c1} \\ V_{c2} \\ V_{c3} \end{bmatrix} \quad (2.25)$$

where

$$a_i = 1 + \frac{4QC_0 \xi_1^2}{\xi_1^2} \frac{(1 + jC_0 \delta_i')^2}{\delta_i'^2} ,$$

$$b_i = a_i \frac{1 + jC_o \delta_i'}{\delta_i'},$$

and

$$c_i = a_i \frac{1 + jC_o \delta_i'}{\delta_i'^2}$$

This matrix once again has the same form as that for the unmodulated TWA. The only change is that  $QC \rightarrow QC\xi_2/\xi_1^2$  and  $\delta \rightarrow \delta'$ .

The general form of the  $i$ th component of circuit voltage found by inverting Eq. 2.25 is

$$\begin{aligned} \frac{V_{ci}}{V} = & \left[ 1 + \frac{1 + jC_o \delta_i'}{1 + jC_o \delta_{i+1}'} \frac{\delta_{i+2}' - \delta_i'}{\delta_{i+1}' - \delta_{i+2}'} \left( \frac{\delta_{i+1}'}{\delta_i'} \right)^2 \right. \\ & \left. + \frac{1 + jC_o \delta_i'}{1 + jC_o \delta_{i+2}'} \frac{\delta_i' - \delta_{i+1}'}{\delta_{i+1}' - \delta_{i+2}'} \left( \frac{\delta_{i+2}'}{\delta_{i+1}'} \right)^2 \right] \left[ 1 + \frac{4QC\xi_2}{\xi_1^2} \frac{1 + jC_o \delta_i'}{\delta_i'^2} \right] \end{aligned} \quad (2.26)$$

where

$$\delta_{i+3}' = \delta_i'$$

A similar result for the wave amplitudes evaluated at a position  $z_o \neq 0$  is given in Appendix B.

The modulation device functions for the small-signal TWA may now be calculated. The total circuit voltage is given as\*

$$V_c(z) = R_e \sum_{i=1}^3 V_{ci} \exp j(\omega t - \beta_{eo} z [1 - C_o \delta_i']) \quad (2.27)$$

---

\* Note that at this point we put in  $\text{Re}(\quad)$ ; this was implied in all previous equations of similar form, however we include it at this point since the following work is dependent on it.

The initial amplitude is a complex number given as

$$V_{ci} = \hat{V}_{ci} \exp j\psi_i, \quad (2.28)$$

where  $\hat{V}_{ci}$  is a real number.

Introduce several more reduced variables, a total phase angle

$$\zeta_i = \psi_i - \beta_{eo} z (1 - C_{oi} y_i) \quad , \quad (2.29a)$$

and a total amplitude

$$a_i = V_{ci} \exp \beta_{eo} C_{oi} x_i z \quad (2.29b)$$

where

$$\delta_i = x_i + jy_i$$

The total line voltage can therefore be expressed in the short form

$$V_c(z,t) = R(z) \cos [\omega t + S(z)] \quad , \quad (2.30a)$$

where

$$\begin{aligned} R^2(z) = & a_1^2 + a_2^2 + a_3^2 + 2a_1 a_2 \cos (\zeta_1 - \zeta_2) \\ & + 2a_2 a_3 \cos (\zeta_2 - \zeta_3) + 2a_3 a_1 \cos (\zeta_3 - \zeta_1) \quad , \quad (2.30b) \end{aligned}$$

and

$$S(z) = \tan^{-1} \frac{a_1 \sin \zeta_1 + a_2 \sin \zeta_2 + a_3 \sin \zeta_3}{a_1 \cos \zeta_1 + a_2 \cos \zeta_2 + a_3 \cos \zeta_3} \quad . \quad (2.30c)$$

For the usual TWA, the output terminal is at a point sufficiently far from the input so that the only wave present is the growing wave.

Under this condition, the amplitude and phase are given as

$$\begin{aligned} R^2(z) &= a_1^2(z) \\ S(z) &= \zeta_1(z) \quad (2.31) \end{aligned}$$

The amplitude and phase at any position  $z$  may be expressed in terms of the modulation by

$$a_1(z) = a_1(z, \Delta V, \Delta I)$$

$$\zeta_1(z) = \zeta_1(z, \Delta V, \Delta I)$$

while for the unmodulated tube

$$a_1(z) = a_1(z, 0, 0)$$

$$\zeta_1(z) = \zeta_1(z, 0, 0)$$

The phase shift resulting from a modulation is therefore given as

$$\begin{aligned} \Delta S &= \zeta_1(z, \Delta V, \Delta I) - \zeta_1(z, 0, 0) \\ &= 2\pi N_s C_o \left\{ y_1(\Delta V, \Delta I) - y_1(0, 0) \right\} + \psi_1(\Delta V, \Delta I) - \psi_1(0, 0) \end{aligned} \quad (2.32)$$

where  $N_s$  is the number of unmodulated stream wavelengths. The amplitude variation during a modulation is given by

$$\Delta a = \frac{\hat{V}_{c1}(\Delta I, \Delta V)}{\hat{V}_{c1}(0, 0)} \exp 2\pi C_o N_s \left\{ x_1(\Delta I, \Delta V) - x_1(0, 0) \right\} \quad (2.33)$$

Equations 2.32 and 2.33 represent the modulation device functions for the small-signal beam-modulated TWA.

In order to calculate the device functions for a short traveling-wave tube such as the Crestatron<sup>4</sup>, it is necessary to consider all three waves. The form in this case becomes

$$\begin{aligned} \Delta S &= S(z, \Delta V, \Delta I) - S(z, 0, 0) \\ \Delta a &= \frac{R(z, \Delta V, \Delta I)}{R(z, 0, 0)} \end{aligned} \quad (2.34)$$

where  $R$  and  $S$  are given by Eqs. 2.30.

### 2.3 Taylor Series Form for the Modulation Device Functions of the Linear TWA

It was mentioned in Section 2.1 that a rather cumbersome way of calculating the device functions for the linear amplifier would be to evaluate the small-signal parameters at many points of the modulation cycle, determine the propagation constants corresponding to this set of parameters, calculate the number of stream wavelengths at each modulation point and finally determine the phase and gain. Assume that the phase-shift and gain have been calculated in this manner. Designate by double primes (") the values of the propagation constants and beam wave number as determined by this method. These results obviously must agree with those found by Eqs. 2.32 and 2.33. Therefore to satisfy the phase relation it is necessary that

$$\beta_{e0} L [1 - C_{01} y_1(\Delta I, \Delta V)] = \beta_e'' L [1 - C'' y_1''(\Delta I, \Delta V)]$$

and

$$\psi(\Delta V, \Delta I) = \psi''(\Delta V, \Delta I) \quad (2.35)$$

Substituting Eq. 2.35 into Eq. 2.32 gives

$$\Delta S = \beta_e'' L [1 - C y_1''(\Delta V, \Delta I)] - \beta_{e0} L [1 - C_{01} y_1(0, 0)] + \Delta \psi \quad (3.36)$$

Equation 2.36 is recognizable as a function which can be expressed as the Taylor Series expansion of  $\beta_e L [1 - C y_1(\Delta V, \Delta I)] + \psi$ . Hence

$$\begin{aligned}
 \Delta S &= \sum_1^{\infty} \frac{1}{n!} \left[ \frac{\partial^n}{\partial V^n} \left\{ \beta_e L[1-Cy_1(\Delta V, 0)] + \psi(\Delta V, 0) \right\} \right]_{V_{O1}, I_{O1}} \Delta V^n \\
 &+ \sum_1^{\infty} \frac{1}{n!} \left[ \frac{\partial^n}{\partial I^n} \left\{ \beta_e L[1-Cy_1(0, \Delta I)] + \psi(0, \Delta I) \right\} \right]_{V_{O1}, I_{O1}} \Delta I^n \\
 &+ \sum_1^{\infty} \frac{1}{n!} \sum_{r=v}^n C_r^n \left[ \frac{\partial^n}{\partial V^r \partial I^{n-r}} \left\{ \beta_e L[1-Cy_1(\Delta V, \Delta I)] \right. \right. \\
 &\left. \left. + \psi(\Delta V, \Delta I) \right\} \right]_{V_{O1}, I_{O1}} \Delta V^r \Delta I^{n-r} \tag{2.37}
 \end{aligned}$$

where  $C_r^n$  is the binomial coefficient.

Similarly the gain can be expressed by a Taylor Series expansion in terms of the modulating signals and the amplitude modulation. Then  $\Delta a$  is given by

$$\begin{aligned}
 \Delta a_{db} &= \sum_1^{\infty} \frac{1}{n!} \left\{ \frac{\partial^n}{\partial V^n} \left[ 8.864 \log_{10} \frac{\hat{V}_1(\Delta V, \Delta I)}{V(0)} + 54.6 CN_{S_1} x_1(\Delta I, \Delta V) \right] \right\}_{V_{O1}, I_{O1}} \Delta V^n \\
 &+ \sum_1^{\infty} \frac{1}{n!} \left\{ \frac{\partial^n}{\partial I^n} \left[ 8.864 \log_{10} \frac{\hat{V}_1(\Delta V, \Delta I)}{V(0)} + 54.6 CN_{S_1} x_1(\Delta I, \Delta V) \right] \right\}_{V_{O1}, I_{O1}} \Delta I^n \\
 &+ \sum_1^{\infty} \frac{1}{n!} \sum_{r=1}^n C_r^n \left\{ \frac{\partial^n}{\partial V^r \partial I^{n-r}} \left[ 8.864 \log_{10} \frac{\hat{V}_1(\Delta V, \Delta I)}{V(0)} \right. \right. \\
 &\left. \left. + 54.6 CN_{S_1} x_1(\Delta V, \Delta I) \right] \right\}_{I_{O1}, V_{O1}} \Delta V^r \Delta I^{n-r} \tag{2.38}
 \end{aligned}$$

Cumming<sup>6</sup> used the Taylor Series approach but did not consider the variation of

$$\hat{V}_1(\Delta V, \Delta I) \exp j\psi_1(\Delta V, \Delta I)$$

The effect of this approximation will be discussed in Chapter III. The evaluation of several of the coefficients of the Taylor Series is given in Appendix C.

#### 2.4 Modulation Device Functions for the Large-Signal TWA

An analysis similar to that given in Section 2.2 will now be performed for the large-signal TWA. When either the input r-f signal or the length of the TWA circuit is increased, the strength of the field acting on the electron increases until saturation effects begin. The large magnitude fields result in r-f velocities and charge-density amplitudes which approach the average values. The average beam velocity will decrease because of the energy being given up to the circuit wave. This is clearly in violation of the small-signal assumption 2 made in Section 2.2.

The large velocity excursions cause crossings of electron trajectories which result in the position being a multivalued function of the interaction region entrance time for the electrons. The multivalued functions can not be described by a hydrodynamical beam. In order to handle both the large amplitude r-f quantities and the multivalued functions, the Lagrangian or particle approach must be used in conjunction with the nonlinear equations of motion of the beam.

In the Lagrangian approach, the beam is considered to be made up of finite discrete particles of charge. The solution is obtained by integrating the equations of motion along the flight line of each particle. The method employed in this section was first used by Nordsieck<sup>18</sup> and then generalized by Rowe<sup>17</sup> to include finite C, space-charge forces and loss.

The method will now be generalized further by including low-frequency beam modulation. The principal assumptions for this analysis are listed in Section 2.1.

The average beam potential and current in the interaction region will be varied as in Eqs. 2.3 and 2.4. The circuit equation is once again independent of the average beam conditions and can be obtained by combining the Eqs. 2.1. The result including loss is,

$$\frac{\partial^2 V_c}{\partial t^2} - v_o^2 \frac{\partial^2 V_c}{\partial z^2} + \frac{R}{L} \frac{\partial V_c}{\partial t} = v_o Z_o \frac{\partial^2 \rho}{\partial t^2} + \frac{R}{L} Z_o \frac{\partial \rho}{\partial t} \quad (2.39)$$

The normal mode theory can not be used in this instance since we can no longer use superposition and the linear operator- $\Gamma$ . The one-dimensional force equation is given in Eq. 2.2 as

$$\frac{du}{dt} = \eta \frac{\partial V}{\partial z} = \eta \left\{ \frac{\partial V_c}{\partial z} + \frac{\partial V_{sc}}{\partial z} \right\} \quad (2.2)$$

The conservation of charge expression for a beam composed of particles<sup>17</sup> given by stating that the charge contained in a bunch at one position  $z_o$  and at time  $t_o$  must be conserved at some other position  $z$  and at a later time  $t$ . Hence

$$\rho(z_o, t_o) dz_o = \rho(z, t) dz \quad (2.40)$$

If  $z_o$  is chosen at the input, then for the modulated beam,

$$\rho(z, t) = - \frac{I_{o1}}{u_{o1}} \left( \frac{\partial z_o}{\partial z} \right)_t \left( \frac{1 + \frac{\Delta I}{I_{o1}}}{M^3} \right)^{1/2} = - \frac{I_{o1}}{u_{o1}} \xi_2 \left( \frac{\partial z_o}{\partial z} \right)_t \quad (2.41)$$

A complete description of the unmodulated TWA may be obtained by integrating the path of each electron entering the interaction region



during one cycle of the r-f signal. For the modulated tube it is necessary to integrate over all electrons entering during one modulation cycle. However, when the quasi-stationary approximation is made, each point in the modulation cycle is treated as a stationary point and once again it becomes necessary to integrate only over one r-f cycle. The electrons entering the interaction region may be identified by reference to an r-f signal at the circuit input. A convenient reference is the phase of the r-f when the electron enters,

$$\phi_{oi} = \omega t_{oi} \quad , \quad (2.42)$$

where  $t_{oi}$  is the arrival time of an electron at the interaction region.

Let us define a distance in terms of  $t_{oi}$  as

$$t_{oi} = \frac{z_{oi_i}}{u_{oi}} = \frac{z_{oi}}{u_{oi} \left(1 + \frac{\Delta V}{V_{oi}}\right)^{1/2}} \quad . \quad (2.43)$$

$z_{oi_i}$  is actually the distance that the  $i$ th electron would travel in time  $t_{oi}$  if its velocity were the unmodulated velocity  $u_{oi}$ , while  $z_{oi}$  is the distance the electron travels in  $t_{oi}$  at the modulated velocity.

The position variable will be replaced by a new variable  $y$  defined in terms of the unmodulated tube.

$$y = \frac{C_o \omega z}{u_{oi}} \quad . \quad (2.44)$$

The interpretation of results can be simplified by defining the normalized variables  $\phi_{oi}$  and  $y$  in terms of the unmodulated tube rather than the modulated tube. A tube of a specific length will always be represented by the same  $y$  value, independent of the modulation condition.

The initial electron phase  $\phi_{oi}$  is assumed to be invariant with modulation. The initial average velocity however is a function of the modulation. This is understandable since the low-frequency modulation does not bunch the beam, and in an unbunched beam the electrons maintain their phase position. The Applegate diagram in Fig. 2.2 illustrates the initial effects of the low-frequency modulation. All bunching and debunching effects are neglected in this diagram.

When the effects of r-f bunching forces and space-charge debunching forces are considered, the trajectories curve and intersect. Some further phase variables must be introduced to describe the interaction flight lines. Consider

$$\phi(z,t) = \omega \left( \frac{z}{u_{o1}} - t \right) - \theta(z) = \phi(z, \phi_{oi}) \quad (2.45)$$

These angles are illustrated in Fig. 2.3. It can be seen from Fig. 2.3 that  $\phi(\phi_{oi}, z)$  is the phase of the  $i$ th electron measured with respect to the circuit wave.  $\phi$  is measured from the electron to the circuit wave.  $\theta(z)$  is the phase of the circuit wave with respect to a fictitious wave traveling at the unmodulated velocity of the beam and is measured from the circuit wave to the fictitious wave.

The most appealing way of solving the equations of motion, from a "physical picture" point of view, would be to integrate all equations with time as the running variable; then at each time the effect of the  $n$  electrons appearing during one r-f cycle would have to be considered, with each electron being at a position  $z$  specified by its flight line. This method is rather involved and extremely difficult to handle. Instead, the group of  $n$  electrons entering during each r-f cycle are assumed to enter the tube simultaneously, but each having a different phase with respect to the r-f

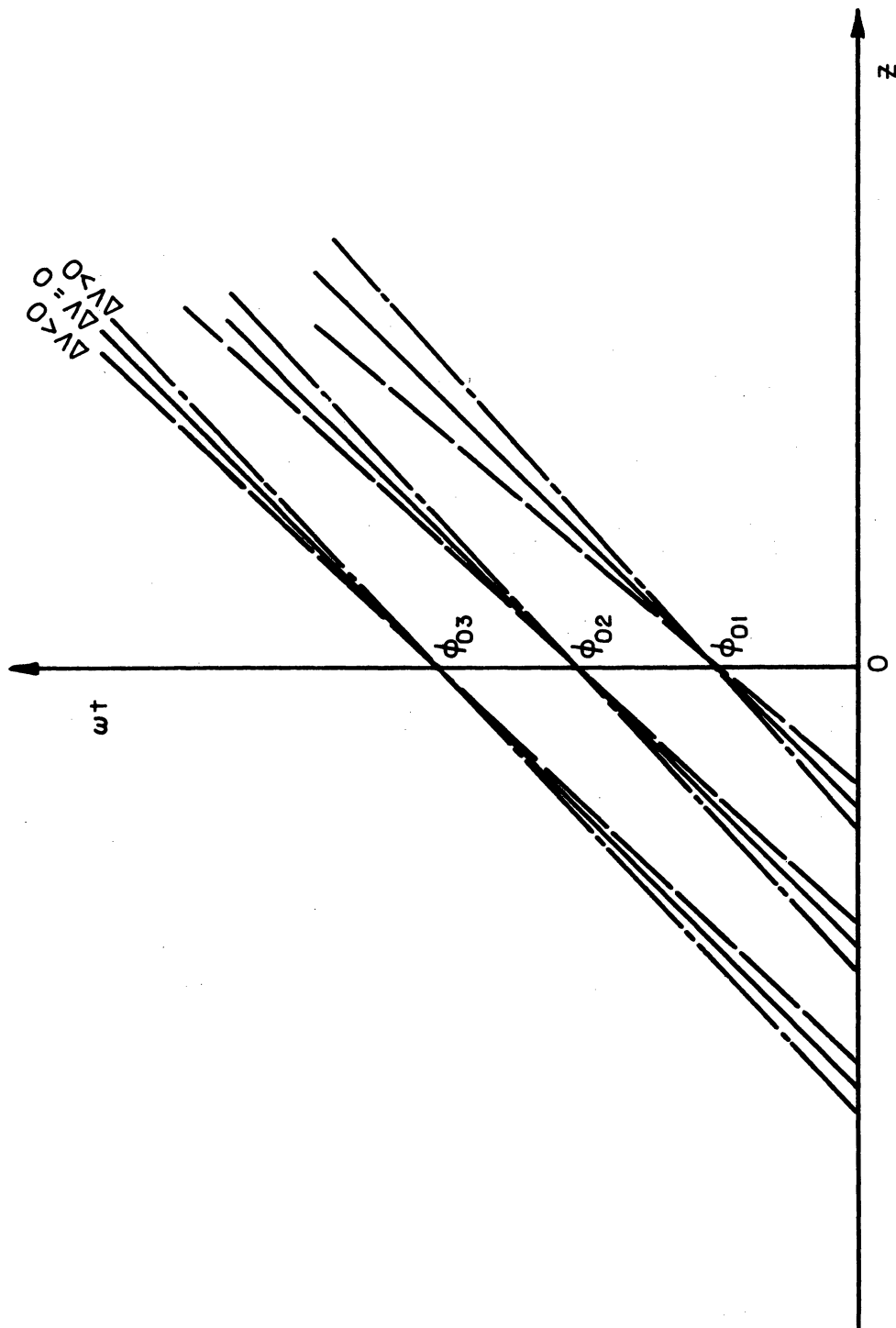


FIG. 2.2 INITIAL EFFECTS OF BEAM-POTENTIAL MODULATION. (NO R-F SIGNAL, SPACE-CHARGE DEBUNCHING NEGLECTED)

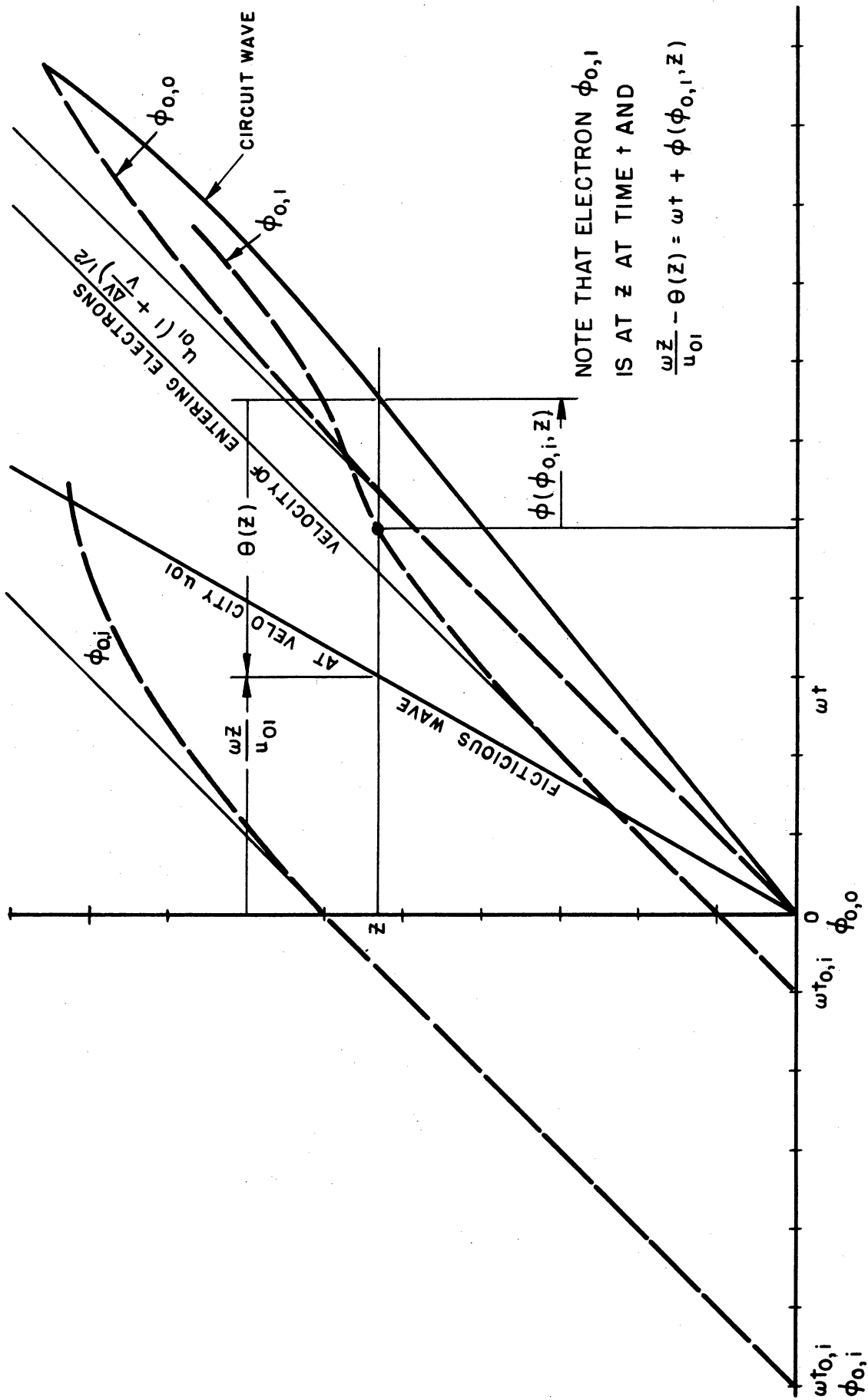


FIG. 2.3 APPLIGATE DIAGRAM OF MODULATED TWA, ILLUSTRATION OF ANGLE RELATIONS.

wave. The equations can then be integrated with respect to distance  $y$ , and the independent variables will be  $\phi_{oi}$  and  $y$ .

Now consider\* the motion of one electron along its trajectory. An expanded drawing of this one line in the vicinity of position  $z$  is shown in Fig. 2.4. The total change of the sum of the angles along this trajectory is given as,\*\*

$$\begin{aligned} \left( \frac{\partial \phi(z, \phi_{oi})}{\partial z} \right)_{\phi_{oi}} + \frac{d\theta(z)}{dz} \\ = \lim_{\Delta z \rightarrow 0} \left\{ \frac{\phi(z+\Delta z, \phi_{oi}) - \phi(z, \phi_{oi})}{\Delta z} + \frac{\theta(z+\Delta z) - \theta(z)}{\Delta z} \right\}. \end{aligned} \quad (2.46)$$

From Fig. 2.4, define the phase difference  $d_3$  as

$$\begin{aligned} d_3 &= -\theta(z) - \phi(\phi_{oi}, z) \\ &= d_2 - \theta(z+\Delta z) - \phi(\phi_{oi}, z+\Delta z) - d_1, \end{aligned}$$

where

$$d_1 = \frac{\omega \Delta z}{u_{ti}}$$

$$d_2 = \frac{\omega \Delta z}{u_{o1}}$$

and

$u_{ti}$  is the total velocity of the  $i$ th electron.

Therefore

$$\phi(\phi_{oi}, z+\Delta z) + \theta(z+\Delta z) - \phi(\phi_{oi}, z) - \theta(z) = \Delta z \left[ \frac{\omega}{u_{o1}} - \frac{\omega}{u_{ti}} \right],$$

---

\* This geometrical interpretation of the phase relation was worked out jointly with J. Meeker of this laboratory.

\*\* The subscripts are included in the partial derivatives to avoid confusion as to which coordinate system is used.

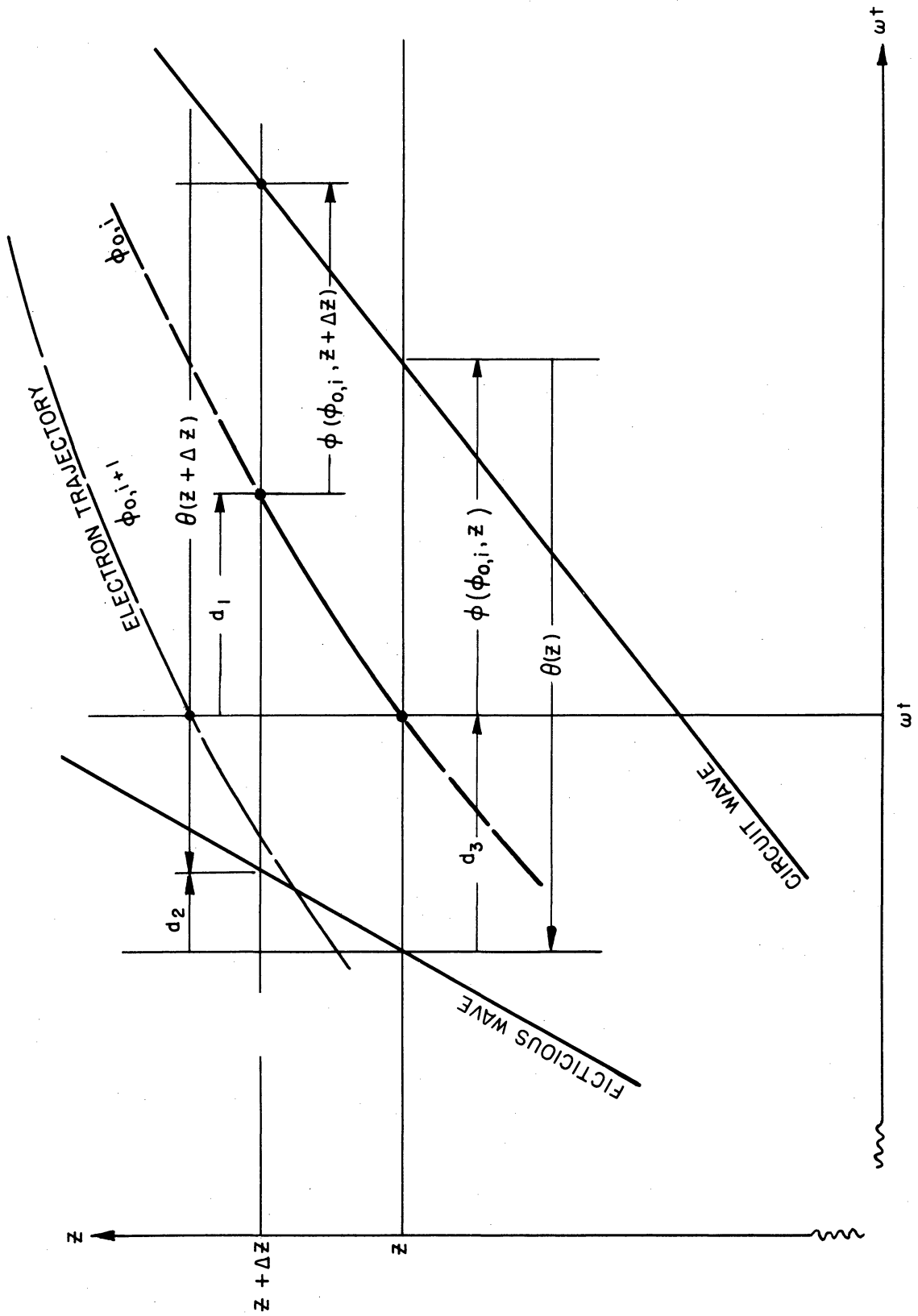


FIG. 2.4 EXPANDED VIEW OF FLIGHT LINES.

and finally, substitution into Eq. 2.46 gives

$$\left(\frac{\partial\phi}{\partial z}\right)_{\phi_{oi}} + \frac{d\theta}{dz} = \left(1 - \frac{u_{o1}}{u_{ti}}\right) \frac{\omega}{u_{o1}} \quad (2.47)$$

Define the total electron velocity as

$$u_{ti} = u_{o1} \left(1 + \frac{\Delta V}{V_{o1}}\right)^{1/2} \left[1 + 2 C_o u(y, \phi_{oi})\right], \quad (2.48)$$

and use the definition of  $y$ , to obtain,

$$\begin{aligned} \left[\frac{\partial\phi}{\partial y}(\phi_{oi}, y)\right]_{\phi_{oi}} + \frac{d\theta(y)}{dy} &= \frac{1}{C_o} \left[1 - \frac{1}{\left(1 + \frac{\Delta V}{V_{o1}}\right)^{1/2} \left[1 + 2C_o u(y, \phi_{oi})\right]}\right] \\ &= \frac{1}{C_o} \left[1 - \frac{1}{\xi_1 [1 + 2C_o u(y, \phi_{oi})]}\right]. \quad (2.49) \end{aligned}$$

Equation 2.49 is the first working equation.

Define the potential  $V'_c$ , due to the circuit wave, but seen by an electron (at the beam radius) at position  $y$  and phase  $\phi$  as,

$$V'_c(y, \phi) = \frac{Z_o I_{o1}}{C_o} M \left(1 + \frac{\Delta I}{I_{o1}}\right) A(y) \cos \phi(y, \phi_{oi}). \quad (2.50)$$

$A(y)$  is assumed to be the normalized amplitude of the circuit wave at position  $y$ . For perfect beam-to-circuit coupling, the potential seen by the electron is the same as the potential at the circuit ( $V'_c = V_c$ ). If perfect coupling is assumed, the following equation is obtained when Eq. 2.50 is substituted into Eq. 2.39.

$$\begin{aligned}
 & -C_o \left( \frac{\omega v_o}{u_{o1}} \right)^2 Z_{o1} I_{o1} M \left( 1 + \frac{\Delta I}{I_{o1}} \right) \left\{ \left[ \frac{d^2 A(y)}{dy^2} - A(y) \left\{ \left( \frac{1}{C_o} - \frac{d\theta(y)}{dy} \right)^2 \right. \right. \right. \\
 & \left. \left. \left. - \left( \frac{u_{o1}}{v_o C_o} \right)^2 \right\} \right] \cos \varphi + \left[ -2 \left( \frac{1}{C_o} - \frac{d\theta}{dy} \right) \frac{dA(y)}{dy} \right. \right. \\
 & \left. \left. + A(y) \frac{d^2 \theta(y)}{dy^2} - \frac{R}{\omega L} \left( \frac{u_{o1}}{v_o} \right)^2 \frac{A(y)}{C_o^2} \right] \sin \varphi \right\} \\
 & = v_o Z_o \frac{\partial^2 \rho}{\partial t^2} + \frac{R}{L} v_o Z_o \frac{\partial \rho}{\partial t} \quad (2.51)
 \end{aligned}$$

Equation 2.50 can also be substituted into the force equation to obtain

$$\begin{aligned}
 & \left( 1 + \frac{\Delta V}{V_{o1}} \right) \left[ 1 + 2C_o u(y, \varphi_o) \right] \frac{\partial u}{\partial y} (\varphi_{oi}, y) \\
 & = M \left( 1 + \frac{\Delta I}{I_{o1}} \right) \left\{ C_o \frac{dA(y)}{dy} \cos \varphi - C_o A \left[ \frac{1}{C_o} - \frac{d\theta}{dy} \right] \sin \varphi \right\} \\
 & + \frac{u_{o1} C_o}{Z_o I_{o1} \omega} \frac{\partial v_{sc}}{\partial z} \quad (2.52)
 \end{aligned}$$



In order to use the conservation of charge expression, Eq. 2.41, it is necessary to evaluate  $\left(\frac{\partial z_o}{\partial z}\right)_t$ .

Recall that Eq. 2.43 states

$$z_o = \phi_o \frac{u_{o1}}{\omega} \left[ 1 + \frac{\Delta V}{V_{o1}} \right]^{1/2}$$

therefore,

$$\left(\frac{\partial z_o}{\partial z}\right)_t = \frac{u_{o1}}{\omega} \left[ 1 + \frac{\Delta V}{V_{o1}} \right]^{1/2} \left(\frac{\partial \phi_o}{\partial z}\right)_t \quad (2.53)$$

Evaluate the total differential of  $\phi(\phi_{oi}, y)$  to obtain

$$d\phi = \left(\frac{\partial \phi}{\partial \phi_o}\right)_y d\phi_o + \left(\frac{\partial \phi}{\partial y}\right)_{\phi_o} dy = \frac{1}{C_o} dy - \frac{d\theta}{dy} - \omega dt \quad ;$$

therefore

$$\left(\frac{\partial \phi}{\partial \phi_o}\right)_y \left(\frac{\partial \phi}{\partial y}\right)_t = \frac{1}{C_o} - \frac{d\theta}{dy} - \left(\frac{\partial \phi}{\partial y}\right)_{\phi_o}$$

After using the first working equation in the above the result is

$$\left(\frac{\partial z_o}{\partial z}\right)_t = \frac{1}{1+2C_o u(y, \phi_{oi})} \frac{1}{\left(\frac{\partial \phi}{\partial \phi_{oi}}\right)_y} \quad (2.54)$$

The conservation of charge expression is therefore given as:

$$\rho(u, \phi_{oi}) = -\frac{I_{o1}}{u_{o1}} \xi_2 \frac{1}{1+2C_o u(y, \phi_{oi})} \frac{1}{\left(\frac{\partial \phi}{\partial \phi_{oi}}\right)_y} \quad (2.55)$$

Due to the nonlinearities, the beam will contain harmonics of the fundamental r-f, however only the fundamental r-f is assumed to interact with the circuit wave. The fundamental component of charge density may be found from a Fourier expansion of the charge density.

$$\rho(u, \varphi_{oi}) = \frac{I_{o1}}{u_{o1} \pi} \xi_2 \sum_{n=0}^{\infty} \left\{ \left( \sin n\varphi \int_0^{2\pi} \frac{\sin n\varphi \left( \frac{\partial \varphi_{oi}}{\partial \varphi} \right)_y}{1+2C_o u(y, \varphi_{oi})} d\varphi \right. \right. \\ \left. \left. + \cos n\varphi \int_0^{2\pi} \frac{\cos n\varphi \left( \frac{\partial \varphi_{oi}}{\partial \varphi} \right)_y}{1+2C_o u(y, \varphi_{oi})} d\varphi \right) \right\} \quad (2.56)$$

The fundamental component of Eq. 2.56 will be used in the circuit equation. There will be  $\sin \varphi$  and  $\cos \varphi$  terms appearing on each side of the resulting equation. Equating the sine and cosine coefficients on each side yields two equations.

$$\frac{d^2 A(y)}{dy^2} - A(y) \left[ \left( \frac{1}{C_o} - \frac{d\theta(y)}{dy} \right)^2 - \frac{(1+C_o b_o)^2}{C_o^2} \right] \\ = - \frac{1+C_o b_o}{\pi C_o} \frac{1}{M^{5/2} \left( 1 + \frac{\Delta I}{I_{o1}} \right)^{1/2}} \left\{ \int_0^{2\pi} \frac{\cos \varphi(\varphi_{oi}, y) d\varphi_o}{1+2C_o u(\varphi_{oi}, y)} \right. \\ \left. + 2C_o d_o \int_0^{2\pi} \frac{\sin \varphi(y, \varphi_{oi}) d\varphi_o}{1+2C_o u(\varphi_{oi}, y)} \right\} \quad (2.57)$$

and

$$\begin{aligned}
 A(y) & \left[ \frac{d^2\theta}{dy^2} - \frac{2d_o}{C_o} (1+C_o b_o)^2 \right] + 2 \frac{dA(y)}{dy} \left( \frac{d\theta(y)}{dy} - \frac{1}{C_o} \right) \\
 & = - \frac{1+C_o b_o}{\pi C_o} \frac{1}{M^{5/2} \left( 1 + \frac{\Delta I}{I_{o1}} \right)^{1/2}} \left\{ \int_0^{2\pi} \frac{\sin \varphi(\varphi_{oi}, y) d\varphi_o}{1+2C_o u(\varphi_{oi}, y)} \right. \\
 & \quad \left. - 2C_o d_o \int_0^{2\pi} \frac{\cos \varphi(\varphi_{oi}, y) d\varphi_o}{1+2C_o u(\varphi_{oi}, y)} \right\} , \quad (2.58)
 \end{aligned}$$

where

$$b_o = \frac{1}{C_o} \left\{ \frac{u_{o1}}{v_o} - 1 \right\} , \quad \text{and}$$

$$2d_o = \frac{R}{\omega L C_o} .$$

The model used to calculate the space-charge potential is a solid beam of electrons flowing within a cylinder having perfect conducting walls. Figure 2.5 illustrates the geometry of the model. The following assumptions are involved in calculating the space-charge potential:

1. There are no transverse fields or electrons moving transversely.
2. There are sufficient ions present to neutralize the average space charge of the beam.
3. The beam is assumed to have a sinusoidal variation of charge density with distance for the first solution to Poisson's equation. The actual variation with distance is used in later work.

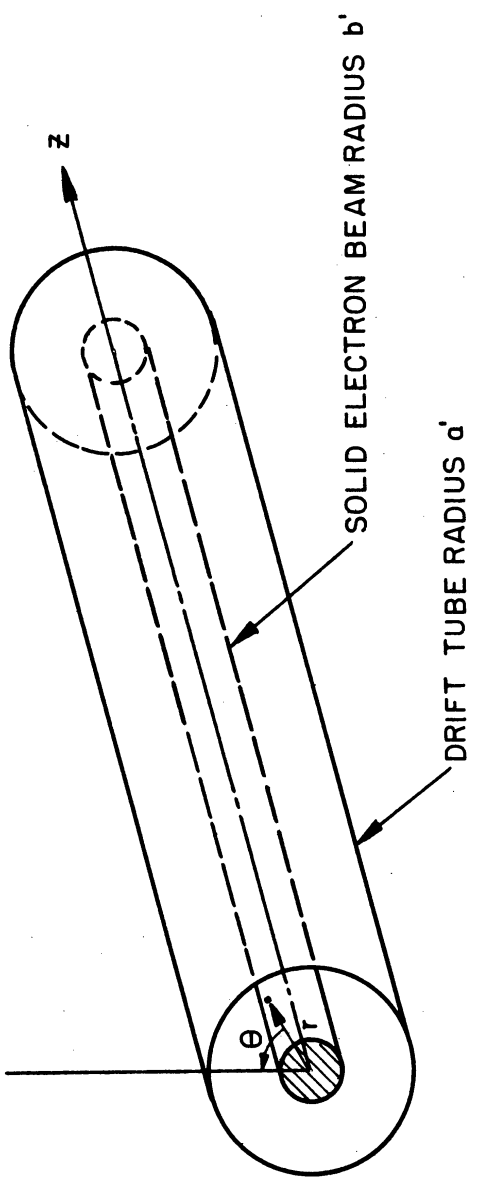


FIG. 2.5 SPACE CHARGE MODEL.

The space-charge potential is defined by Poisson's equation:

$$\nabla^2 V_{sc} = - \frac{\rho_o e^{-j\beta z}}{\epsilon_o \pi b'^2} \quad (2.59)$$

The sinusoidal variation of charge density is in accordance with assumption 3 above. The wave number  $\beta$  is the cold wave number of the circuit wave.

Equation 2.59 can be integrated and the boundary conditions for the geometry used. The result is the familiar space-charge field expression as determined by several authors<sup>17,19</sup> in the past,

$$E_{sc} = \frac{j\rho_o e^{-j\beta z}}{\epsilon \pi b'^2 \beta} R^2(\beta b') \quad (2.60)$$

where  $R$  is the plasma-frequency reduction factor given as

$$R^2 = 1 - \frac{\beta b'}{I_o(\beta a')} \left[ I_1(\beta b') K_o(\beta a') + I_o(\beta a') K_1(\beta b') \right]$$

Curves of the reduction factor as a function of beam to circuit radii ratio and  $\beta b'$  are found in the literature<sup>17</sup>. The dimensionless quantity  $\beta b'$  may be defined as

$$B \triangleq \beta b' \quad .$$

The sinusoidal variation of space-charge density is now dropped and the actual variation is used, therefore

$$E_{sc} = \frac{j\rho(z)R^2}{\epsilon \pi b'^2 \beta} \quad (2.61)$$

When the Fourier expansion for charge is introduced, the space-charge field may be expressed as

$$E_s = \frac{1}{\pi} \operatorname{Re} \sum_{1}^{\infty} \frac{jRn^2}{n\beta} \frac{e^{-jn\phi}}{\pi\epsilon b'^2} \int_0^{2\pi} \rho e^{jn\phi} d\phi$$

Inverting the order of summation and integration, this expression becomes

$$E_s = \frac{2}{\pi\epsilon b'^2} \frac{1}{\beta} \int_0^{2\pi} \rho F(\phi-\phi') d\phi' \quad (2.62)$$

where

$$F(\phi-\phi') = \sum_{1}^{\infty} \frac{\sin n(\phi-\phi') R_n^2}{2\pi n}$$

F is the space-charge weighting factor and relates the force of an electron at phase  $\phi$  and one at phase  $\phi'$ . Curves of the space-charge weighting function for various values of stream diameter can be found in the literature<sup>17, 47</sup>.

The radian plasma frequency is defined by the relation

$$\omega_{po}^2 = \frac{I_{o1} |\eta|}{\pi\epsilon b'^2 u_{o1}} ;$$

and the cold wave number of the circuit as:

$$\beta = \beta_{eo} (1+C_o b_o)$$

These two definitions along with the form for  $\rho$  given by Eq. 2.55 leads to the final form for the space-charge field as

$$E_s = \frac{2\omega u_{o1}}{|\eta|(1+C_o b_o)} \left(\frac{\omega_{po}}{\omega}\right)^2 \xi_2 \int_0^{2\pi} \frac{F(\phi-\phi') d\phi'_o}{1+2C_o u(\phi'_o, y)} \quad (2.63)$$

The final form for the force equation, Eq. 2.52, is then given as

$$\begin{aligned}
 & \left\{ 1 + 2C_o u(\varphi_{oi}, y) \right\} \frac{\partial u}{\partial y} (\varphi_{oi}, y) \\
 &= - \frac{1}{M^2} A(y) \left[ 1 - \frac{d\theta}{dy} C_o \right] \sin \varphi(\varphi_{oi}, y) \\
 &+ \frac{C_o}{M^2} \frac{dA(y)}{dy} \cos \varphi(\varphi_{oi}, y) \\
 &- \frac{1}{(1+C_o b_o) M^2 \xi_1} \left( \frac{\omega p_o}{\omega C_o} \right)^2 \int_0^{2\pi} \frac{F(\varphi - \varphi')}{1 + 2C_o u(\varphi_{oi}, y)} d\varphi' \quad (2.64)
 \end{aligned}$$

Equation 2.64 is the last working equation. Note that for no modulation, Eqs. 2.49, 2.57, 2.58 and 2.64 reduce to the usual large-signal TWA equations.<sup>17</sup>

It is to be noted that in the above calculation of space-charge potential, the force exerted on a particular electron by all other electrons was calculated assuming that all electrons were at a position  $y$ , but in general each had a different phase. This method of calculation is consistent with the manner in which the problem is integrated, however it is not an exact method of calculating the force. The force on an electron is actually exerted by electrons distributed in space, but we have here assumed that it suffices to calculate the force using a distribution in phase or time. Figure 2.6 illustrates the possible configurations. It is felt by this author that the assumption that the distribution in phase is approximately equal to the distribution in space is consistent with other assumptions. A recent paper by Rowe<sup>47</sup> further illustrates the equivalence of the two distributions. In this paper Rowe obtains good agreement between the nonlinear TWA performance calculated using the above method and Tien's<sup>53</sup> method in which the space-charge field is calculated using the space distribution.

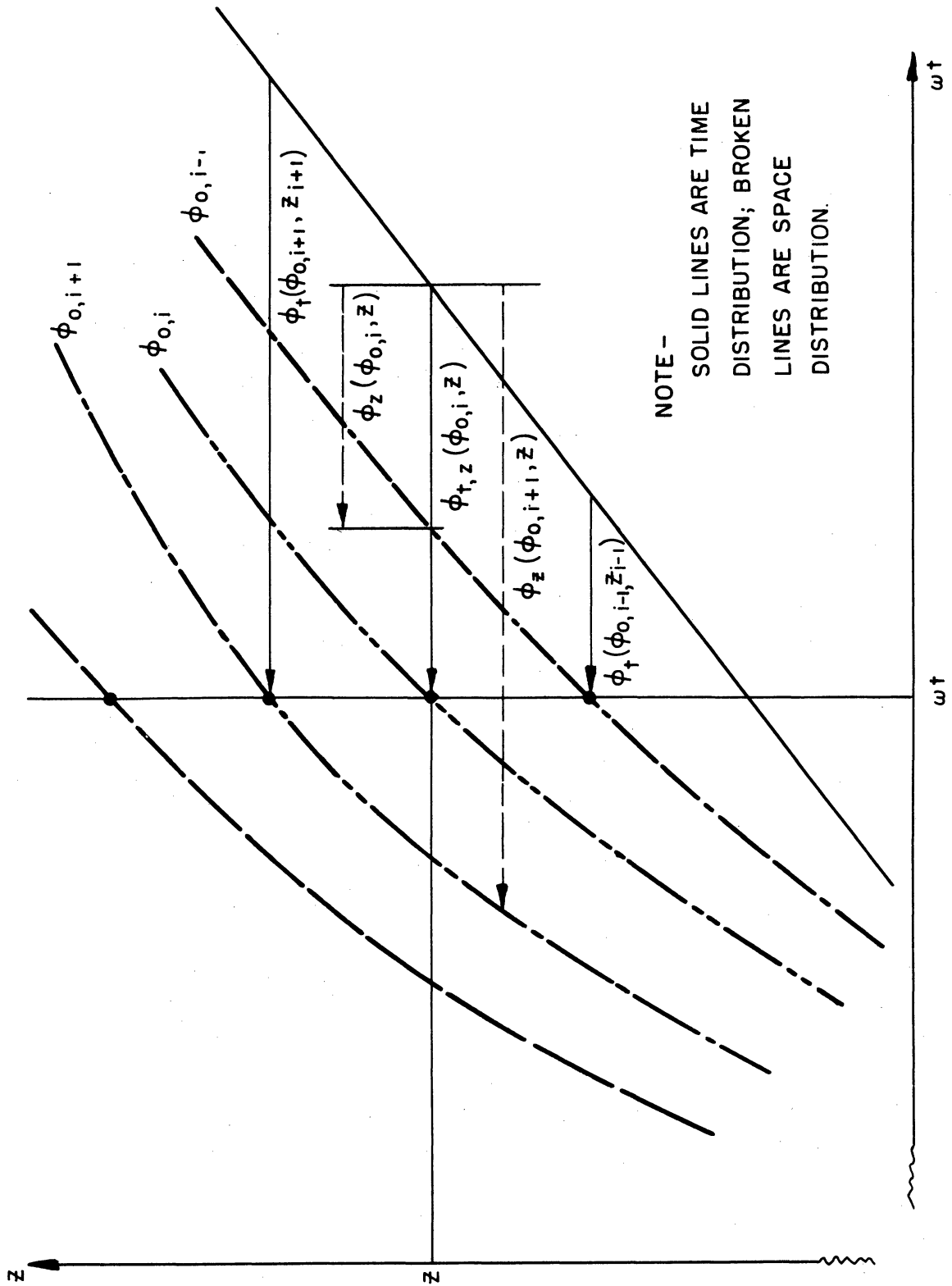


FIG. 2.6 FLIGHT LINES SHOWING ELECTRON DISTRIBUTION IN SPACE AND TIME.



The small signal space-charge parameter of the unmodulated tube is introduced through the equation

$$QC_o \approx \frac{1}{4C_o^2} \left( \frac{\frac{\omega_{po}}{\omega} R}{1 + \frac{\omega_{po}}{\omega}} \right)^2$$

where R is  $R(\beta b')$ , the plasma-frequency reduction factor.

In summary, Eqs. 2.49, 2.57, 2.58 and 2.64 represent the working equations for the large-signal beam modulated tube in terms of the circuit r-f voltage  $A(y)$ , the electron velocity  $u(\phi_{oi}, y)$ , the electron phase  $\phi(\phi_{oi}, y)$  and the circuit wave phase  $\theta(y)$ . The independent variables are the normalized length  $y$ , the electron initial phase  $\phi_{oi}$  and the modulation  $\Delta I$  and  $\Delta V$ . The modulation equations reduce to the ordinary TWA equations. It is necessary to introduce the boundary conditions at  $y=0$ . The boundary conditions are listed below:

1. Since the electrons enter the interaction region with no r-f disturbances, the r-f velocity is zero so that

$$u(\phi_{oi}, 0) = 0 \quad \text{for } i = 1 \dots n.$$

2. The initial phases of the entering particles are uniformly spaced since the beam is unbunched, therefore

$$\phi_{o,i} = \frac{2\pi i}{n} \quad i = 1 \dots n \quad (32 \text{ electrons are used})$$

3. The phase difference between the circuit wave and the fictitious wave (see Fig. 2.3) is zero at the origin.
4. An initial amplitude for  $A(0)$  is arbitrarily chosen but it is still small enough so that the amplifier behaves linearly near the input.

5.  $(d\theta/dy)_0$  and  $(dA/dy)_0$  can be evaluated using the small-signal analysis; this was done by Rowe<sup>17</sup> using all three waves and Nordsieck<sup>18</sup> using only the growing wave, however this method involving the small signal-analysis further complicates the modulation problem.

Consider the circuit equation given in Eq. 2.1. If loss is included this becomes

$$\frac{\partial v_c}{\partial z} + I_c R + j\beta_0 Z_0 I_c = 0 \quad (2.2a)$$

For a matched line

$$\frac{V_c(0)}{I_c(0)} = Z_0,$$

therefore after normalizing, Eq. 2.2a evaluated at the input becomes

$$\left(\frac{\partial v_c}{\partial y}\right)_0 = - \left[ 2d_0 + j \frac{1+C_0 b_0}{C_0} \right] v_c(0) \quad (2.65)$$

Using the definition of the line potential given by Eq. 2.50 in Eq. 2.65 one obtains the boundary conditions

$$\left(\frac{dA}{dy}\right)_0 = - 2d_0 A(0)$$

$$\left(\frac{d\theta}{dy}\right)_0 = - b_0 \quad (2.66)$$

These values are in agreement with the initial values found by Rowe using a different method.

If the circuit equation, Eq. 2.57, is evaluated at the input, the integrals will vanish since the beam enters unmodulated. Therefore in order to obtain conditions given by Eq. 2.66, it is necessary that  $(d^2A/dy^2)_0$  vanish. This is approximately true, in fact this term is neglected altogether in Nordsieck's work. This is not justified at a position distant from the input.

The modulation device functions can now be calculated. The phase modulation is given as

$$\Delta S = \theta(y, \Delta I, \Delta V) - \theta(y, 0, 0) \quad (2.67)$$

and the amplitude modulation

$$\Delta a_{db} = A(y, \Delta I, \Delta V) - A(y, 0, 0) \quad (2.68)$$

The equations necessary for calculating the modulation device functions were derived in the preceding chapter. Two distinct methods of calculation were described, one applicable for small r-f signals involved the solution of the linear equations describing the hydrodynamic type beam while the second method was for large r-f signals and involved the solution of the set of nonlinear equations describing the particle type beam. In this chapter some typical modulation device functions will be shown.

### 3.1 Small-Signal Modulation Device Functions

There are three distinct steps involved in the determination of the modulation device functions for the linear amplifier, if one uses the direct method of solution as presented in Section 2.2. It is necessary first to determine the propagation constants as functions of the low-frequency beam modulation, secondly to calculate the effect of the modulation on the initial loss parameter, and finally to combine these two steps for a tube of specified length in order to determine its modulation device functions.

3.1.1 Propagation Constants as Functions of the Modulation-Signal Amplitudes. The characteristic equation for the low-frequency beam-modulated TWA was given in Eq. 2.16. The roots of this quartic equation are the propagation constants. Since one of the roots represents a backward traveling wave, which is far from synchronism, only the three roots representing forward waves are considered. The roots are, in general complex and are given as

$$\delta_i(\xi_1, \xi_2) = x_i(\xi_1, \xi_2) + jy_i(\xi_1, \xi_2) \quad (3.1)$$

where  $i = 1, 2, 3,$

and

$$\xi_1 = \left(1 + \frac{\Delta V}{V_{O1}}\right)^{1/2}$$

$$\xi_2 = \frac{1 + \frac{\Delta I}{I_{O1}}}{\xi_1} .$$

To conform to previous convention, the root corresponding to  $i = 1$  represents the slow and growing wave, the wave corresponding to  $i = 2$  is the slow and declining wave and finally the wave for  $i = 3$  is the fast wave. Recall that the waves propagate as

$$\exp \left\{ j\beta_{e0} z (1 - C_{0i} y_i) + \beta_{e0} C_{0i} x_i z \right\} .$$

Figures 3.1 through 3.6 are curves of the propagation constants as functions of the normalized beam-potential modulation amplitude with constant beam current, and also as functions of the normalized beam-current modulation amplitude for constant beam potential. In all curves the gain parameter for unmodulated operation is selected to be 0.10. The other parameter values for unmodulated operation are listed on the curves. For all curves, the velocity injection parameter  $b_0$  is adjusted to maximize the small-signal gain.

The voltage modulation amplitudes are kept within  $\pm 20\%$  of the beam voltage while the current is allowed to vary from  $20\%$  to  $200\%$  of the unmodulated beam current. It is the author's opinion that modulation amplitudes for system applications will fall within these limits.

The linear variation of  $y_1(\xi_1)$ , the imaginary part of the propagation constants of the slow and growing wave, as a function of the beam-potential modulation with constant current has an important bearing on

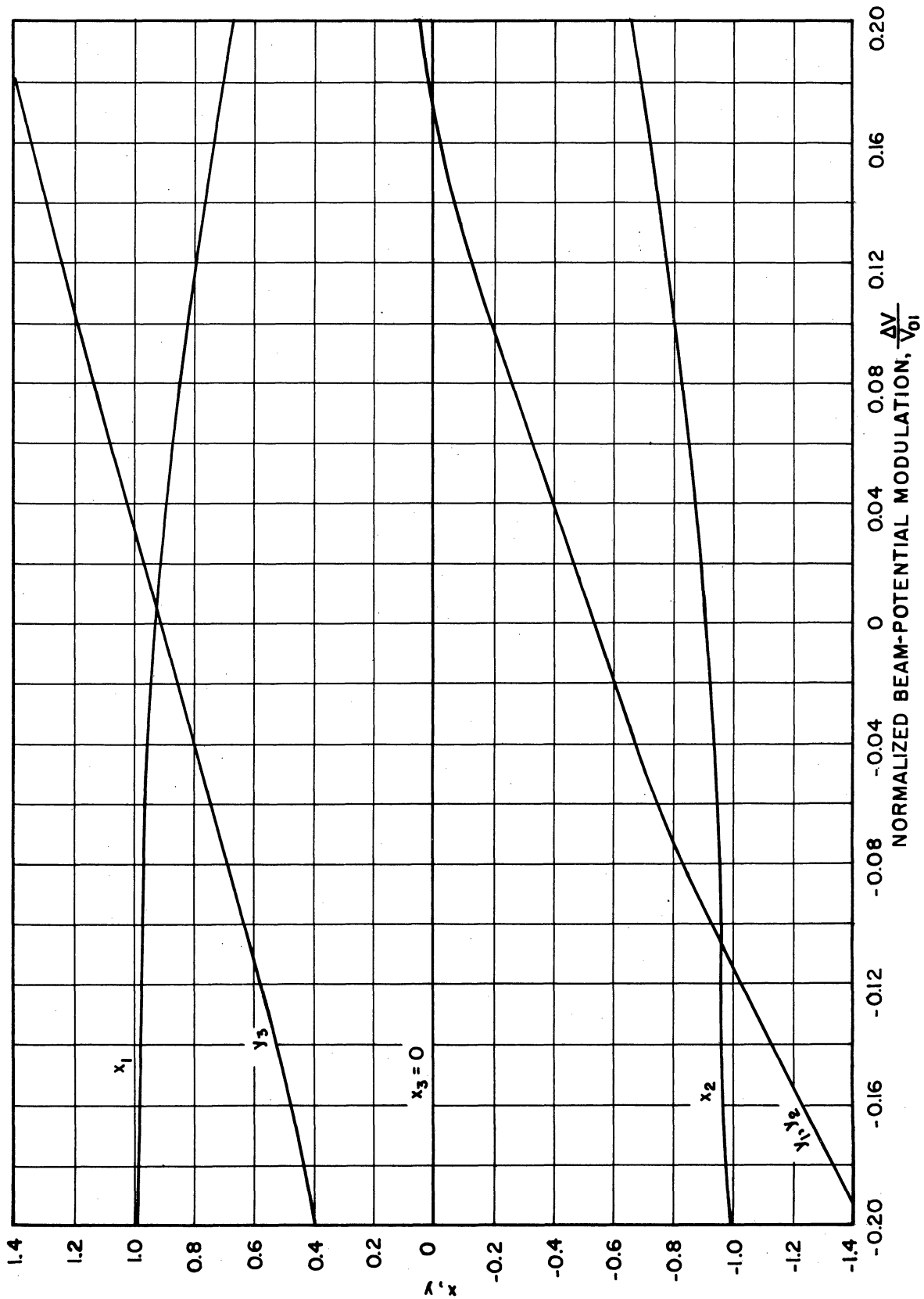


FIG. 3.1 SMALL-SIGNAL PROPAGATION CONSTANTS FOR TWA WITH MODULATED BEAM POTENTIAL. ( $C_0 = 0.10, Q_{C_0} = 0, b_0 = 0.1525, d_0 = 0, \Delta I = 0$ )

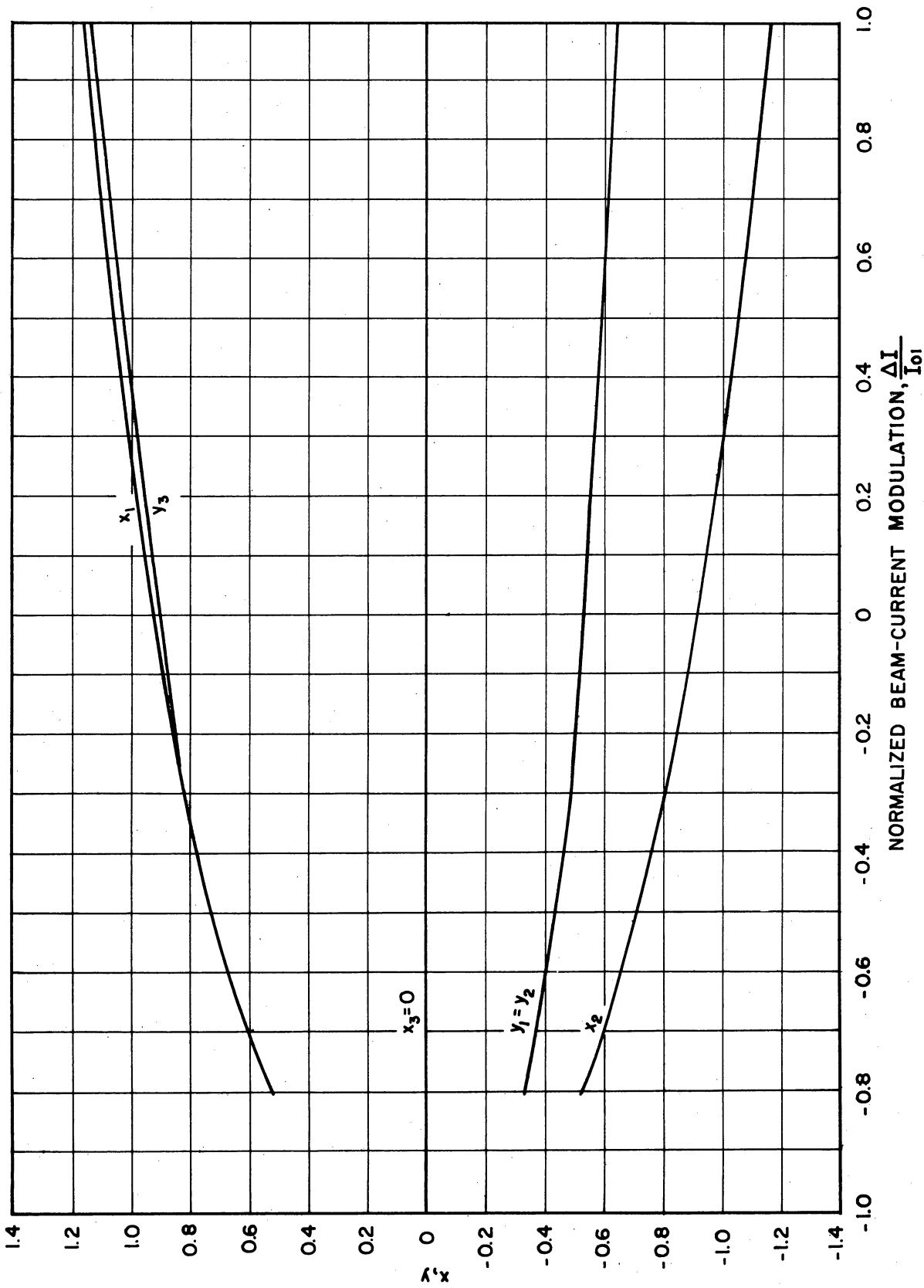


FIG. 3.2 SMALL-SIGNAL PROPAGATION CONSTANTS FOR TWA WITH MODULATED BEAM CURRENT. ( $C_0=0.10, Q C_0=0, b_0=0.1525, d_0=0, \Delta V=0$ )

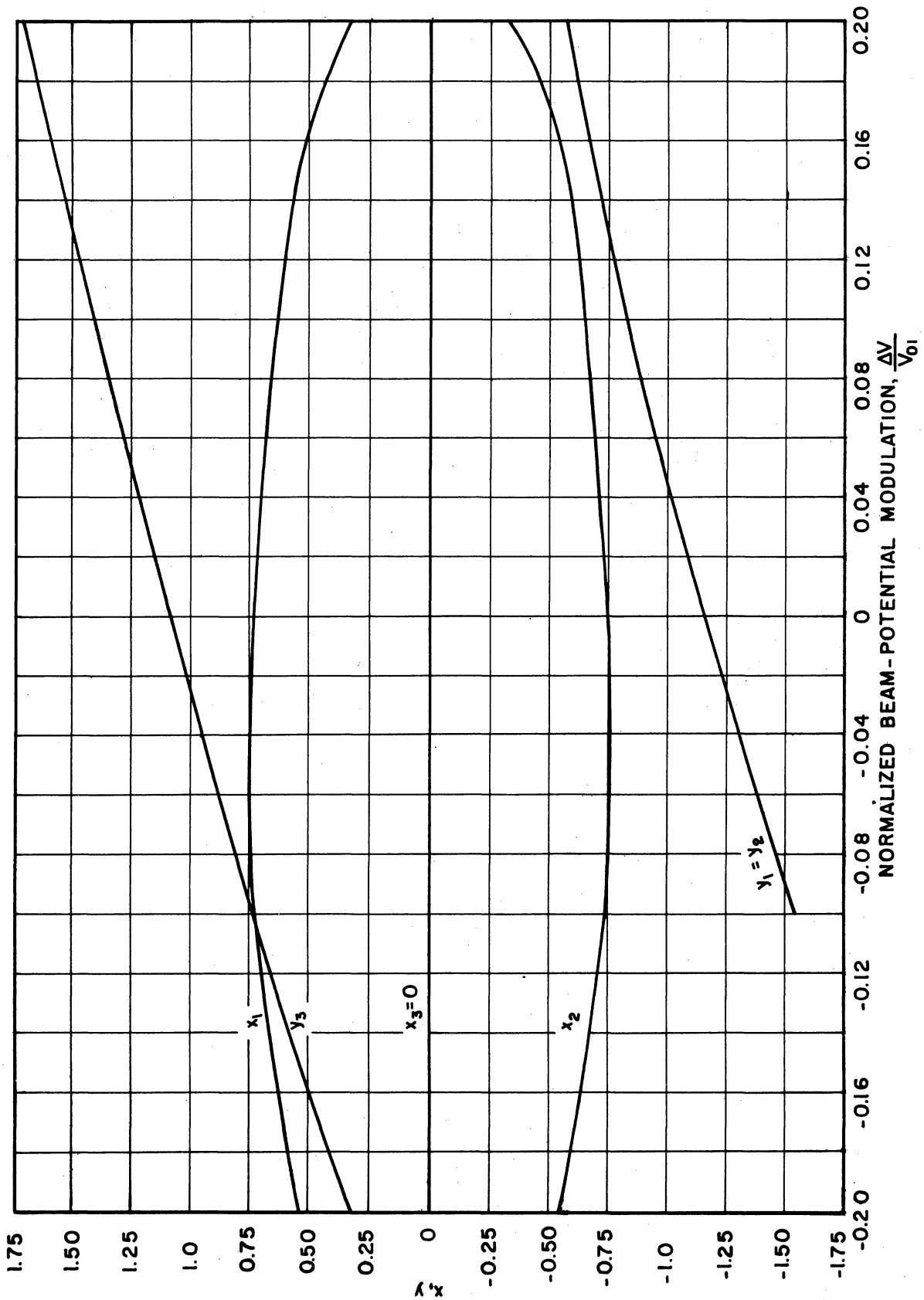


FIG. 3.3 SMALL-SIGNAL PROPAGATION CONSTANTS FOR TWA WITH MODULATED BEAM POTENTIAL. ( $C_0=0.10$ ,  $qC_0=0.250$ ,  $b_0=1.0$ ,  $d_0=0$ ,  $\Delta I=0$ )



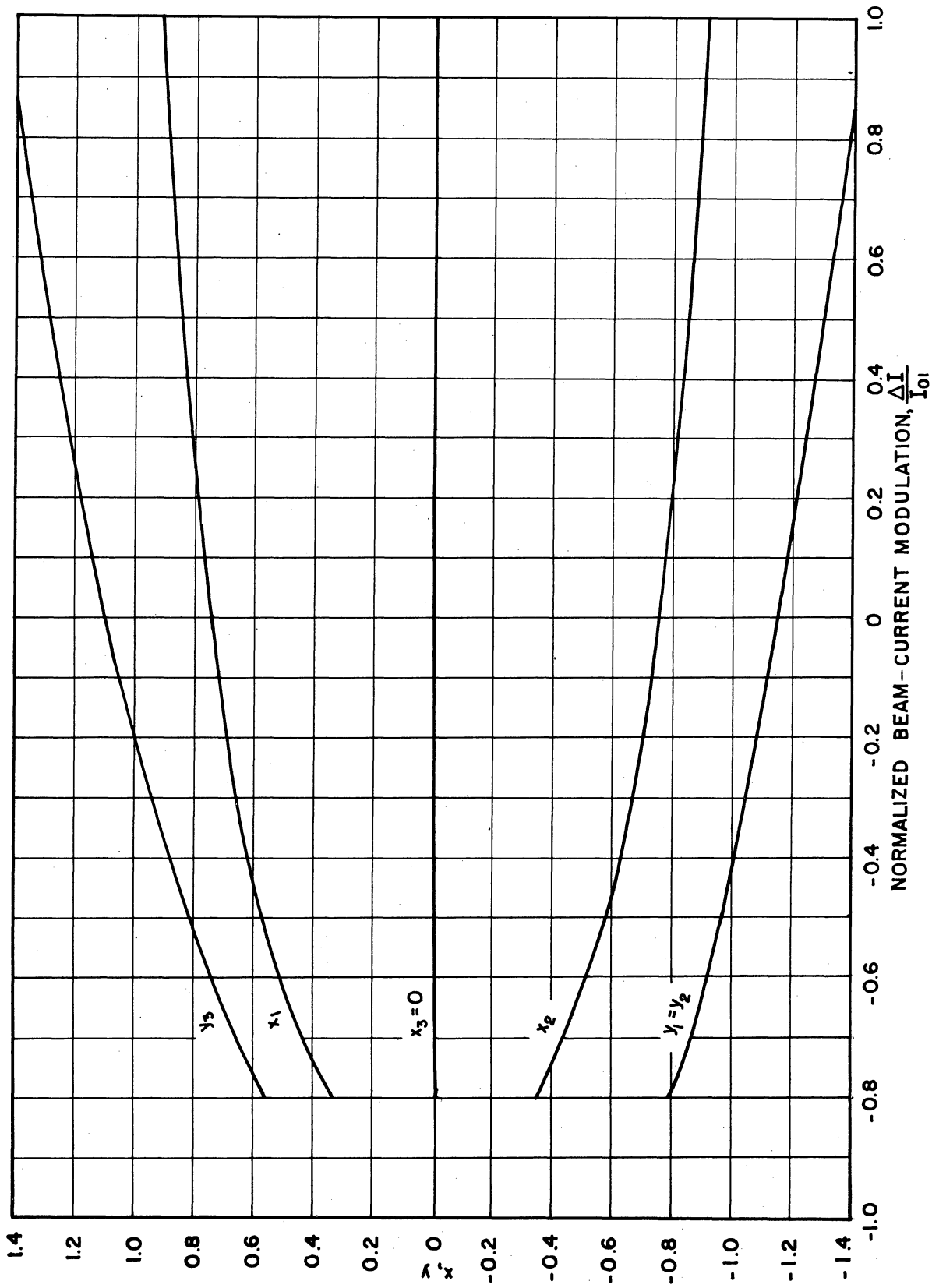


FIG. 3.4 SMALL-SIGNAL PROPAGATION CONSTANTS FOR TWA WITH MODULATED BEAM CURRENT. ( $C_0 = 0.10$ ,  $QC_0 = 0.250$ ,  $b_0 = 1.0$ ,  $d_0 = 0$ ,  $\Delta V = 0$ )

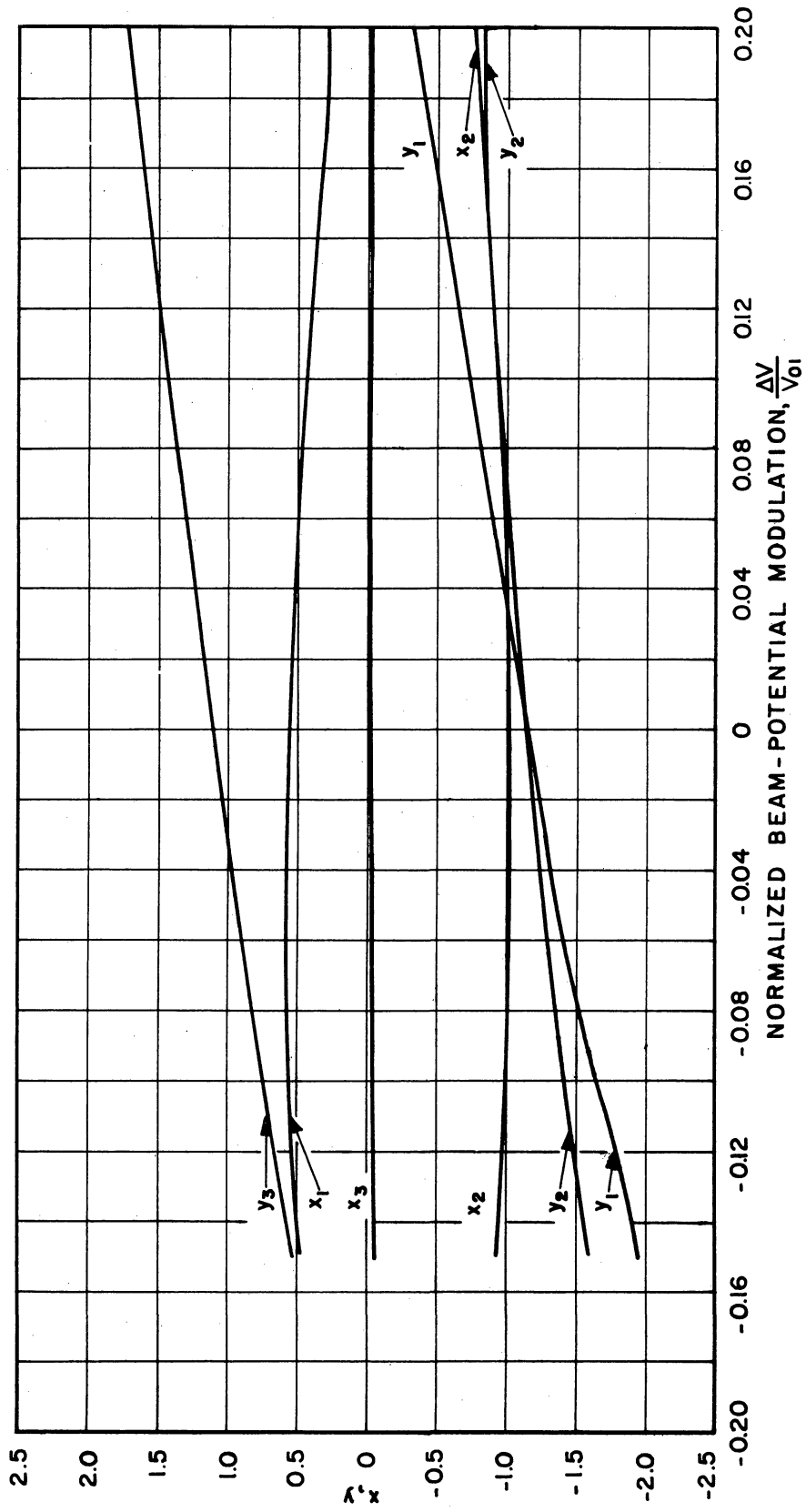


FIG. 3.5 SMALL-SIGNAL PROPAGATION CONSTANTS FOR TWA WITH MODULATED BEAM POTENTIAL. ( $C_0=0.10, Q C_0=0.250, b_0=1.0, d_0=0.5, \Delta I=0$ )

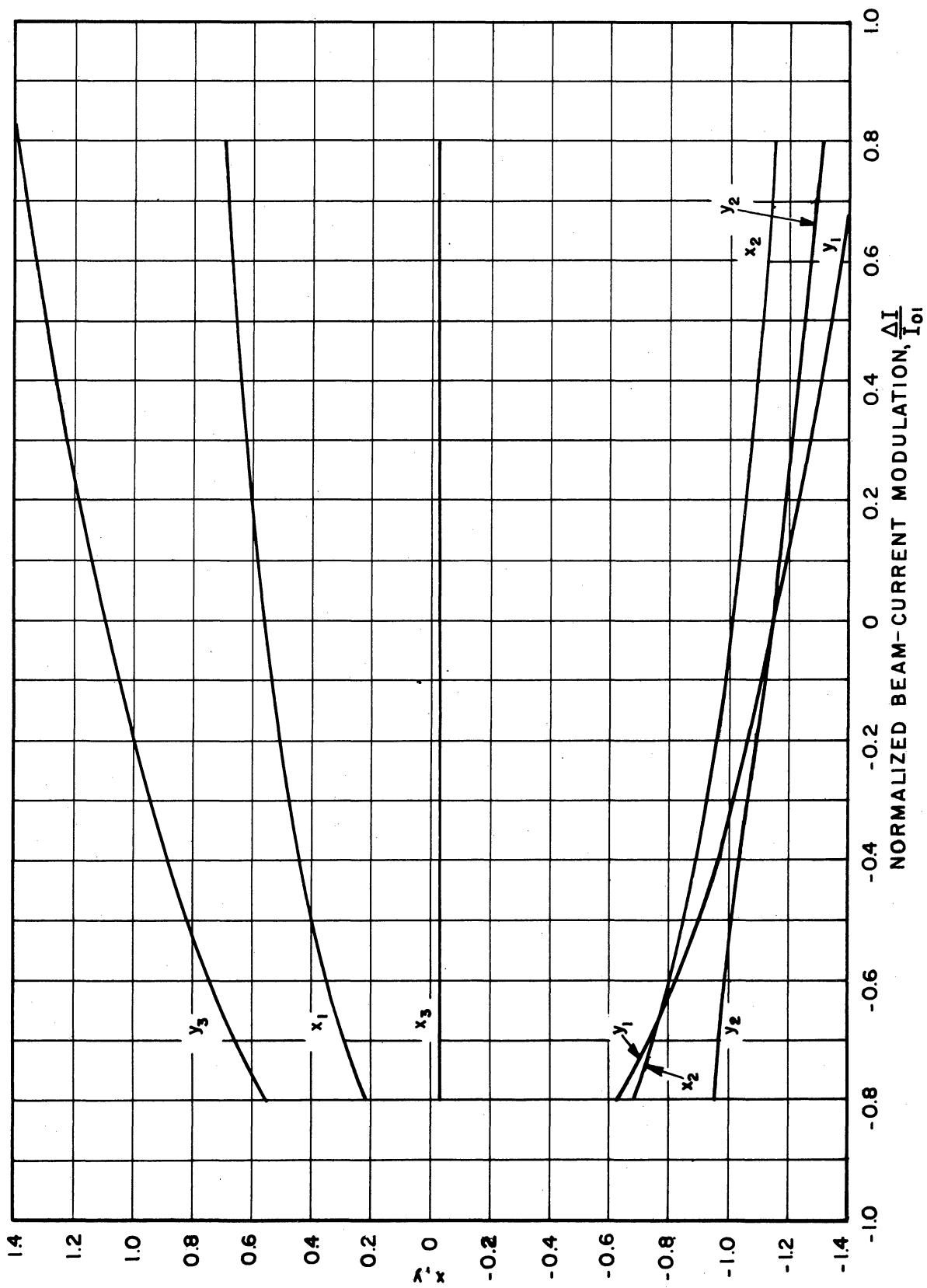


FIG. 3.6 SMALL-SIGNAL PROPAGATION CONSTANTS FOR TWA WITH MODULATED BEAM CURRENT. ( $C_0=0.10$ ,  $QC_0=0.250$ ,  $b_0=1.0$ ,  $d_0=0.50$ ,  $\Delta V=0$ )

the applicability of TWA's as phase modulators. Note that good linearity is apparently obtained for all cases considered in this report when the voltage swing is between  $\pm 5\%$ . The slope of  $y_1(\xi_2)$  as a function of the normalized beam-current modulation amplitude, with constant potential, is much less than that for the voltage modulation.

The variation of the real part of the propagation constant,  $x_1$ , during the modulation is of the same order of magnitude for both current and potential modulation. It is now possible to calculate the phase modulation in radians per stream wavelength and the amplitude modulation in db per stream wavelength exclusive of the phase and amplitude modulation introduced by the modulation of the initial loss parameter. If the main interaction region is defined as the region in which the signal grows after the growing wave has been set up, then this phase and amplitude modulation will be that taking place in the main interaction region.

The phase modulation produced per stream wavelength in the main interaction region can be calculated using Eq. 2.32.

$$\frac{\Delta S'}{N_s} = \frac{\Delta S - \Delta \psi}{N_s} = 2\pi C_o \left[ y_1(\Delta V, \Delta I) - y_1(0, 0) \right] . \quad (3.2)$$

The amplitude modulation produced per stream wavelength in the main interaction region can be calculated from Eq. 2.33.

$$\frac{\Delta a' \text{db}}{N_s} = 54.6 C_o \left[ x_1(\Delta V, \Delta I) - x_1(0, 0) \right] . \quad (3.3)$$

Equations 3.2 and 3.3 are plotted in Figs. 3.7 and 3.10 for the propagation constants shown in Figs. 3.1 through 3.6.

3.1.2 The Effect of Low-Frequency Beam Modulations on the Initial Loss Parameter A. It can be seen from Eqs. 2.32 and 2.33 that the total phase shift and gain are each composed of a component which varies with

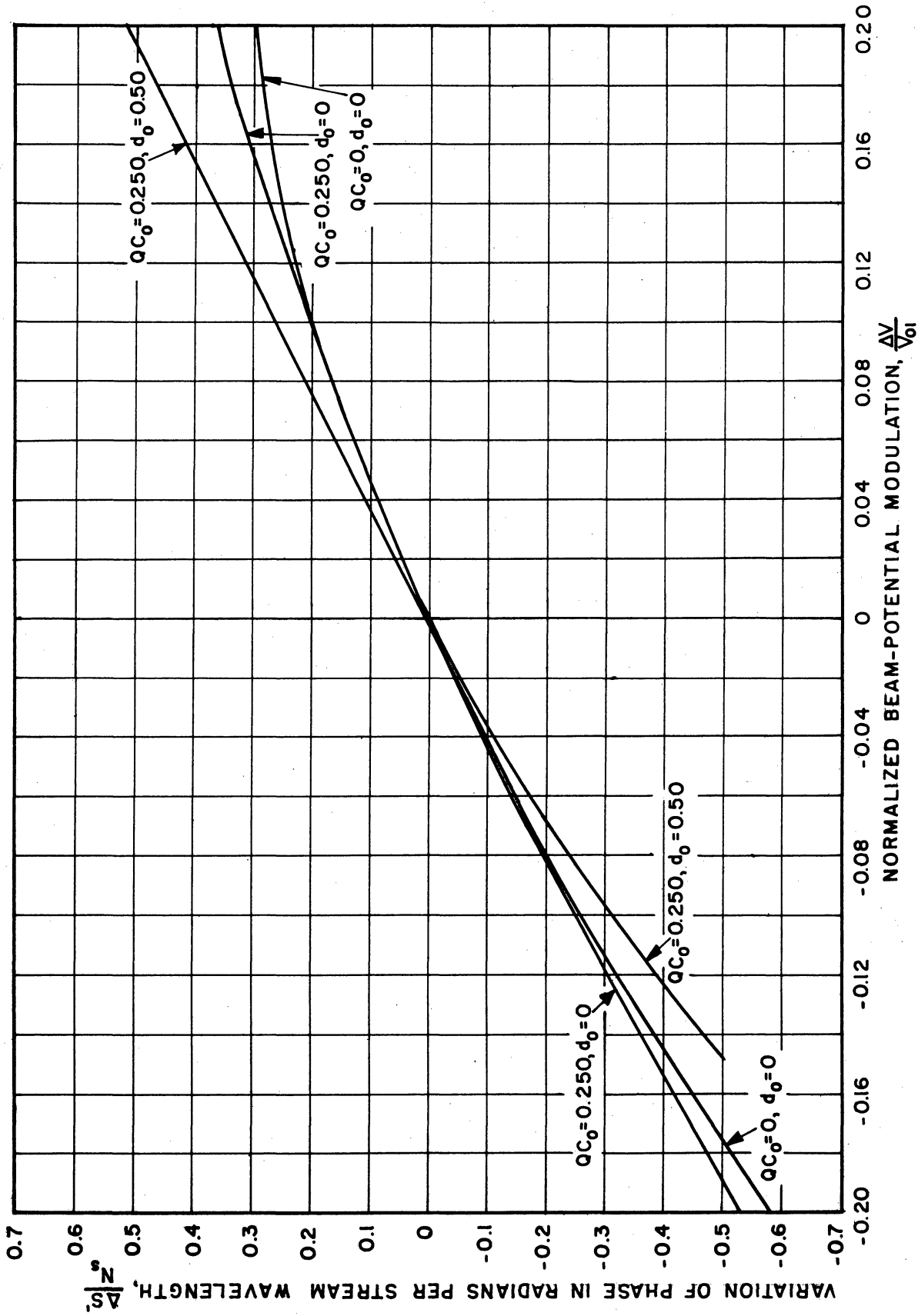


FIG. 37 PHASE VARIATION IN THE MAIN INTERACTION REGION DURING BEAM-POTENTIAL MODULATION ( $C_0=0.10, \Delta I=Q, b_0$  ADJUSTED FOR MAXIMUM GAIN)

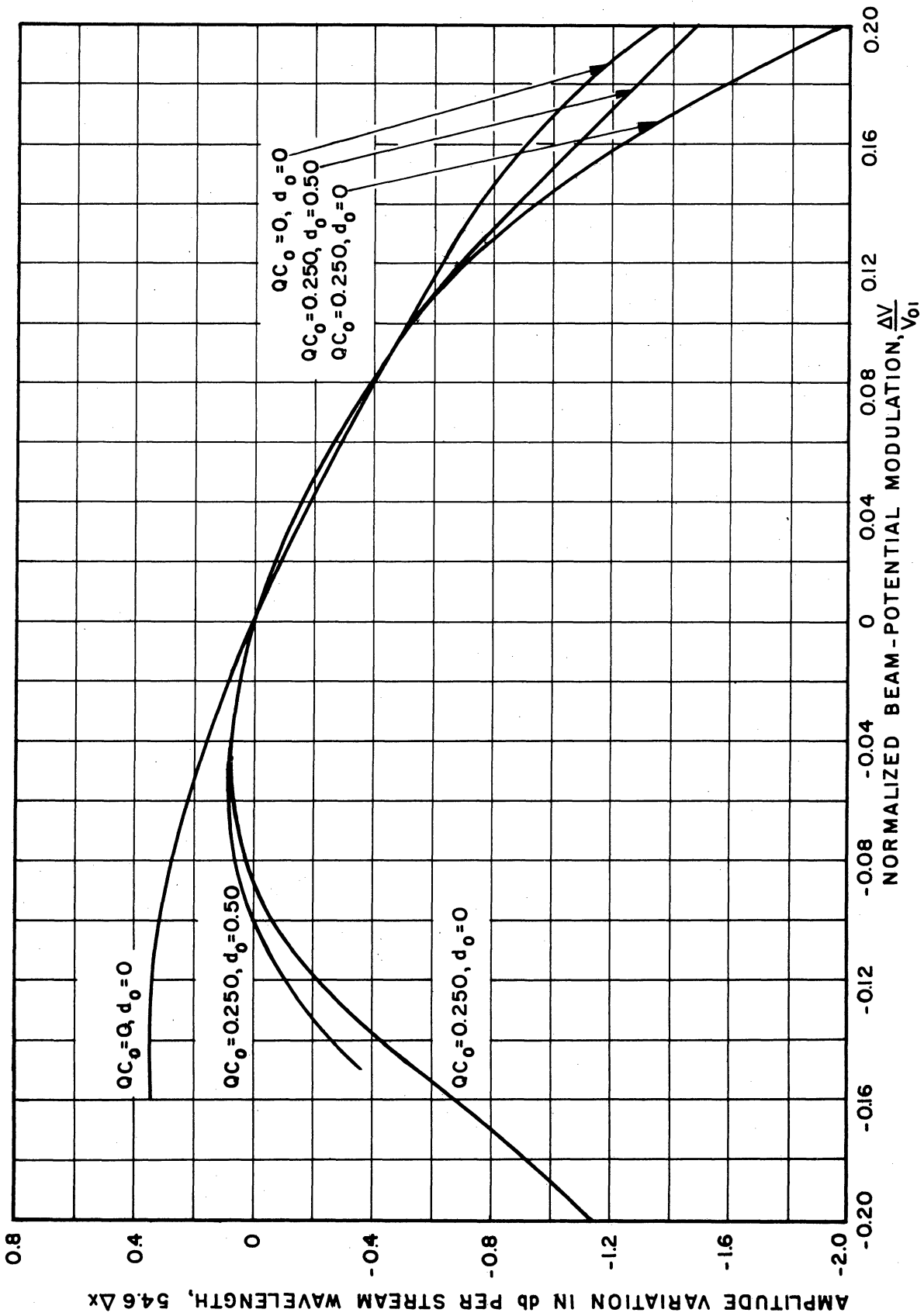


FIG. 3.8 AMPLITUDE VARIATION IN THE MAIN INTERACTION REGION DURING BEAM-POTENTIAL MODULATION ( $c_0 = 0.10, \Delta I = 0, b_0$  ADJUSTED FOR MAXIMUM GAIN)

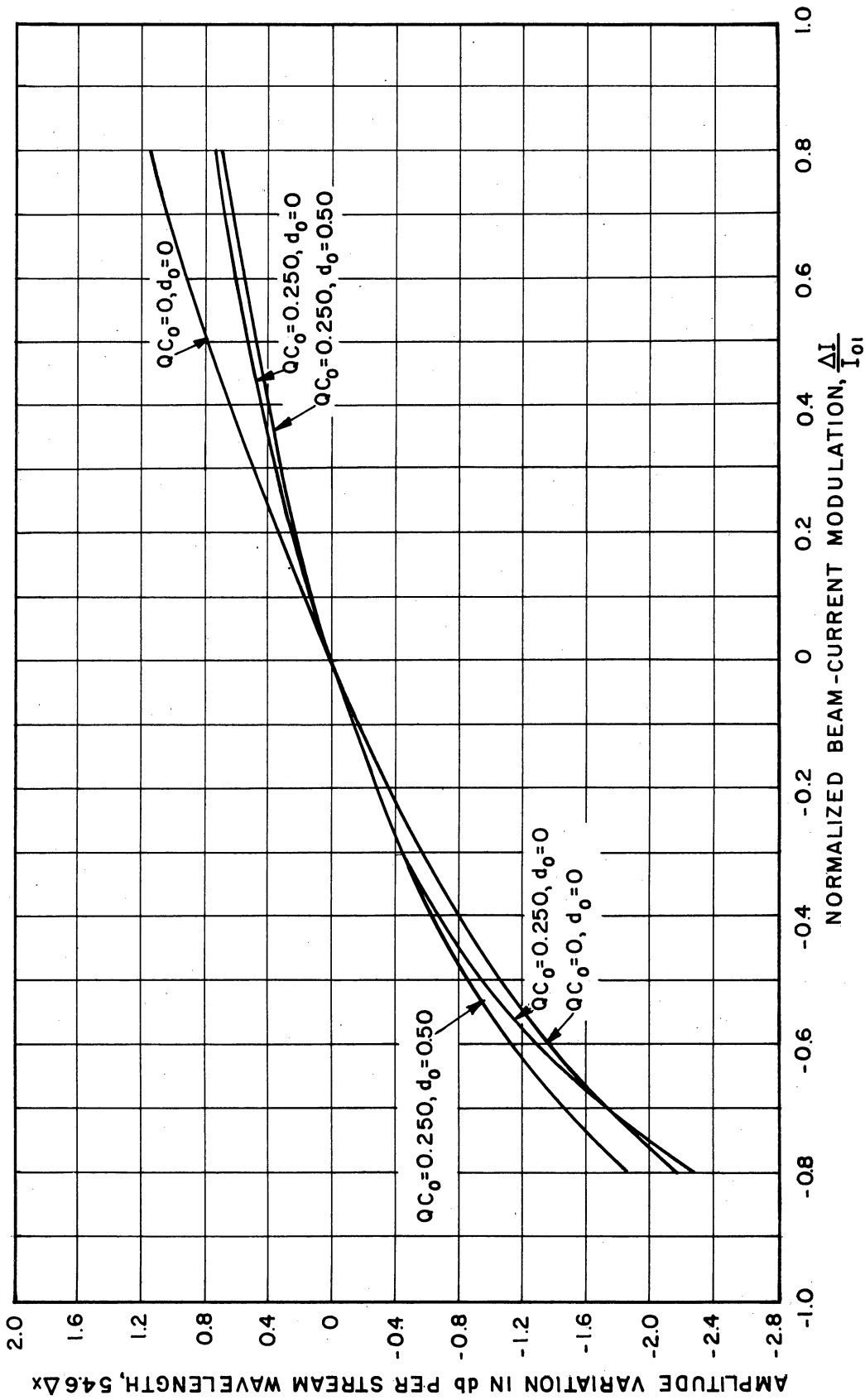


FIG. 3.9 AMPLITUDE VARIATION IN THE MAIN INTERACTION REGION DURING BEAM-CURRENT MODULATION. ( $C_0=0.10, \Delta V=0, b_0$  ADJUSTED FOR MAXIMUM GAIN)

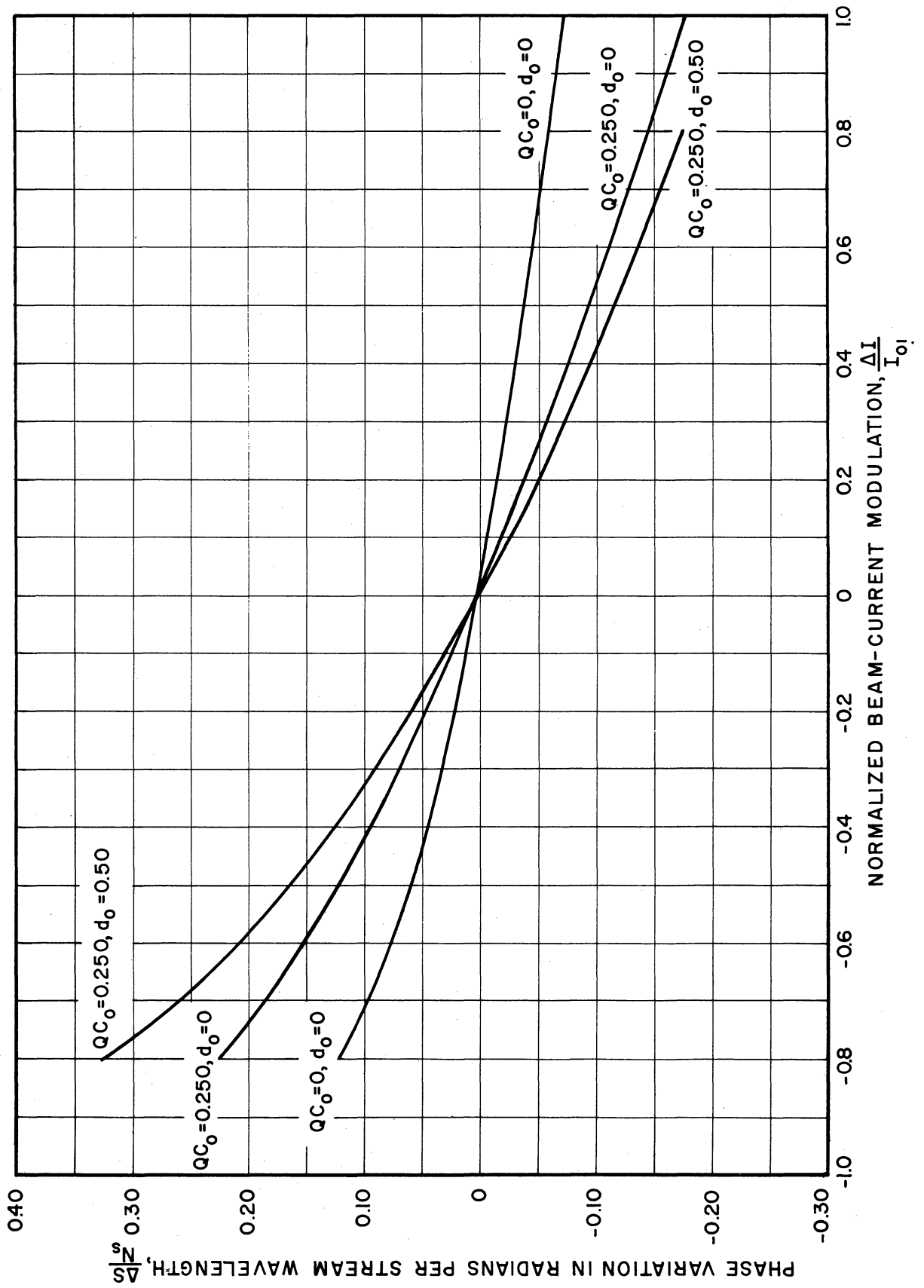


FIG. 3.10 PHASE VARIATION IN THE MAIN INTERACTION REGION DURING BEAM-CURRENT MODULATION. ( $C_0=0.10, \Delta V=0, b_0$  ADJUSTED FOR MAXIMUM GAIN)



the number of stream wavelengths and a component which is independent of the number of stream wavelengths. The components dependent upon the length of the tube have been discussed in Section 3.1.1 and were called the phase modulation and amplitude modulation in the main interaction region. In this section the component independent of circuit length, the initial loss parameter, will be considered. It should be noted that the effect of modulation upon the initial loss parameter does not affect the overall modulation properties of a long tube as much as it would a short tube; also for a given gain, modulation of A becomes more significant for a high-C short tube, since the gain is proportional to  $CN_s$ .

The effect of modulation on the initial loss parameter is determined from the amplitude and phase of the quantity  $A = V_{c1}/V$  as given in Eq. 2.26. Curves of the amplitude and phase modulations are shown in Figs. 3.11 through 3.14. The value of the initial loss parameter with no modulation is  $A_0$ .

The initial loss parameter will vary over a much wider range during a voltage modulation than during a current modulation. Also, the addition of loss and space charge tends to increase the range over which the initial loss will vary. Note that for a  $\pm 20\%$  variation of the beam current, the phase of A will vary  $\pm 1$  radian, while for a  $\pm 80\%$  variation of the beam current, the phase varies only  $+ 0.3$  to  $- 0.5$  radians. Over a similar range of modulations, the amplitude of A can vary between 0 and - 4 db for a voltage variation, while for a current modulation, it will vary between  $+ 0.8$  and  $- 0.6$  db. Hence, a consideration of the modulation of A, during a voltage modulation is more important than during a current modulation. Some insight into the reason for this can be obtained by referring to work published by Brewer and Birdsall<sup>21</sup> in which

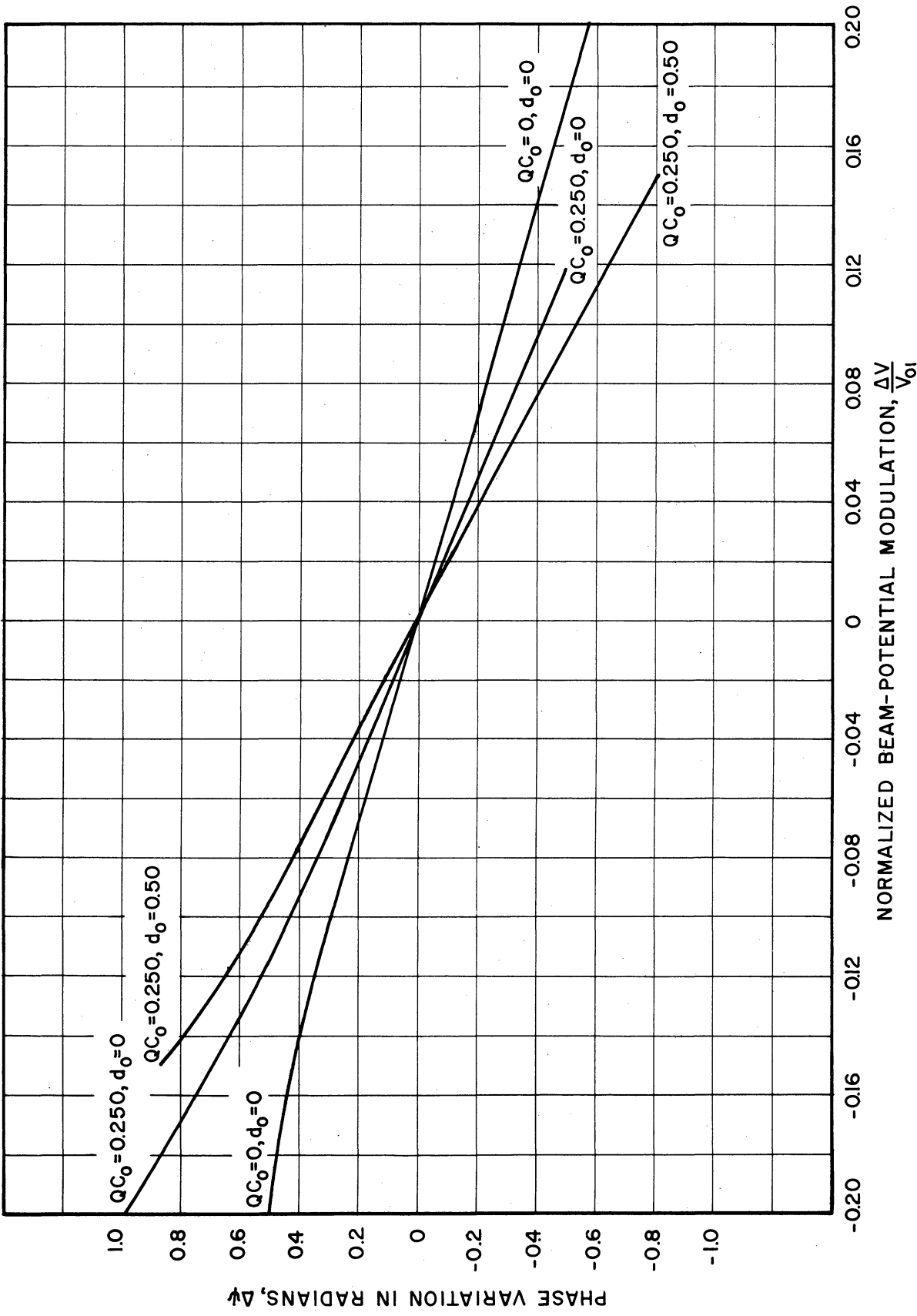


FIG. 3.11 VARIATION OF THE PHASE OF A DURING BEAM-POTENTIAL MODULATION. ( $C_0=0.10, \Delta I=0, b_0$  ADJUSTED FOR MAXIMUM GAIN)

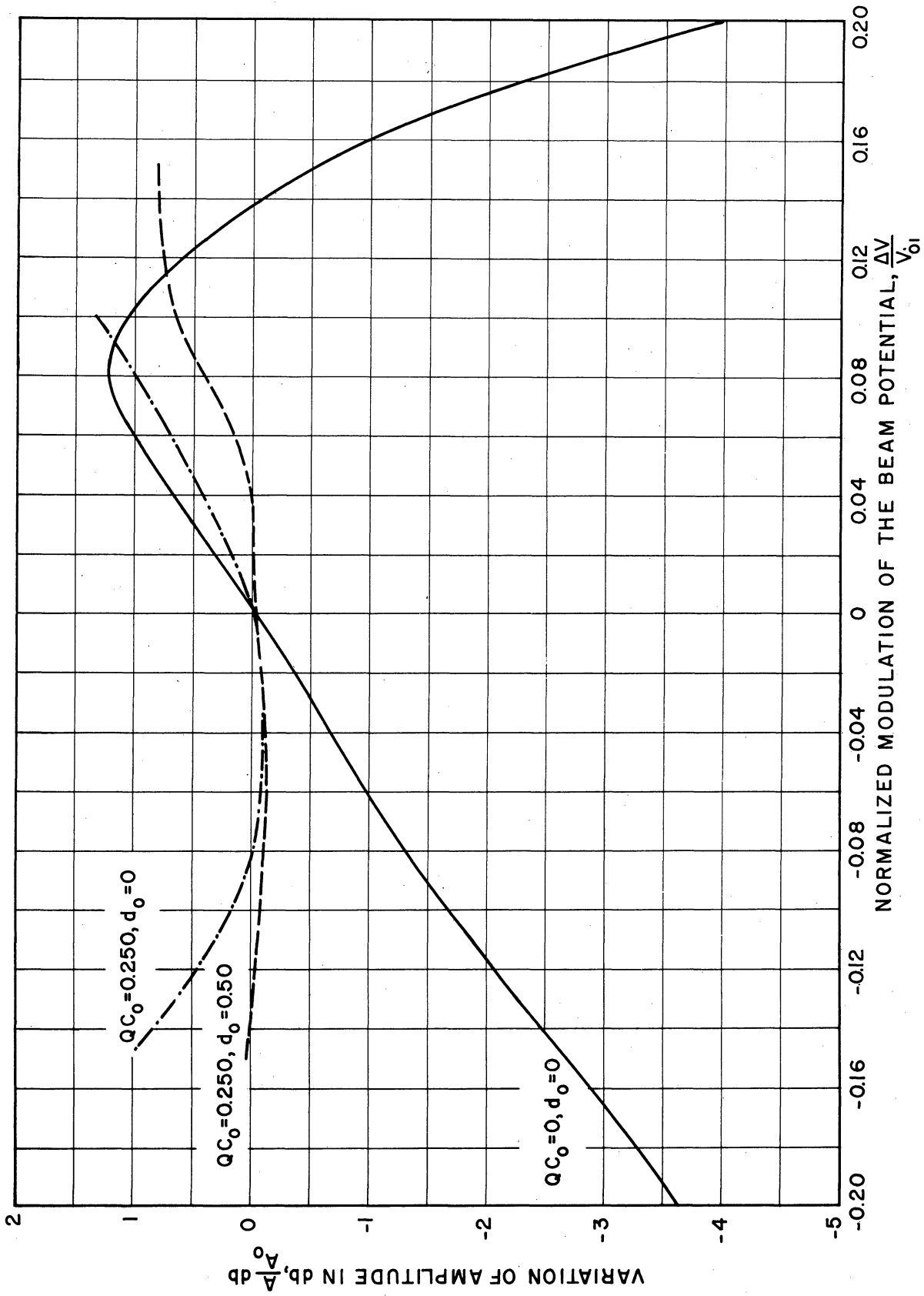


FIG. 3.12 VARIATION OF THE MAGNITUDE OF A DURING BEAM-POTENTIAL MODULATION ( $C_0=0.10, \Delta I=0, b_0$  ADJUSTED FOR MAXIMUM GAIN)

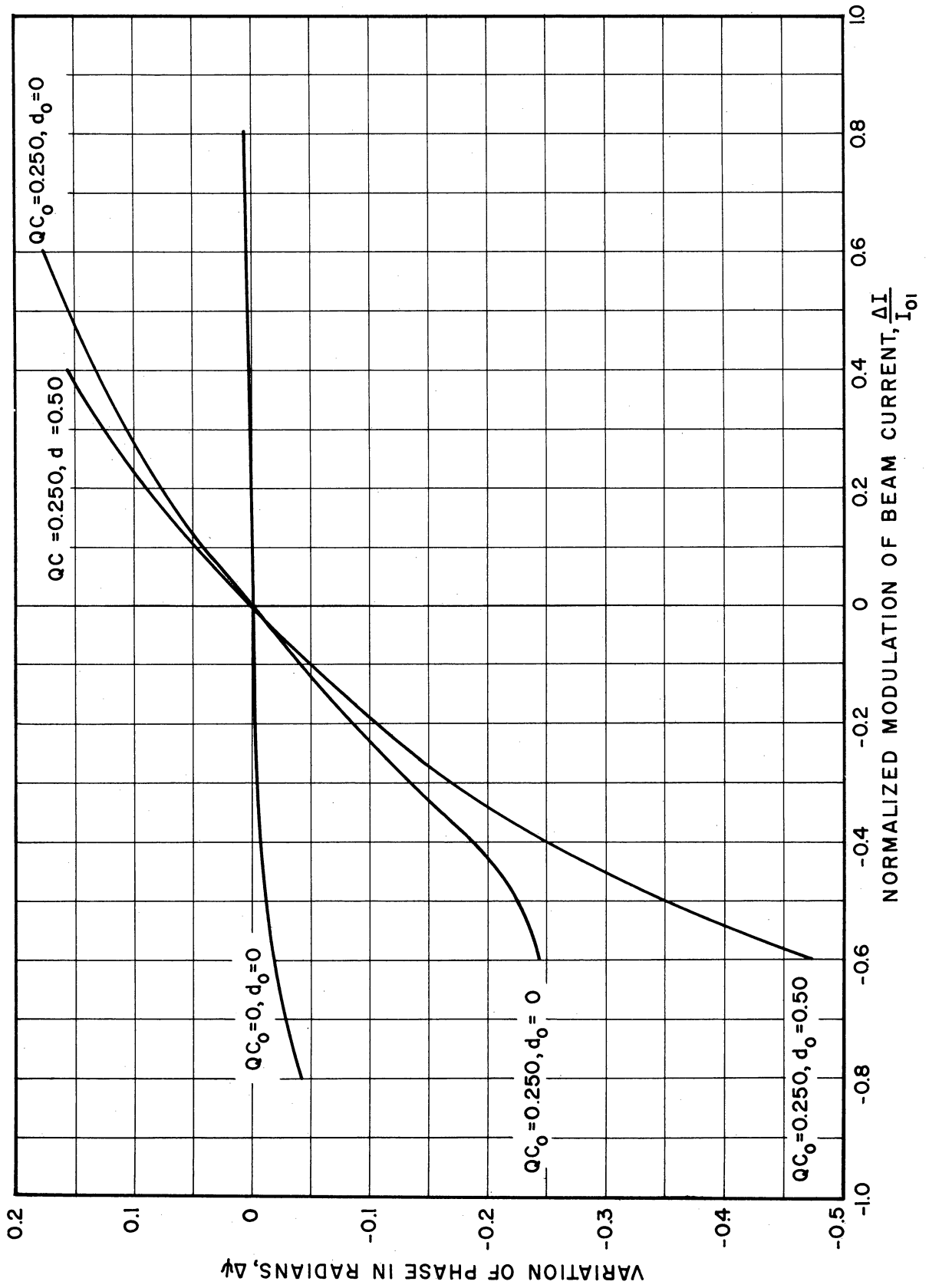


FIG. 3.13 VARIATION OF THE PHASE OF A DURING BEAM-CURRENT MODULATION. ( $C_0=0.10, \Delta V=0, b_0$  ADJUSTED FOR MAXIMUM GAIN)

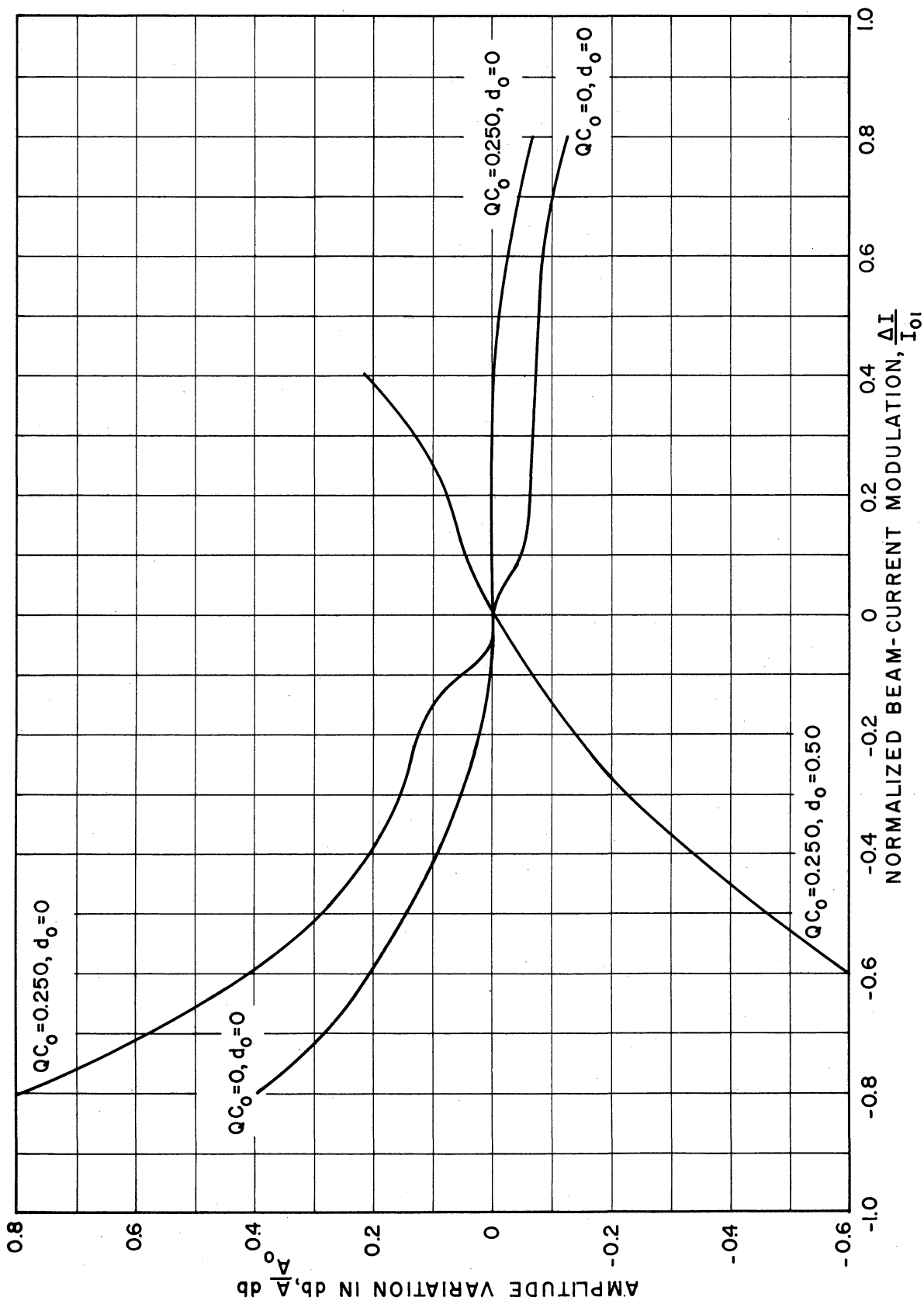


FIG. 3.14 VARIATION OF THE MAGNITUDE OF A DURING BEAM-CURRENT MODULATION. ( $C_0 = 0.10$ ,  $\Delta V = 0, b_0$  ADJUSTED FOR MAXIMUM GAIN)

it can be seen that  $|A|$  varies greatly with  $b$  but does not change very much with the other parameters.

3.1.3 Linear Modulation Device Functions. The linear modulation device functions are calculated from the results of Sections 3.1.1 and 3.1.2. The total phase modulation in radians is given as

$$\Delta S = \Delta\psi + 2\pi C_o N_s [y_1(\Delta V, \Delta I) - y_1(0, 0)] \quad (3.4)$$

and the total amplitude modulation in db is given as

$$\Delta a_{db} = 20 \log_{10} \frac{V_{c1}(\Delta I, \Delta V)}{V_{c1}(0, 0)} + 54.6 C_o N_s [x(\Delta V, \Delta I) - x_1(0, 0)] \quad (3.5)$$

The modulation device functions can be calculated therefore, only if the tube length is specified. Several modulation device functions are shown in Figs. 3.15 through 3.18. Each function is calculated for two stream wavelength values.

From the curves of voltage modulations it can be seen that the phase-modulation index and the amplitude distortion will increase as the tube length is increased. Also, the effect of space charge tends to decrease the phase-modulation index. Loss, however, will increase the phase-modulation index, and also increase the linear range. Space charge tends to accentuate the amplitude variation, while loss might be helpful in smoothing the amplitude variation.

The phase modulation curves show a linear phase response for a voltage modulation of  $\pm 5\%$  for a tube of 20 stream wavelengths. The deviation from a linear phase response is  $9\%$  for a  $10\%$  voltage modulation. Note that the inherent AM during this phase modulation is about 5 db for a  $\pm 5\%$  voltage modulation and about 10 db for a  $\pm 10\%$  voltage modulation.

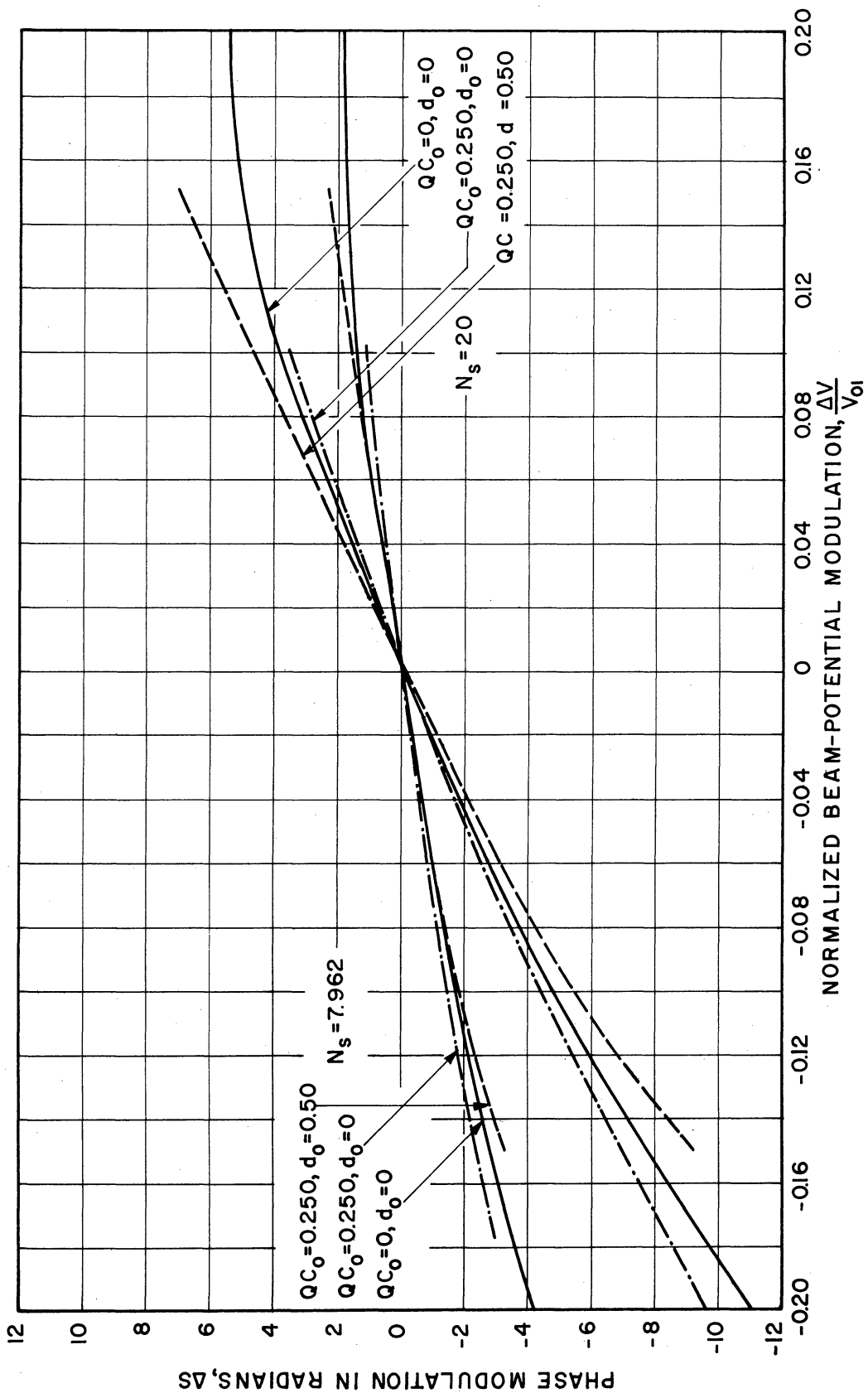


FIG. 3.15 PHASE-MODULATION DEVICE FUNCTIONS FOR BEAM-POTENTIAL MODULATION. ( $C_0=0.10, \Delta I=0, b_0$  ADJUSTED FOR MAXIMUM GAIN)

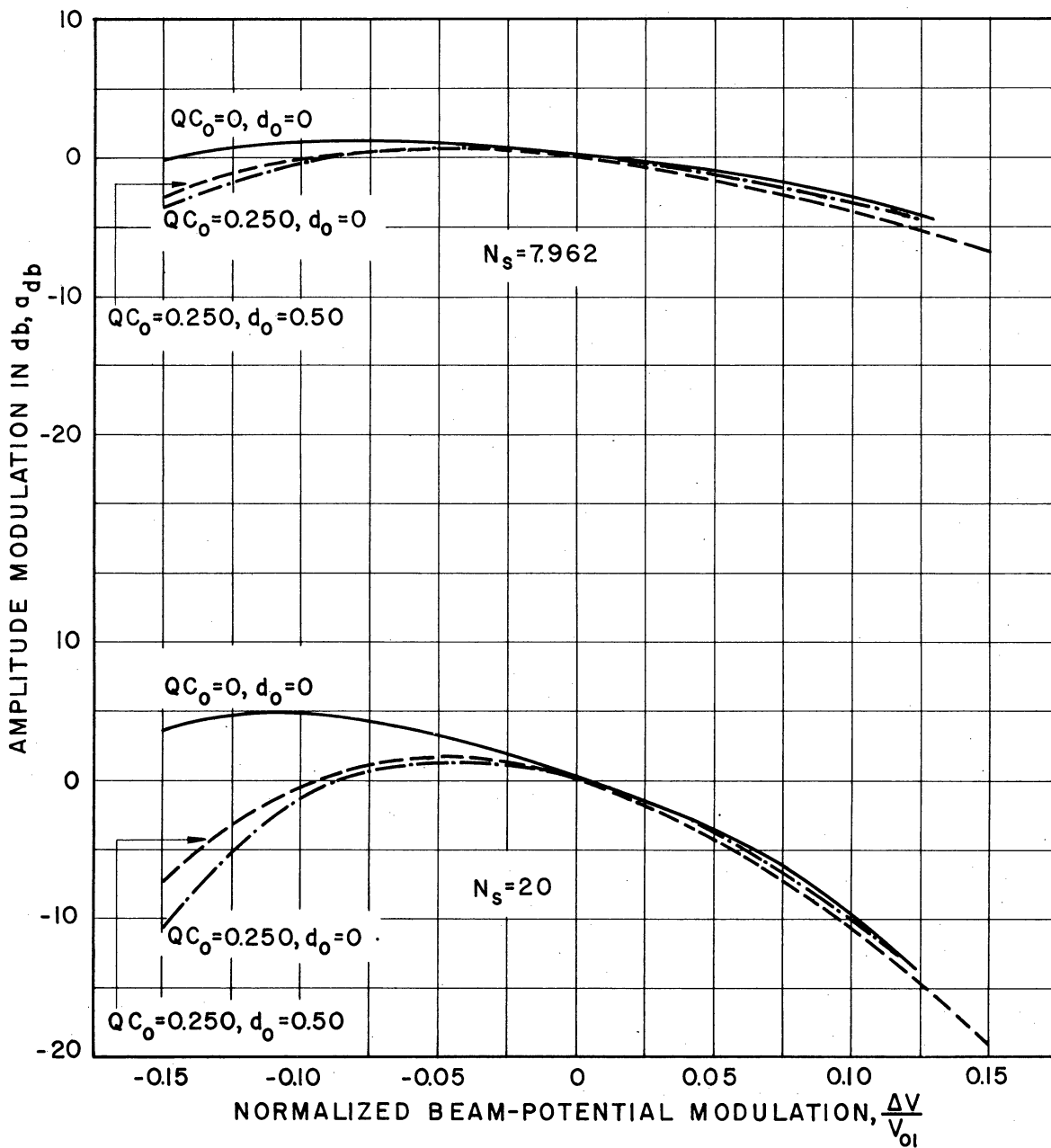


FIG. 3.16 AMPLITUDE-MODULATION DEVICE FUNCTIONS FOR BEAM-POTENTIAL MODULATION. ( $C_0 = 0.10, \Delta I = 0, b_0$  ADJUSTED FOR MAXIMUM GAIN)



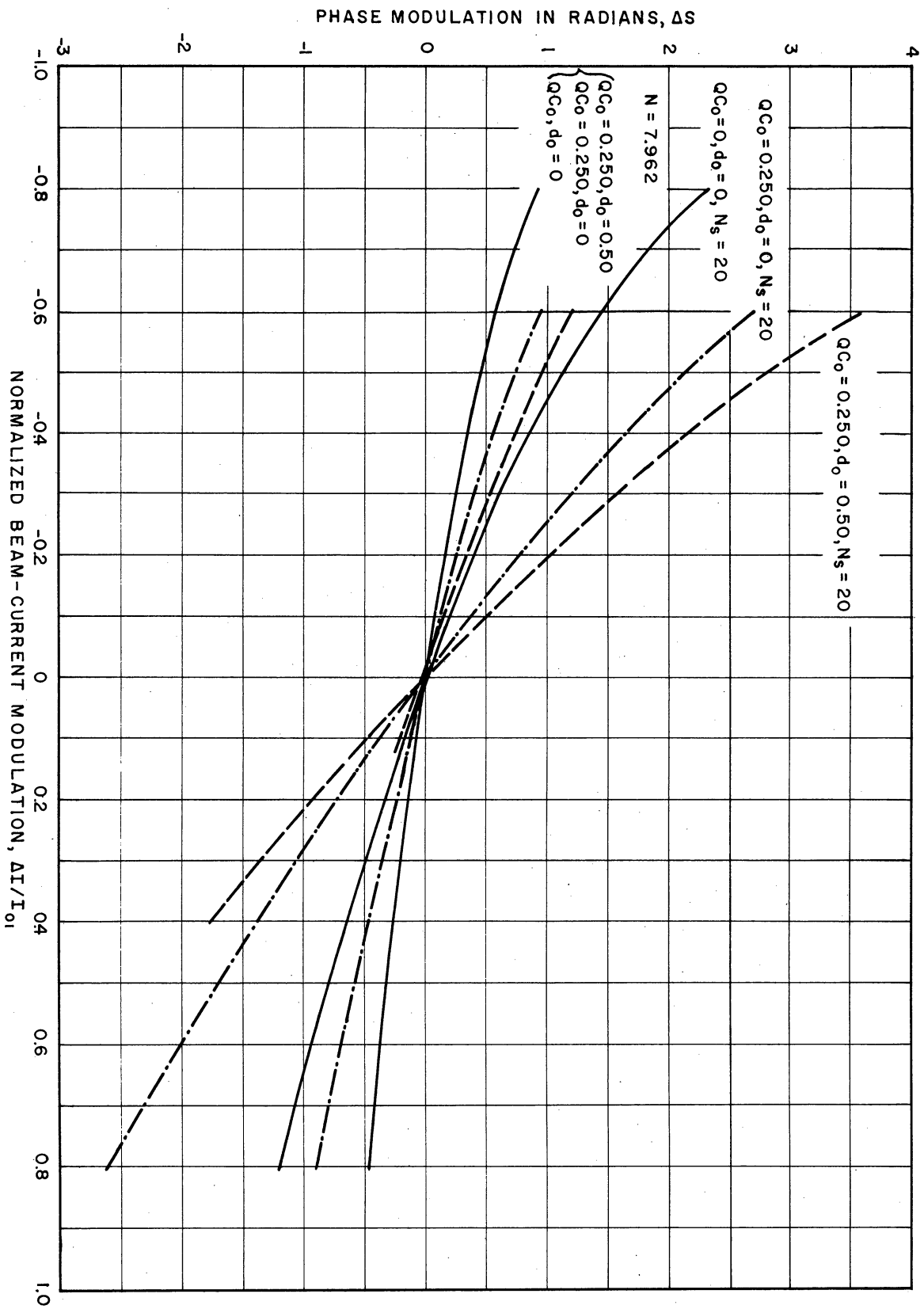


FIG. 3.17 PHASE-MODULATION DEVICE FUNCTIONS FOR BEAM-CURRENT MODULATION ( $C = 0.10, \Delta V = 0, b_0$  ADJUSTED FOR MAXIMUM GAIN)

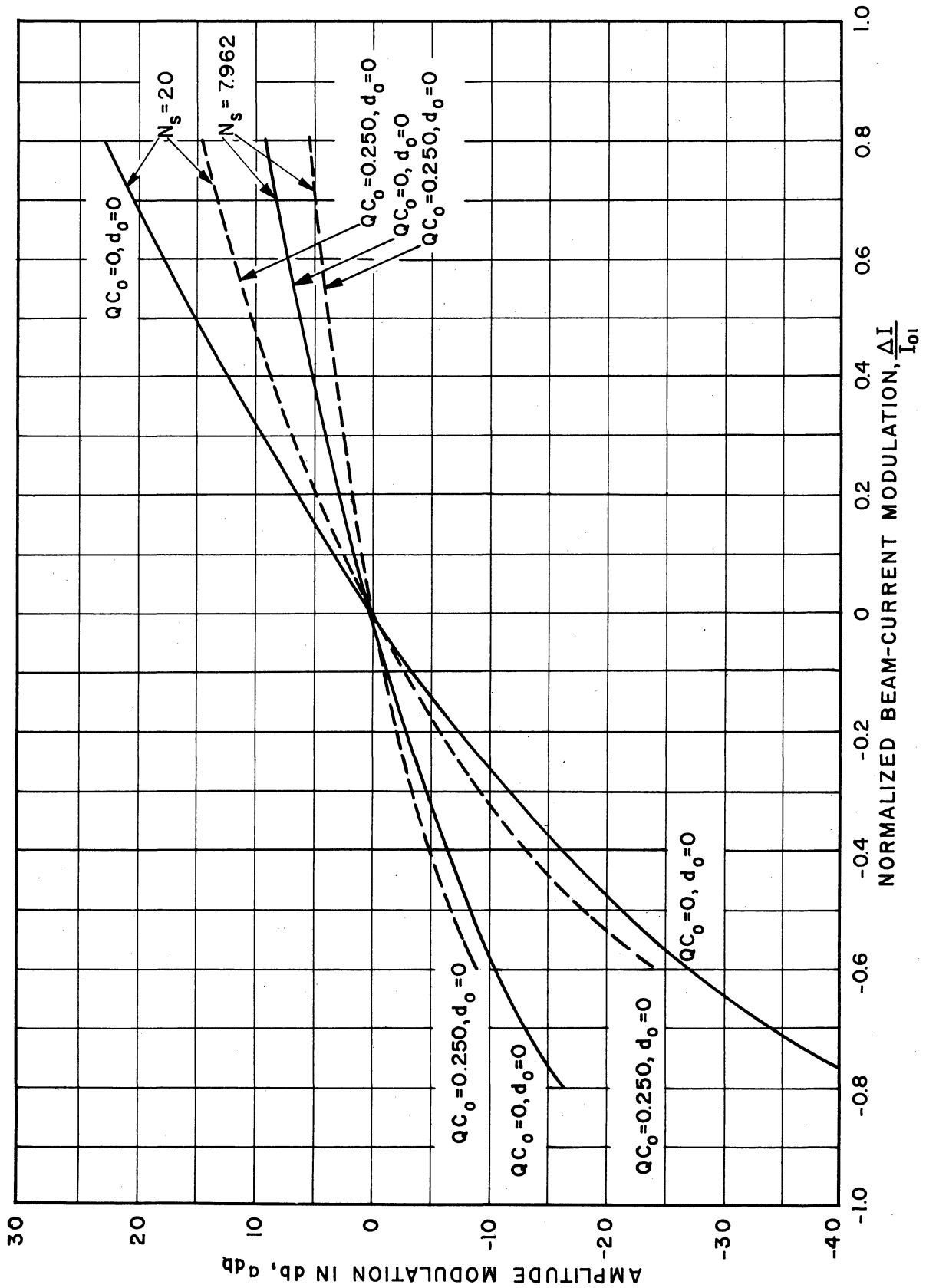


FIG. 3.18 AMPLITUDE-MODULATION DEVICE FUNCTIONS FOR BEAM-CURRENT MODULATION.  
( $C_0 = 0.10, \Delta V = 0, b_0$  ADJUSTED FOR MAXIMUM GAIN)

The current modulation curves indicate a very limited range of linear AM, which becomes a higher than linear variation with large modulating signals. The inherent PM during current modulation is very much smaller than that during voltage modulation. For the same percentage modulation, the PM during voltage modulation is approximately related to the PM during current modulation by

$$\Delta S_{AM} \approx - C \Delta S_{PM} .$$

3.1.4 Taylor Series Approximations to the Device Functions. The form of the second-order Taylor series approximation for the device functions was given in Section 2.3 and the coefficients were evaluated for the simple case of  $QC_0 = d_0 = 0$ . The modulation of the initial loss parameter A was also calculated using the Taylor series method. The results are shown in Figs. 3.19 and 3.20 and are compared with the results using the previous method and those obtained using the nonlinear equations, which will be discussed in Section 3.2. Note that the agreement for the phase modulation is excellent between all three methods, when the initial loss parameter variations are taken into account. The amplitude modulation data shows that agreement between the exact modulation method and the nonlinear calculations is excellent whereas errors of about 0.5 db result with 10% voltage modulation when the Taylor series is used. The tube represented in Figs. 3.19 and 3.20 is a relatively short tube (of about 8 wavelengths). This short tube was used so that the effect of neglecting the variation of A would be emphasized and also to insure that nonlinearities would not affect results. This allowed comparison of the three methods used to analyze the modulated TWA.

It is possible to approximate the phase shift by a rather simple formula for small-modulation amplitudes. For small variations of the

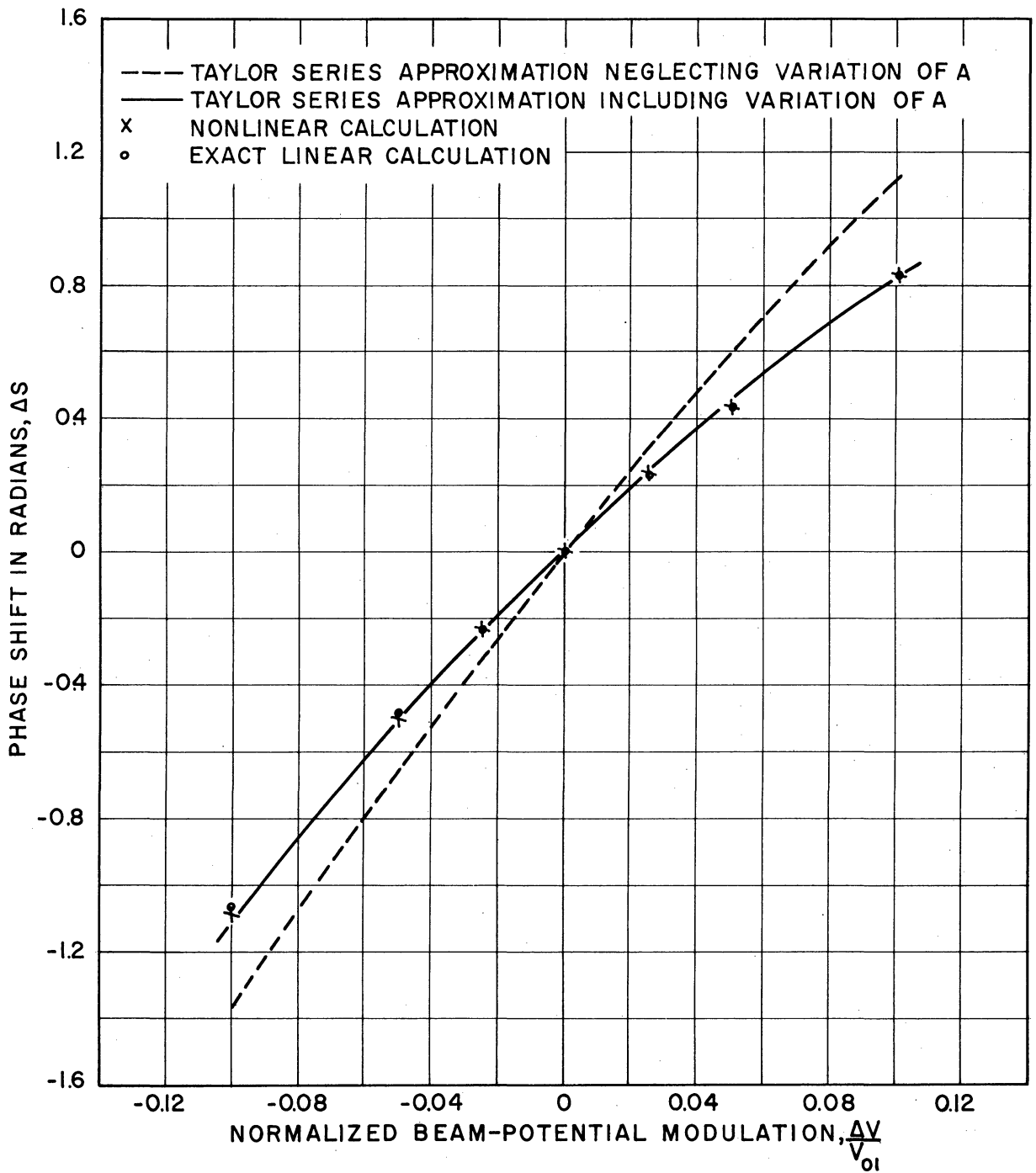


FIG. 3.19 VARIATION OF PHASE DURING BEAM-POTENTIAL MODULATION. ( $C_0=0.10$ ,  $QC_0=0$ ,  $d_0=0$ ,  $b_0=0.1525$ ,  $\Delta I=0$ ,  $\gamma=3.4$ )

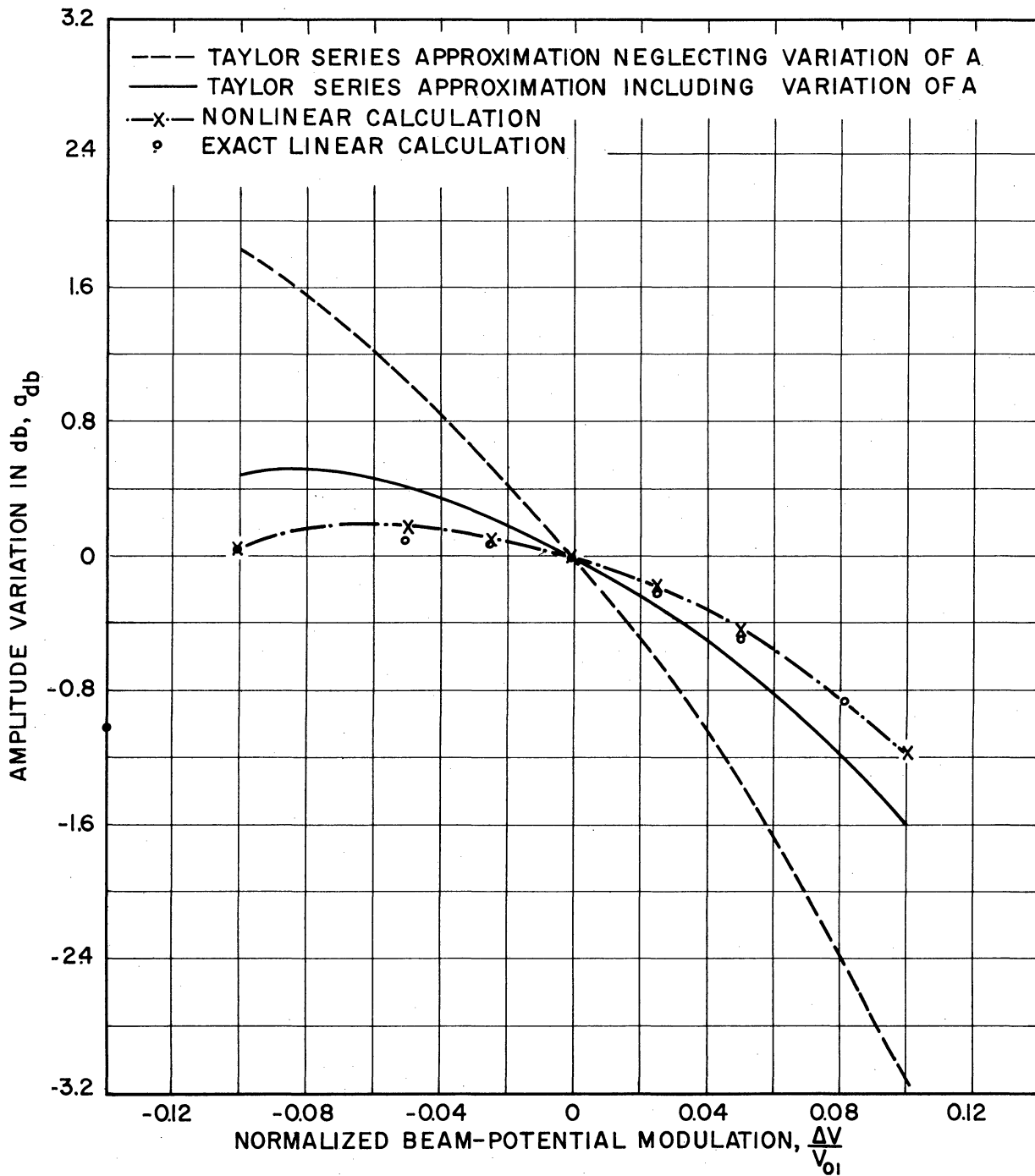


FIG. 3.20 VARIATION OF AMPLITUDE DURING BEAM-POTENTIAL MODULATION. ( $C_0=0.10, QC_0=0, d_0=0, b_0=0.1525, \Delta I=0, y=3.4$ )

beam potential and current, the phase shift is approximately a linear function of the modulation. If the tube is sufficiently long to enable the modulation of A to be neglected, the phase shift is given as

$$\frac{\Delta S}{2\pi N_s} \approx - \left[ \frac{1}{3} + 0.0407 b_o - \frac{2}{9} QC_o - C_o \left\{ 0.833y_{10} + 0.278 b_o - 0.0928 b_o^2 - 1.127 b_o d_o - \frac{5}{9} QC_o \right\} \right] \frac{\Delta V}{V_{o1}} \quad (3.6)$$

and

$$\frac{\Delta S}{2\pi N_s} \approx C_o \left[ \frac{y_{10}}{3} - \frac{2}{9} QC_o - 0.0369 d_o - \frac{8}{9} C_o QC_o + 0.0369 b_o^2 - 0.064 b_o d_o \right] \frac{\Delta I}{I_{o1}} \quad (3.7)$$

Equation 3.6 can be compared to the approximation for the linearized phase shift as a function of beam potential as determined by Beam and Blattner<sup>11</sup> using a curve fitting technique to approximate Pierce's curves. Their result using the above symbols\* is

$$\frac{\Delta S}{2\pi N_g} = \left[ 0.29 - \frac{C_o y_o}{2} - 0.035 (1 + C_o b_o) QC_o - 0.21 b_o C_o \right] \frac{\Delta V}{V_{o1}} \quad (3.8)$$

The phase shift as computed by Eqs. 3.6 and 3.8 are compared in Fig. 3.21. The figure demonstrates the closer agreement with the exact value obtained by using Eq. 3.6 rather than 3.8.

The fact that the phase shift can be fairly well predicted using the linear Eq. 3.6 will be useful later on in providing information for use in TWA modulator design. Unfortunately, the amplitude modulation

---

\* In their report Beam and Blattner define the shift in phase as the negative of the phase angle used in this dissertation.

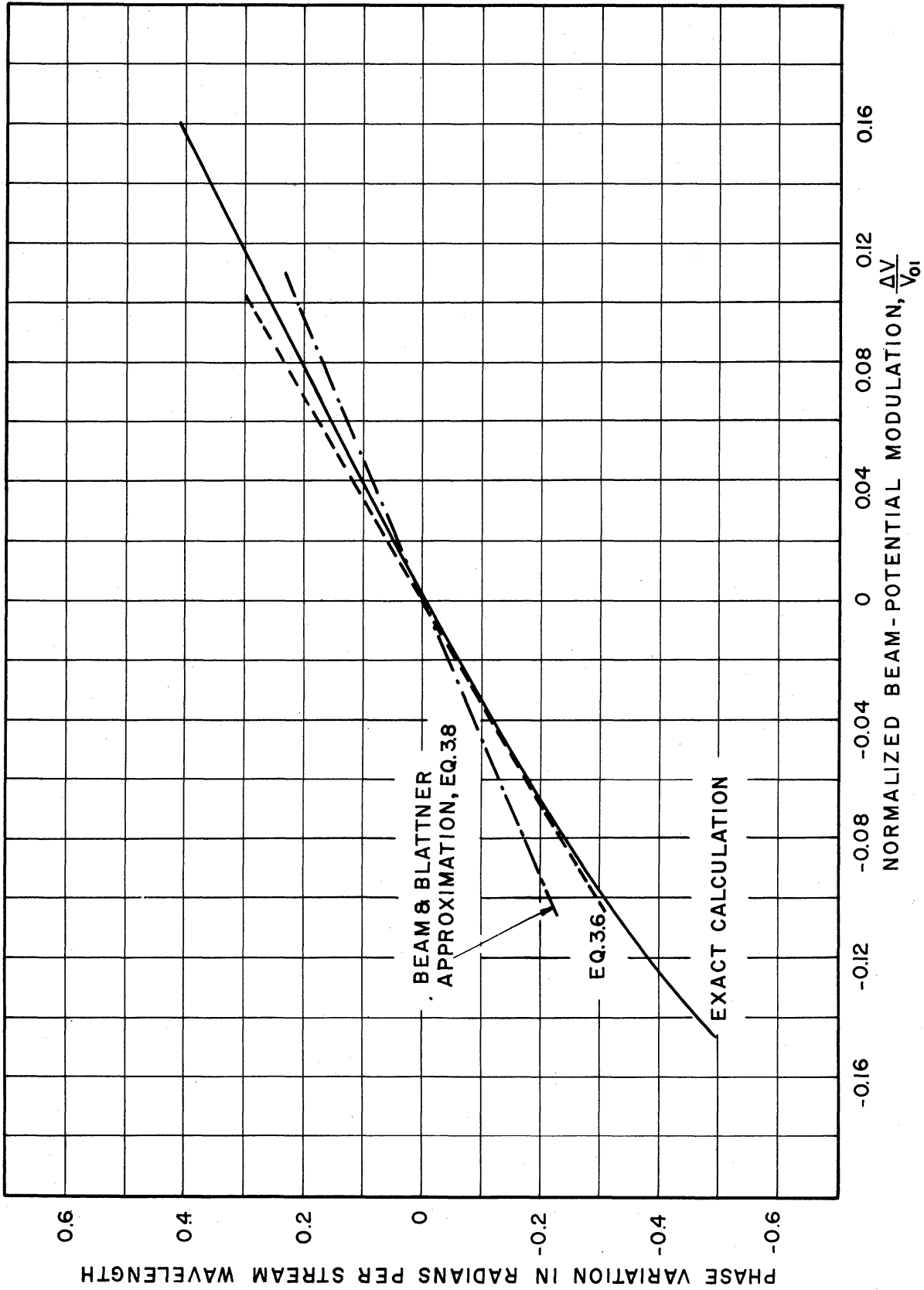


FIG. 3.21 COMPARISON OF PHASE VARIATIONS DURING BEAM-POTENTIAL MODULATION.  
( $C_0=0.10, Q C_0=0.250, b_0=1.0, d_0=0.50, \Delta I=0$ )

cannot be given in a simple form. The equation would have to be second order and would involve many more terms than the phase shift approximation.

### 3.2 Results for the Modulation Device Functions for the Large-Signal Amplifier

The equations for obtaining the large-signal TWA modulation device functions were given in Section 2.4. These equations were solved on an IBM-704 digital computer for several values of the parameters. The technique of solving the large-signal TWA equations on a digital computer has previously been discussed by Rowe<sup>17</sup>. Several device functions for the large-signal tubes are shown in Figs. 3.22 through 3.29. As pointed out in the previous section, the curves agree well with the linear calculations for short lengths where the tube is still operating linearly. A very interesting result is that as saturation is approached it appears that the phase modulation during a voltage modulation becomes more nearly linear than for the unsaturated tube. Working near saturation will tend to limit the inherent AM. Note that as saturation is approached, the modulation voltage at which maximum gain occurs shifts to higher values. This is in line with theoretical predictions by Rowe<sup>4</sup> and measurements by Caldwell<sup>37</sup>.

The AM characteristics during a current modulation were only carried out for relatively small-modulation levels. These characteristics show that a range of linear amplitude modulation is possible. However, near saturation, there is little change in amplitude as one might expect.

The foregoing data indicates that it is feasible, from a theoretical point of view to operate a voltage-modulated tube near saturation



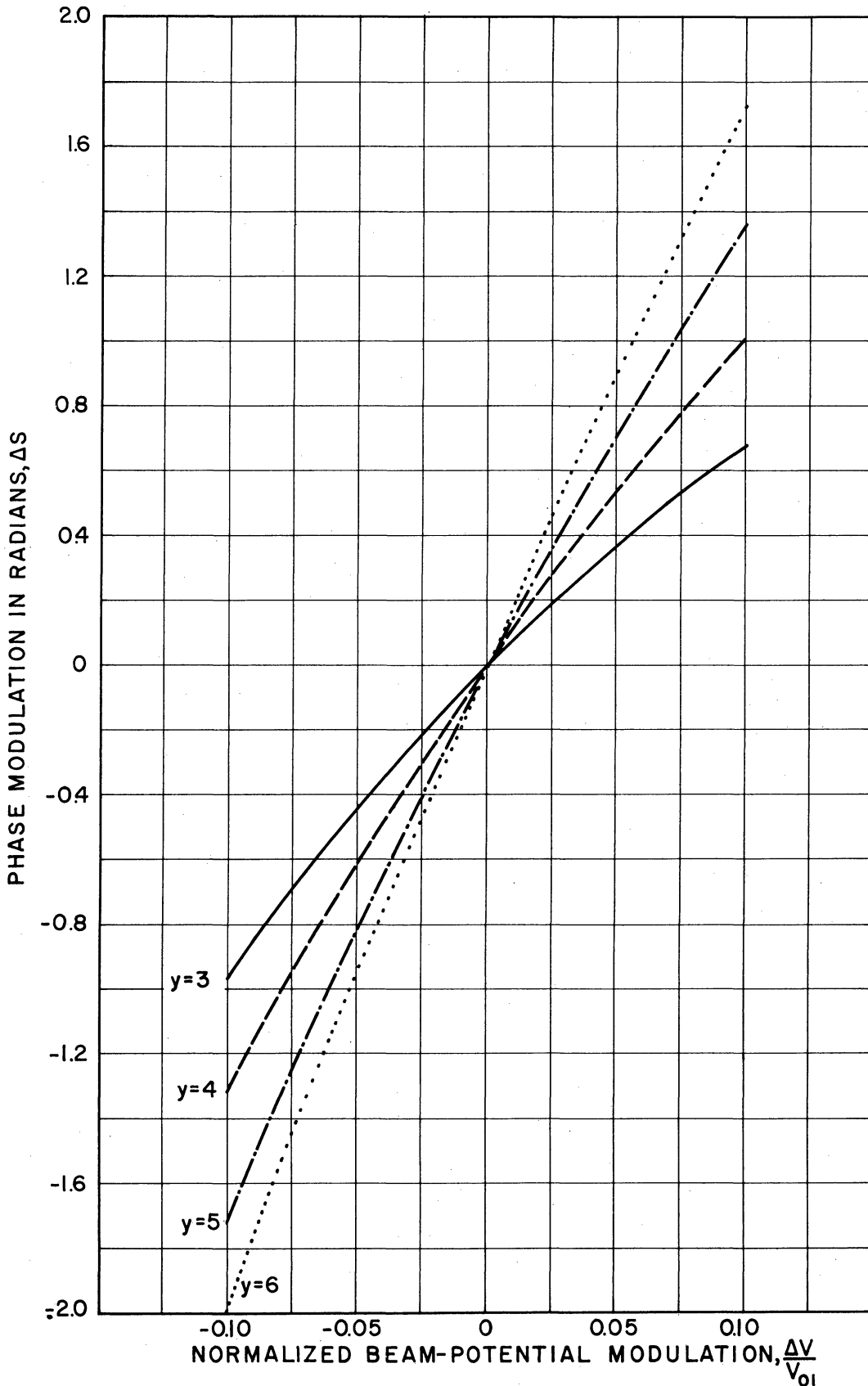


FIG. 3.22 PHASE-MODULATION DEVICE FUNCTIONS DURING BEAM-POTENTIAL MODULATION, LARGE-SIGNAL CALCULATION. ( $C_0=0.10$ ,  $QC_0=0$ ,  $d_0=0$ ,  $b_0=0.1525$ ,  $\Delta I=0$ )

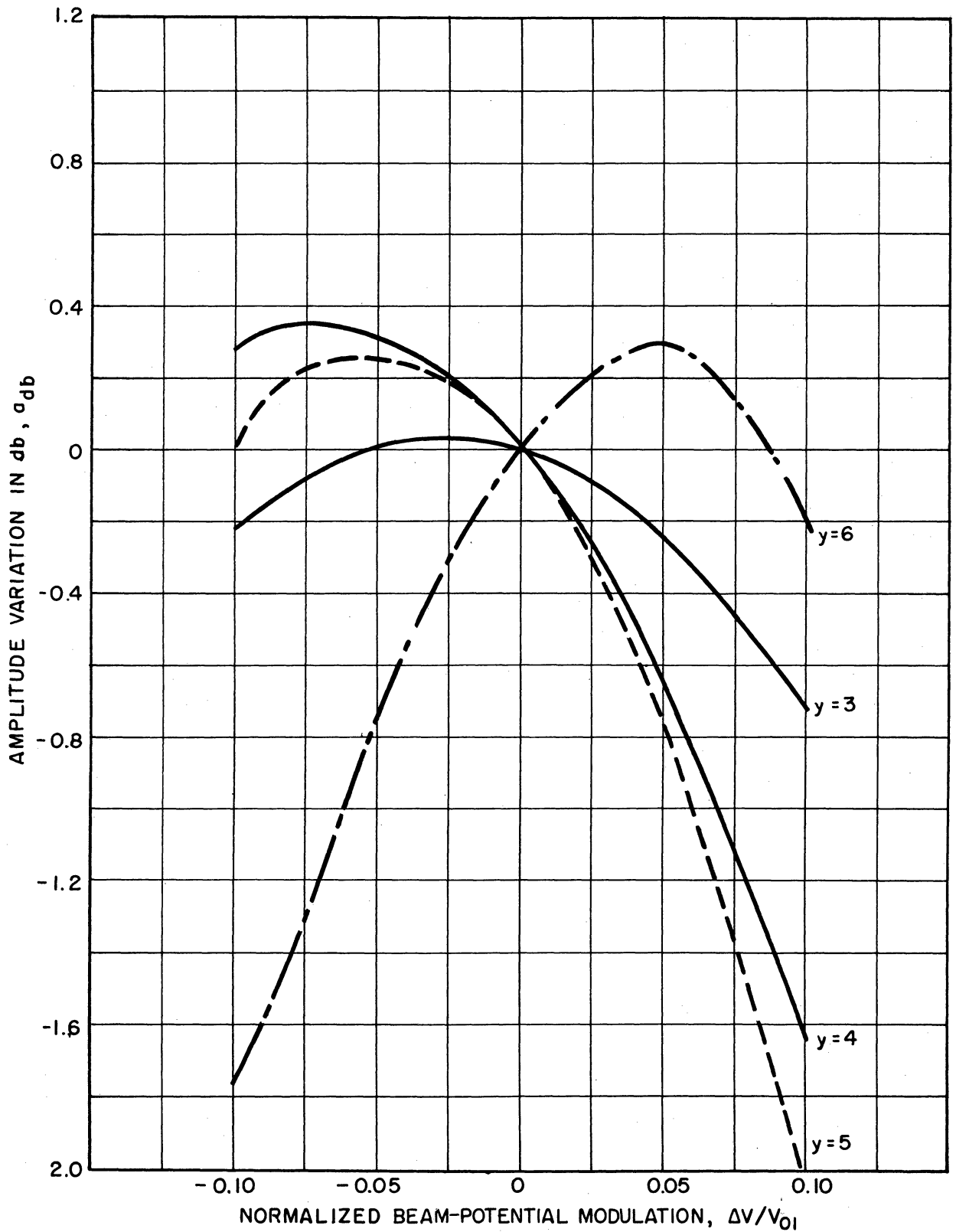


FIG. 3.23 AMPLITUDE-MODULATION DEVICE FUNCTION DURING BEAM-POTENTIAL MODULATION, LARGE-SIGNAL CALCULATION. ( $C_0=0.10$ ,  $QC_0=0$ ,  $d_0=0$ ,  $b_0=0.1525$ ,  $\Delta I=0$ )

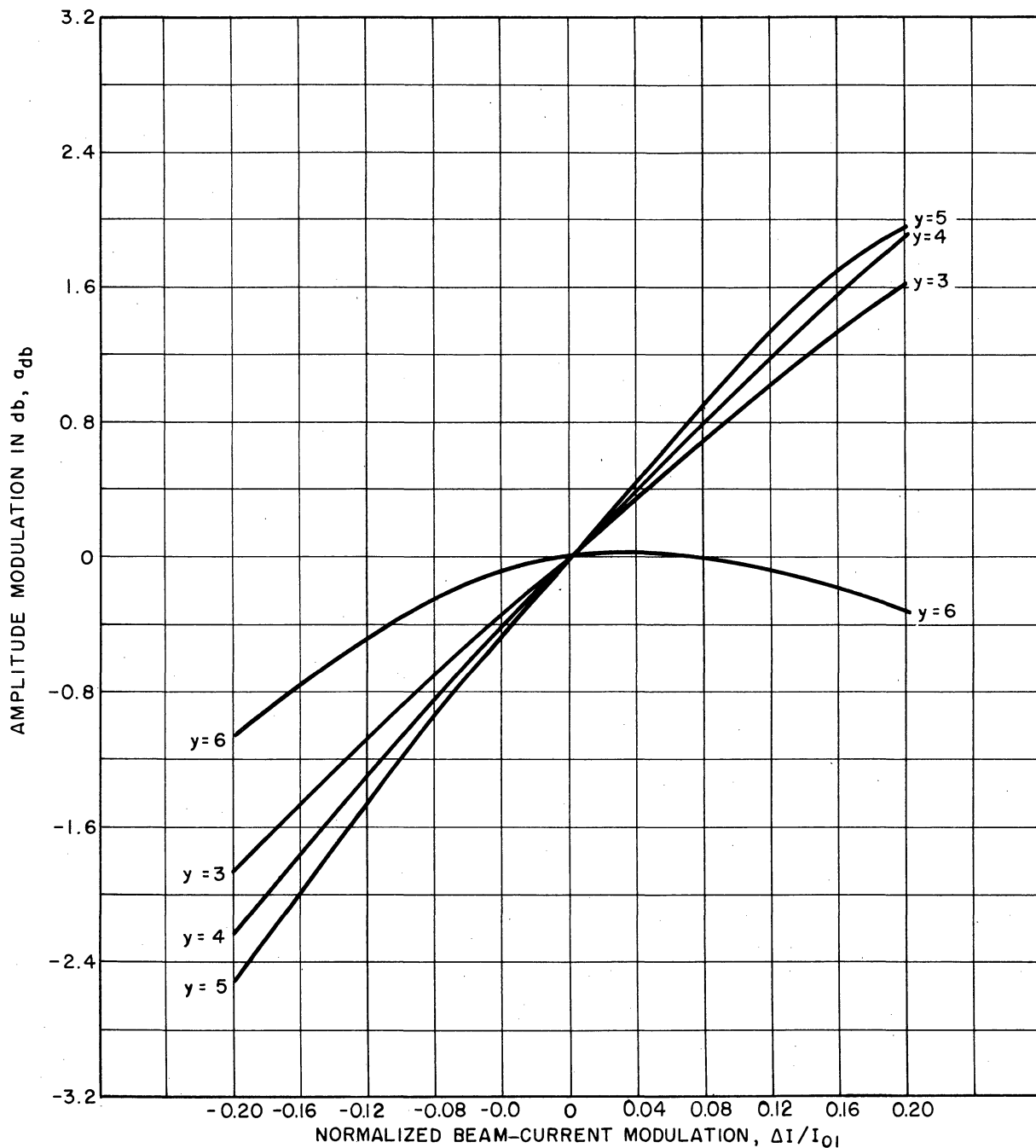


FIG. 3.24 AMPLITUDE-MODULATION DEVICE FUNCTION DURING BEAM-CURRENT MODULATION, LARGE-SIGNAL CALCULATION. ( $C_0=0.10$ ,  $QC_0=0$ ,  $d_0=0$ ,  $b_0=0.1525$ ,  $\Delta V=0$ )

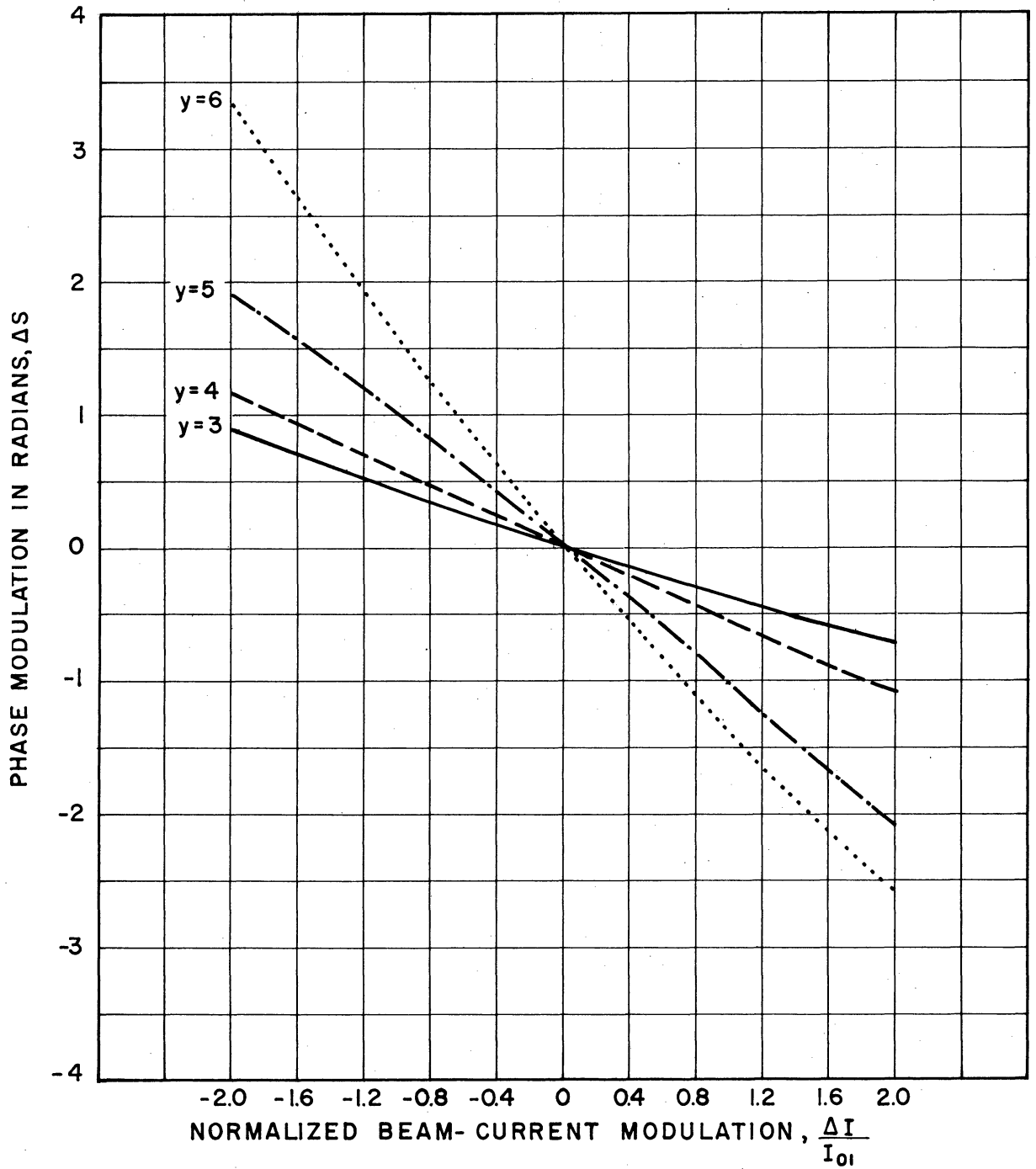


FIG. 3.25 PHASE-MODULATION DEVICE FUNCTION DURING BEAM-CURRENT MODULATION, LARGE-SIGNAL CALCULATION. ( $C_0=0.10, QC_0=0, d_0=0, b_0=0.1525, \Delta V=0$ )

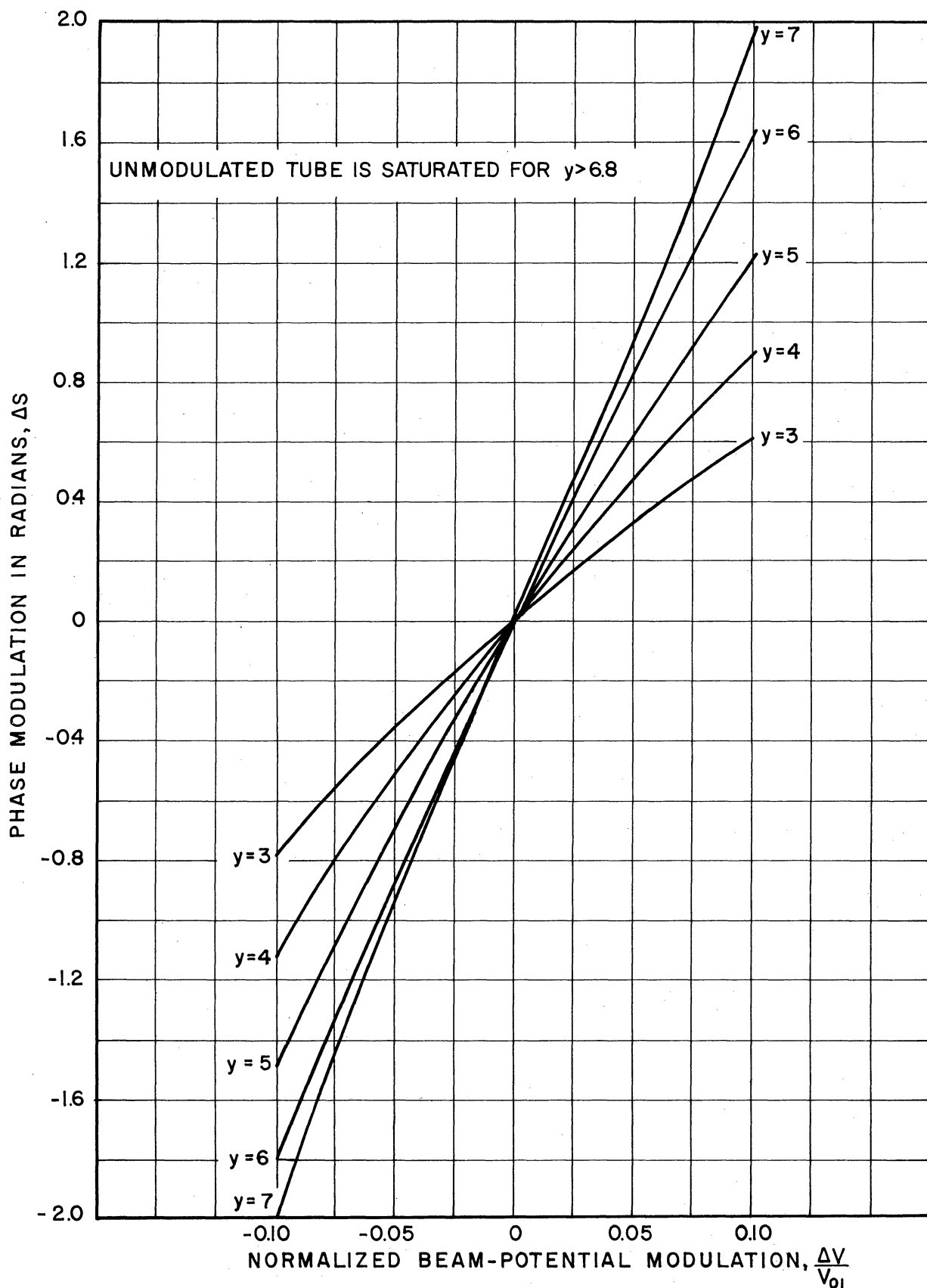


FIG. 3.26 PHASE-MODULATION DEVICE FUNCTION DURING BEAM-POTENTIAL MODULATION, LARGE-SIGNAL CALCULATION, ( $C_0=0.10, QC_0=0.125, d_0=0, b_0=0.65, B=1.0, \frac{a_1}{b}=2.0$ )

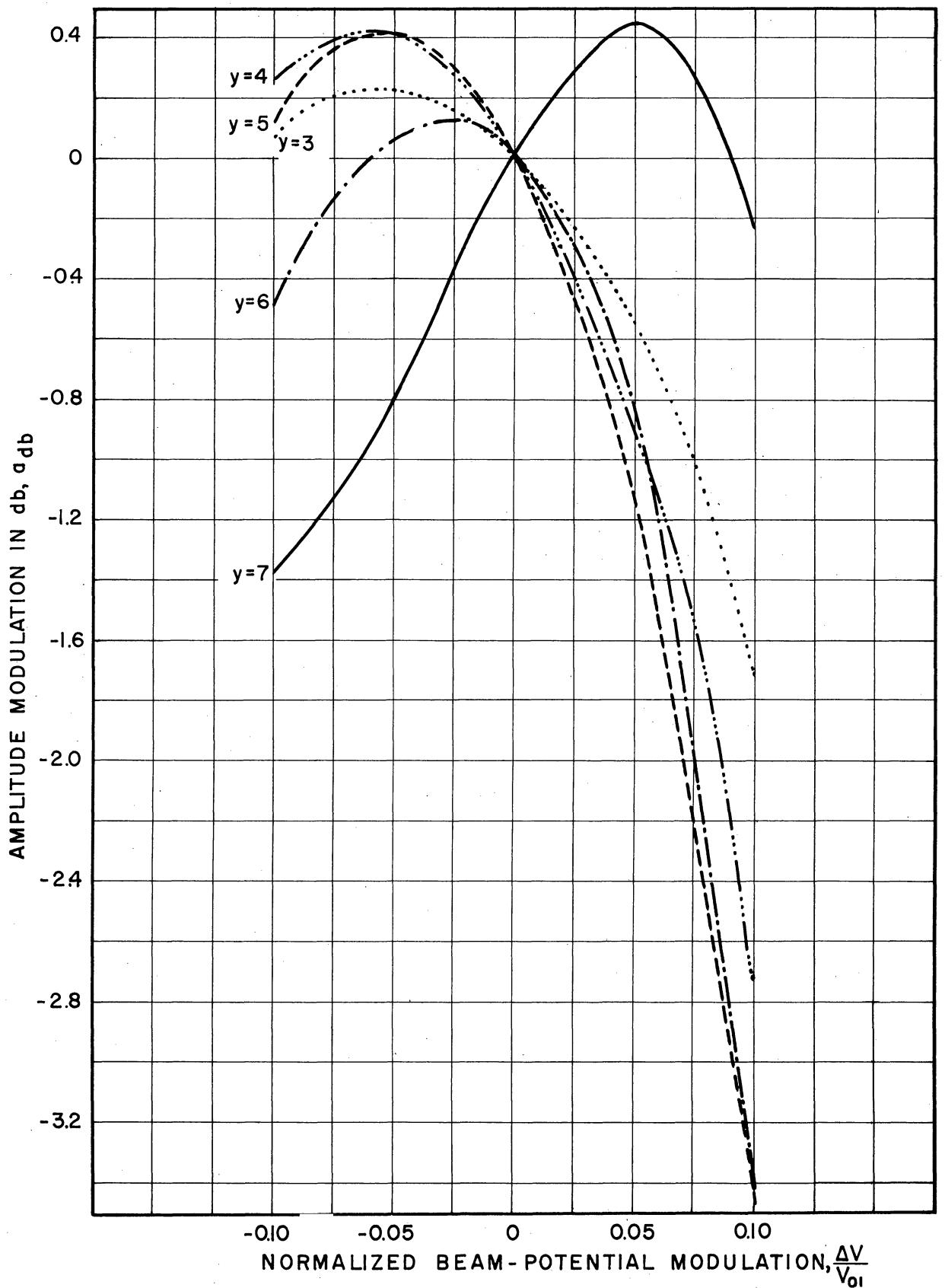


FIG. 3.27 AMPLITUDE-MODULATION DEVICE FUNCTION DURING BEAM-POTENTIAL MODULATION, LARGE-SIGNAL CALCULATION. ( $C_0=0.10$ ,  $QC_0=0.125$ ,  $d_0=0$ ,  $b_0=0.65$ ,  $B=1.0$ ,  $\frac{a_1}{b_1}=2.0$ )

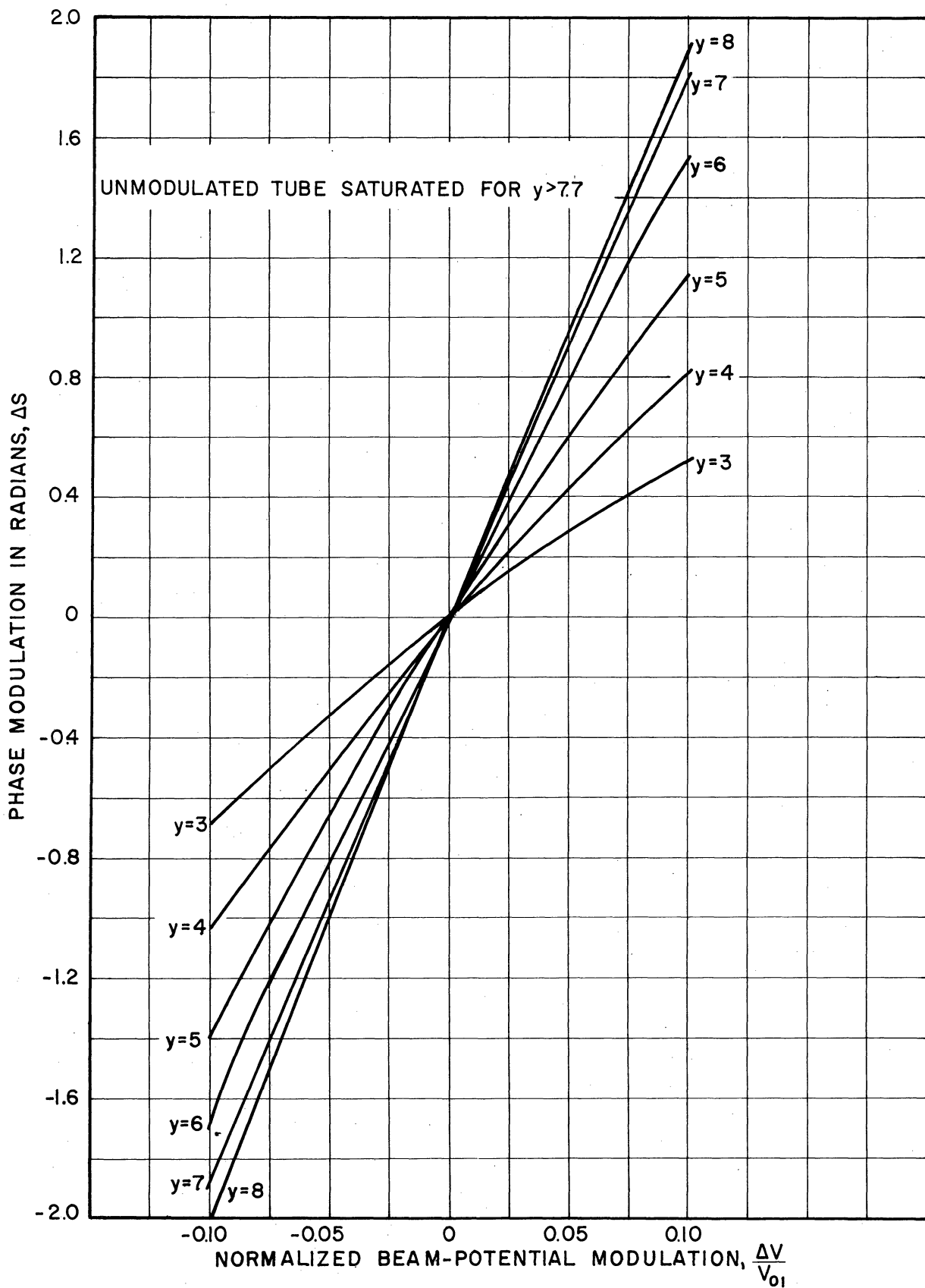


FIG. 3.28 PHASE-MODULATION DEVICE FUNCTION DURING BEAM-POTENTIAL MODULATION, LARGE-SIGNAL CALCULATION. ( $C_0=0.10$ ,  $QC_0=0.250$ ,  $d_0=0$ ,  $b_0=1.0$ ,  $B=1.0$ ,  $\frac{a'}{b}=2.0$ )

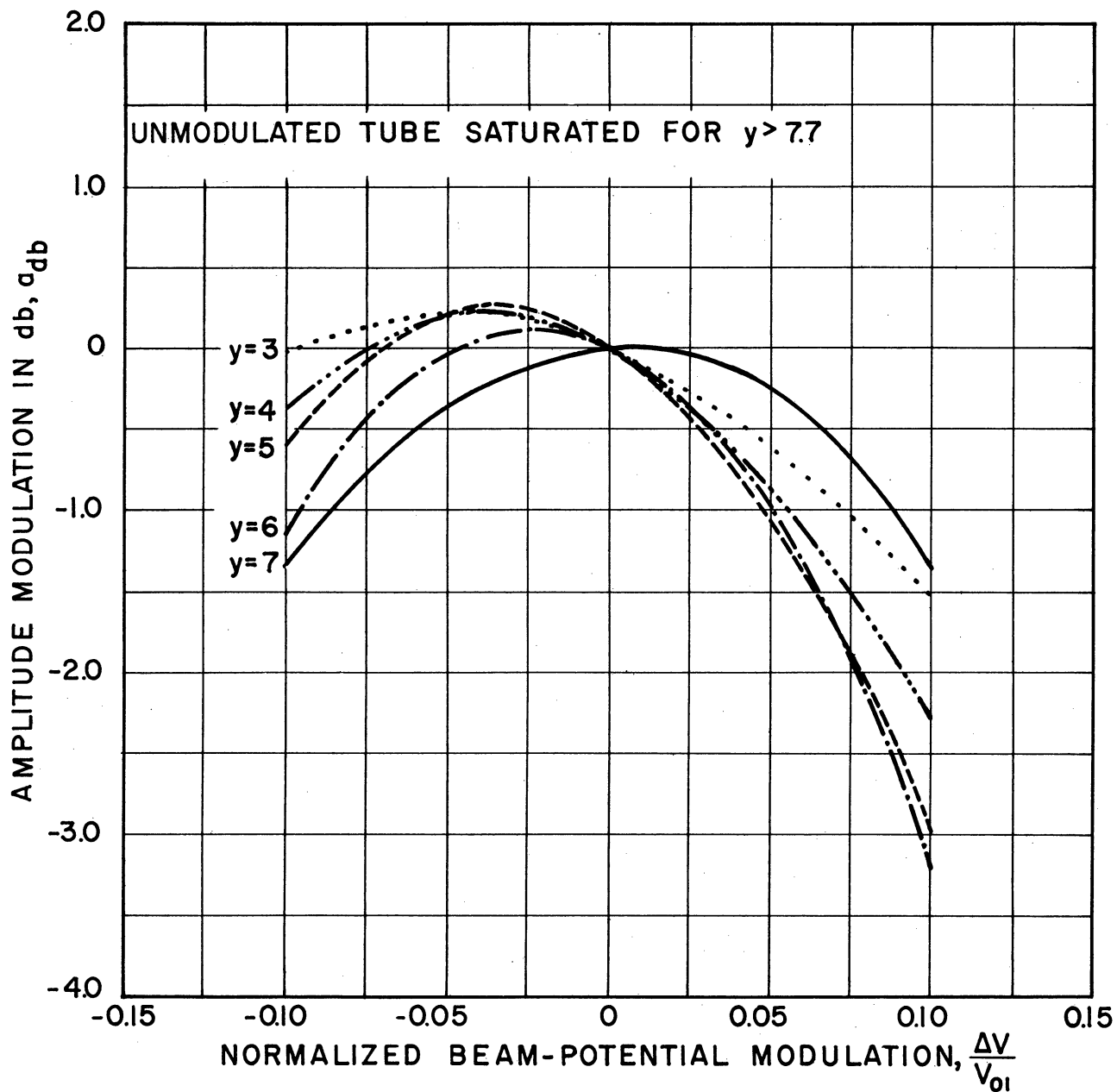


FIG. 3.29 AMPLITUDE-MODULATION DEVICE FUNCTION DURING BEAM-POTENTIAL MODULATION, LARGE-SIGNAL CALCULATION. ( $C_0=0.10, QC_0=0.250, d_0=0, b_0=1.0, B=1.0, \frac{a^1}{b^1}=2.0$ )



and still obtain a satisfactory operation as a phase modulator, while at the same time minimizing the inherent AM.

### 3.3 Experimental Modulation Device Functions

3.3.1 Measurement Technique. The modulation device functions are determined experimentally by measuring the phase and amplitude modulation as a function of modulation signals. The circuit used is shown in Fig. 3.30. The gain measurements and resultant amplitude modulations are found by using a power bridge. The phase shift is determined by first adjusting the probe in the slotted line for a null indication of the voltage standing wave ratio meter at the unmodulated operation, then at each stationary modulation amplitude, readjusting the probe to a new minimum. The phase shift from the unmodulated value is then given by

$$\Delta\theta = 2\beta\Delta z , \quad (3.9)$$

where

$\Delta\theta$  = phase shift in radians

$\beta$  = propagation in slotted line, and

$\Delta z$  = distance between minima.

3.3.2 Results. Measurements were made on a Hewlett-Packard 490-B TWA. This particular tube is a low level S-band model with a maximum output of 10 milliwatts. The device functions were measured at several different frequencies across the S-band.

The phase and amplitude modulation device functions for a beam-voltage modulated small-signal or linear type of operation are shown in Figs. 3.31 and 3.32 and for the saturated case in Figs. 3.33 and 3.34. It is found that an input level of 0 dbm drove the tube well into the saturation region.

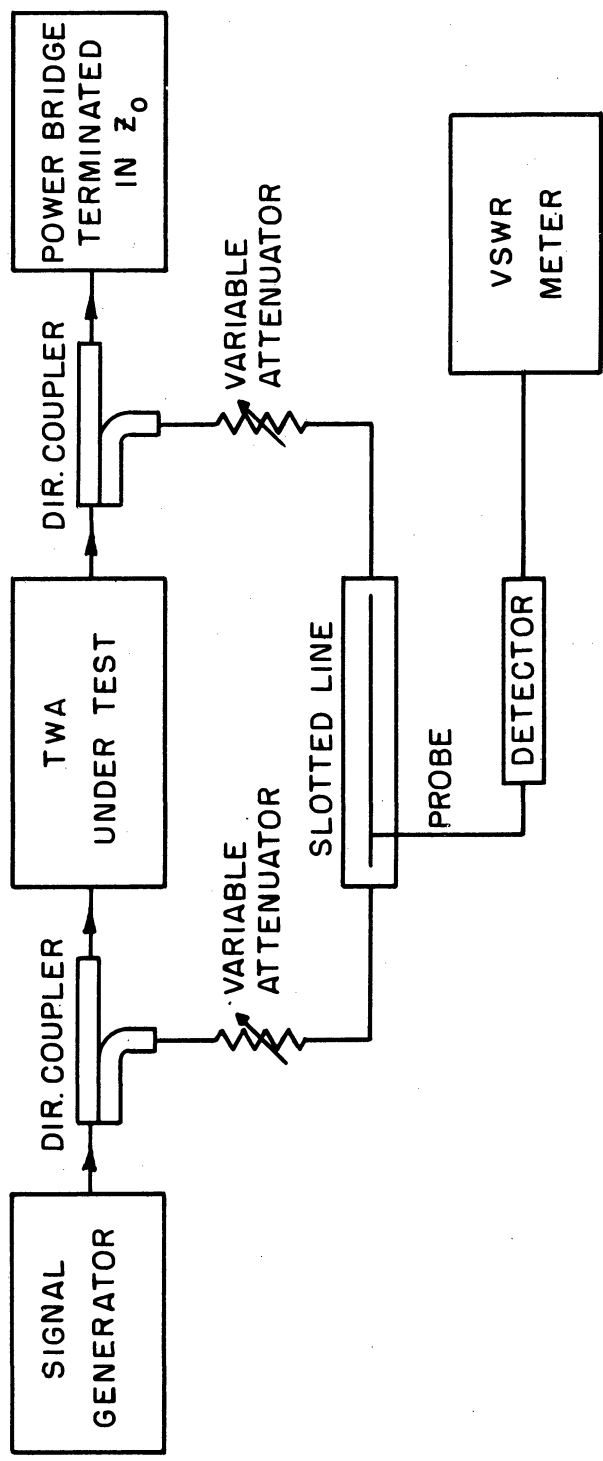


FIG.3.30 BLOCK DIAGRAM OF EQUIPMENT SETUP FOR MEASUREMENT OF MODULATION DEVICE FUNCTIONS.

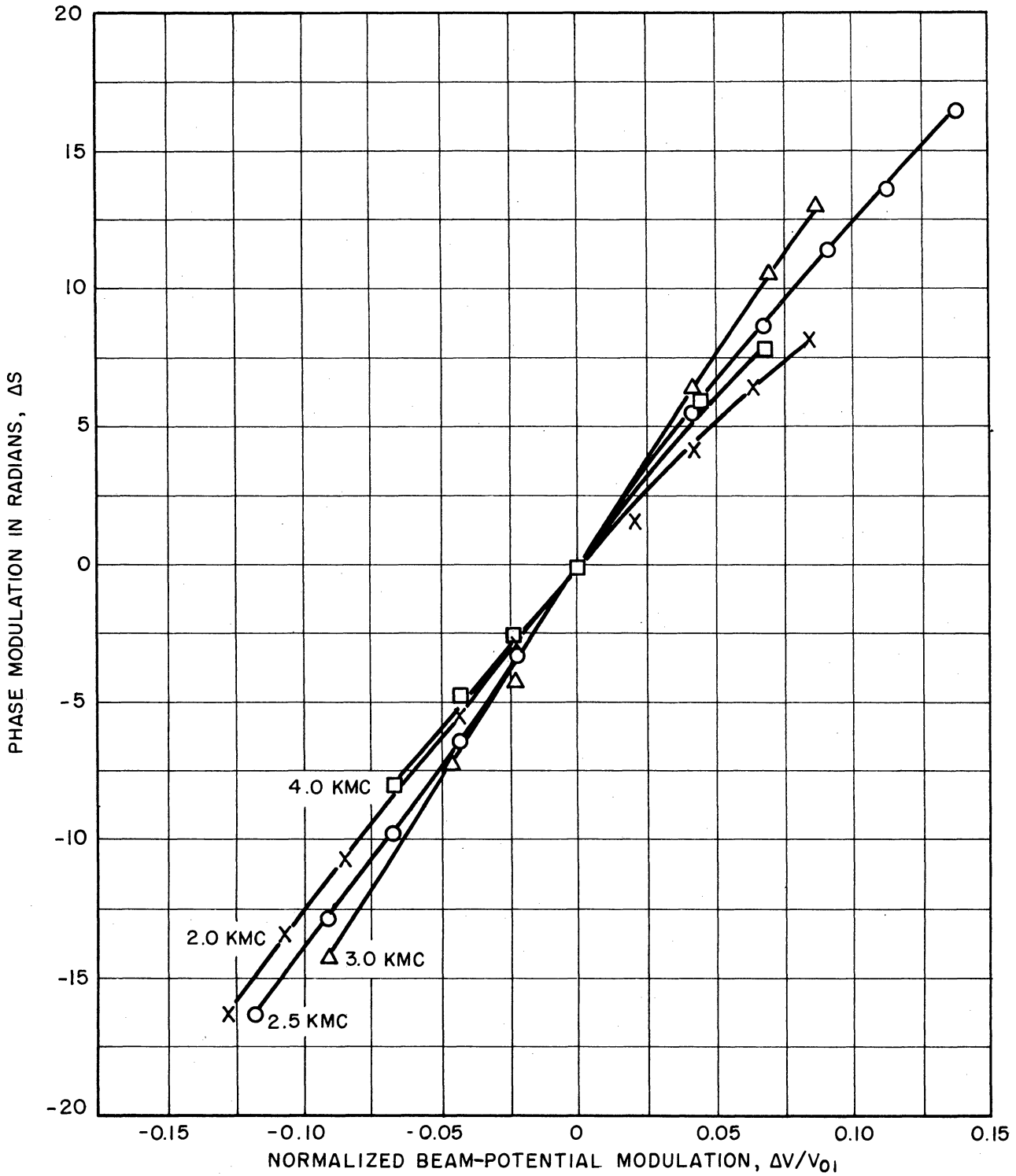


FIG. 3.31 MEASURED PHASE-MODULATION DEVICE FUNCTIONS DURING BEAM-POTENTIAL MODULATION, SMALL-SIGNAL OPERATION. (HEWLETT-PACKARD TWA 490-B,  $I_0 = 3 \text{ ma}$ ,  $P_{IN} = -35 \text{ dbm}$ )

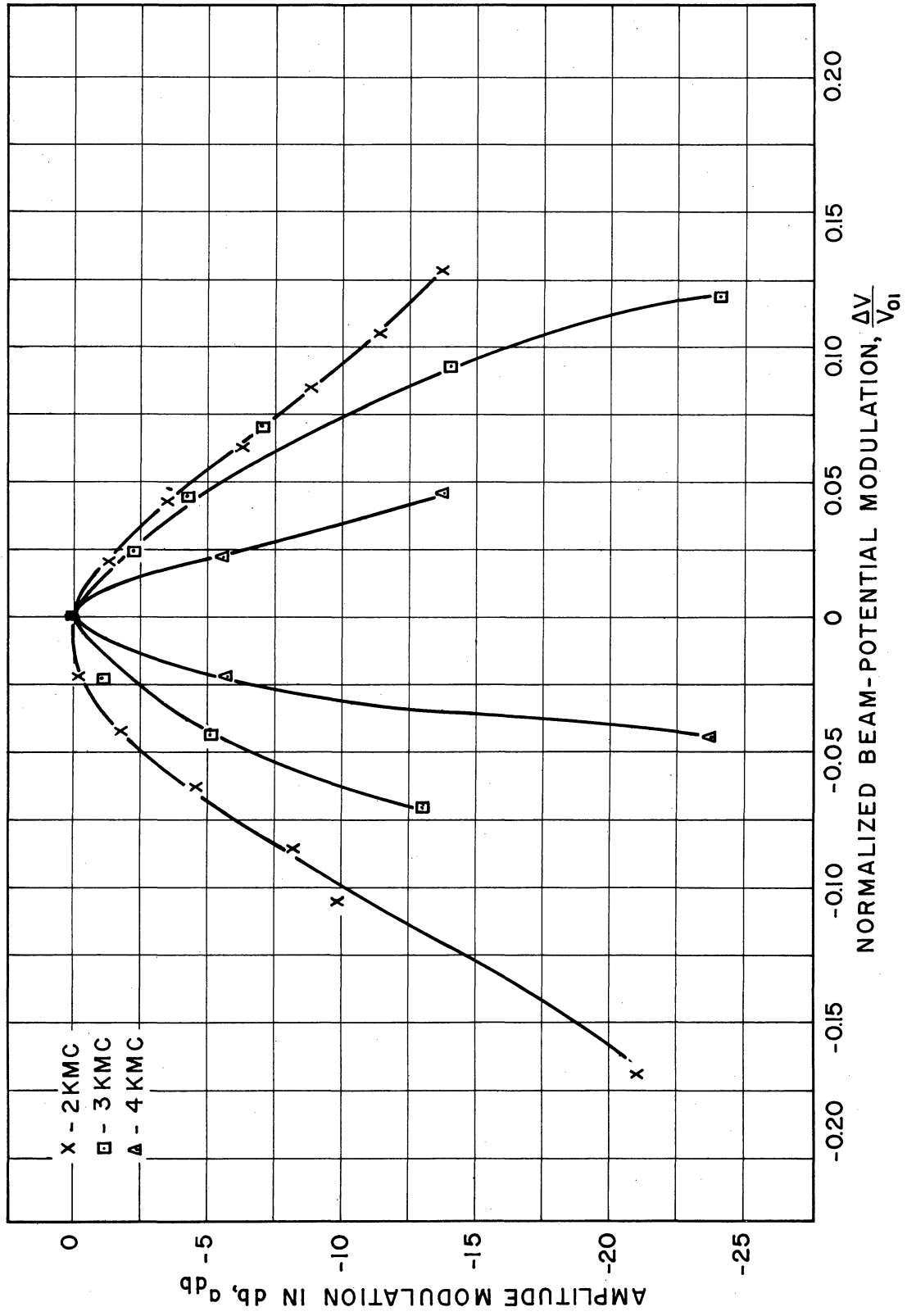


FIG. 3.32 MEASURED AMPLITUDE-MODULATION DEVICE FUNCTIONS DURING BEAM-POTENTIAL MODULATION, SMALL-SIGNAL OPERATION. (HEWLETT-PACKARD TWA 490-B,  $I_0 = 3\text{ma}$ ,  $P_{in} = -35\text{dbm}$ )

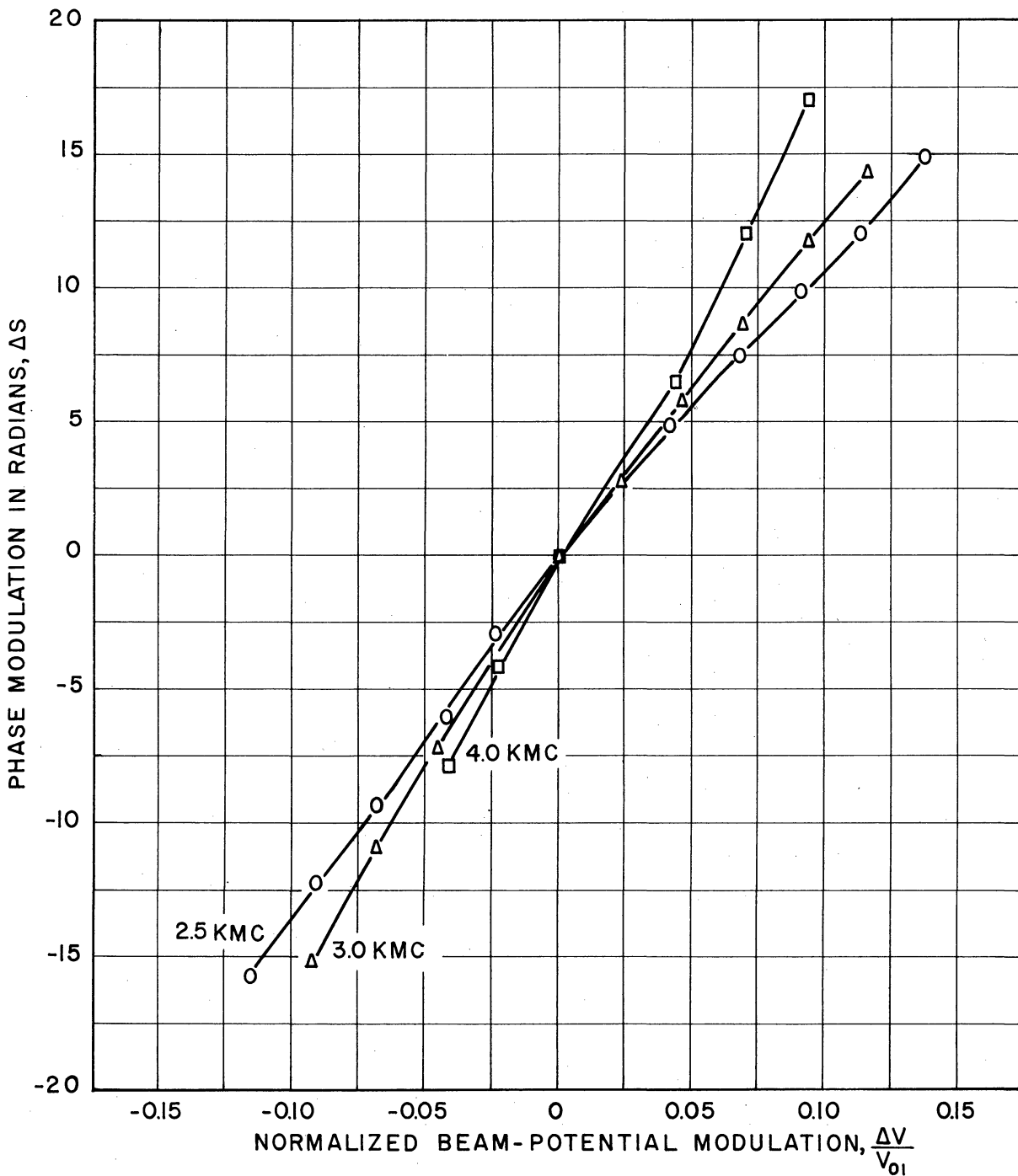


FIG. 3.33 MEASURED PHASE-MODULATION DEVICE FUNCTIONS DURING BEAM-POTENTIAL MODULATION, LARGE-SIGNAL OPERATION. (HEWLETT-PACKARD TWA 490-B,  $I_o = 3\text{ma}$ ,  $P_{in} = 0\text{dbm}$ )

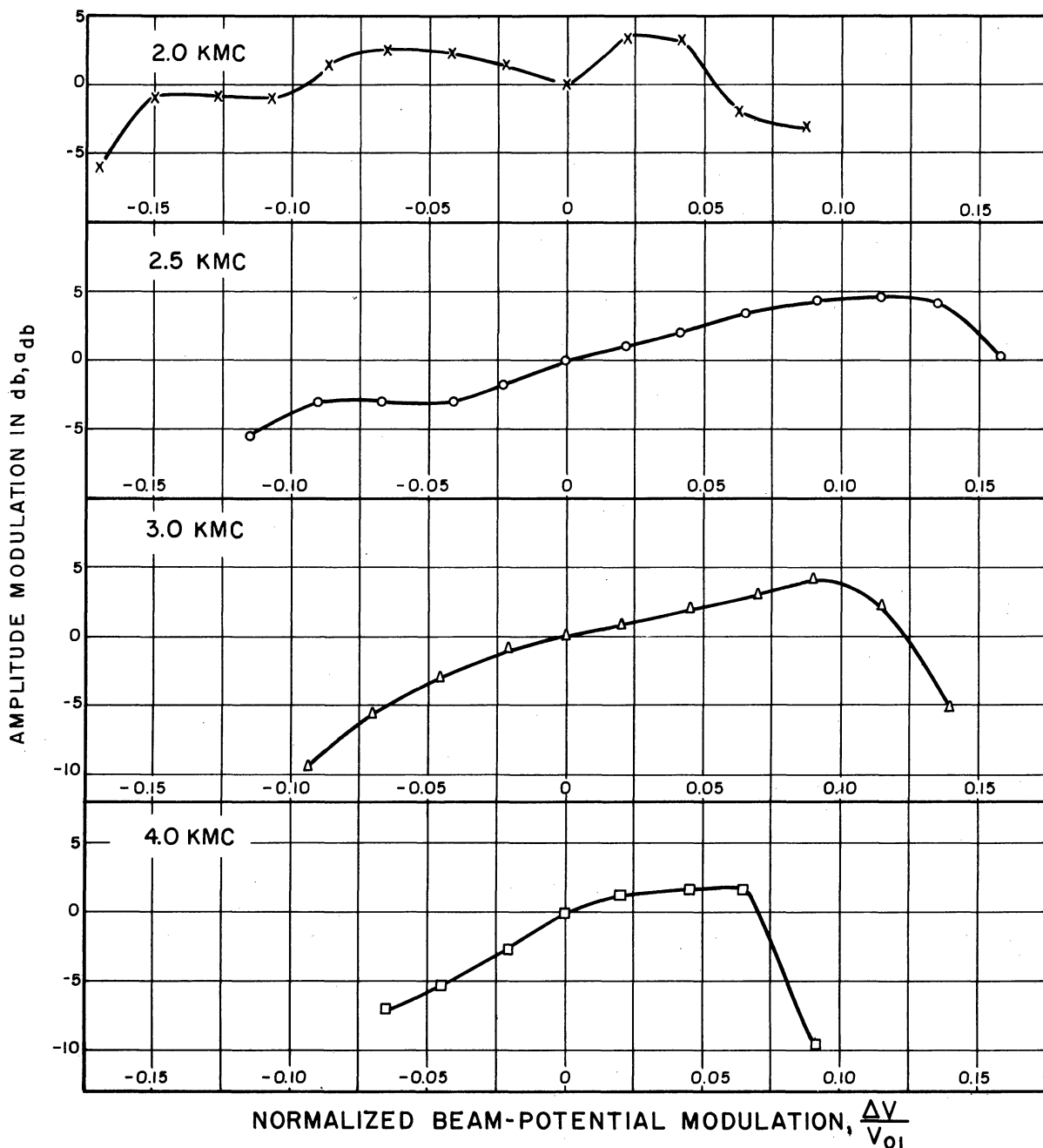


Fig. 3.34 MEASURED AMPLITUDE MODULATION DURING BEAM-POTENTIAL MODULATION, LARGE-SIGNAL OPERATION. (HEWLETT-PACKARD TWA-490-B,  $I_0 = 3 \text{ ma}$ ,  $P_{in} = 0 \text{ dbm}$ )

The linear and nonlinear operation device functions for a current-modulated amplifier are shown in Figs. 3.35 and 3.36. The inherent PM during AM was smaller than the measurement error. In order to keep within operating levels as specified by the manufacturer, only negative values of  $\Delta I/I_0$  are used so as to avoid operation with cathode current above three milliamperes.

### 3.3.3 Comparison between Experimental and Theoretical Results.

The tube parameters can be calculated from a knowledge of dimensions and operating conditions. The tube dimensions are shown in Fig. 3.37. Note that there are five boundaries in this tube between the sections of different loss. In an exact analysis the phase shift introduced at each boundary would have to be accounted for; this however, would make the calculations extremely tedious. In an attempt to simplify the calculations, an average loss figure was taken for the entire tube and the additional modulation introduced at each boundary was assumed to be cancelled by the modulation introduced at the following boundary. This assumption is validated by good agreement between measured and computed results. Since this is a long tube ( $N_s \approx 40$ ), the modulation of the initial loss parameter is neglected.

The tube parameters and operating conditions at 2 kmc are listed below.

$$\begin{aligned}\gamma'_a &= 2.12 \\ C_o &= 0.061 \\ QC_o &= 0.215 \\ b_o &= 0.90 \text{ (Maximum small-signal gain)} \\ N_s &= 38.79 \\ V_{o1} &= 470 \text{ volts}\end{aligned}$$

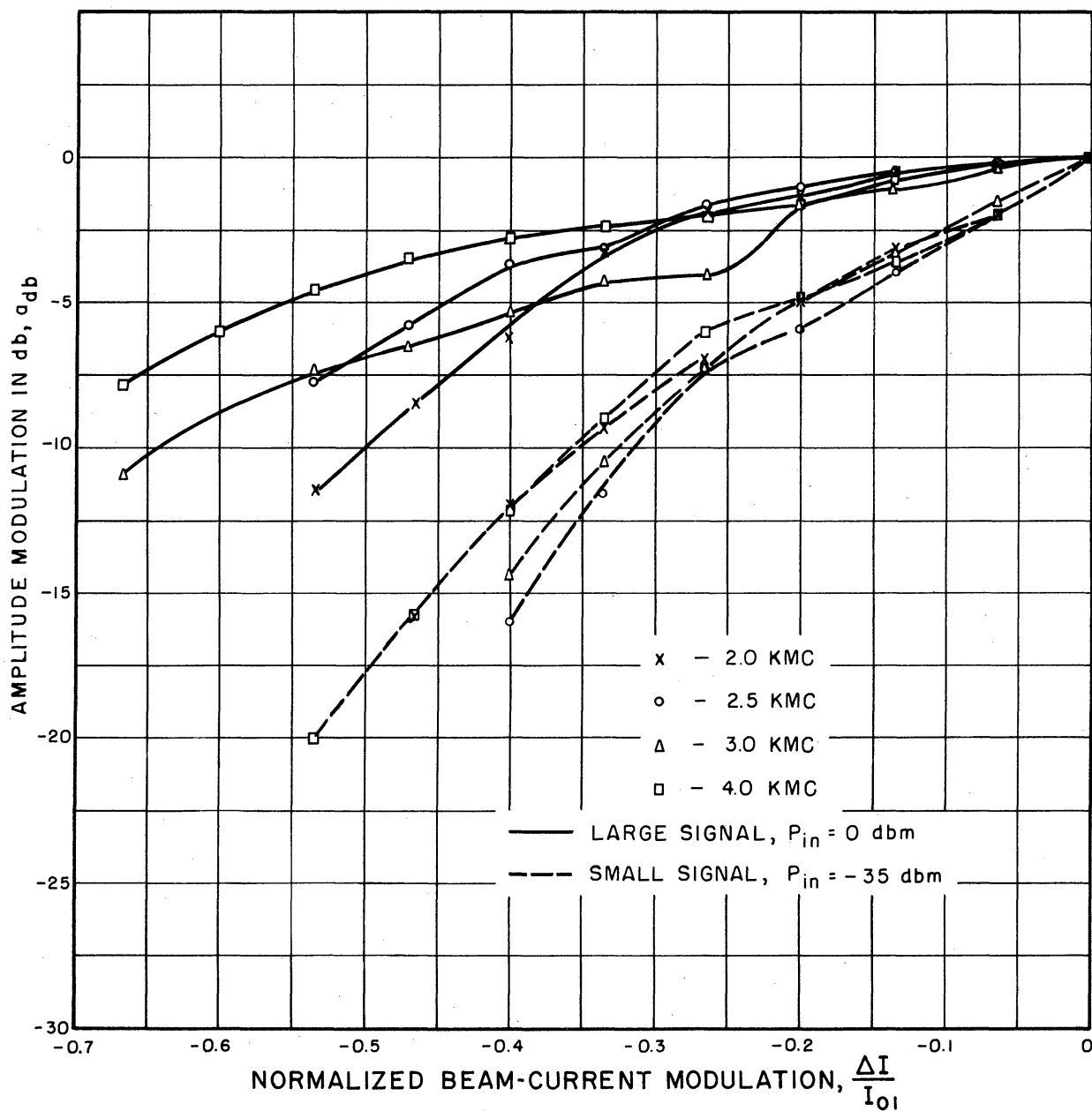


FIG.3.35 MEASURED AMPLITUDE-MODULATION DEVICE FUNCTIONS DURING BEAM-CURRENT MODULATION. (HEWLETT-PACKARD TWA 490-B,  $I_0 = 3$  ma)



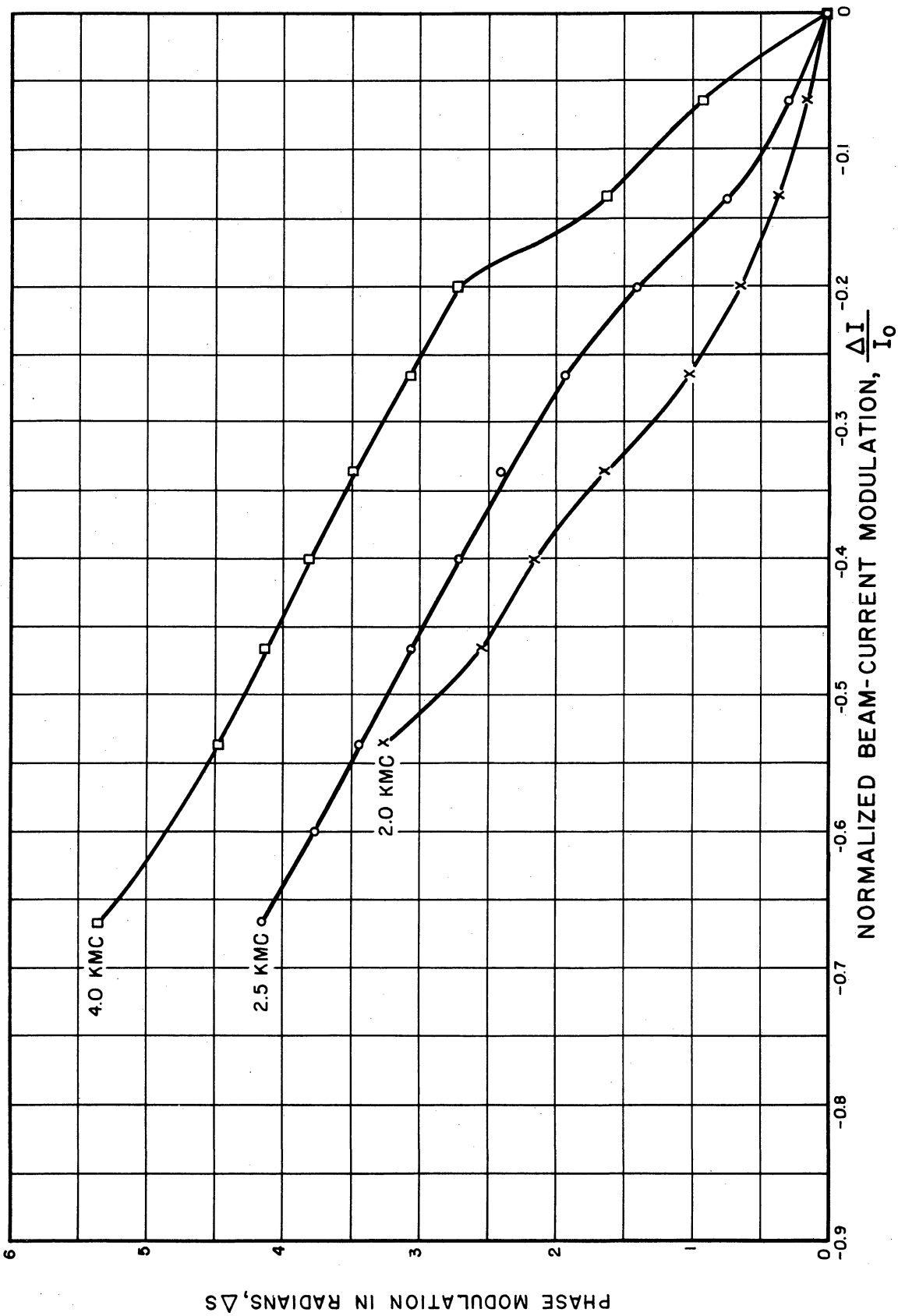
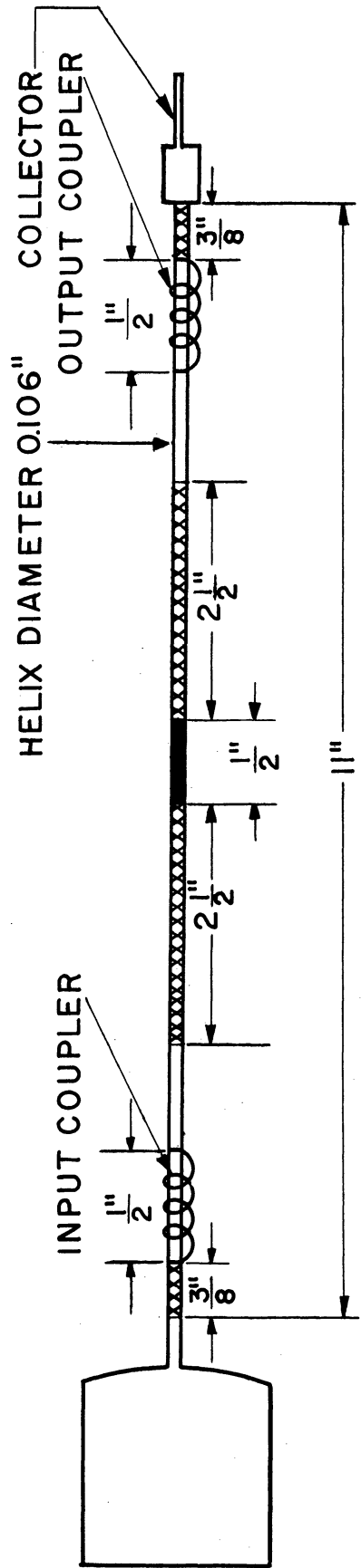


FIG. 3.36 MEASURED PHASE-MODULATION DEVICE FUNCTIONS DURING BEAM-CURRENT MODULATION, LARGE-SIGNAL OPERATION. (HEWLETT-PACKARD TWA 490-B,  $I_0 = 3 \text{ ma}$ ,  $P_{in} = 0 \text{ dbm}$ )



EFFECTIVE TUBE LENGTH FROM CENTER TO CENTER OF COUPLERS IS  $9\frac{3}{4}$ \"/>

■ - INTERNAL AQUADAG ATTENUATOR - 50db.

XXXX EXTERNAL COUPLED HELIX ATTENUATOR 25db TOTAL. COT  $\psi=18.2$

FIG. 3.37 SCHEMATIC DRAWING OF TWA (HUGGINS HA1-HP) USED IN HEWLETT-PACKARD TWA 490-B.

$$I_0 = 3 \text{ milliamps}$$

$$\text{DLF} = 70\%$$

The value of the small-signal velocity injection parameter listed above is computed from an average dispersion curve supplied by the manufacturer. With this particular  $b_0$ , the calculated maximum gain did not occur at the same voltage as the measured gain. The difference between the calculated and experimental values may have been caused by errors in the voltage readings, potential depression within the beam, and errors in the dispersion curves. In order to eliminate these errors, the theoretical curves were shifted so that the maximum gains occurred at the same beam potential.

The experimental and measured device functions for small signal operation at 2 kmc are compared in Figs. 3.38 through 3.41. Agreement is excellent for the beam potential modulation. There is, however, a difference between the theoretical and measured amplitude modulation for a beam-potential modulation with a large positive modulation amplitude. The reason for this is that only one wave was accounted for in the theoretical results and that, at large amplitudes, Crestatron<sup>4</sup> action sets in and accounts for the additional gain.

The agreement is only fair for the beam-current modulation. This is explained by the fact that it was not possible to measure the beam current accurately.

No theoretical calculations were made to obtain a check on the large-signal data; however, the results can be qualitatively analyzed. There is definitely a shift in the maximum of the gain pattern to higher values of modulation voltage as the signal level is raised. Furthermore the amplitude variation does decrease as the signal level is increased. The results for voltage modulation do not seem to indicate that operation

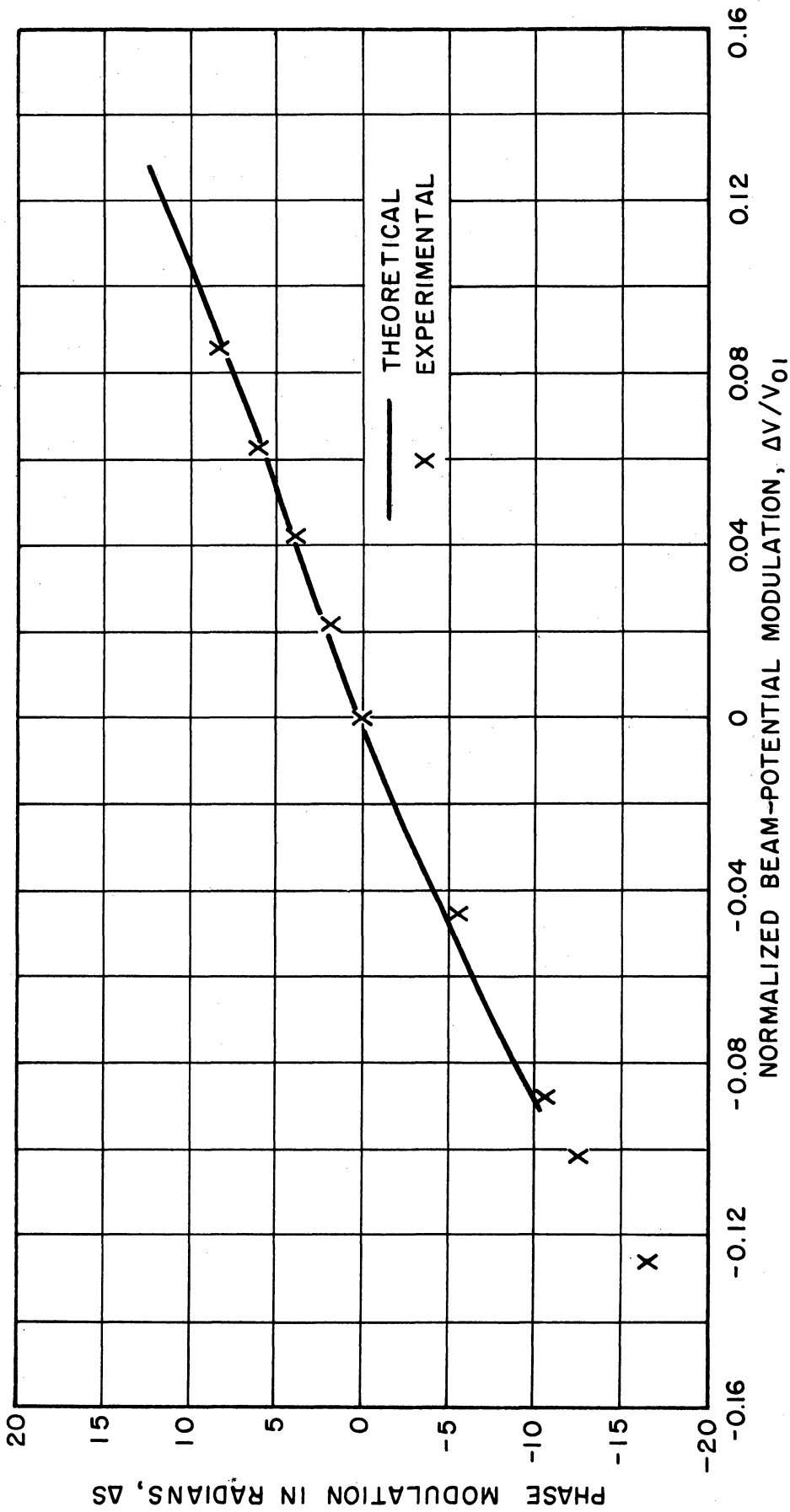


FIG. 3.38 PHASE-MODULATION DEVICE FUNCTION DURING BEAM-POTENTIAL MODULATION, SMALL-SIGNAL OPERATION. (HEWLETT-PACKARD TWA 490-B, 2KMC,  $I_0 = 3\text{ma}$ )

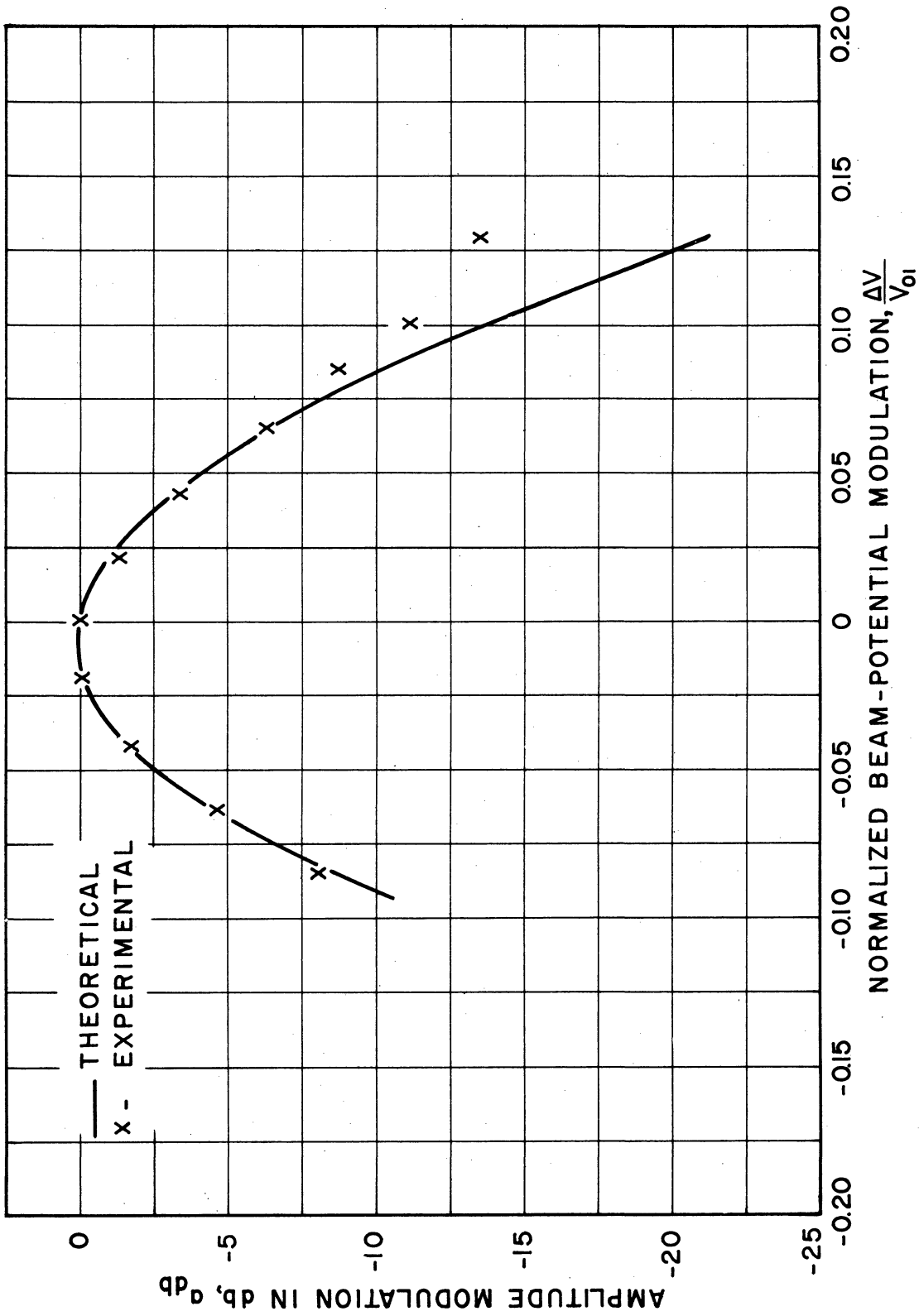


FIG. 3.39 AMPLITUDE-MODULATION DEVICE FUNCTION DURING BEAM-POTENTIAL MODULATION, SMALL-SIGNAL OPERATION. (HEWLETT-PACKARD TWA 490-B, 2 KMC,  $I_0 = 3\text{ma}$ )

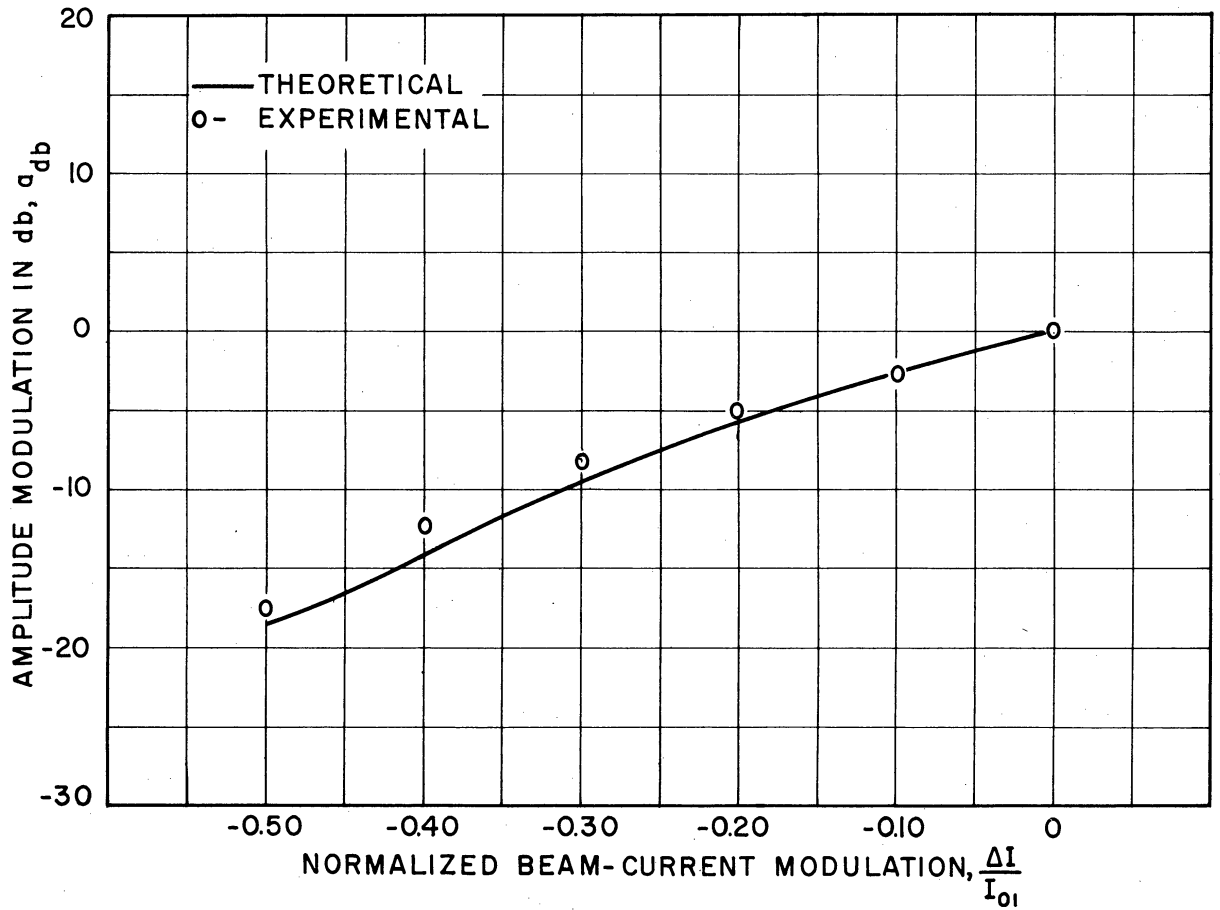


FIG. 3.40 AMPLITUDE-MODULATION DEVICE FUNCTION DURING BEAM-CURRENT MODULATION, SMALL-SIGNAL OPERATION. (HEWLETT-PACKARD TWA 490-B, 2KMC,  $I_0 = 3\text{ma}$ )

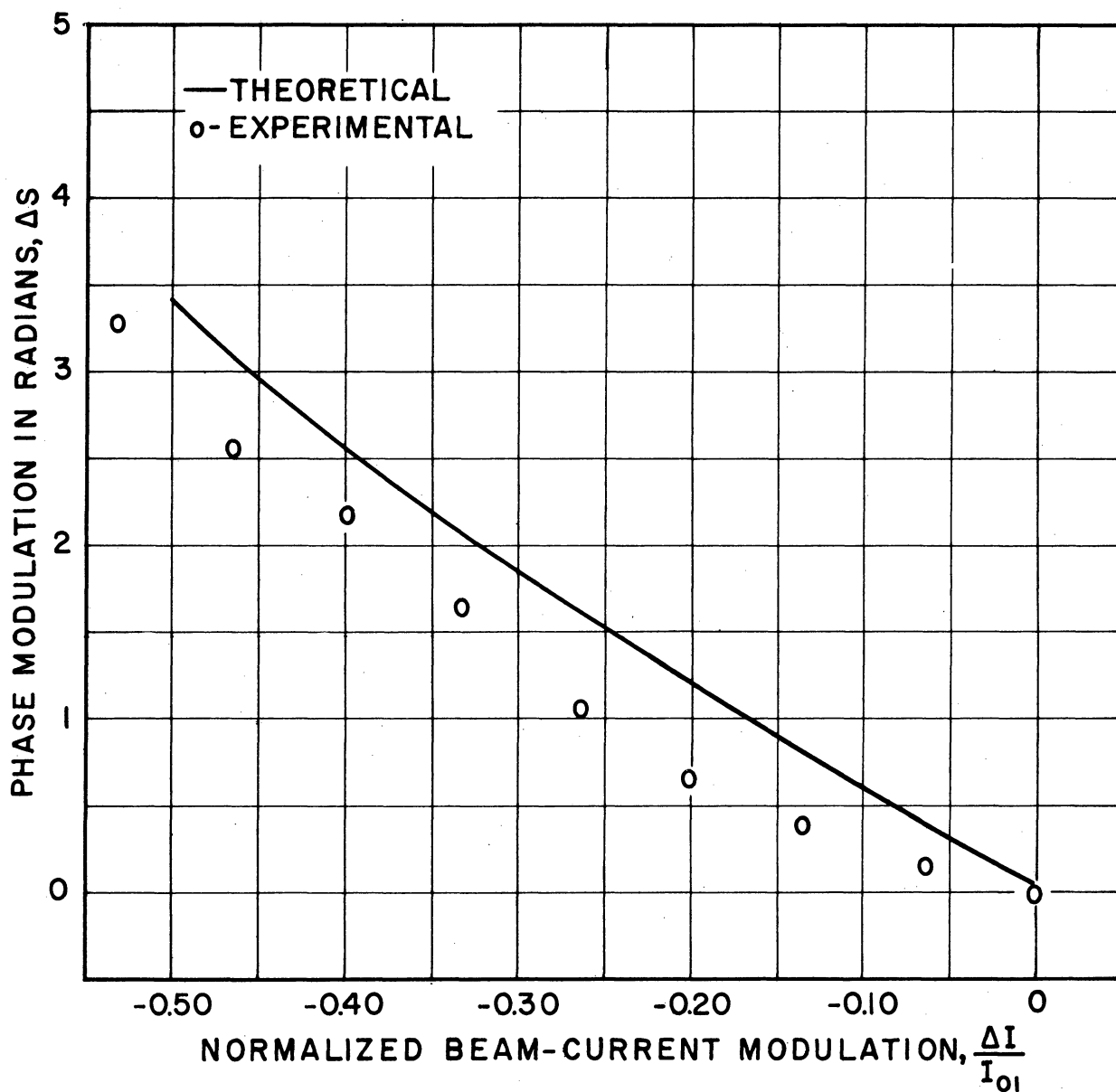


FIG. 3.41 PHASE-MODULATION DEVICE FUNCTION DURING BEAM-CURRENT MODULATION, SMALL-SIGNAL OPERATION.(HEWLETT-PACKARD TWA 490-B, 2KMC,  $I_0=3ma$ )

near saturation increases the linear range of phase modulation, however the range over which the linear phase shift is obtained is not any less for saturation operation than it is for small-signal operation. The flattening of the AM curves for a current modulation as the signal level is increased agrees with the theory.

### 3.4 Summary of Results and Remarks on Traveling-Wave Amplifiers for Modulation Applications

The important results described in this chapter are summarized below. Information on the use of these results in the design of traveling-wave amplifiers for modulation applications is provided.

1. An approximately linear phase modulation of the carrier can be produced by varying the beam potential. There will be a large accompanying amplitude modulation. The phase-linearity and phase-modulation index are almost independent of the carrier level and in some cases improve as the carrier signal is increased to the saturation level. It is possible to reduce the resulting amplitude modulation when using large carrier signals.
2. Amplitude modulation can be produced by varying the beam current. The accompanying phase modulation will be small. The amplitude-modulation index decreases as the carrier signal is increased. A linear variation of amplitude (in db) can be obtained over a limited range of the beam current.
3. For a specific gain, a long low-C, modulated tube has higher phase- and amplitude-modulation indices than the short high-C tube.
4. The characteristics obtained by including the variations of the initial loss parameter,  $A$ , lead to less favorable results than



those found using the approximation that A is invariant with modulation. Space charge and loss tend to accentuate the detrimental effects. It is more important to consider variations of A during voltage modulation than during current modulation. The modulation effects on A are also more important in the short, high-C tube than the long, low-C tube.

5. a). Voltage-Modulated Amplifier

Space charge tends to decrease the overall phase-modulation index and increase the overall amplitude-modulation index. Loss increases both the overall phase-modulation index and the range over which linearity is obtained while decreasing the overall amplitude modulation.

b). Current-Modulated Amplifier

Both loss and space charge reduce the overall amplitude modulation and increase the overall phase modulation.

The following remarks can be made regarding the TWA as a modulator. In order to obtain large-phase modulation indices it is probably best to use a long, low C, voltage modulated tube. Some loss should be included not only to prevent oscillation but to increase the linear range of phase modulation. In this case, however, there will be substantial AM introduced. The AM can be minimized by raising the r-f level to saturation\*; this can be done without seriously affecting the phase linearity. If the inherent AM is still too great, the designer will have to go to a shorter, higher C tube (keeping  $CN_s$  constant if a specific gain is required) and use greater modulation amplitudes. From the shape

---

\* Since a saturated tube without beam modulation converts carrier amplitude variations to phase variations, this method cannot be used in those cases where the input carrier is amplitude modulated.

of the curves, it appears that a simultaneous voltage and current modulation can be used to advantage in minimizing the inherent AM during PM.

For those cases where a large PM index is not required, a higher C tube is a better choice if one is again to minimize the inherent AM. The current modulated TWA operating under linear conditions will serve as a modulator giving AM with little phase distortion.

CHAPTER IV. FREQUENCY SPECTRUM OF THE TRAVELING-WAVE AMPLIFIER  
WITH A LOW-FREQUENCY BEAM MODULATION

4.1 General Modulation Theory

The output spectrum of a traveling-wave amplifier undergoing a low-frequency beam modulation will now be obtained. This discussion is confined to modulations of either the average beam potential or the average beam current, but not of both simultaneously. Spurious modulation effects, (AM during PM and PM during AM), will be considered, but independent simultaneous modulations will not be discussed. The method presented, however, is adaptable to the case of independent modulations. The low modulation frequency assumptions listed in Section 2.1 apply for the material presented in the chapter.

The spectra calculated in this section are for signals having a phase and amplitude which vary in accordance with a specified modulation. Actually, modulation of the average beam potential perturbs the transit time. Under the conditions for low modulation frequencies, the spectra of phase modulated and of transit-time modulated devices are the same. This is more fully discussed in Section 4.5. All modulating signals considered will be periodic, and furthermore, it is assumed that the modulations are applied to a tube that was in cw unmodulated operation prior to being modulated. In view of the periodic nature of this problem, the amplitude and position of the spectral lines will be found from a Fourier series expansion of the output signal.

An output r-f wave that has been amplitude and phase modulated by the same signal can be represented as:

$$\frac{E}{E_0} = G(\xi) \cos [\omega_c t + \phi(\xi)] \quad , \quad (4.1)$$

where  $\xi$  = periodic lower frequency modulating signal,

$G(\xi)$  = normalized amplitude function,

$E$  = output r-f field,

$E_0$  = unmodulated output r-f field, and

$\phi(\xi)$  = phase shift through the tube relative to the input signal.

The modulating signal  $\xi$  is applied for the purpose of perturbing either  $G$  or  $\phi$ . This modulation simultaneously results in an inherent perturbation of  $\phi$  or  $G$  respectively. Both  $G$  and  $\phi$  are real functions. Equation 4.1 may be written in exponential form as

$$\frac{E}{E_0} = \frac{1}{2} G(\xi) \left[ \exp j[\omega_c t + \phi(\xi)] + \exp - j[\omega_c t + \phi(\xi)] \right] \quad (4.2)$$

The output r-f signal will possibly contain harmonics of the carrier frequency  $\omega_c^*$ , harmonics of the fundamental frequency  $\omega_a$  of the modulating signal  $\xi$  and combinations of the harmonics called the intermodulation or crossmodulation frequencies  $n\omega_c + m\omega_a$ . Therefore the output r-f field can be expanded in the doubly periodic series

$$\frac{E}{E_0} = \sum_{n=-\infty}^{\infty} \sum_{m=-\infty}^{\infty} A_{nm} \exp j(n\omega_c + m\omega_a)t \quad (4.3)$$

For many traveling-wave amplifiers it can safely be assumed that the impedance of the circuit to harmonics of the carrier will be rather low so that the unmodulated output will contain only the carrier fundamental. Similarly it is assumed that the modulated tube will contain only cross modulation frequencies with the carrier fundamental. For low

---

\* The carrier frequency  $\omega_c$  is not to be confused with the cyclotron frequency.

modulating frequencies Eq. 4.3 can be approximated as

$$\frac{E}{E_0} \approx \sum_{m=-\infty}^{\infty} A_{1m} \exp j(\omega_c + m\omega_a)t + A_{-1m} \exp j(-\omega_c + m\omega_a)t. \quad (4.4)$$

Equation 4.4 can be written as

$$\frac{E}{E_0} = \sum_{m=-\infty}^{\infty} 2\text{Re} \left\{ A_{1m} \exp j(\omega_c + m\omega_a)t \right\}. \quad (4.5)$$

A comparison of Eq. 4.5 with Eq. 4.2 shows that

$$\frac{1}{2} G(\xi) \exp j\varphi(\xi) = \sum_{m=-\infty}^{\infty} A_{1m} \exp jm\omega_a t, \quad (4.6)$$

therefore

$$A_{1m} = \frac{1}{4\pi} \int_0^{2\pi} G(\xi) \exp j[\varphi(\xi) - m\omega_a t] d\omega_a t. \quad (4.7)$$

From Eq. 4.5b one can see that the amplitude of the spectral line at the sideband  $\omega_c + m\omega_a$  is given as

$$2\text{Re}(A_{1m}).$$

Therefore in order to find the spectrum amplitudes, it is necessary to perform the integration indicated in Eq. 4.7. For certain forms of  $\xi$ , the integration becomes rather involved. There is, however, an alternate method for calculating the amplitudes. The integrations arising in the second method are simpler, however they are so at the expense of having the amplitudes given in open form.

Consider the expression given in Eq. 4.6 and expand each term on the left side in a Fourier series. Therefore

$$\frac{1}{2} G(\xi) \exp j \varphi(\xi) = \frac{1}{2} \left( \sum_{l=-\infty}^{\infty} G_l \exp j n \omega_a t \right) \left( \sum_{s=-\infty}^{\infty} F_s \exp j s \omega_a t \right) , \quad (4.8a)$$

where

$$G_l = \frac{1}{2\pi} \int_0^{2\pi} G(\xi) (\exp [-j l \omega_a t]) d\omega_a t ,$$

$$F_s = \frac{1}{2\pi} \int_0^{2\pi} [\exp j(\varphi(\xi) - s \omega_a t)] d\omega_a t . \quad (4.8b)$$

Since the product involved in Eq. 4.8a is of two series each with indices running from  $-\infty$  to  $+\infty$ , the product may be expressed as

$$\frac{1}{2} G(\xi) \exp j \varphi(\xi) = \sum_{m=-\infty}^{\infty} \sum_{k=-\infty}^{\infty} G_k F_{m-k} \exp j m \omega_a t , \quad (4.9)$$

where the results of Appendix D have been used.

Matching similar frequency terms in Eqs. 4.9 and 4.6 gives the open form for  $A_{1m}$  as

$$A_{1m} = \frac{1}{2} \sum_{k=-\infty}^{\infty} G_k F_{m-k} . \quad (4.10)$$

Note that in general the integration involved in evaluating  $G$  and  $F$  as given in Eq. 4.8b will be simpler than that given in Eq. 4.7.

The spectrum amplitudes can be calculated by either of the two methods given above; however in order to use either method one must have an analytical form for  $G(\xi)$  and  $\varphi(\xi)$ . Obviously  $G$  and  $\varphi$  are the

modulation device functions. An analytical form was given for the small-signal amplifier by using a Taylor series expansion. The errors introduced by truncating the Taylor series are described in Chapter III. Alternately, representation of the device functions can be obtained by fitting a polynomial to the curves of the device functions calculated by the exact linear method or by the nonlinear method. Additional terms are required in the polynomial to fit the curves as the amplitude of the modulating signal is increased. It shall now be assumed that a quadratic approximation will suffice to describe the device functions. Therefore the normalized device functions are approximated as

$$G(\xi) = 1 + h_1 \xi + h_2 \xi^2$$

$$\varphi(\xi) = \varphi_0 (1 + p_1 \xi + p_2 \xi^2) \quad , \quad (4.11)$$

where  $\varphi_0$  is the unmodulated phase shift through the tube. The particular values of  $h$  and  $p$  will depend on the unmodulated tube parameters and the method of modulation used.

Equations 4.11 can now be substituted into the preceding integrals to obtain

$$G_o = 1 + \frac{1}{2\pi} \int_0^{2\pi} (h_1 \xi + h_2 \xi^2) d\omega_a t \quad , \quad (4.12a)$$

$$G_m = \frac{1}{2\pi} \int_0^{2\pi} (h_1 \xi + h_2 \xi^2) (\exp [-jm\omega_a t]) d\omega_a t \quad , \quad (4.12b)$$

$$\varphi - j\varphi_0 = \frac{1}{2\pi} \int_0^{2\pi} \exp [j(\varphi_0 p_1 \xi + \varphi_0 p_2 \xi^2 - m\omega_a t)] d\omega_a t \quad , \quad (4.12c)$$

and

$$2A_{1m} \exp[-j\phi_0] = F_m \exp[-j\phi_0] + \frac{1}{2\pi} \int_0^{2\pi} (h_1 \xi + h_2 \xi^2) \exp[j\phi_0 p_1 \xi + \phi_0 p_2 \xi^2 - m\omega_a t] d\omega_a t \quad (4.12d)$$

The spectra of particular forms of the modulating signal  $\xi$  will now be calculated.

#### 4.2 Sinusoidal Modulation

The most common signal used in modulation theory is the sinusoidal signal. Assume that  $\xi$  is given as

$$\xi = q \sin \omega_a t \quad (4.13)$$

The evaluation of Eq. 4.12d becomes exceedingly difficult with this form of  $\xi$  so that it is necessary to resort to the open form to find the spectral amplitudes. When Eqs. 4.13, 4.12a and 4.12b are combined, the following results are found;

$$\begin{aligned} G_0 &= 1 + \frac{h_2}{2} q^2 \\ G_1 &= -jq \frac{h_1}{2} \\ G_{-1} &= jq \frac{h_1}{2} \\ G_2 &= -q^2 \frac{h_2}{4} \\ G_{-2} &= -q^2 \frac{h_2}{4} \\ G_n &= 0 \quad \text{for } |n| > 2. \end{aligned} \quad (4.14)$$



The sum involved in the calculation of  $A_{1m}$  for a sinusoidal modulation therefore is closed. The terms that must be considered are listed below.

$$2A_{1m} = G_0 F_m + G_1 F_{m+1} + G_{-1} F_{m+1} + G_2 F_{m-2} + G_{-2} F_{m+2} \quad (4.15)$$

Finding the  $G_m$  terms involves more difficulty than evaluating the  $F_m$  terms. Substitute Eq. 4.13 into Eq. 4.12c, hence

$$F_m \exp - j\phi_0 = \frac{\exp j \frac{q^2 \phi_0 p^2}{2}}{2\pi} \int_0^{2\pi} \exp j(\phi_0 p_1 q \sin \omega_a t) - \frac{\phi_0 p_2}{2} q^2 \cos [2\omega_a t - n\omega_a t] d\omega_a t \quad (4.16)$$

By using the Jacobi-Anger<sup>23</sup> formula it is possible to introduce the expansion

$$\exp \left[ - j \frac{\phi_0 p^2}{2} q^2 \right] = \sum_{k=-\infty}^{\infty} j^k \exp (2jk\omega_a t) J_k \left( - q^2 \frac{\phi_0 p^2}{2} \right) ,$$

where  $J_k$  is the Bessel function of order  $k$ .

Substitution of this series and inversion of the order of integration and summation yields

$$F_m \exp \left[ - j \left( \phi_0 + \frac{\phi_0 q^2 p^2}{2} \right) \right] = \sum_{k=-\infty}^{\infty} j^k J_k \left( - q^2 \frac{\phi_0 p^2}{2} \right) \frac{1}{2\pi} \int_0^{2\pi} \exp j \left( q\phi_0 p_1 \sin \omega_a t - (m-2k)\omega_a t \right) d\omega_a t .$$

The integral in the above equation is easily recognized as one appearing in ordinary modulation theory and can be integrated<sup>24</sup> to give

$$F_m \exp\left[-j\left(\varphi_0 + \frac{\varphi_0 q^2 p_2}{2}\right)\right] = \sum_{k=-\infty}^{\infty} j^k J_k\left(-\frac{\varphi_0 q^2 p_2}{2}\right) J_{2k-m}(-q\varphi_0 p_1) \quad (4.17)$$

Equation 4.17 can be substituted into Eq. 4.15 to complete the evaluation of the sideband amplitudes. Each sideband frequency has a phase shift

$$\varphi_0 + \varphi_0 \frac{q^2 p_2}{2} \quad (4.18a)$$

and an amplitude

$$\begin{aligned} 2R_e A_{1m} = & \sum_k (-1)^k J_{2k}\left(-q^2 \frac{\varphi_0 p_2}{2}\right) \left\{ \left(1 + \frac{h_2 q^2}{2}\right) J_{4k-m}(-\varphi_0 p_1 q) \right. \\ & - q^2 \frac{h_2}{4} \left[ J_{4k-n-2}(-q\varphi_0 p_1) + J_{4k-n+2}(-q\varphi_0 p_1) \right] \left. \right\} \\ & - J_{2k+1} \frac{h_1 q}{2} \left[ J_{4k-n+1}(-\varphi_0 p_1 q) - J_{4k-n+3}(-\varphi_0 p_1 q) \right] \quad (4.18b) \end{aligned}$$

Equations 4.18 give the general sideband amplitudes for the quadratically approximated TWA modulated by a sinusoidal signal. It is interesting to study some degenerate forms of Eqs. 4.18.

For the case of small-modulation amplitudes, it is possible to approximate the phase shift with a linear function. Under this condition  $p_2 = 0$  and the summation in Eqs. 4.18 vanishes for all  $k$  except  $k = 0$ . Therefore the linear phase TWA that is sinusoidally modulated

has sidebands with amplitudes

$$2\text{Re}A_{1m} = (-1)^m \left( 1 + \frac{h_2 q^2}{2} \right) J_m(-\phi_0 q p_1)$$

$$- \frac{q^2 h_2}{4} \left[ (-1)^{m+2} J_{m+2}(-\phi_0 p_1 q) + (-1)^{m-2} J_{m-2}(-\phi_0 p_1 q) \right].$$

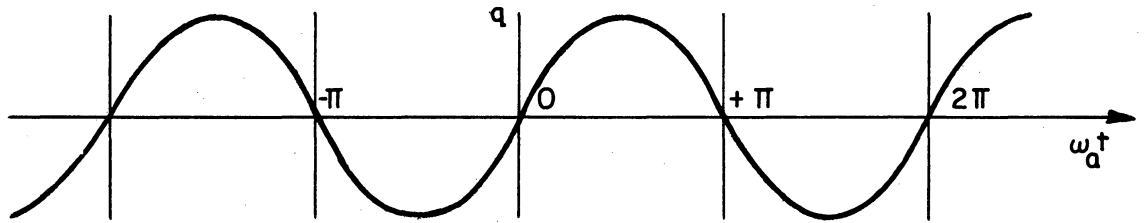
Finally the TWA with no output AM has amplitudes given by the familiar result

$$2\text{Re}A_{1m} = (-1)^m J_m(-\phi_0 q p_1)$$

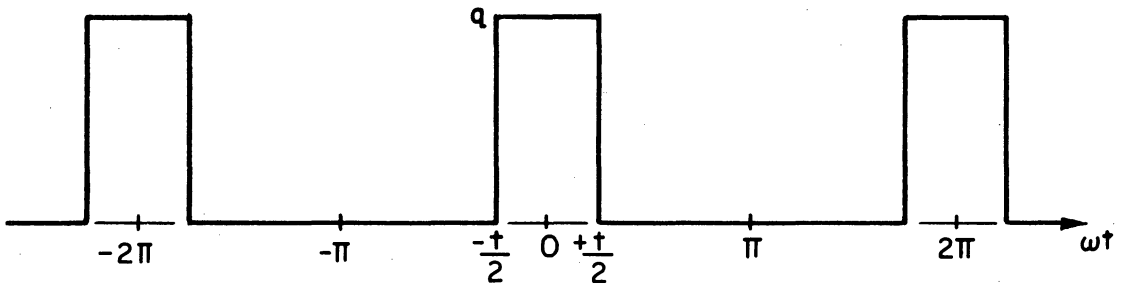
### 4.3 Pulse Modulation

Another common modulation form is by a train of pulses. The pulse modulated tube will now be investigated. This particular case is again for the tube in unmodulated operation when pulses are applied to the average beam potential or current. This analysis is not to be confused with that of the tube where the beam is cut on and off by pulses; this would be a purely transient analysis and would certainly not fall under those cases describable by the Taylor series approximation to the quasi-static function. The pulse modulation applied to the operating tube however can be described to an extent by the quasi-static approach. The modulation signal is shown in Fig. 4.1b.

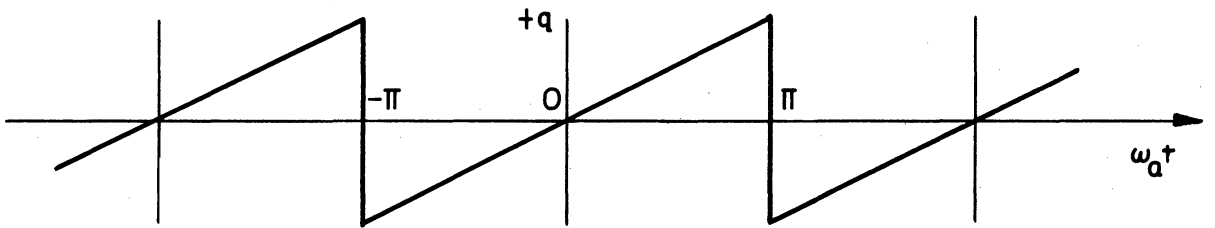
The additional assumption is now introduced, that the duty cycle is sufficiently low so that the average value of either the beam current or potential is unaltered from the unmodulated case. For the wave shape shown in Fig. 4.1b, the signal is described as



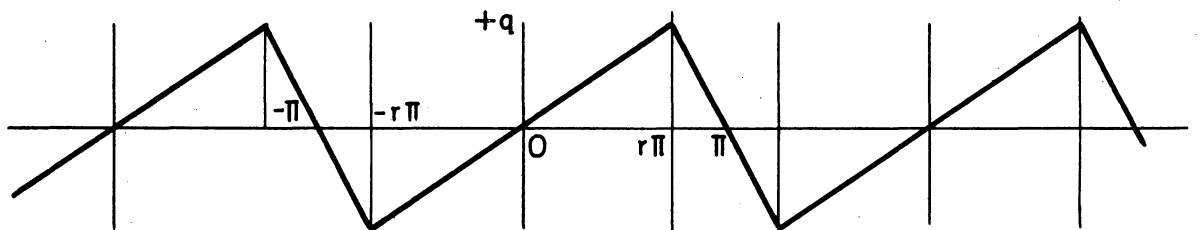
(a.)



(b.)



(c.)



(d.)

FIG. 4.1 MODULATING WAVE FORMS. (a.) SINUSOIDAL, (b.) PULSE (c.) IDEAL SAWTOOTH, (d.) SAWTOOTH WITH FINITE FLYBACK TIME.

$$\begin{aligned} \xi &= 0 && \text{for } -\pi < \omega_a t < -\frac{\pi\tau}{T} \\ \xi &= q && \text{for } -\frac{\pi\tau}{T} < \omega_a t < \frac{\pi\tau}{T} \\ \xi &= 0 && \text{for } +\frac{\pi\tau}{T} < \omega_a t < \pi \end{aligned} \quad (4.19)$$

$\xi$  as given in Eq. 4.19 can be substituted into Eqs. 4.12c and 4.12d to obtain the sideband amplitudes. The result is given by

$$2A_{im} \exp[-j\phi_0] = \frac{\tau}{T} \left( \frac{\sin \frac{\pi m \tau}{T}}{\frac{\pi m \tau}{T}} \right) \left\{ 1 + (1+h_1 q+h_2 q^2) \exp j (\phi_0 p_1 q + \phi_0 p_2 q^2) \right\}. \quad (4.20)$$

The limits of integration were changed to  $-\pi$  and  $\pi$ .

The spectrum is seen to be composed of two sets of lines. One set is the usual  $(\sin x)/x$  distribution but it arrives at the output at the same phase as the unmodulated signal would, and the second set similarly has a  $(\sin x)/x$  pattern but arrives with a delay dependent upon the phase-modulation characteristic, and an amplitude dependent upon the amplitude-modulation characteristics.

#### 4.4 Sawtooth Modulation

The two previous sections were concerned with modulations primarily used to impart information onto an r-f wave. There are certain applications when it becomes desirable to translate the energy at the carrier frequency to one of the sidebands and have very little energy in the other sidebands or at the original carrier frequency. This is possible using a TWA with a sawtooth-modulated beam velocity. This method of frequency translation using a TWA was first devised and analyzed by Cumming<sup>6</sup>. He named this method of frequency translation "Serrodyne" operation. In this section a mathematical discussion of sawtooth

modulation is given while a physical picture of how sawtooth modulation can produce frequency shifting is given in the following section.

Rather than attempting the general solution, first a simple case will be investigated. An ideal amplifier for frequency shifting is one with a linear phase characteristic and no amplitude variation ( $p_2 = h_1 = h_2 = 0$ ). An ideal sawtooth for frequency shifting is one with no fly-back time. This signal is shown in Fig. 4.1c. The ideal signal is then applied to the ideal amplifier.

The mathematical representation of the sawtooth signal is

$$\xi = \frac{q}{\pi} \omega_a t, \quad -\pi < \omega_a t < \pi \quad . \quad (4.21)$$

Using 4.21 in 4.12d with the limits going from  $-\pi$  to  $+\pi$  gives the sideband amplitude as

$$2A_{1m} e^{-j\varphi_0} = F_m e^{-j\varphi_0} = \frac{\sin\left(\frac{p_1 q \varphi_0}{\pi} - m\right) \pi}{\left(\frac{p_1 q \varphi_0}{\pi} - m\right) \pi} \quad . \quad (4.22)$$

If the tube length and modulation signal amplitude are adjusted so that

$$\frac{p_1 q \varphi_0}{\pi} = n' \quad (\text{an integer}) \quad ,$$

then the amplitude of the sideband at  $m = n'$  will be unity and all other sideband amplitudes will vanish. This is truly the desired frequency shifter. In practice this ideal operation is extremely difficult to achieve. Consider now some departures from the ideal. Apply a sawtooth with finite fly-back time as shown in Fig. 4.1d to the ideal tube. For this signal,  $\xi$  is described as

$$\begin{aligned} \xi &= -\frac{q}{1-r} \left( 1 + \frac{\omega_a t}{\pi} \right) && \text{for } -\pi < \omega_a t < -r\pi \\ \xi &= \frac{q}{r\pi} \omega_a t && \text{for } -r\pi < \omega_a t < r\pi \\ \xi &= \frac{q}{1-r} \left( 1 - \frac{\omega_a t}{\pi} \right) && \text{for } r\pi < \omega_a t < \pi \end{aligned} \quad (4.23)$$

The sideband amplitudes are given as

$$\begin{aligned} 2A_{1m} e^{-j\phi_0} &= r \frac{\sin\left(\frac{p_1 \phi_0 q}{r\pi} - m\right) r\pi}{\left(\frac{p_1 \phi_0 q}{r\pi} - m\right)} \\ &+ \frac{\sin\left[\left(\frac{p_1 \phi_0 q}{(1-r)\pi} + m\right)\pi - \frac{qp_1 \phi_0}{1-r}\right] - \sin\left[\left(\frac{p_1 \phi_0 q}{(1-r)} + m\right)r\pi - \frac{qp_1 \phi_0}{1-r}\right]}{\left(\frac{p_1 \phi_0 q}{(1-r)\pi} + m\right)\pi} \end{aligned} \quad (4.24)$$

Clearly the effect of finite fly-back time is to create a large number of sidebands.

Finally apply the perfect sawtooth to the nonideal tube. The integrals of Eq. 4.12 can be evaluated using the Fresnel integral forms<sup>23</sup>,

$$C(x) = \frac{2}{\pi} \int_0^{x^{1/2}} \cos t^2 dt$$

and

$$S(x) = \frac{2}{\pi} \int_0^{x^{1/2}} \sin t^2 dt$$

These are tabulated functions; the results are,

$$A_{1m} e^{-j\phi_0} = F_m e^{-j\phi_0} + \frac{q h_1 e^{-j\alpha^2}}{2\pi^2 \beta} \left\{ \frac{j}{2\beta} \left( e^{jP_2} - e^{jP_1} \right) - \alpha \left( \frac{\pi}{2} \right)^{1/2} \left[ C(P_1) - C(P_2) + jS(P_1) - jS(P_2) \right] \right\} + j e^{jP_1} \left[ \frac{\alpha}{\beta} - \frac{P_1^{1/2}}{\beta^2} \right] - j e^{jP_2} \left[ \frac{\alpha}{\beta} - \frac{P_2^{1/2}}{\beta^2} \right]. \quad (4.25a)$$

$$F_m e^{-j\phi_0} = \frac{e^{-j\alpha^2}}{\beta} \left( \frac{\pi}{2} \right)^{1/2} \left[ C(P_1) - C(P_2) + jS_1(P_1) - jS(P_2) \right]. \quad (4.25b)$$

where

$$\alpha = \frac{\frac{q\phi_0 p_1}{\pi} - m}{2q^2 \frac{\phi_0 p_2}{\pi^2}}$$

$$\beta = \frac{q^2 \phi_0 p_2}{\pi}$$

$$P_1 = \beta(\pi + \alpha)^2$$

$$P_2 = \beta(\alpha - \pi)^2$$

and  $C(X)$  and  $S(X)$  represent the Fresnel integrals mentioned above.

#### 4.5 Physical Description of Frequency Translation by Sawtooth Modulation

In the preceding section, the mathematical formulation of the Serrodyne frequency translator was presented. Since the concept of changing the frequency of a signal while it propagates on a structure may appear difficult to understand, it has been decided to repeat the



physical picture given by Cumming<sup>6</sup> and others<sup>51</sup> to explain Serrodyne operation. This explanation will be for the ideal situation.

Consider a signal with time variation described as

$$\cos (\omega_c t + \varphi) \quad .$$

Now assume that the phase  $\varphi$  is made to vary linearly with time, therefore

$$\frac{d\varphi}{dt} = \text{constant} = 2\pi F \quad ,$$

and

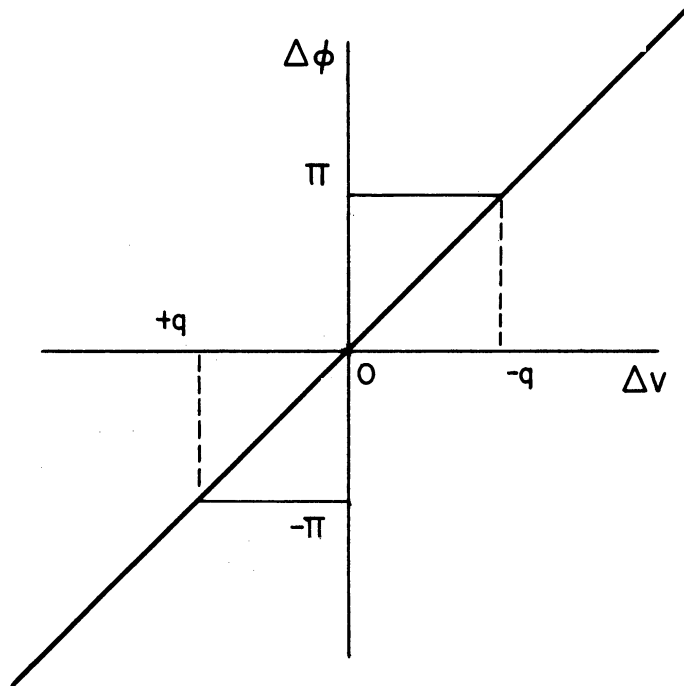
$$\varphi = 2\pi \int F dt = 2\pi F t + \varphi_0 \quad .$$

The time variation of the signal can be described as

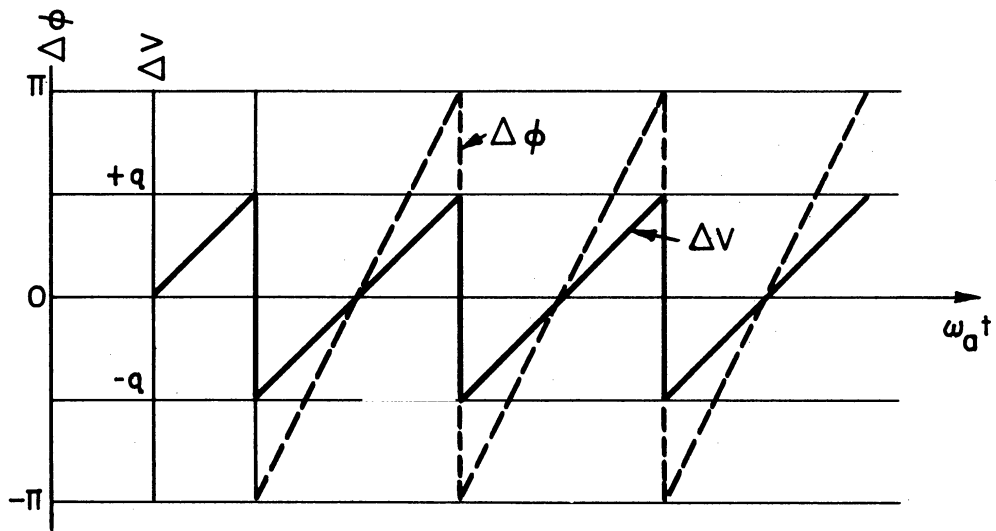
$$\cos [(\omega_c + 2\pi F)t + \varphi_0]$$

and the frequency has been shifted  $F$  cycles. Unfortunately this type of frequency shifting requires that the phase change indefinitely in a linear fashion. Of course this cannot be done but it can be approximated by a sawtooth wave as shown in Fig. 4.2. The necessary phase conditions for sawtooth operation are also shown in the figure. Therefore if the phase can be made to change  $2\pi$  radians  $F$  times a second, the frequency will be shifted  $F$  cycles. In practice this linear change in phase is obtained by a sawtooth modulating the circuit potential.

Let us now consider this shifting action from the point of view of modulating the transit time. The transit time (as the phase) is almost a linear function of circuit potential; by modulating the average circuit potential we are actually varying the transit time. Assume that a large bunch of electrons enter the interaction region during each r-f cycle. Figure 4.3 illustrates the flight lines over more than one



a. IDEAL PHASE-MODULATION DEVICE FUNCTION.



b. MODULATION VOLTAGE AND PHASE VS. TIME.

FIG. 4.2 IDEAL PHASE CONDITIONS FOR SERRODYNE.

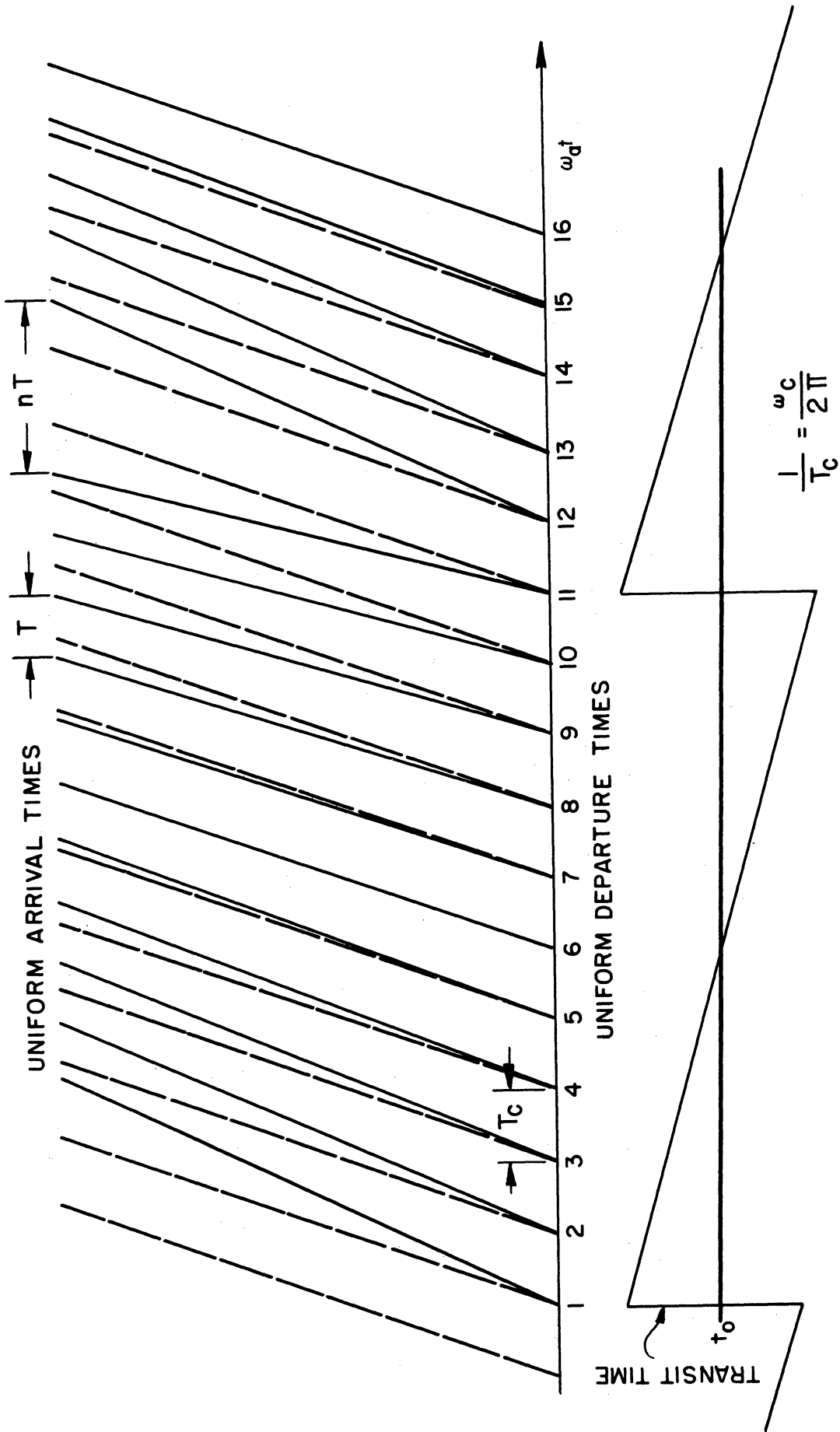


FIG. 4.3 FLIGHT LINE DIAGRAM OF SERRODYNE.

modulating cycle. Each flight line represents the entire bunch of electrons that entered during an r-f cycle. Since one bunch enters during each r-f cycle the bunches are initially evenly spaced in time, separated by  $1/f_c$  seconds where  $f_c$  is the carrier frequency. If the tube is unmodulated the bunches arrive at the output still evenly spaced at  $1/f_c$  seconds. The gain mechanism has taken place within each bunch and the electrons constituting the bunch surely have changed position but the time orientation from bunch to bunch is unchanged. When the transit time is modulated, the bunches arrive in a different time orientation than they had at the entrance. For a linear transit time modulation, the bunches arrive still uniformly spaced but with a different spacing than  $1/f_c$  seconds. Assume this new spacing is  $1/f_t$  seconds, the carrier frequency has been shifted to  $f_t$  cycles per second. To get perfect frequency translation it is necessary to satisfy the phasing conditions shown in Fig. 4.3, i.e., the space between the bunches must be an integral number of  $1/f_c$  periods.

#### 4.6 Differences in Spectrum for TTM and PM

Cumming has shown that the output spectra of a transit-time modulated device and a phase-modulated device for the same modulation input are different. The difference is attributed to the fact that transit-time modulation alters a time delay which follows the generation of a periodic time function while phase modulation alters the phase during the time that the periodic function is being generated. Using Cumming's notation, the normalized spectral amplitude of the nth side-band in the vicinity of a TTM is given by

$$I = M_n [q, (1 + \rho_c) r_t \omega_c] \quad ,$$

where  $q$  is the depth of AM factor,  $r_t$  is the peak deviation in transit time over the modulation cycle,  $\rho_c$  is the ratio of the lowest frequency of the modulation signal to the r-f ( $\omega_a/\omega_c$ ).

The spectral line amplitude of a similar component with PM is given as

$$I = M_n(q, r_p) \quad ,$$

where  $r_p$  is the peak phase deviation and  $M_n$  is the same function as above.

For low modulation frequencies,  $\rho_c \ll 1$ . The product of time deviation and frequency is just the phase deviation, so that for low modulation frequencies the spectrum for TTM and PM will be the same. Furthermore, if one uses the quasi-stationary device functions, he must not use high-modulation frequencies as previously pointed out, hence, when conditions for the quasi-stationary approximation are valid, the PM and TTM spectra are the same.

## CHAPTER V. LOW-FREQUENCY BEAM MODULATIONS OF OTHER O-TYPE DEVICES

It is necessary to write two sets of equations to analyze an O-type electron tube. These are, of course, the electro-kinetic or ballistic equations which describe the motion of electrons in the tube, and the electromagnetic equations which describe the wave supported by the r-f structure surrounding the beam. All O-type devices amenable to one-dimensional analyses are characterized by the same ballistic equation although its form may be varied in some applications for reasons of mathematical simplicity. The circuit equation does assume different forms as the modes of propagation are varied from tube to tube. In a low-frequency beam modulation study of O-type devices, it is possible to use quasi-stationary ballistic equations very similar to those derived in Chapter 2 for the TWA, and in addition the circuit equation peculiar to the device under study.

In this chapter the modulation characteristics of two O-type tubes, the Crestatron and the Backward-Wave Oscillator (BWO) will be discussed. These two devices are similar in that gain is obtained by a beating of three waves rather than by an exponential growth of one wave as in the TWA. The Crestatron and BWO differ by the fact that the energy flows in the beam and the circuit are in the same direction for the Crestatron while they are oppositely directed in the BWO. In view of the energy flow considerations it can be seen that the Crestatron is stable while the BWO is inherently unstable. Since the unmodulated operation of these devices has been well covered in the literature, the remaining discussion will be primarily devoted to a study of their modulation characteristics.

### 5.1 Low-Frequency Beam Modulations of a Crestatron

The Crestatron<sup>4</sup> is a shortened TWA with the electron beam injected at a greater velocity than the cold-circuit phase velocity. For a tube with  $C$  of 0.10 the beam velocity is about 30-40% higher than the circuit velocity, while for a  $C$  of 0.05 the beam velocity is about 10% higher than the circuit velocity. With these velocity differences there is no exponential growth, however, the circuit is not completely decoupled from the beam and three waves are set up which propagate with different phase velocities and produce an interference pattern. If the tube length is adjusted to the crest of the circuit voltage interference pattern, a net gain is obtained. The modulation equations derived in Section 2.2 apply to the Crestatron when all three waves are taken into account during the computation of the amplitude and phase modulation. The modulation device functions for the Crestatron are given in Eqs. 2.30 and 2.34. The modulation characteristics for a hypothetical Crestatron without space charge and loss have been computed. The following unmodulated parameters were chosen,

$$\begin{aligned}C_o &= 0.10 \\QC_o &= 0 \\d_o &= 0 \\b_o &= 2.4\end{aligned}$$

Under these operating conditions, a gain of 6.54 db was obtained with a tube length of  $2\pi C_o N_s = 144^\circ$ . The variations of the modulation propagation constants as functions of the beam average potential and current modulation can be determined from the secular equation for the TWA, Eq. 2.16. Plots of the propagation constants are shown in Figs. 5.1 and 5.2. It can be seen from these curves that as the average beam voltage is

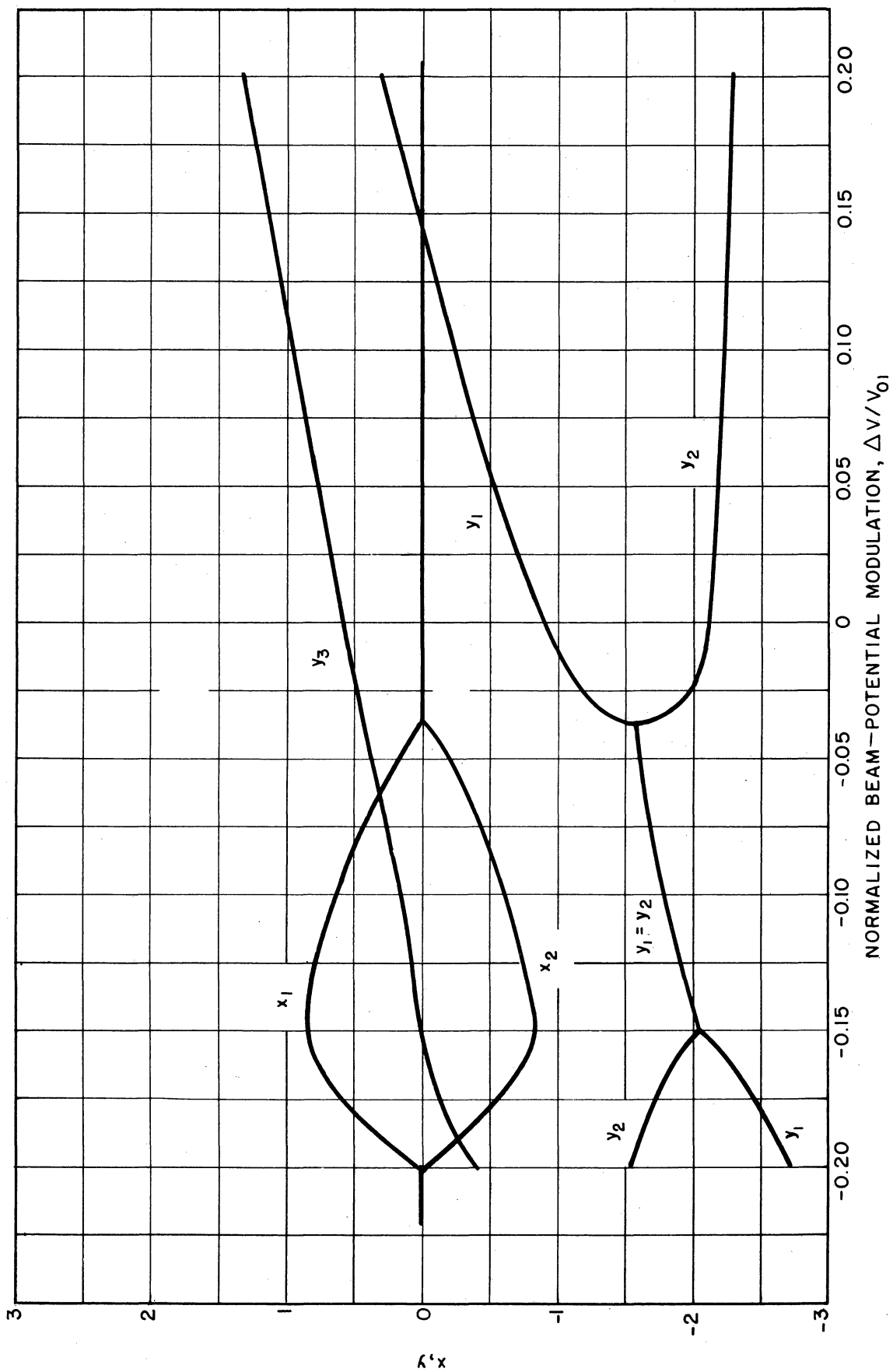


FIG. 5.1 PROPAGATION CONSTANTS FOR A CRESTATRON WITH MODULATED BEAM POTENTIAL. ( $C_0 = 0.10$ ,  $d_0 = 0$ ,  $QC_0 = 0$ ,  $b_0 = 2.4$ )



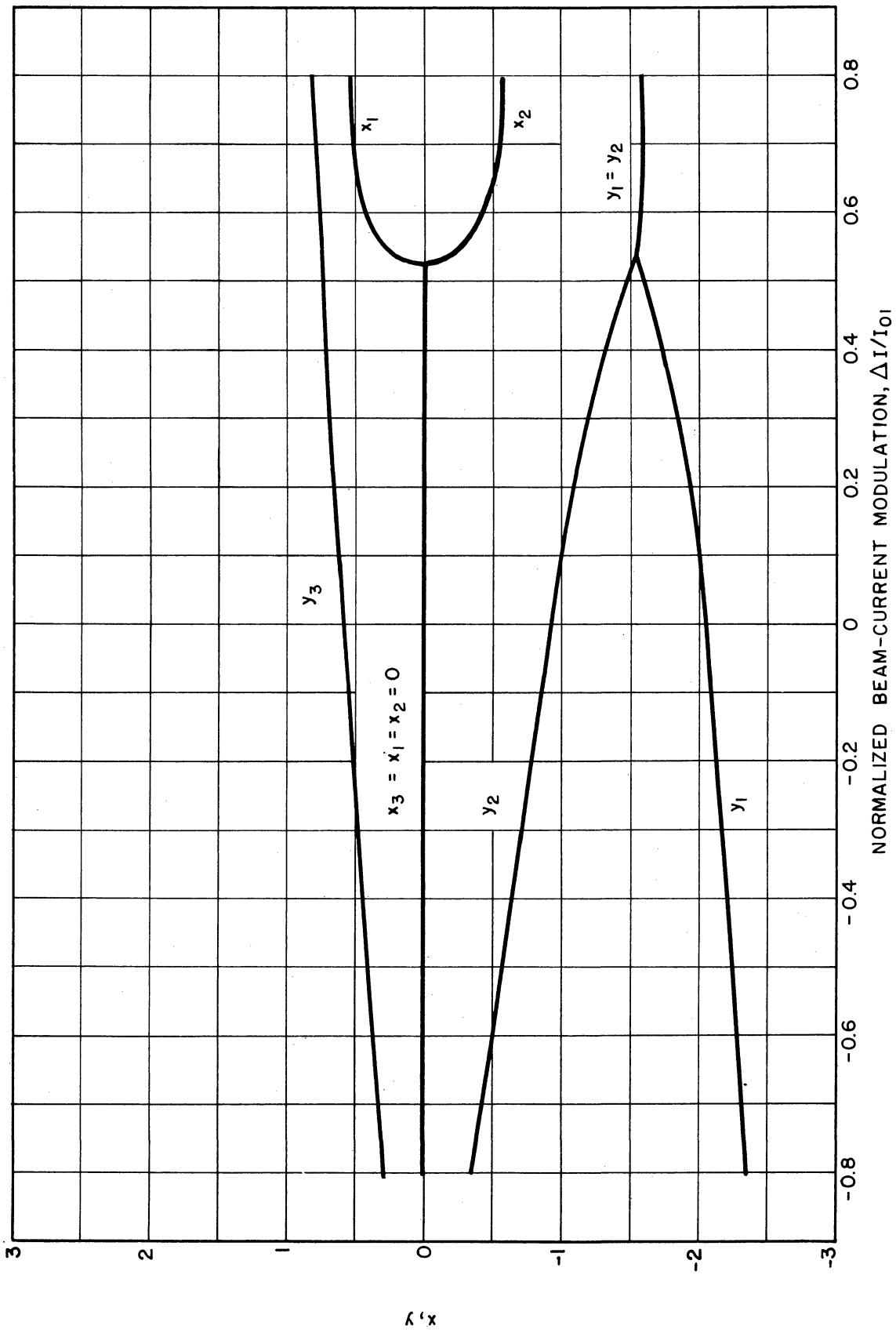


FIG. 5.2 PROPAGATION CONSTANTS FOR A CRESTATRON WITH MODULATED BEAM CURRENT.  
( $C_0 = 0.10, d_0 = 0, Q_{C0} = 0, b_0 = 2.4$ )

reduced or as the current level is increased, the tube will go over to normal TWA operation with growing-wave gain.

The variation of the wave amplitudes can be calculated from Eq. 2.25. This is shown in Figs. 5.3 and 5.4. For the parameter values chosen, the phase of the initial wave amplitudes is either 0 or 180° so that Figs. 5.3 and 5.4 give a complete description of the wave amplitudes.

Finally the modulation device functions are plotted in Figs. 5.5 and 5.6. A linear amplitude-modulation is obtained over a moderate range of both beam-potential and current modulations. The change in phase is greater during the beam-current modulation. It appears that the beam-voltage modulated Crestatron might be useful as an amplitude-modulation device with a linear amplitude variation (in db) and with little spurious phase modulation. It must be emphasized however that only relatively low modulation indices can be obtained since the Crestatron is a low gain device.

## 5.2 Low-Frequency Beam Modulations of a Backward-Wave Oscillator

A detailed modulation study of the BWO would involve determining the change in frequency and power level of the operating oscillator as its average beam potential and current are varied. The characteristics of the operating or unmodulated BWO can only be determined from a nonlinear analysis of the device since it is the nonlinearities that ultimately determine the operation levels and frequency. Nonlinear analysis of the unmodulated BWO have been carried out by Sedin<sup>39</sup> and by Rowe<sup>40</sup>. Sedin modified Nordsieck's<sup>18</sup> TWA equations by changing the sign of the circuit impedance, while Rowe\* used the more general interaction equation and

---

\* Some of Rowe's calculations with space charge present contain an error due to a wrong sign in the space-charge term.

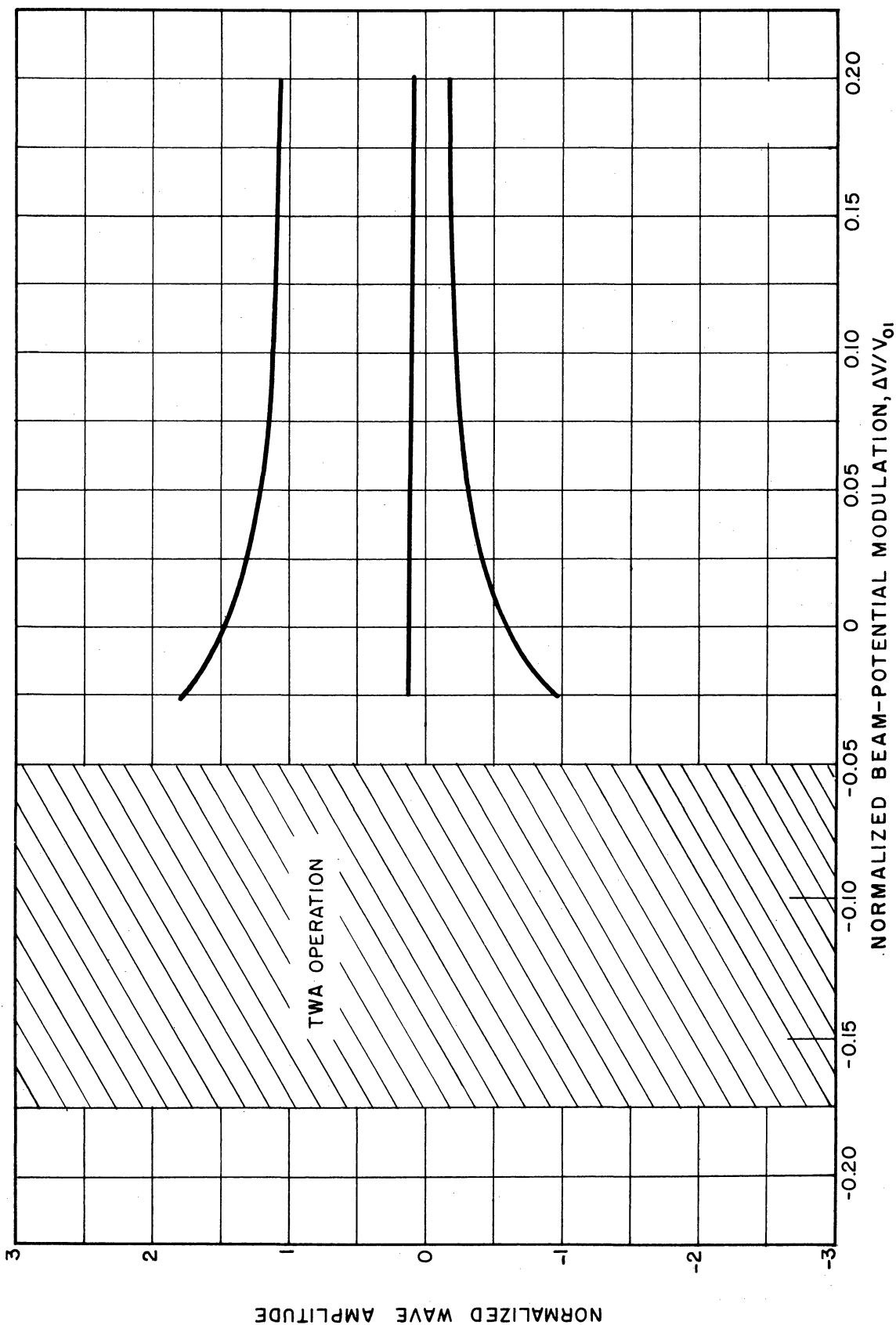


FIG. 5.3 VARIATION OF CRESTATRON WAVE AMPLITUDES DURING BEAM-POTENTIAL MODULATION  
( $C_0 = 0.10$ ,  $d_0 = 0$ ,  $QC_0 = 0$ ,  $b_0 = 2.4$ )

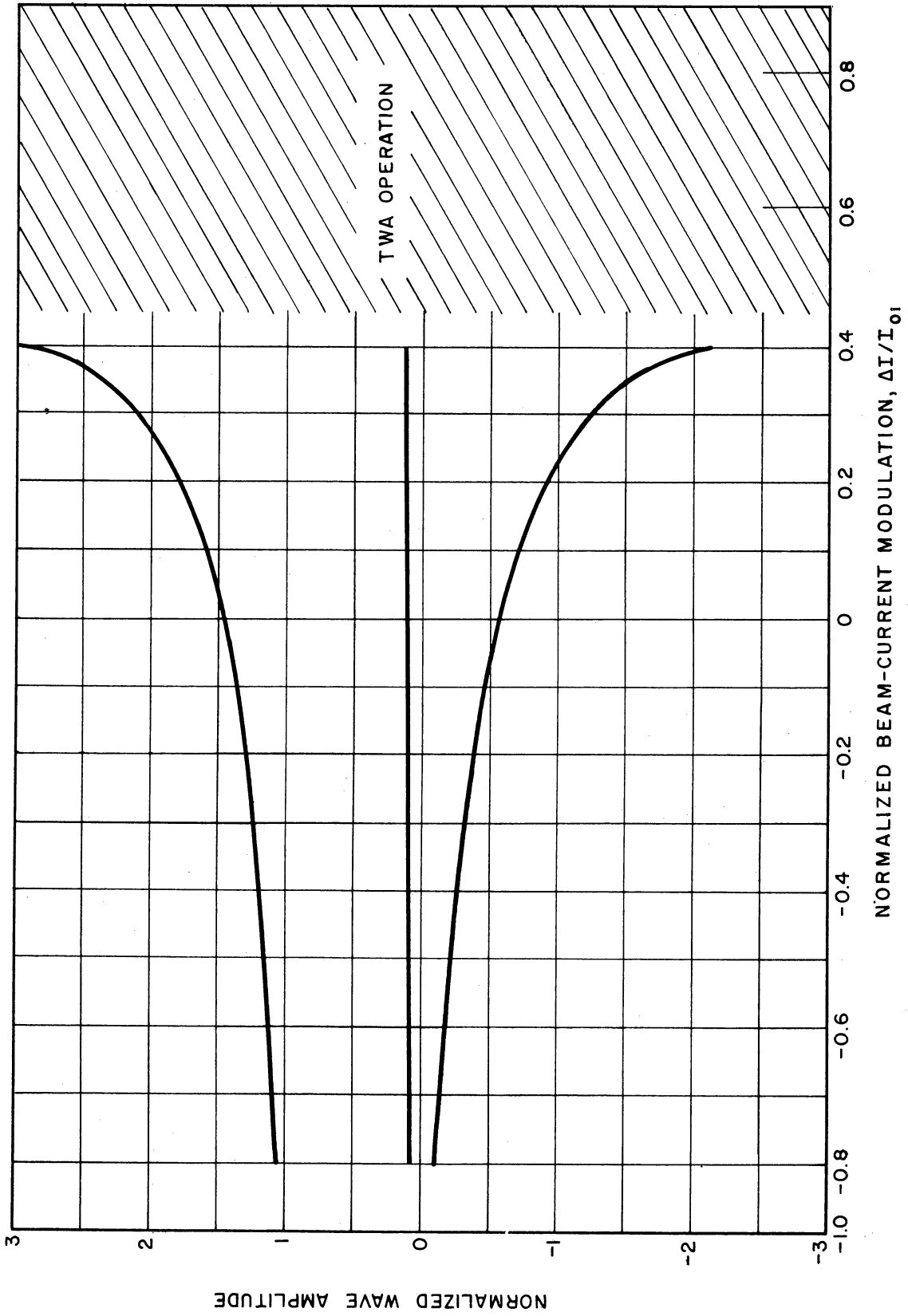


FIG. 5.4 VARIATION OF CRESTATRON WAVE AMPLITUDES DURING BEAM-CURRENT MODULATION.  
( $C_0 = 0.10$ ,  $d_0 = 0$ ,  $QC_0 = 0$ ,  $b_0 = 2.4$ )

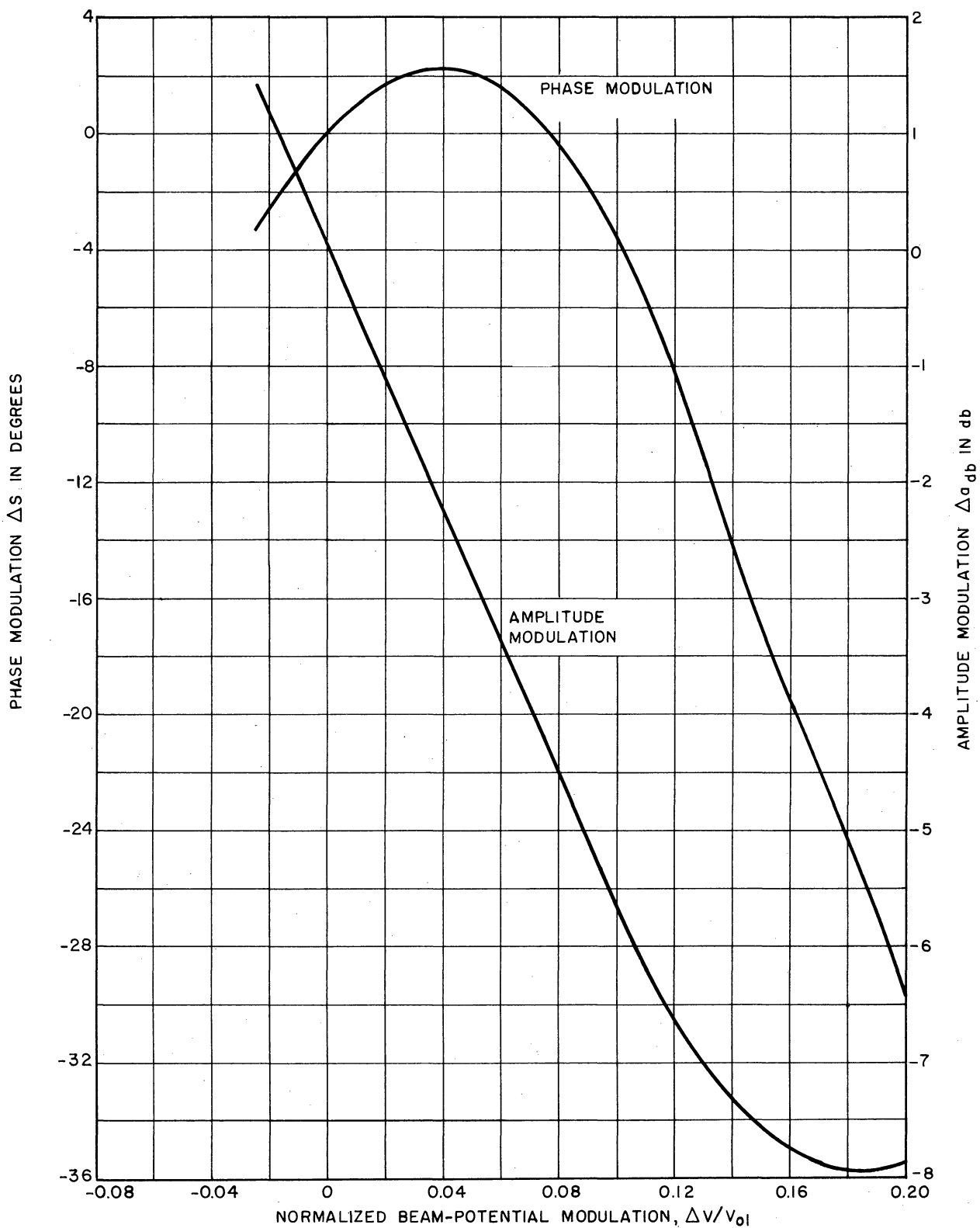


FIG. 5.5 MODULATION DEVICE FUNCTIONS FOR CRESTATRON WITH BEAM-POTENTIAL MODULATION. ( $C_0=0.10$ ,  $d_0=0$ ,  $QC_0=0$ ,  $b_0=2.4$ )

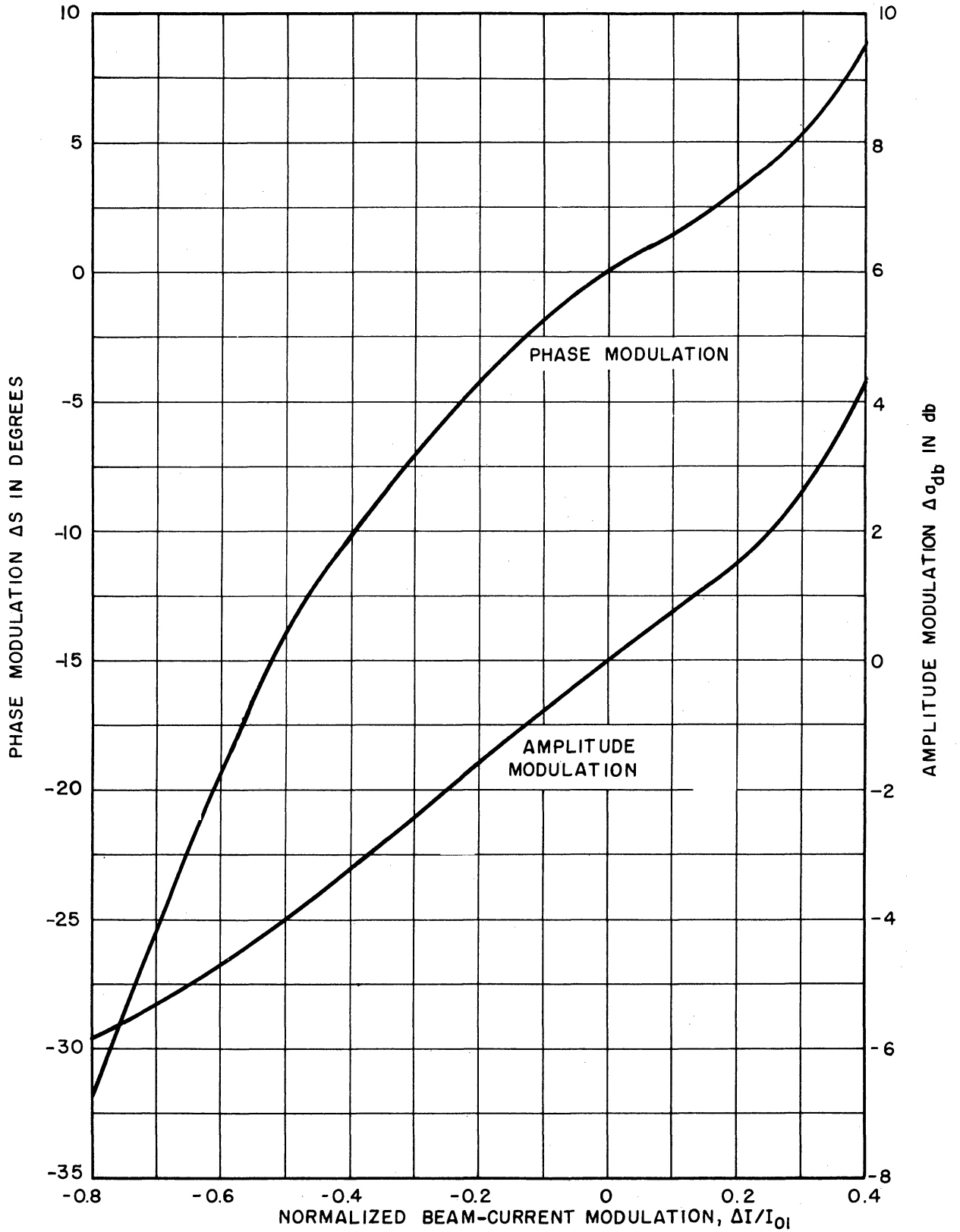


FIG. 5.6 MODULATION DEVICE FUNCTIONS FOR CRESTATRON WITH BEAM-CURRENT MODULATION. ( $C_0 = 0.10$ ,  $d_0 = 0$ ,  $QC_0 = 0$ ,  $b_0 = 2.4$ )

also changed the sign of the impedance. In each of these papers the authors experienced considerable difficulty and expense in determining operating points. The major difficulty is that the boundary conditions have to be found by a trial and error procedure. This involves integrating the BWO equations for a series of trial boundary conditions. The conditions that result in a zero line voltage somewhere along the tube represent an operating point.

In a modulation study of the BWO, it is necessary to include in addition to the variable average beam parameters a variable frequency as a function of the average beam conditions. Allowing the frequency to vary means that dispersion and impedance variation effects must be accounted for; this implies that an r-f structure must be specified. After selecting an r-f structure a set of quasi-stationary equations can be derived to describe the modulation characteristics. The solution of these equations would involve a difficult trial and error procedure which involves not only guessing of the boundary conditions but would further entail guessing the new frequency. In view of the difficulties that would be encountered, it was decided not to attempt to solve the modulation problem using the Lagrangian approach. Due to the severe bunching effects shown theoretically by Sedin<sup>39</sup> and experimentally by Gewartowski<sup>44</sup> it was decided that a hydrodynamical model using nonlinear equations would not be valid. The modulation study presented below will discuss only the effect of modulation on the start-oscillation conditions.

#### 5.2.1 The Effect of Modulation on the Start-Oscillation Conditions

At start oscillation, the BWO behaves as a linear device and therefore can be investigated using the small-signal approach developed for the TWA but with a change in the sign of the impedance terms. This method involves

determining propagation constants, wave amplitudes and finally the necessary conditions on tube length and velocity injection parameter  $b$  to drive the line voltage to zero at some point along the circuit. This is essentially the approach of Heffner<sup>41</sup> and Johnson<sup>42</sup>. A more straightforward, but not as accurate method would be to program the differential equations on an analog computer and determine the start-oscillation conditions by a trial and error procedure. The advantage of using the analog computer is that one can easily vary parameters by changing a potentiometer setting. The latter method is the one to be used in the modulation study. Grow<sup>43</sup> has previously solved for the start-oscillation conditions using an analog computer.

The model used for BWO study is shown in Fig. 5.7. The linearized ballistic equations for the modulated BWO are the same as those given for the linear TWA and are written below. As mentioned above, the frequency is a function of the modulation conditions\* and is no longer a constant as with the TWA.

$$\eta E_T + j \omega(M)v + u_{o1} \left(1 + \frac{\Delta V}{V_{o1}}\right)^{1/2} \frac{dv}{dz} = 0 \quad (5.1)$$

$$\rho_{o1} \left(\frac{1 + \frac{\Delta I}{I_{o1}}}{M^3}\right)^{1/2} \frac{dv}{dz} + u_{o1} \left(1 + \frac{\Delta V}{V_{o1}}\right)^{1/2} \frac{d\rho}{dz} + j\omega(M)\rho = 0 \quad (5.2)$$

$E_T$  is the total field acting on an electron. The fundamental space-charge field can be found using a technique similar to that used for the large-signal TWA with the result

---

\*  $\omega(M)$  is defined as the operating frequency as a function of the applied modulation.



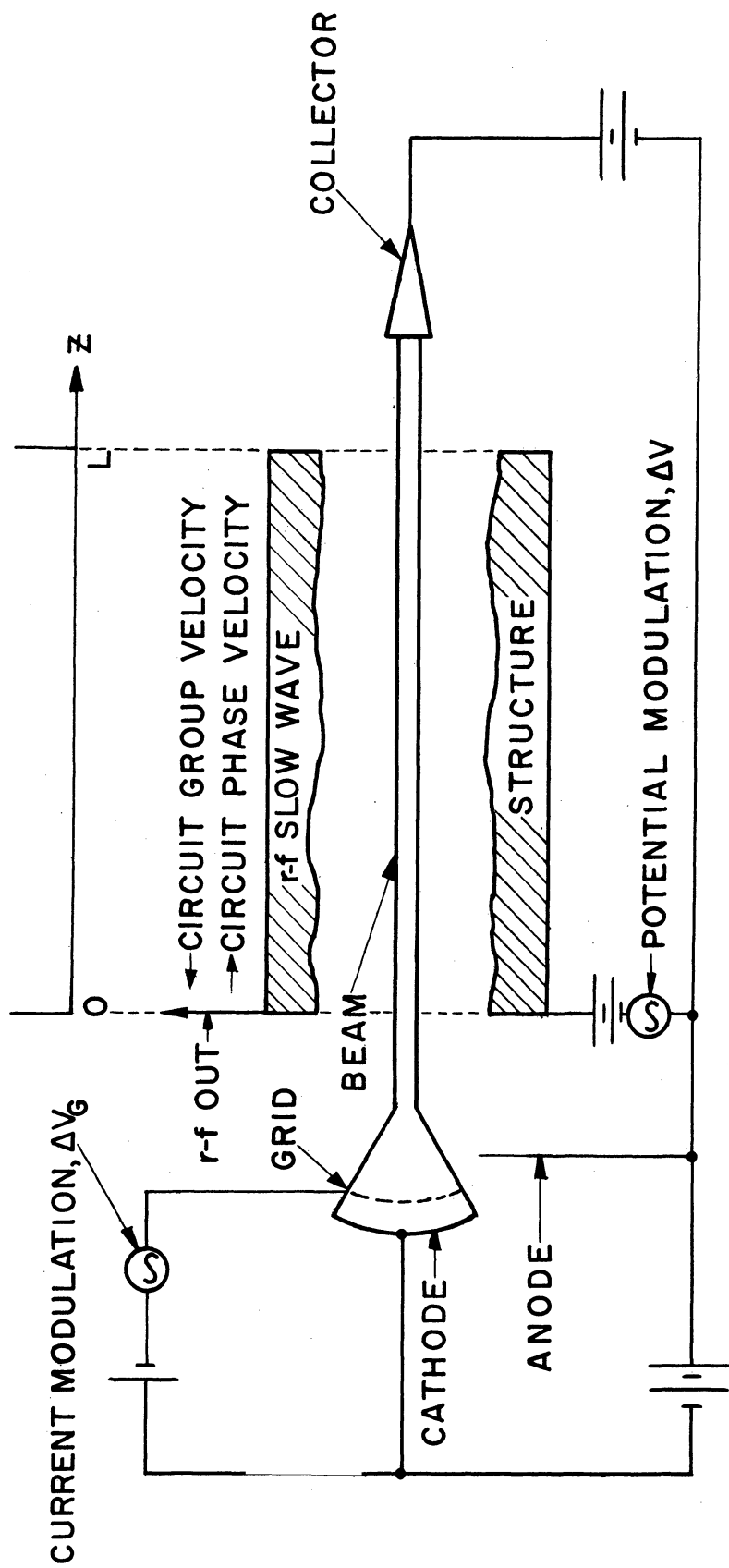


FIG. 5.7 MODEL FOR ANALYSIS OF MODULATED BWO

$$E_s = j \frac{u_{o1}^2 \omega_{po}^2}{I_{o1} |\eta|} \frac{R^2(M)}{\omega(M)} \frac{v_{c1}(M)}{u_{o1}} \rho \quad (5.3)$$

where  $R(M)$  = Plasma Frequency Reduction factor

$v_{c1}(M)$  = cold-circuit phase velocity of the interacting circuit mode.

The circuit equation for the BWO, allowing for variable frequency can be written as

$$\begin{aligned} \frac{d^2V}{dz^2} + \beta_o^2(M)V + j \frac{R_e(M)\beta_o(M)}{Z_o(M)} V \\ = -\omega(M)Z_o(M)\beta_o(M)\rho - jR_e(M)\omega(M)\rho \quad , \quad (5.4) \end{aligned}$$

where  $\beta_o(M)$  = cold radian wave number of interacting circuit mode

$R_e$  = series circuit resistance, see Fig. 5.7

$Z_o$  = characteristic circuit impedance of interacting mode.

At this point it is convenient to introduce several normalizing factors and also to assume that the loss is constant with frequency. This last assumption is questionable but in the BWO, the loss is usually kept quite small so that neglecting variations of this factor which contributes very little will not appreciably change the final result. Define

$$\xi_1 = \left(1 + \frac{\Delta V}{V_{o1}}\right)^{1/2}$$

$$\xi_2 = \left(1 + \frac{\Delta I}{I_{o1}}\right)^{1/2}$$

also

$$\zeta_1 = \frac{\beta_o(M)}{\beta_{o1}(M=1)}$$

$$\zeta_2 = \frac{Z_o(M=1)}{Z_o(M)}$$

$$\zeta_3 = \frac{\omega(M)}{\omega_o}$$

$$F(M) = \frac{R^2(M)}{R^2(M=1)} \frac{1}{\zeta_1}$$

$$y = \beta_{eo} C_o z \quad (5.5)$$

When the factors of Eq. 5.5, and definitions of  $C_o, QC_o, b_o$  and  $d_o$  given in Eq. 2.13 are introduced into Eqs. 5.1 through 5.4, the following is obtained,

$$\xi_2 \frac{dv}{dy} + \xi_1 \frac{d\rho}{dy} + \frac{j\rho}{C_o} = 0 \quad (5.6)$$

$$\frac{1}{2} \frac{dV}{dy} + j \frac{4C_o QC_o}{(1-2C_o \sqrt{QC_o})^2} \frac{\rho}{1+C_o b_o} \frac{F(M)}{\zeta_3} = \xi_1 \frac{dv}{dy} + j \frac{v}{C_o} \quad (5.7)$$

$$\begin{aligned} \frac{d^2V}{dy^2} + \left( \frac{1+C_o b_o}{C_o} \right)^2 \left( \frac{\xi_1}{\zeta_3} \right)^2 V + 2j \frac{d_o}{C_o} (1+C_o b_o) \frac{\xi_1 \xi_2}{\zeta_3} V \\ = 4C_o (1+C_o b_o) \frac{\xi_1}{\zeta_2 \zeta_3} \rho + j \frac{8C_o^2 d_o}{\zeta_3} \rho \quad (5.8) \end{aligned}$$

The above equations are the normalized equations representing the modulated BWO. The solution of this set of equations on an analog computer is discussed in Appendix E.

The boundary conditions for the BWO are that the beam enters the circuit region with no bunching,

$$v(0) = \rho(0) = 0 \quad , \quad (5.9)$$

and that the impedance seen looking into the circuit at the r-f output is

$$Z_o = - \frac{V(0)}{I(0)} \quad . \quad (5.10)$$

In the linear analysis, the signal level at the r-f output is arbitrary. For the arbitrary signal level, Eqs. 5.9 and 5.10 are equivalent to

$$\left( \frac{dV}{dy} \right)_{y=0} = - V(0) \left[ j\zeta_2\zeta_3 \frac{1+C_o b_o}{C_o} - 2d_o\zeta_2\zeta_3 \right] \quad (5.11)$$

As mentioned above, in order to solve the equations it is necessary to specify a structure. The r-f circuit selected is the bifilar helix. The important properties of the bifilar helix are given in the literature<sup>45, 46</sup> and are shown in Fig. 5.8. The normalized frequency parameters  $\zeta_1$ ,  $\zeta_2$ ,  $\zeta_3$  may be calculated using Fig. 5.8. The parameters  $\zeta_1$  and  $\zeta_2$  can easily be determined in terms of the frequency parameter. This is shown in Fig. 5.10. The frequency parameter is to be determined by trial and error. An initial value may be estimated from the  $\omega$ - $\beta$  diagram for a particular unmodulated point. A typical  $ka'$  for an unmodulated BWO is 0.3; using this  $ka'$ , a series of initial guesses for the frequency as a function of  $\zeta_1$  are shown in Fig. 5.9. The factor F is shown in Fig. 5.11 for an annular beam. The data for the plasma frequency reduction of a hollow beam was taken from a paper by Branch and Mihran<sup>48</sup>.

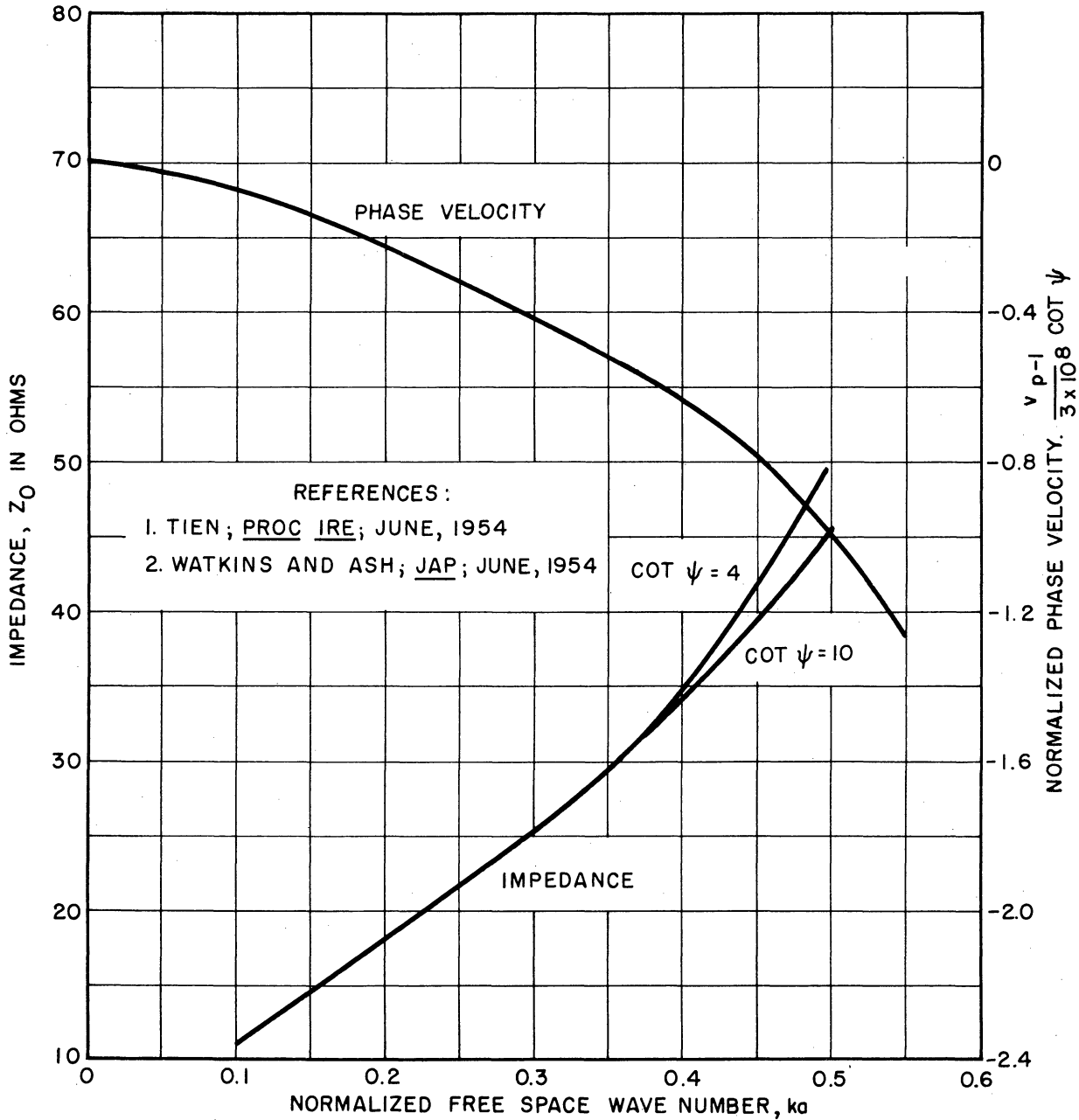


FIG. 5.8 IMPEDANCE<sup>1</sup> AND PHASE VELOCITY<sup>2</sup> CHARACTERISTICS OF (-1) MODE OF BIFILAR HELIX.

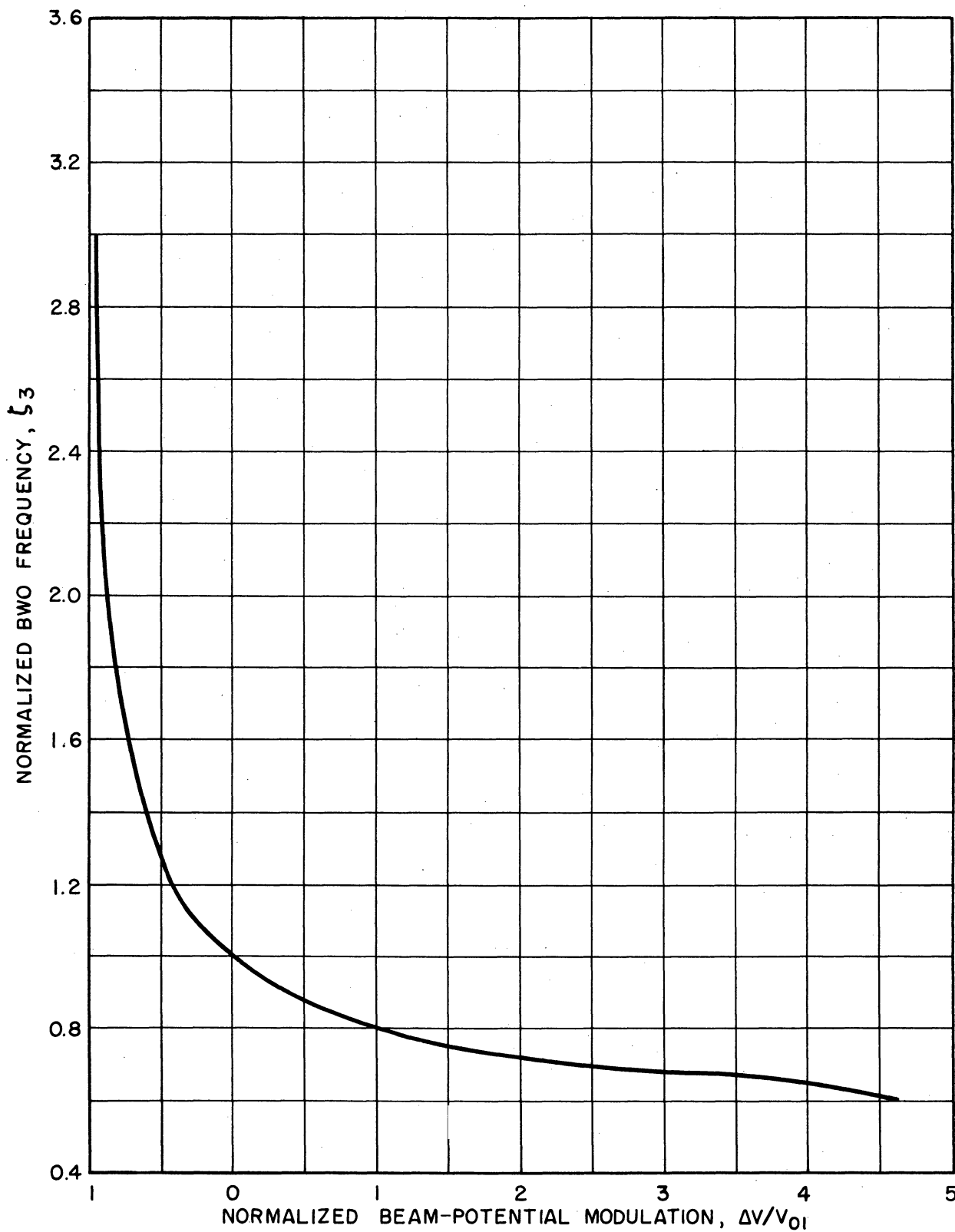


FIG. 5.9 FIRST ESTIMATE OF NORMALIZED FREQUENCY,  $\zeta_3$ , OBTAINED FROM  $\omega$ - $\beta$  DIAGRAM. (BIFILAR HELIX; AT  $\Delta V=0$ ,  $k_a=0.30$ )

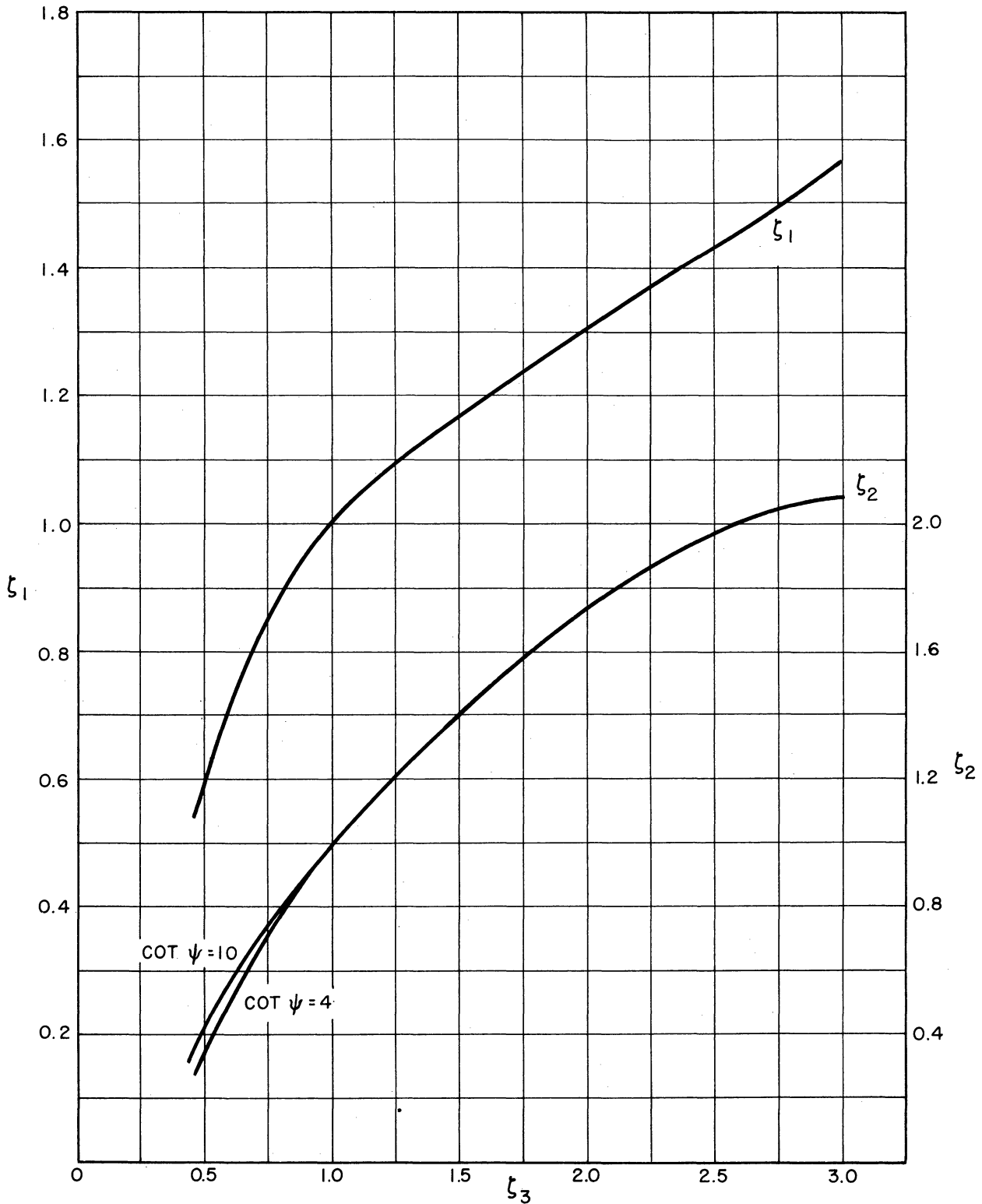


FIG. 5.10 BWO MODULATION PARAMETERS  $\zeta_1$  AND  $\zeta_2$  AS FUNCTIONS OF FREQUENCY,  $\zeta_3$ . (BIFILAR HELIX; AT  $\Delta V = 0$ ,  $k\alpha = 0.30$ )

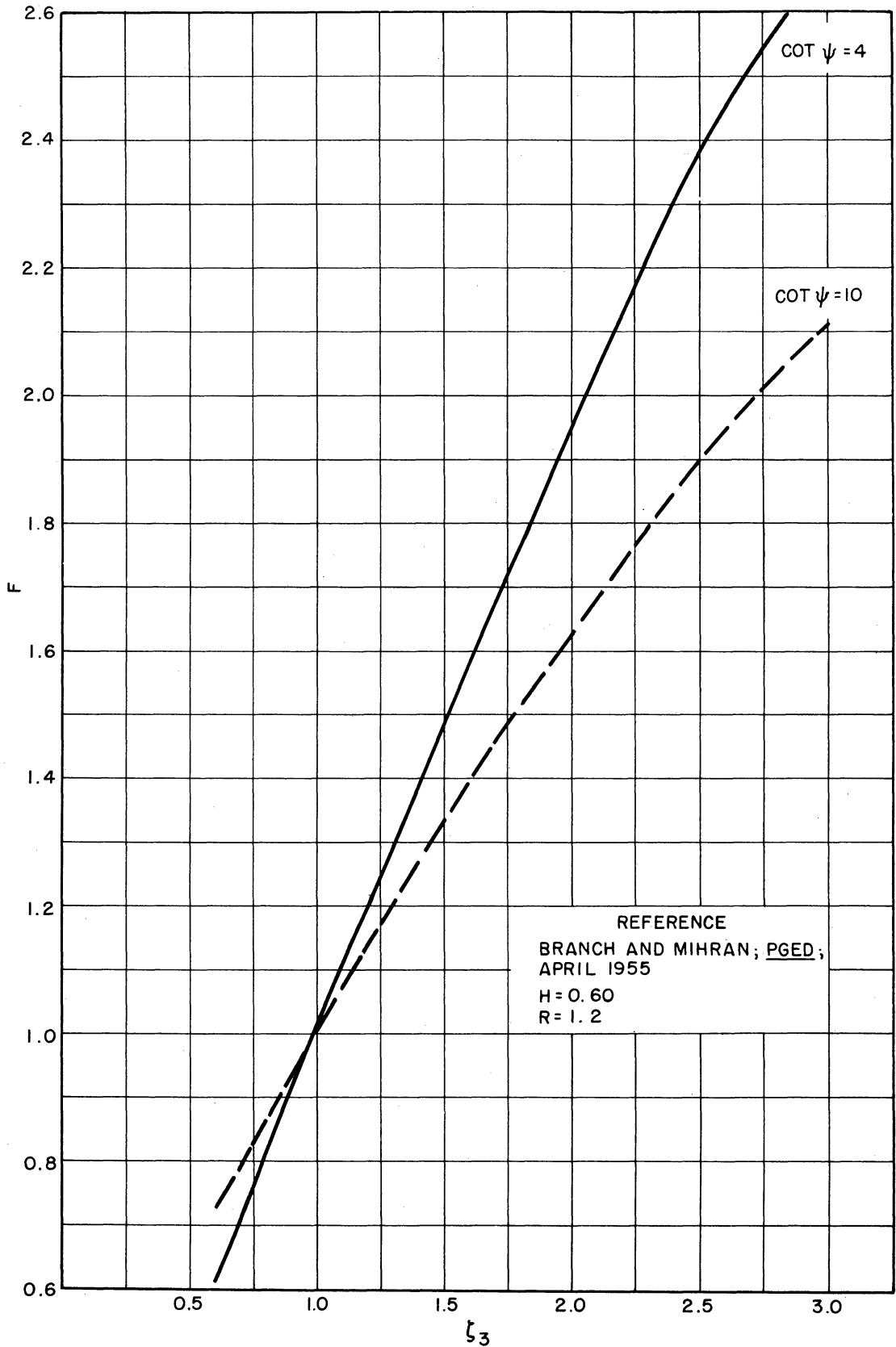


FIG. 5.11 BWO MODULATION PARAMETER  $F$  AS FUNCTION OF FREQUENCY,  $\zeta_3$ . (BIFILAR HELIX; AT  $\Delta V = 0$ ,  $k\alpha = 0.30$ ; ANNULAR BEAM,  $H = 0.6$ ,  $R = 1.2$ )



Using the above curves and the technique outlined in Appendix E, the effect of a beam-voltage modulation on the required normalized start oscillation length and the normalized starting frequency of a typical BWO was determined. The results are shown in Figs. 5.12, 5.13, 5.14 and 5.15. The final frequencies are compared with the initial estimates on Figs. 5.12 and 5.14. It can be seen that the initial values are quite accurate at low modulation amplitudes, but are in error as  $\Delta V/V_{01}$  increases.

This particular method of calculating the start-oscillation conditions is recommended when the variation of starting frequency and required lengths is desired once an unmodulated operating point has been chosen. This method has the advantage of using only one set of parameter values.

5.2.2 Modulation of the BWO with Currents Higher than Start-Oscillation Current. As the current or the tube length is increased beyond the start-oscillation conditions, nonlinearities rapidly set in to limit the power output for a specific d-c beam input. As mentioned above, the Eulerian model must be abandoned in a nonlinear description of the BWO because of the severe bunching that takes place. The Lagrangian equations for the BWO can be derived in a manner similar to the derivation of the nonlinear TWA equations.

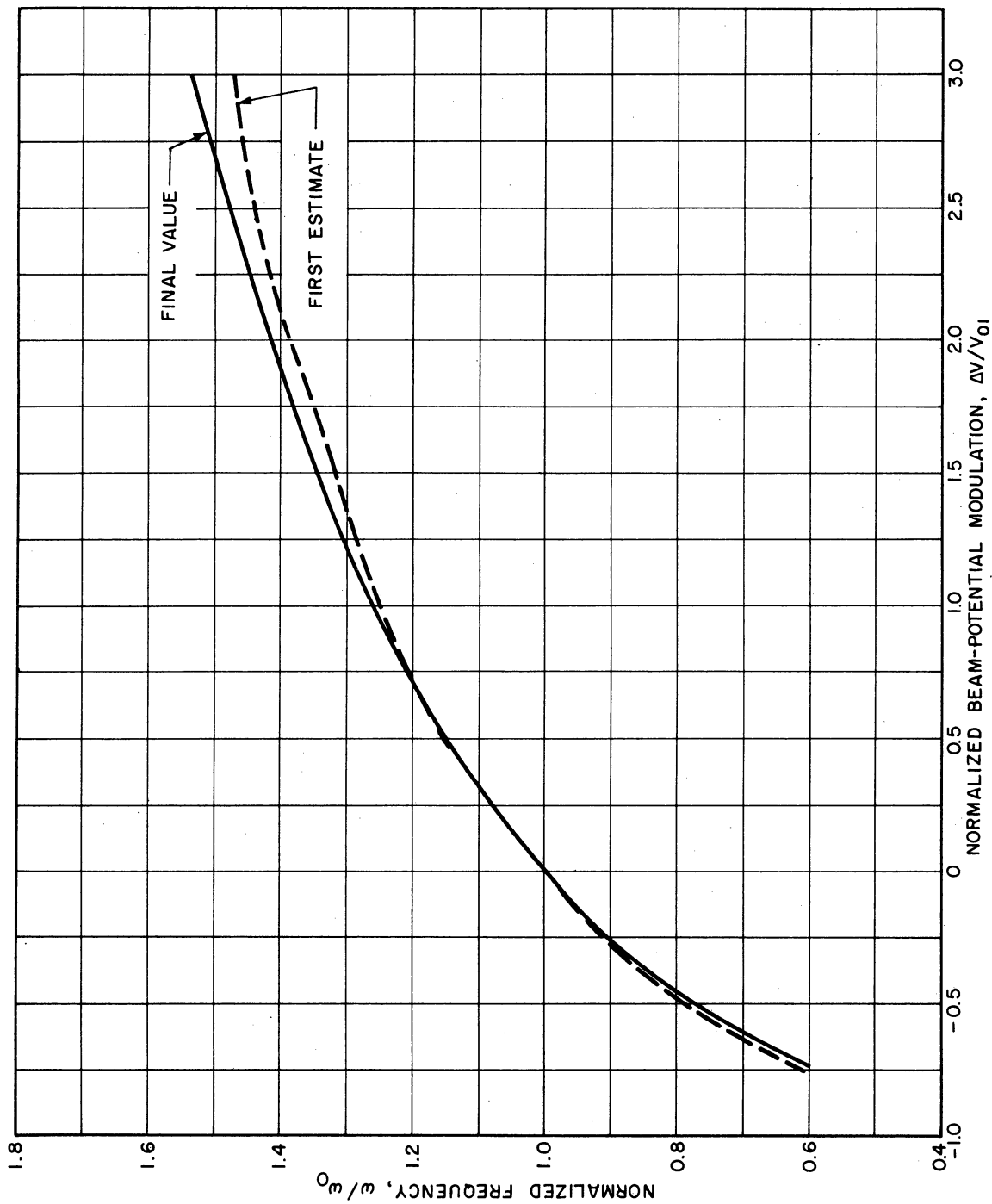


FIG. 5.12 VARIATION OF START-OSCILLATION FREQUENCY OF BWO AS FUNCTION OF BEAM-POTENTIAL MODULATION. ( $C_0=0.05$ ,  $QC_0=0$ ,  $d_0=0$ ,  $b_0=1.56$ ; BIFILAR HELIX; ANNULAR BEAM,  $H=0.60$ ,  $R=1.2$ ; AT  $\Delta V=0$ ,  $k_a=0.30$ )

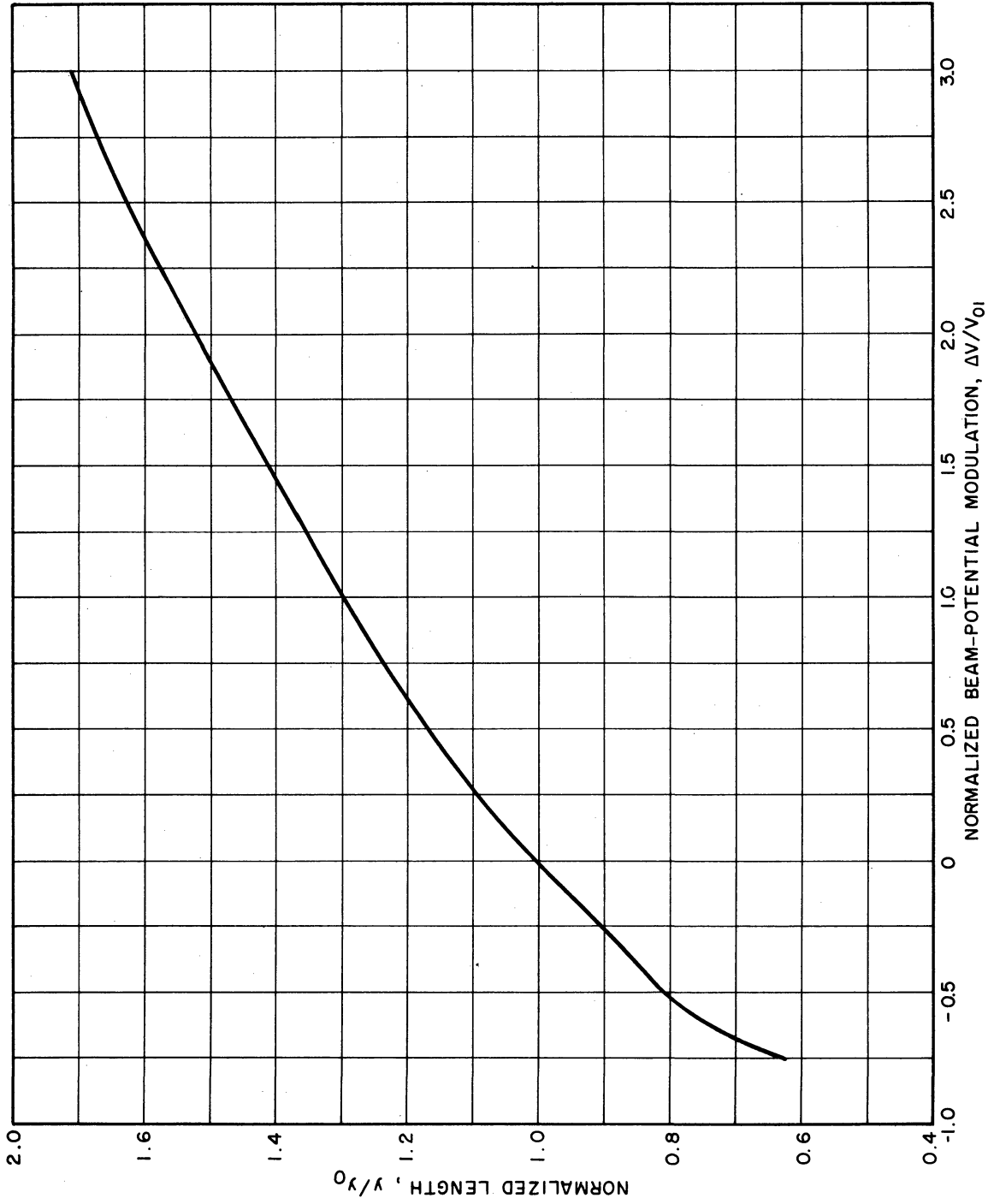


FIG. 5.13 VARIATION OF START-OSCILLATION LENGTH OF BWO AS FUNCTION OF BEAM-POTENTIAL MODULATION. ( $C_0=0.05$ ,  $QC_0=0$ ,  $d_0=0$ ,  $b_0=1.56$ ; BIFILAR HELIX; ANNULAR BEAM,  $H=0.60$ ,  $R=1.2$ ; AT  $\Delta V=0$ ,  $k\sigma=0.30$ )

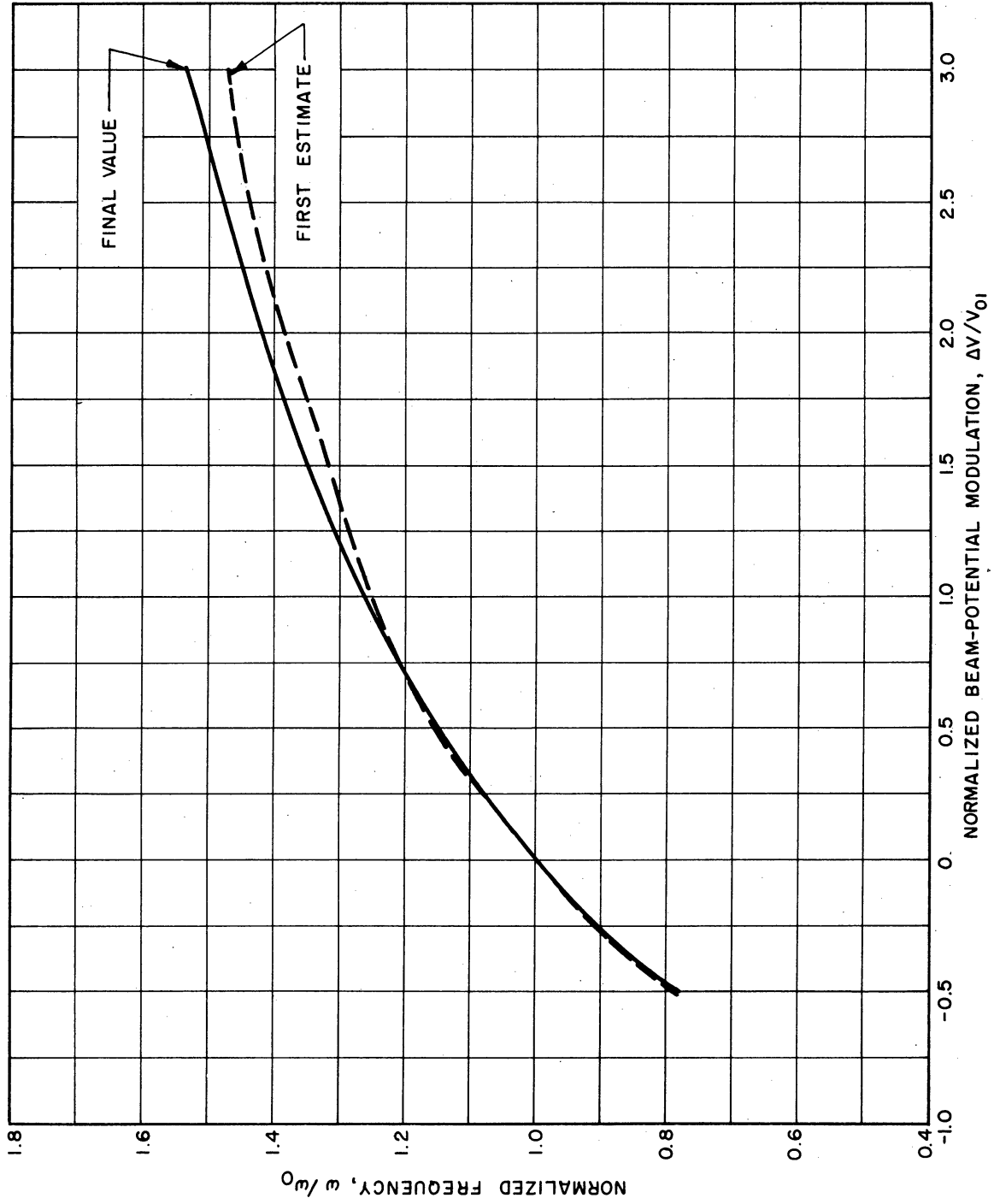


FIG. 5.14 VARIATION OF START-OSCILLATION FREQUENCY OF BWO AS FUNCTION OF BEAM - POTENTIAL MODULATION. ( $C_0=0.05$ ,  $QC_0=0.20$ ,  $d_0=0$ ,  $b_0=1.59$ ; BIFILAR HELIX; ANNULAR BEAM,  $H=0.60$ ,  $R=1.2$ , AT  $\Delta V=0$ ,  $k_a=0.30$ )

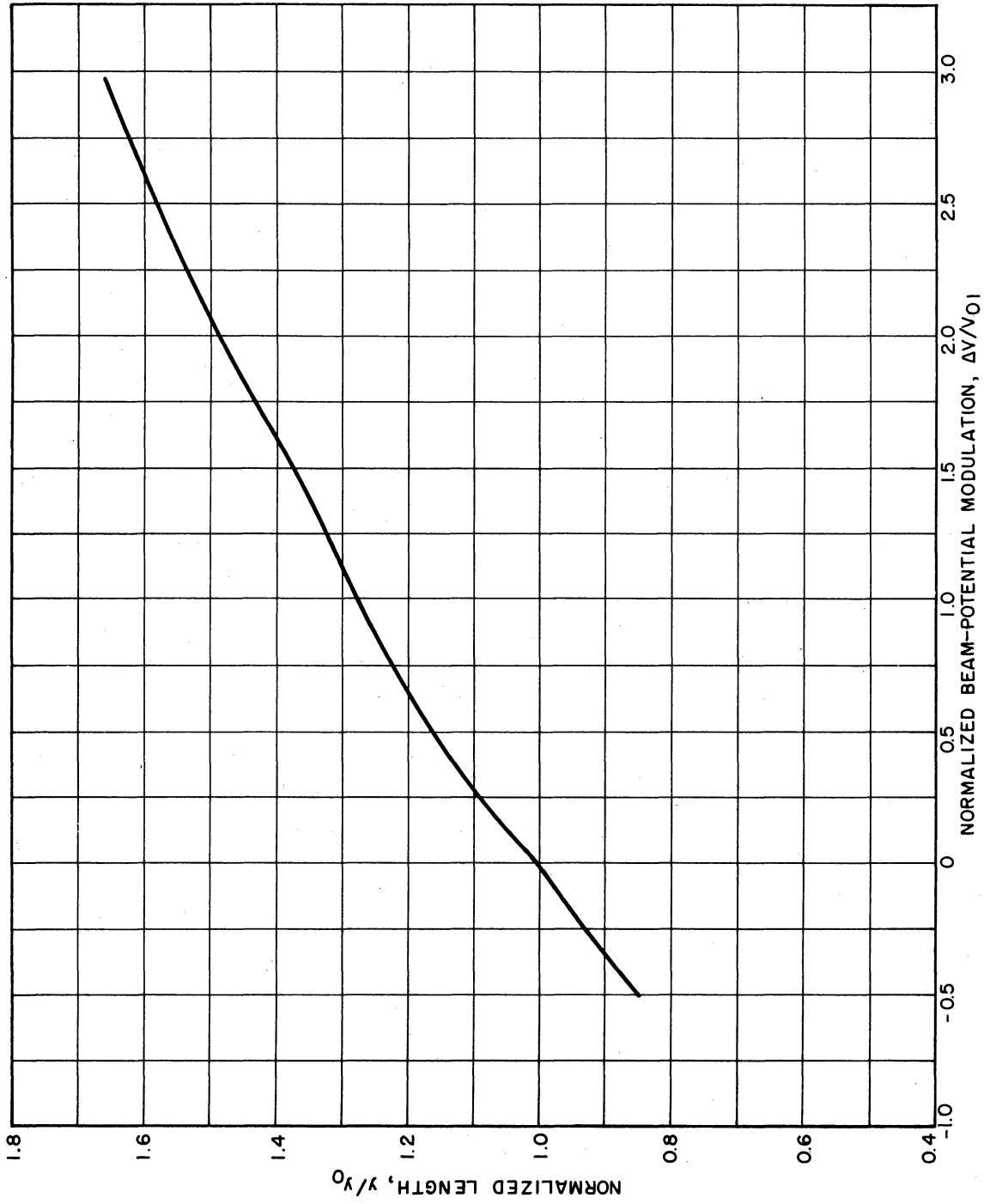


FIG. 5.15 VARIATION OF START-OSCILLATION LENGTH OF BWO AS FUNCTION OF BEAM - POTENTIAL MODULATION. ( $C_0=0.05$ ,  $Q_{C0}=0.02$ ,  $d_0=0$ ,  $b_0=1.59$ ; BIFILAR HELIX; ANNULAR BEAM,  $H=0.60$ ,  $R=1.2$ ; AT  $\Delta V=0$ ,  $k\alpha=0.30$ )

## CHAPTER VI. HIGH-FREQUENCY BEAM MODULATIONS

### 6.1 Introduction

The preceding chapters dealt with beam modulations at frequencies much lower than the r-f signal carried by the beam. Beam modulations at a rate comparable to the r-f will now be considered. This implies dropping the low-frequency restrictions listed in Section 2.1. Therefore time dependence of the modulations will have to be taken into account in the equations of motion. Another distinction that will be made is to permit the sideband signals to propagate at different velocities and see different impedances than the carrier.

For most applications of high-frequency modulations, the nonlinearities of the beam are used to generate sidebands. This principle is used in the traveling-wave tube mixer, frequency multiplier and divider, and the longitudinal-beam parametric amplifier. In all of these cases, two r-f signals are applied to the beam.

There is another type of high-frequency beam modulation in which only one frequency is used. This is called the single-frequency modulation and arises when a bunched beam enters an interaction region where the signal on the circuit is at the same frequency as the one producing the bunching. Obviously this is the noise or prebunched beam problem. Pierce<sup>1</sup> has analyzed the propagation of noise waves in a TWA where the noise signal is assumed to originate near the cathode at the carrier frequency. This noise bunches the beam and induces currents in the circuit which then grow as the beam travels through the interaction region. The prebunched signal may be coherent as in the case of the severed helix, or the helix output circuit on a klystron. Another example of coherent prebunching is the introduction of a prebunched beam into the circuit

region to produce higher efficiency or gain. This phenomenon is present under study by J. E. Rowe and J. G. Meeker of this laboratory.

When treating the small-signal tube, one uses the same propagation constants as found for the unmodulated tube. The initial wave amplitudes are different and are calculated by inverting the matrix shown in Appendix B.

Similarly, prebunching in a large-signal tube can be treated by using the same working equations as found for the unmodulated tube\*, but changing the initial conditions to conform to the prebunching. The initial phase  $\phi_{oi}$  and initial velocity  $u_{oi}(0)$  are calculated from a knowledge of the beam prebunching. The initial derivatives,  $(d\theta/dy)_o$  and  $(dA/dy)_o$  can be found directly from the small-signal equations or by using the working equations. When using the working equations to find the initial conditions, one must realize that the integrals encountered which describe the Fourier series components of charge density, do not vanish as they did before. It is now necessary to integrate over a cycle of r-f at the input to evaluate the charge density.

The subject matter of interest in this chapter is the interaction of two signals of different frequencies when both are simultaneously applied to a beam. The beam nonlinearities are introduced through the nonlinear Eulerian equations describing the hydrodynamical model of the beam. This method is certainly open to question since in general crossings of electron trajectories are apt to occur. Unfortunately the difficulties that would be encountered using a particle approach for this problem result in unwieldy equations so that for the purpose of the

---

\* The unmodulated equations are found by setting  $\Delta V = \Delta I = 0$  in Section 2.4.

high-frequency beam modulation, the stream is treated as a fluid, although nonlinearities are preserved.

In this chapter, the general form of the two-frequency beam modulated case will be studied. The specific solution for the longitudinal-beam parametric amplifier will be obtained from the general equations.

## 6.2 General Formulation of the Two-Frequency Problem

Consider a beam confined to axial flow within an enclosure. The enclosure may be a circuit capable of supporting a slow electromagnetic wave, or may be merely a drift tube which only reduces the plasma frequency. Assume that the beam has been modulated simultaneously by two different radio frequencies, and that at some point within the enclosure the modulation is strong enough to produce nonlinearities. In the presence of these nonlinearities, the signals of different frequencies no longer act orthogonally as they would if applied to a linear system. The signals will therefore interact and produce a large number of sidebands.

If the applied frequencies are  $\omega_1$  and  $\omega_2$ , the intermodulation or sideband frequencies will appear as spectral lines at the frequencies

$$|n\omega_1 \pm m\omega_2| \quad ,$$

where  $n$  and  $m$  may take on any integral value.

The electro-kinetic variables may be expanded in a double Fourier series of the applied frequencies. This expansion is similar to the one given in Chapter IV for the output wave of a TWA undergoing a low-frequency beam modulation. There is however a marked difference in that the low-frequency case sidebands behave in the same manner as the carrier, whereas each sideband in the high frequency modulations can react very differently in the interaction process. The expansions of the variables



are shown below.

$$\text{Charge density, } \rho(z,t) = \sum_{n=-\infty}^{\infty} \sum_{m=-\infty}^{\infty} \rho_{nm}(z) \exp j(n\omega_1+m\omega_2)t$$

$$\text{Total beam velocity, } v(z,t) = \sum_{n=-\infty}^{\infty} \sum_{m=-\infty}^{\infty} v_{nm}(z) \exp j(n\omega_1+m\omega_2)t$$

$$\text{Electric field intensity, } E(z,t) = \sum_{n=-\infty}^{\infty} \sum_{m=-\infty}^{\infty} E_{nm}(z) \exp j(n\omega_1+m\omega_2)t$$

$$\text{Convection current, } i(z,t) = \sum_{n=-\infty}^{\infty} \sum_{m=-\infty}^{\infty} i_{nm}(z) \exp j(n\omega_1+m\omega_2)t. \quad (6.1)$$

The Eulerian formulation will be used to describe the nonlinear interaction as mentioned in Section 6.1. The ballistic equations have been presented previously but are repeated again for reference. For a one-dimensional beam

$$\frac{\partial v}{\partial t} + v \frac{\partial v}{\partial z} = - \eta E \quad , \quad (6.2)$$

$$\frac{\partial i}{\partial z} + \frac{\partial \rho}{\partial t} = 0 \quad , \quad (6.3)$$

$$i = \rho v \quad . \quad (6.4)$$

The total electric field  $E$ , is composed of the superposition of the space-charge  $E_{sc}$  and an electromagnetic field  $E_c$ . The space-charge field is determined from Poisson's equation. In calculating the space-charge field, the geometry shall be considered as in previous chapters

by introducing the plasma-frequency reduction factor.

Poisson's equation is

$$\nabla \cdot \mathbf{E} = \frac{\rho}{\sigma \epsilon_0} , \quad (6.5)$$

where  $\sigma$  is the beam cross-sectional area.

The electromagnetic field is found from the forced Telegrapher's equation

$$\frac{\partial^2 V_c}{\partial z^2} - \frac{1}{v_c^2} \frac{\partial^2 V_c}{\partial t^2} + \frac{Z_0}{v_c} \frac{\partial^2 \rho}{\partial t^2} = 0 . \quad (6.6)$$

where

$$\mathbf{E}_c = - \nabla V_c ,$$

$v_c$  is the circuit velocity, and  $Z_0$  the impedance. The relations between the Fourier coefficient of Eqs. 6.1 can be found by substituting the above expansions into Eqs. 6.2 through 6.6.

It must be pointed out that there are degenerate frequencies possible. There can be many combinations of  $n$  and  $m$  such that  $n\omega_1 + m\omega_2$  are equal to a specific frequency. In this case, either a total variable can be defined to cover all those cases or the individual components can be found and added vectorially to obtain the resultant. A very important degenerate case, the parametric amplifier, is considered later on.

From the continuity Eq. 6.3,

$$\frac{di_{nm}}{dz} = - j(n\omega_1 + m\omega_2)\rho_{nm} . \quad (6.7)$$

The nmth component of Poisson's equation in one dimension reads

$$\frac{dE_{snm}}{dz} = \frac{R_{nm}^2 \rho_{nm}}{\sigma \epsilon_0}, \quad (6.8)$$

where  $R_{nm}$  is the plasma-frequency reduction factor at a frequency  $n\omega_1 + m\omega_2$ . There exists no d-c field within a neutralized one-dimensional beam, therefore the space-charge field can be expressed by

$$\frac{dE_{snm}}{dz} = j \frac{R_{nm}^2}{\epsilon_0 \sigma} \frac{1}{n\omega_1 + m\omega_2} \frac{di_{nm}}{dz}. \quad (6.9)$$

Note that in Eq. 6.9 the denominator  $n\omega_1 + m\omega_2$  never goes to zero since  $E$  is an a-c quantity. Equation 6.9 can be integrated to obtain the space-charge field

$$E_{snm}(z) = j \frac{R_{nm}^2}{\sigma \epsilon_0} \frac{i_{nm}(z)}{n\omega_1 + m\omega_2}. \quad (6.10)$$

The convection current as defined by Eq. 6.4 is the product of two infinite series. By virtue of the extension of the Cauchy product as shown in Appendix D, the Fourier series amplitudes of the current are

$$i_{nm} = \sum_{r,s=-\infty}^{\infty} \rho_{rs} v_{n-r,m-s}. \quad (6.11)$$

The summation can be separated into three terms as shown below.

$$i_{nm} = \sum_{r,s=-\infty}^{\infty}{}' \rho_{rs} v_{n-r,m-s} + \rho_0 v_{nm} + \sum_{r,s}{}'' \rho_{ors} v_{n-r,m-s}. \quad (6.12)$$

The first summation ( $\sum'$ ) is over all terms where  $n\omega_1 + s\omega_2$  does not vanish, the second term is for  $r,s$  equal to zero simultaneously and the

third summation ( $\sum''$ ) is for all other terms where  $r\omega_1 + s\omega_2$  vanishes. The vanishing of the frequency  $r\omega_1 + s\omega_2$  indicates a d-c term in the charge. Using the continuity relation, Eq. 6.7, permits Eq. 6.12 to be stated as

$$i_{nm} = j \sum_{r,s=-\infty}^{\infty} \left[ \frac{v_{n-r,m-s}}{r\omega_1+s\omega_2} \frac{di_{rs}}{dz} + v_{nm} \rho_o \right] + \sum'' \rho_{ors} V_{n-r,m-s} \quad (6.13)$$

The expression for the space-charge field can be substituted into the force equation to obtain the following relation for the nmth frequency;

$$j(n\omega_1+m\omega_2)v_{nm} + \sum_{r,s=-\infty}^{\infty} v_{rs} \frac{dv_{n-r,m-s}}{dz} = -j \eta \frac{R_{nm}^2 i_{nm}}{\epsilon_o \sigma (n\omega_1+m\omega_2)} + \eta \frac{dV_{cnm}}{dz} \quad (6.14)$$

The above form of the force equation applies only for non d-c terms. The nmth component of the circuit equation can be written as

$$\frac{d^2v_{cnm}}{dz^2} + \frac{(n\omega_1+m\omega_2)^2}{v_{cnm}^2} V_{cnm} - j \frac{Z_{onm}}{v_{cnm}} (n\omega_1+m\omega_2) \frac{di_{nm}}{dz} = 0 \quad (6.15)$$

Equations 6.13, 6.14 and 6.15, when used with the boundary conditions, describe the mixing interaction. Unfortunately this set of equations represents an infinite number of simultaneous nonlinear differential equations. To facilitate the solution of these equations and also because of the very nature of mixing devices, it will be assumed that one of the signals has a very large amplitude while the other is quite small. The large signal is the local oscillator or pump signal and has radian frequency  $\omega_1$ . The smaller amplitude signal mixes with the pump to produce sidebands, however the only sidebands to be considered will

be those occurring at  $\omega_1 \pm \omega_2$ . The sidebands around the second harmonic of the pump  $2\omega_1 \pm \omega_2$  may certainly be significant, however they will not be considered.

The nonlinearities shall be removed from the equations for the signal and sideband propagation by assuming that the pump or local oscillator signal propagates in the same known manner as it would if no signal were impressed at  $\omega_2$ . This assumption, (called the r-f linearization), is equivalent to the linearization used in the usual small-signal TWA or space-charge wave theory where it is assumed that the average velocity of the beam is invariant with distance. Once again just as in the small-signal TWA the transfer of energy is neglected.

Introduce the further assumption, (d-c linearization), that even though the pump signal is large, the r-f velocity disturbance at the pump frequency will be much less than the d-c beam velocity. Use of the r-f and d-c linearization permits the equations for the pump of ( $n=1, m=0$ ) frequency to be written in the form shown below.

$$\begin{aligned}
 i_{10} &= j \frac{u_0}{\omega_1} \frac{di_{10}}{dz} + v_{10} \rho_0 \\
 j\omega_1 v_{10} + u_0 \frac{dv_{10}}{dz} &= -j\eta \frac{R_{10}^2}{\sigma \epsilon_0 \omega_1} i_{10} + \eta \frac{dv_{c10}}{dz} \\
 \frac{d^2 v_{c10}}{dz^2} + \omega_1^2 \frac{V_{c10}}{v_{c10}^2} - j \frac{Z_{o10}}{v_{c10}} \omega_1 \frac{di_{10}}{dz} &= 0 \quad . \quad (6.16)
 \end{aligned}$$

Equations 6.16 are easily recognized; for positive  $Z_{o10}$  they represent a TWA, for negative  $Z_{o10}$  a BWO or BWA\* and finally, for vanishing  $Z_{o10}$  (implies  $V_{c10}$  also vanishes), they represent the space-charge wave

---

\* Backward-wave amplifier.

equations. When the solutions of Eqs. 6.16 are substituted into Eqs. 6.13, 6.14 and 6.15, a set of linear differential equations with variable coefficients will be obtained.

These equations are listed below for the nondegenerate frequency case. Note that in the equations, because of the "realness" of the variables

$$f_{-n-m} = f_{nm}^* .$$

Upper sideband (n=1,m=1)

$$i_{11} = j \left\{ \frac{v_{01}}{\omega_1} \frac{di_{10}}{dz} + \frac{v_{10}}{\omega_2} \frac{di_{01}}{dz} + \frac{u_0}{\omega_1 + \omega_2} \frac{di_{11}}{dz} \right\} + v_{11} \rho_0 , \quad (6.17a)$$

$$j(\omega_1 + \omega_2)v_{11} + \frac{d}{dz} (v_{10}v_{01}) + u_0 \frac{dv_{11}}{dz} = -j\eta \frac{R_{11}^2 i_{11}}{\epsilon_0 \sigma(\omega_1 + \omega_2)} + \eta \frac{dV_{c11}}{dz} , \quad (6.17b)$$

and

$$\frac{d^2 V_{c11}}{dz^2} + \frac{(\omega_1 + \omega_2)^2}{v_{c11}^2} V_{c11} - j \frac{Z_{011}}{v_{c11}} (\omega_1 + \omega_2) \frac{di_{11}}{dz} = 0 . \quad (6.17c)$$

Lower sideband (n=1,m=-1)

$$i_{1-1} = j \left( \frac{v_{10}}{-\omega_2} \frac{di_{01}^*}{dz} + \frac{u_0}{\omega_1 - \omega_2} \frac{di_{1-1}}{dz} + \frac{v_{01}^*}{\omega_1} \frac{di_{10}}{dz} \right) + v_{1-1} \rho_0 , \quad (6.18a)$$

$$j(\omega_1 - \omega_2)v_{1-1} + \frac{d}{dz} (v_{01}^* v_{10}) + u_0 \frac{dv_{1-1}}{dz} = -j\eta \frac{R_{1-1}^2 i_{1-1}}{\epsilon_0 \sigma(\omega_1 - \omega_2)} + \eta \frac{dV_{c1-1}}{dz} , \quad (6.18b)$$

and

$$\frac{d^2 V_{c1-1}}{dz^2} + \frac{(\omega_1 - \omega_2)^2}{v_{c1-1}^2} V_{c1-1} - j \frac{Z_{01-1}}{v_{c1-1}} (\omega_1 - \omega_2) \frac{di_{1-1}}{dz} = 0 . \quad (6.18c)$$

Signal Frequency (n=0,m=1)

$$i_{o1} = j \left[ \frac{v_{11}}{-\omega_1} \frac{di_{10}^*}{dz} + \frac{v_{1-1}^*}{\omega_1} \frac{di_{10}}{dz} + \frac{v_{10}}{\omega_2 - \omega_1} \frac{di_{1-1}^*}{dz} + \frac{u_o}{\omega_2} \frac{di_{o1}}{dz} + \frac{v_{10}^*}{\omega_1 + \omega_2} \frac{di_{11}}{dz} \right] + v_{o1} \rho_o, \quad (6.19a)$$

$$j\omega_2 v_{o1} + \frac{d}{dz} (v_{11} v_{10}^* + v_{1-1}^* v_{10}) + u_o \frac{dv_{o1}}{dz} = -j\eta \frac{R^2 i_{o1} i_{o1}}{\epsilon_o \omega_2} + \eta \frac{dV_{co1}}{dz}, \quad (6.19b)$$

$$\frac{d^2 V_{co1}}{dz^2} + \frac{\omega_2^2}{v_{co1}^2} V_{co1} - j \frac{Z_{oo1}}{v_{co1}} \omega_2 \frac{di_{o1}}{dz} = 0. \quad (6.19c)$$

The simultaneous solution of Eqs. 6.17, 6.18 and 6.19 subject to the sufficient boundary conditions constitutes a solution to the problem. Even though the problem has been greatly simplified, its solution still represents an arduous task. A further simplification can be introduced by assuming that the coupling of the pump and signal to the sidebands is relatively weak; therefore, the signal frequency remains unperturbed and its propagation may be described by a set of equations similar to Eqs. 6.16 with all (n=1,m=0) terms changed to (n=0,m=1) and  $\omega_1$  terms changed to  $\omega_2$ .

The unperturbed signal frequency variables can then be substituted into Eqs. 6.17 and 6.18 to calculate the weak sideband signals.

DeGrasse's<sup>15</sup> work on the traveling-wave tube mixer contains expressions similar to the simplified set of sideband equations mentioned above.

DeGrasse makes the further approximation of neglecting the (n=1,m=1) term in Eq. 6.17.

Once having derived the general upper and lower sideband equations and the signal frequency equation, one can introduce many configurations of circuits for different applications. Then by judicious approximations, the equations can be simplified to a usable form.

A special case will now be studied, that of the longitudinal-beam parametric amplifier.

### 6.3 Longitudinal-Beam Parametric Amplifier

This particular device has promise of being a high-gain low-noise amplifier. It was first introduced by Louisell and Quate<sup>16</sup> and later discussed by Haus<sup>27</sup>. The unique feature of this amplifier is that it does not require a circuit in the interaction region and operates on fast-wave coupled modes. As with most parametric amplifiers, it can best be analyzed by considering the pump at twice the signal frequency, although in actual operation an improvement is obtained by working at some other frequency. A mathematical description is given first, and then a physical picture of the coupling and noise properties follows.

#### 6.3.1 Mathematical Description.

6.3.1.1 Characteristic Equation. Since the pump frequency is twice the signal frequency, the lower sideband ( $n=1, m=-1$ ) and the signal ( $n=0, m=1$ ) are at the same frequency; this is then a degenerate case as was previously mentioned. Other degeneracies occur for the second harmonic of the signal corresponding to the fundamental of the pump and also for the third harmonic of the signal corresponding to the upper sideband. With these degeneracies in mind, the schedule of possible combinations of frequency terms arising in Eqs. 6.17 to 6.19 must be revised. The components at the signal and lower sideband can be combined into one term at the signal frequency denoted merely by  $\omega$ . The terms are combined by adding the revised equations. The circuit voltage  $V_c$  is set equal to zero in view of the fact that the enclosure is a drift tube.



Now introduce the following parameters,

$$\begin{aligned} \omega_1 &= 2\omega_2 = 2\omega, \\ \frac{-\eta\rho_o}{\sigma\epsilon_o} &= \omega_p^2; \quad \omega_q = \omega_{qo1} = R_{o1}\omega_p, \\ \frac{R_{1o}}{R_{o1}} &= \frac{R_{1o}}{R_{1-1}} = \frac{\omega_{q1o}}{\omega_{qo1}} = 2a', \\ \frac{R_{11}}{R_{o1}} &= \frac{\omega_{q11}}{\omega_{qo1}} = 3b'. \end{aligned} \quad (6.20)$$

The upper and lower sideband equations now assume the form

$$i_1 = j \left[ \frac{v_{11}}{-2\omega} \frac{di_{1o}^*}{dz} + \frac{v_1^*}{2\omega} \frac{di_{1o}}{dz} - \frac{v_{1o}}{\omega} \frac{di_1^*}{dz} + \frac{u_o}{\omega} \frac{di_1}{dz} + \frac{v_{1o}^*}{3\omega} \frac{di_{11}}{dz} \right] + v_1 \rho_o, \quad (6.21a)$$

$$j\omega v_1 + \frac{d}{dz} (v_{11} v_{1o}^* + v_1^* v_{1o}) + u_o \frac{dv_1}{dz} = -j \frac{\omega^2 i_1}{\beta_e I_o} \quad (6.21b)$$

and

$$i_{11} = j \left[ \frac{v_1}{2\omega} \frac{di_{1o}}{dz} + \frac{v_{1o}}{\omega} \frac{di_1}{dz} + \frac{u_o}{3\omega} \frac{di_{11}}{dz} \right] + v_{11} \rho_o \quad (6.22a)$$

$$3j\omega v_{11} + \frac{d}{dz} (v_{1o} v_1) + u_o \frac{dv_{11}}{dz} = -j \frac{3\omega^2}{\beta_e I_o} b'^2 i_{11}. \quad (6.22b)$$

The pump equations, Eqs. 6.16, are given as

$$i_{1o} = j \frac{u_o}{2\omega} \frac{di_{1o}}{dz} + v_{1o} \rho_o, \quad (6.23a)$$

$$j\omega v_{1o} + u_o \frac{dv_{1o}}{dz} = -j \frac{2\omega^2 a'^2}{\beta_e I_o} i_{1o}, \quad (6.23b)$$

which are recognizable as the space-charge wave equations. As is well known, the solution of Eqs. 6.23 is composed of both a fast and a slow wave. Assume that only one wave is excited, either the fast or the slow but not both simultaneously. Methods of exciting a single space-charge wave are discussed in Appendix H. When the amplitude of the current perturbation at the pump signal is expressed as  $mI_0$ , where  $m$  is a depth-of-modulation factor, the solution to Eqs. 6.23 is given as

$$i_{10} = -I_0 + \frac{m}{2} I_0 \exp\left[-2j\beta_e \left(1 - \frac{a'\omega_q}{\omega}\right) z\right]$$

$$v_{10} = u_0 - \frac{a'\omega_q}{\omega} \frac{m}{2} u_0 \exp\left[-2j\beta_e \left(1 - \frac{a'\omega_q}{\omega}\right) z\right]. \quad (6.24)$$

Following Louisell and Quate's notation, for a slow wave,  $a'$  is negative, while for the fast wave it is positive.

The signal and upper sideband currents can be eliminated by combining the two equations in both Eqs. 6.22 and 6.23. The resultant second-order equations for velocity are:

$$\begin{aligned} \frac{d^2 v_1}{dz^2} + \frac{v_{10}}{u_0} \frac{d^2 v_1^*}{dz^2} + \frac{1}{u_0} \frac{d^2}{dz^2} (v_{11} v_{10}^* + v_{10}^* v_{11}) \\ + \frac{1}{u_0} \frac{v_{10}}{u_0} \frac{d^2}{dz^2} (v_{11}^* v_{10} + v_{10} v_{11}^*) + \frac{1}{u_0} \frac{v_{10}^*}{u_0} \frac{1}{9b'^2} \frac{d^2}{dz^2} (v_{10} v_1) \\ + \frac{v_{10}^*}{u_0} \frac{1}{9b'^2} \frac{d^2 v_{11}}{dz^2} + 2j\beta_e \frac{dv_1}{dz} - j \frac{v_{10}}{u_0} \beta_e \frac{dv_1^*}{dz} + j \frac{v_{10}^*}{u_0} \frac{\beta_e}{3} \frac{1}{b'^2} \frac{dv_{11}}{dz} \\ + j \frac{\beta_e}{u_0} \frac{d}{dz} \left[ v_{11} v_{10}^* + v_{10}^* v_{11} \right] - (\beta_e^2 - \beta_q^2) v_1 - j \frac{v_{10}^*}{u_0} \frac{\omega_q^2}{2\omega I_0} \frac{di_{10}}{dz} \\ + j \frac{\omega_q^2}{I_0} \frac{v_{11}}{2\omega u_0} \frac{di_{10}^*}{dz} = 0 \end{aligned} \quad (6.25)$$

and

$$\begin{aligned} & \frac{d^2 v_{11}}{dz^2} + \frac{v_{10}}{u_0} g_{b'2} \frac{d^2 v_1}{dz^2} + \frac{v_{10}}{u_0^2} g_{b'2} \frac{d^2}{dz^2} (v_{11} v_{10}^* + v_1^* v_{10}) \\ & + \frac{1}{u_0} \frac{d^2}{dz^2} (v_{10} v_1) + 6j\beta_e \frac{dv_{11}}{dz} + j \frac{v_{10}}{u_0} \beta_e g_{b'2} \frac{dv_1}{dz} \\ & + 3j \frac{\beta_e}{u_0} \frac{d}{dz} (v_{10} v_1) - 9 \left[ \beta_e^2 - \beta_q^2 b'^2 \right] v_{11} - j \frac{v_1}{u_0} \frac{g_{b'2}}{2\omega} \frac{\omega_q^2}{I_0} \frac{di_{10}}{dz} = 0 \quad (6.26) \end{aligned}$$

where  $\beta_q = \frac{\omega_q}{u_0}$ .

Assume the following forms of solutions,

$$\begin{aligned} v_1 &= u_1(z) \exp \left[ -j\beta_e \left( 1 - \frac{a'\omega_q}{\omega} \right) z \right] \\ v_{11} &= u_{11}(z) \exp \left[ -3j\beta_e \left( 1 - \frac{a'\omega_q}{\omega} \right) z \right] . \end{aligned} \quad (6.27)$$

Substitute Eqs. 6.27 and 6.24 into Eqs. 6.25 and 6.26, furthermore assume that the beam is not very dense, therefore

$$\frac{a'\omega_q}{\omega} \ll 1 .$$

After considerable work the following simplified equations are obtained;

$$\begin{aligned} & \frac{d^2 u_1}{dz^2} + 2j\beta_q a' \frac{du_1}{dz} - \beta_q^2 \left[ a'^2 \left( 1 + \frac{|m|^2}{4} \right) - 1 + \frac{a'^2}{b'^2} \frac{|m|^2}{4} \right] u_1 \\ & - \beta_q^2 \frac{m}{2} (1 + 2a'^2) u_1^* + j\beta_q a' \frac{m^*}{2} \left[ 1 + \frac{1}{3b'^2} \right] \frac{du_{11}}{dz} \\ & - \beta_q^2 \frac{m^*}{2} \left[ 1 + a'^2 \left\{ 1 + \frac{1}{b'^2} \right\} \right] u_{11} - a'^2 \beta_q^2 \frac{m^2}{4} u_{11}^* = 0 . \end{aligned} \quad (6.28)$$

and

$$\begin{aligned}
 \frac{d^2 u_{11}}{dz^2} + 6j\beta_q a' \frac{du_{11}}{dz} - 9\beta_q^2 \left[ a'^2 \left( 1 + b'^2 \frac{|m|^2}{4} \right) - b'^2 \right] u_{11} \\
 + j\beta_q a' \frac{3m}{2} \left[ 1 + 3b'^2 \right] \frac{du_{11}}{dz} - 9\beta_q^2 \frac{m}{2} \left[ a'^2 (1 + b'^2) + b'^2 \right] u_{11} \\
 - 9a'^2 b'^2 \beta_q^2 \frac{m^2}{4} u_{11}^* = 0 .
 \end{aligned} \tag{6.29}$$

The same equations have been derived in Appendix G using an extension of the method of Louisell and Quate<sup>16</sup>.

Equations 6.28 and 6.29 and the complex conjugates of these equations completely describe the system. The equations are a set of four linear homogeneous differential equations with constant coefficients. The solutions<sup>28</sup> will therefore be exponentials. An operator

$$\frac{d}{dz} = \beta_q \mu$$

may be introduced. When this is done the equations assume the algebraic form

$$\begin{aligned}
 \varphi_1(\mu)u_1 + \psi_1(\mu)u_1^* + \zeta_1(\mu)u_{11} + \xi_1(\mu)u_{11}^* &= 0 \\
 \psi_1^*(\mu)u_1 + \varphi_1^*(\mu)u_1^* + \xi_1^*(\mu)u_{11} + \zeta_1^*(\mu)u_{11}^* &= 0 \\
 \varphi_2(\mu)u_1 + \psi_2(\mu)u_1^* + \zeta_2(\mu)u_{11} + \xi_2(\mu)u_{11}^* &= 0 \\
 \psi_2^*(\mu)u_1 + \varphi_2^*(\mu)u_1^* + \xi_2^*(\mu)u_{11} + \zeta_2^*(\mu)u_{11}^* &= 0
 \end{aligned} \tag{6.30}$$

where  $\varphi_1 \dots \xi_2^*$  are operators. The condition that this homogeneous set have a nontrivial solution is that the determinant of the coefficients vanish.

$$\begin{vmatrix}
 \varphi_1(\mu) & \psi_1(\mu) & \zeta_1(\mu) & \xi_1(\mu) \\
 \psi_1^*(\mu) & \varphi_1^*(\mu) & \xi_1^*(\mu) & \zeta_1^*(\mu) \\
 \varphi_2(\mu) & \psi_2(\mu) & \zeta_2(\mu) & \xi_2(\mu) \\
 \psi_2^*(\mu) & \varphi_2^*(\mu) & \xi_2^*(\mu) & \zeta_2^*(\mu)
 \end{vmatrix} = 0 \tag{6.31}$$

The expansion of this determinant is the characteristic equation of the beam-type parametric amplifier. The roots of the equation will be the propagation constants, For the parametric amplifier there will be eight waves.

The characteristic equation may be determined in another fashion by using the real and imaginary parts of the velocities. Once again four equations result. The system in terms of the real and imaginary components of the velocity is given as:

$$\begin{bmatrix}
 \varphi_3(\mu) & \psi_3(\mu) & \zeta_3(\mu) & \xi_3(\mu) \\
 \varphi_4(\mu) & \psi_4(\mu) & \zeta_4(\mu) & \xi_4(\mu) \\
 \varphi_5(\mu) & \psi_5(\mu) & \zeta_5(\mu) & \xi_5(\mu) \\
 \varphi_6(\mu) & \psi_6(\mu) & \zeta_6(\mu) & \xi_6(\mu)
 \end{bmatrix} \times \begin{bmatrix}
 u_{1R} \\
 u_{1i} \\
 u_{11R} \\
 u_{11i}
 \end{bmatrix} = 0 \tag{6.32}$$

where

$$u_1 = u_{1R} + ju_{1i}$$

$$u_{11} = u_{11R} + ju_{11i} .$$

The characteristic equation determined by setting the determinant of the coefficients equal to zero is identical with that found using Eq. 6.31.

The complete characteristic equation is given in Appendix F. It is pointed out in this appendix that the quantities a' and b' appear in even powers therefore, the same characteristic equation holds for fast- and slow-wave pump signals. For the case of a small radius beam, a' = b' = 1 the characteristic equation of Appendix F reduces to

$$\begin{aligned} \mu^8 + \mu^6 \left( 40 + \frac{5}{2} |m|^2 \right) + \mu^4 \left( 144 + \frac{381}{4} |m|^2 + \frac{43}{16} |m|^4 \right) \\ + \mu^2 \left[ 405 |m|^2 + \frac{504}{8} |m|^4 - \frac{27}{32} |m|^6 \right] \\ + \frac{6561}{16} |m|^4 - \frac{2187}{64} |m|^6 + \frac{81}{256} |m|^8 = 0 \quad . \end{aligned} \quad (6.33)$$

For small depth of modulation levels  $m \ll 1$  and the roots of Eq. 6.33 can be approximated as

$$\begin{aligned} \mu_1 &= 2j \\ \mu_2 &= -2j \\ \mu_3 &= 6j \\ \mu_4 &= -6j \\ \mu_5 &= (0.375 + j 1.24) |m| \\ \mu_6 &= (-0.375 - j 1.24) |m| \\ \mu_7 &= (0.375 - j 1.24) |m| \\ \mu_8 &= (-0.375 + j 1.24) |m| \quad . \end{aligned}$$

6.3.1.2 Boundary Conditions. In the preceding section it was shown that eight waves propagate in this model of the longitudinal-beam parametric amplifier. The amplitudes of these waves will now be determined. Two sets of four simultaneous differential equations giving the same characteristic equation were presented in Section 6.3.1.1. The second set, given in Eq. 6.32, will be used to find the wave amplitudes. The real and imaginary velocity components may be stated in terms of their wave amplitudes and propagation constants as

$$\begin{aligned}
 u_{1R} &= \sum_{i=1}^8 \epsilon_i \exp \beta_q \mu_i z , \\
 u_{1i} &= \sum_{i=1}^8 \eta_i \exp \beta_q \mu_i z , \\
 u_{11R} &= \sum_{i=1}^8 \tau_i \exp \beta_q \mu_i z , \\
 u_{11i} &= \sum_{i=1}^8 \pi_i \exp \beta_q \mu_i z .
 \end{aligned} \tag{6.34}$$

Obviously there are 32 constants to determine, however, not all of these constants are independent. Forsyth<sup>28</sup> points out that the number of independent constants in such a system of linear equations is equal to the highest power of  $\mu$  occurring in the characteristic or secular equation. For the parametric amplifier there are only eight independent constants. These independent constants are determined from the boundary conditions, that is the value of the real and imaginary velocity components and the distance derivatives of velocity at the start of the tube. This leaves twenty-four relations to determine the remaining

constants.

Substitute the solutions represented by Eqs. 6.34 into the system given in Eq. 6.32. The result for the first equation of Eq. 6.32 is

$$\begin{aligned}
 & [\epsilon_1 \phi_3(\beta_{q\mu_1}) + \eta_1 \psi_3(\beta_{q\mu_1}) + \tau_1 \zeta_3(\beta_{q\mu_1}) + \pi_1 \xi_3(\beta_{q\mu_1})] \exp \beta_{q\mu_1} z \\
 & + [\epsilon_2 \phi_3(\beta_{q\mu_2}) + \eta_2 \psi_3(\beta_{q\mu_2}) + \tau_2 \zeta_3(\beta_{q\mu_2}) + \pi_2 \xi_3(\beta_{q\mu_2})] \exp \beta_{q\mu_2} z \\
 & + \dots \\
 & + [\epsilon_8 \phi_3(\beta_{q\mu_8}) + \eta_8 \psi_3(\beta_{q\mu_8}) + \tau_8 \zeta_3(\beta_{q\mu_8}) + \pi_8 \xi_3(\beta_{q\mu_8})] \exp \beta_{q\mu_8} z \\
 & = 0 .
 \end{aligned}$$

This expression must be valid for any value of  $z$ , therefore, each coefficient must independently vanish. This can be repeated for any two of the three remaining equations of Eq. 6.31 with similar results. The relations of the amplitudes  $\eta_i$ ,  $\tau$ , and  $\pi_i$  to the  $\epsilon_i$  are expressed in the following matrix equation.

$$\begin{bmatrix} -\phi_3(\beta_{q\mu_i})\epsilon_i \\ -\phi_4(\beta_{q\mu_i})\epsilon_i \\ -\phi_5(\beta_{q\mu_i})\epsilon_i \end{bmatrix} = \begin{bmatrix} \psi_3(\beta_{q\mu_i}) & \zeta_3(\beta_{q\mu_i}) & \xi_3(\beta_{q\mu_i}) \\ \psi_4(\beta_{q\mu_i}) & \zeta_4(\beta_{q\mu_i}) & \xi_4(\beta_{q\mu_i}) \\ \psi_5(\beta_{q\mu_i}) & \zeta_5(\beta_{q\mu_i}) & \xi_5(\beta_{q\mu_i}) \end{bmatrix} \begin{bmatrix} \eta_i \\ \tau_i \\ \pi_i \end{bmatrix}, \quad (6.35)$$

which is found by using the first three equations of Eq. 6.32. Equation 6.35 applies to all values of the index  $i$  running from 1 through 8. Inverting Eq. 6.35 for each value of the index gives the required twenty-four relations. The expanded matrix elements are shown in Appendix D.

The eight known boundary conditions are found from the real and imaginary velocity and current components of the sideband frequencies



evaluated at the input. Assuming that an input is applied only at the signal frequency\*, the inputs are

$$\begin{aligned}
 v_1(0) &= v_{1in} \\
 i_1(0) &= i_{1in} \\
 v_{11}(0) &= 0 \\
 i_{11}(0) &= 0 \quad . \quad (6.36a)
 \end{aligned}$$

The eight conditions are found by separating the velocity and current into real and imaginary parts to obtain

$$\begin{aligned}
 v_{1R}(0) &= v_{1inR} \\
 v_{1i}(0) &= v_{1inI} \\
 i_{1R}(0) &= i_{1inR} \\
 i_{1i}(0) &= i_{1inI} \\
 v_{11R}(0) &= v_{11i}(0) = i_{11R}(0) = i_{11i}(0) = 0 \quad . \quad (6.36b)
 \end{aligned}$$

The velocities can be used directly in the problem, however, the currents must be used in calculating the velocity derivatives at the input. This is necessary since the equations describing the propagation are in terms of the velocity.

Both the input signal and pump waves propagate as space-charge waves before interaction takes place. Recall that for this analysis

---

\* A pump signal is of course also applied and its propagation is assumed to be known as is indicated in Eq. 6.38.

these space-charge waves will be either slow or fast but both will not simultaneously be present. In a "single" space-charge wave the current and velocity amplitudes are related through

$$i_1(0) = (-1)^s \frac{\omega}{\omega_q} \frac{I_o}{u_o} v_1(0) \quad (6.37)$$

where  $s = +1$  for fast wave,

$s = +2$  for slow wave.

The pump velocity and current amplitudes were previously introduced as

$$i_{10}(0) = \frac{mI_o}{2}$$

and

$$v_{10}(0) = -\frac{a'\omega_q}{\omega} \frac{m}{2} u_o \quad (6.38)$$

where  $a' > 0$  for fast waves

$a' < 0$  for slow waves,

and  $m = |m| \exp j\theta$ .

Evaluate Eqs. 6.21b and 6.22b at the input using the conditions given in Eqs 6.36 through Eq. 6.38. Therefore

$$\begin{aligned} \left(\frac{dv_1}{dz}\right)_o - \frac{a'\omega_q}{\omega} \frac{m}{2} \left(\frac{dv_1^*}{dz}\right)_o - \frac{a'\omega_q}{\omega} \frac{m^*}{2} \left(\frac{dv_{11}}{dz}\right)_o \\ = -j \left( \beta_e + (-1)^s \beta_q \right) v_{1in} - 2j\beta_q a' \frac{m}{2} \left( 1 - \frac{a'\omega_q}{\omega} \right) v_{1in}^* \quad (6.39) \end{aligned}$$

$$\left(\frac{dv_{11}}{dz}\right)_o - \frac{a'\omega_q}{\omega} \frac{m}{2} \left(\frac{dv_1}{dz}\right)_o = -2j\beta_q a' \frac{m}{2} \left( 1 - \frac{a'\omega_q}{\omega} \right) v_{1in} \quad (6.40)$$

The above equations can be simplified by introducing the form for the velocity given in Eq. 6.27 and also the approximation that  $a'\omega_q/\omega \ll 1$ ; this is then separated into real and imaginary parts to obtain:

$$\begin{aligned} \left(\frac{du_{1R}}{dz}\right)_0 &= \beta_q(a'+(-1)^s) v_{1in i} + \beta_q a' \frac{|m|}{2} [v_{1in R} \sin \theta - v_{1in i} \cos \theta] \\ \left(\frac{du_{1i}}{dz}\right)_0 &= -\beta_q(a'+(-1)^s) v_{1in R} - \beta_q a' \frac{|m|}{2} [v_{1in R} \cos \theta + v_{1in i} \sin \theta] \\ \left(\frac{du_{11R}}{dz}\right)_0 &= 3\beta_q a' \frac{|m|}{2} [v_{1in R} \sin \theta + v_{1in i} \cos \theta] \\ \left(\frac{du_{11i}}{dz}\right)_0 &= 3\beta_q a' \frac{|m|}{2} [v_{1in i} \sin \theta - v_{1in R} \cos \theta] . \end{aligned} \quad (6.41)$$

The initial values of the derivatives can be matched to the derivatives of Eq. 6.34 evaluated at  $z = 0$ .

$$\begin{aligned} \left(\frac{du_{1R}}{dz}\right)_0 &= \beta_q \sum_{i=1}^8 \mu_i \epsilon_i \\ \left(\frac{du_{1i}}{dz}\right)_0 &= \beta_q \sum_{i=1}^8 \mu_i \eta_i \\ \left(\frac{du_{11R}}{dz}\right)_0 &= \beta_q \sum_{i=1}^8 \mu_i \tau_i \\ \left(\frac{du_{11i}}{dz}\right)_0 &= \beta_q \sum_{i=1}^8 \mu_i \pi_i , \end{aligned} \quad (6.42)$$

while the initial velocity values are

$$\begin{aligned}
 u_{1R}(0) &= v_{1inR} = \sum_{i=1}^8 \epsilon_i \\
 u_{1i}(0) &= v_{1ini} = \sum_{i=1}^8 \eta_i \\
 u_{11R}(0) &= 0 = \sum_{i=1}^8 \tau_i \\
 u_{11i}(0) &= 0 = \sum_{i=1}^8 \pi_i \quad . \quad (6.43)
 \end{aligned}$$

The  $\eta$ ,  $\tau$ , and  $\pi$  coefficients were expressed in terms of the  $\epsilon$  coefficients in Eq. 6.35, therefore Eqs. 6.42 and 6.43 represent a set of eight linear equations with eight  $\epsilon_i$  as the unknowns. When the following normalizations are made,

$$\begin{aligned}
 \eta_i &= \bar{\eta}_i \epsilon_i \\
 \tau_i &= \bar{\tau}_i \epsilon_i \\
 \pi_i &= \bar{\pi}_i \epsilon_i \quad , \quad (6.44)
 \end{aligned}$$

the matrix equation describing the 8 x 8 system can be expressed as

$$\left[ \begin{array}{l} v_{1inR} \\ v_{1ini} \\ 0 \\ 0 \\ (a'+(-1)^s)v_{1ini} + a' \frac{|m|}{2} [v_{1inR} \sin \theta - v_{1ini} \cos \theta] \\ -(a'+(-1)^s)v_{1inR} - a' \frac{|m|}{2} [v_{1inR} \cos \theta + v_{1ini} \sin \theta] \\ 3a' \frac{|m|}{2} [v_{1inR} \sin \theta + v_{1ini} \cos \theta] \\ 3a' \frac{|m|}{2} [v_{1ini} \sin \theta - v_{1inR} \cos \theta] \end{array} \right] = \left[ \begin{array}{l} 1 \quad 1 \quad \dots \quad 1 \\ \bar{\eta}_1 \quad \bar{\eta}_2 \quad \dots \quad \bar{\eta}_8 \\ \bar{\tau}_1 \quad \bar{\tau}_2 \quad \dots \quad \bar{\tau}_8 \\ \bar{\pi}_1 \quad \bar{\pi}_2 \quad \dots \quad \bar{\pi}_8 \\ \mu_1 \quad \mu_2 \quad \dots \quad \mu_8 \\ \bar{\eta}_1^{\mu_1} \quad \bar{\eta}_2^{\mu_2} \dots \bar{\eta}_8^{\mu_8} \\ \bar{\tau}_1^{\mu_1} \quad \bar{\tau}_2^{\mu_2} \dots \bar{\tau}_8^{\mu_8} \\ \bar{\pi}_1^{\mu_1} \quad \bar{\pi}_2^{\mu_2} \dots \bar{\pi}_8^{\mu_8} \end{array} \right] \left[ \begin{array}{l} \epsilon_1 \\ \epsilon_2 \\ \epsilon_3 \\ \epsilon_4 \\ \epsilon_5 \\ \epsilon_6 \\ \epsilon_7 \\ \epsilon_8 \end{array} \right]$$

(6.45)

The wave amplitudes are then expressed by inverting Eq. 6.44. As mentioned above, the expanded matrix equations for evaluating  $\eta_1 \dots \pi_8$  are shown in Appendix I.

6.3.1.3 Numerical Results for the Longitudinal-Beam Parametric Amplifier. The eight roots of the polynomial obtained by expanding Eqs. 6.31 are the propagation constants for the longitudinal-beam amplifier. In order to evaluate the propagation constants, it is necessary to specify the geometry (ratio of beam to drift tube radius) and the pump amplitude  $m$ . The plasma-frequency reduction factor for a very thin beam is a linear function of frequency so that the constants  $a'$  and  $b'$  are unity. An approximate form of the propagation constants as a function of pump amplitude was given in Section 6.3.1.1 for the special case of  $a' = b' = 1.0$ . More accurate values of the roots were obtained by using an IBM 704 computer. The propagation constants as a function of pump amplitude for  $a' = b' = 1.0$  are shown in Figs. 6.1 and 6.2. It can be seen that the approximate values obtained in Section 6.3.1.1 are fairly accurate.

The propagation constants for a thicker beam are shown in Figs. 6.3 and 6.4. The beam used for this case has a radius that is one half of the drift tube radius. The "radian wave number" of the beam at the signal frequency (defined as  $\beta_e = \omega/u_0$ ) times the beam radius is assumed to be 0.5. Under these conditions the parameters  $a'$  and  $b'$  are given as

$$a' = 0.697$$

$$b' = 0.573 \quad .$$

It can be seen from Fig. 6.4 that when a thicker beam is used, there will be a threshold value of pumping amplitude. For pumping signals with amplitudes below the threshold value there will be no

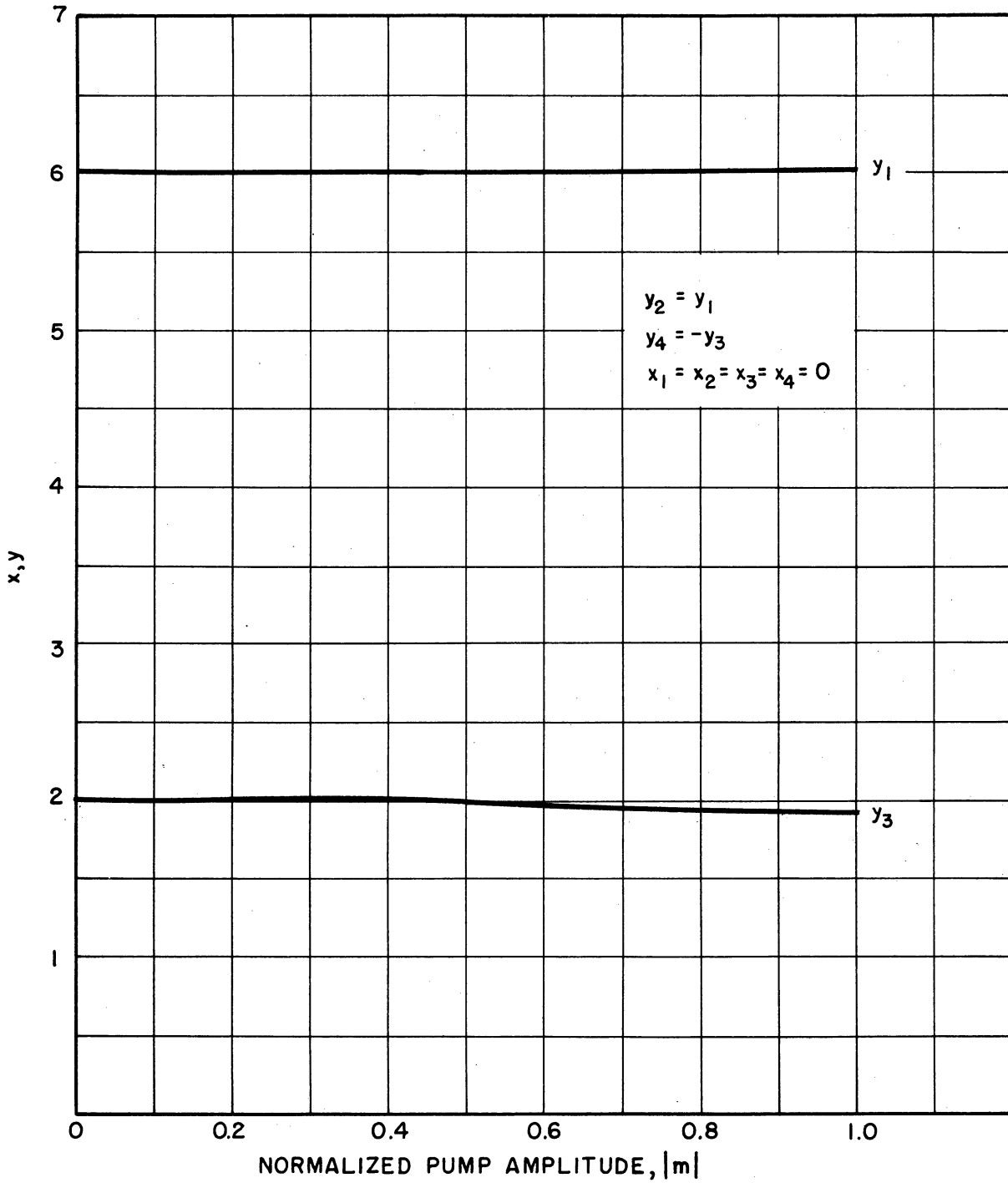


FIG. 6.1 LONGITUDINAL-BEAM PARAMETRIC-AMPLIFIER PROPAGATION CONSTANTS ( $\mu_1 \dots \mu_4$ ) AS FUNCTIONS OF THE PUMP AMPLITUDE ( $a' = b' = 1.0$ ).

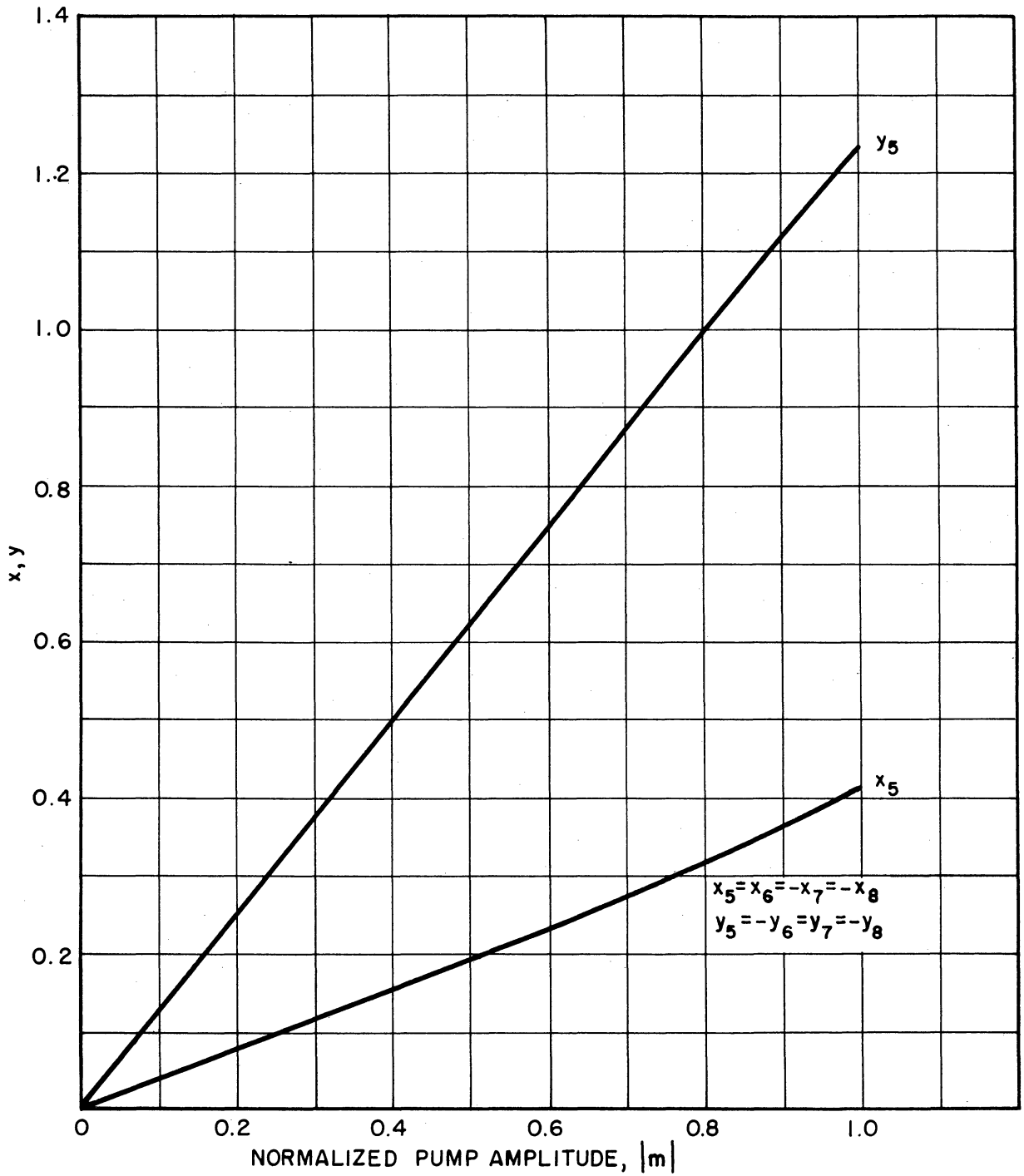


FIG. 6.2 LONGITUDINAL-BEAM PARAMETRIC-AMPLIFIER PROPAGATION CONSTANTS ( $\mu_5 \dots \mu_8$ ) AS FUNCTIONS OF THE PUMP AMPLITUDE ( $a' = b' = 1.0$ ).



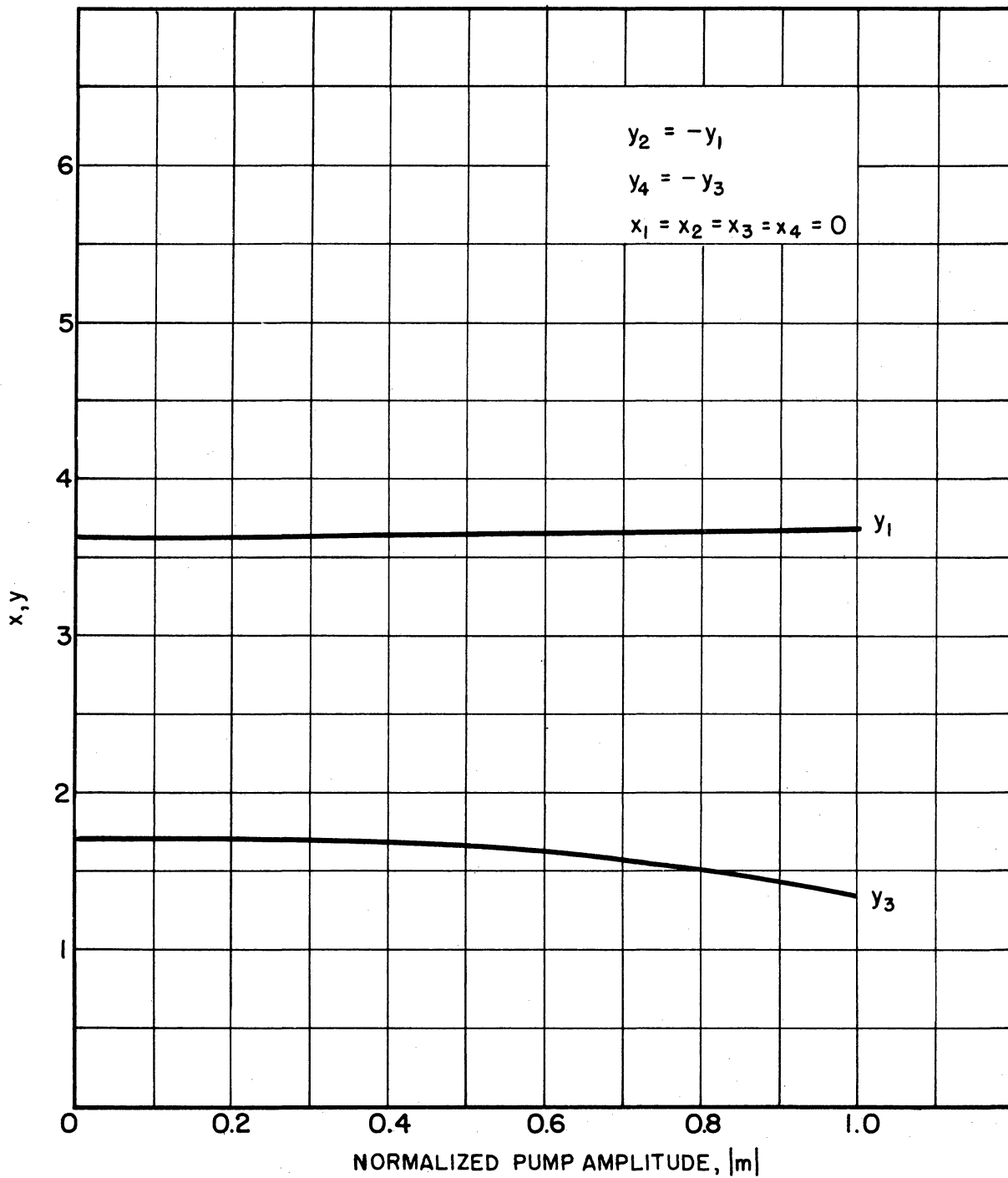


FIG. 6.3 LONGITUDINAL-BEAM PARAMETRIC-AMPLIFIER PROPAGATION CONSTANTS ( $\mu_1, \mu_4$ ) AS FUNCTIONS OF THE PUMP AMPLITUDE ( $a' = 0.697, b' = 0.513$ ).

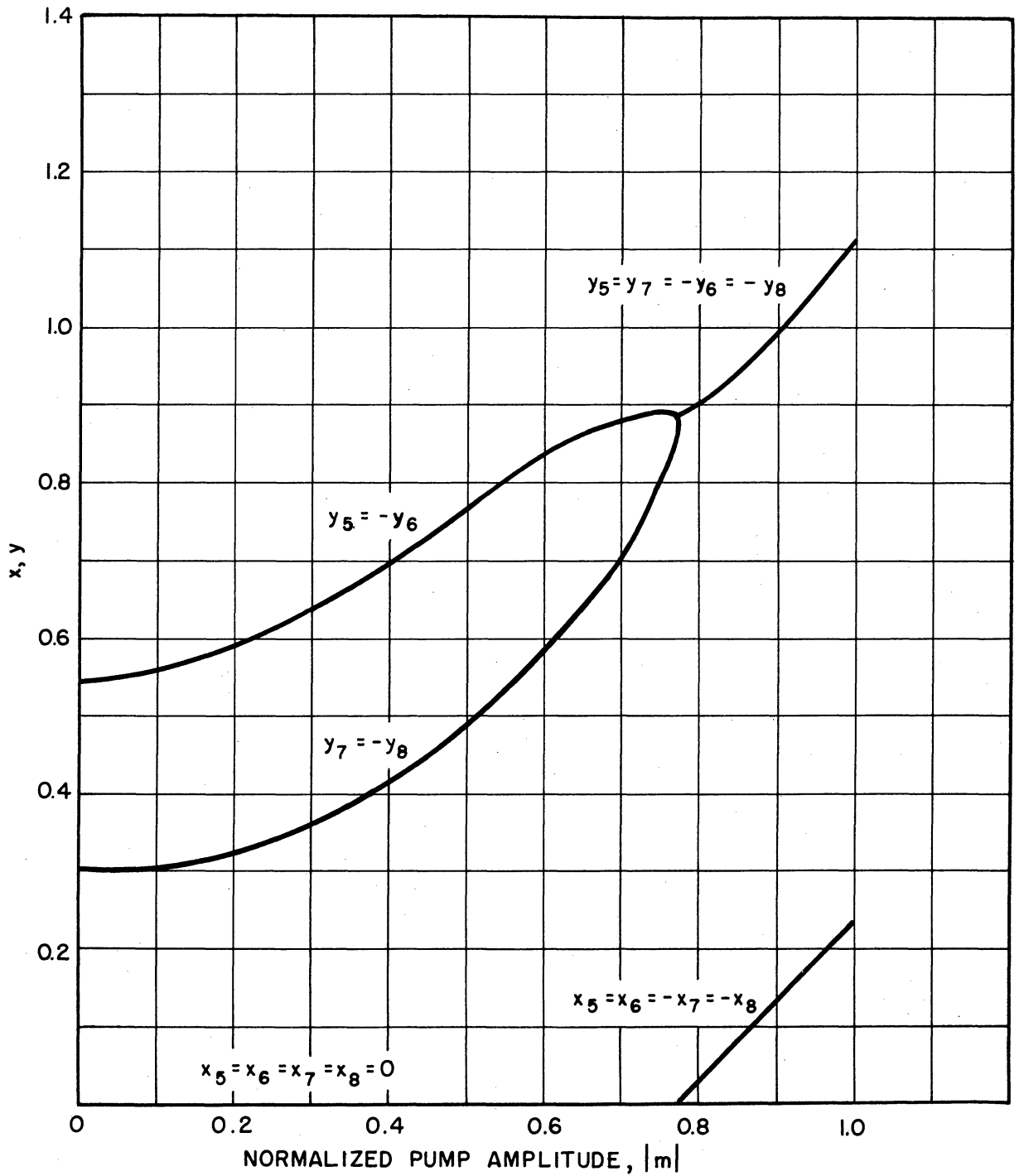


FIG. 6.4 LONGITUDINAL-BEAM PARAMETRIC-AMPLIFIER PROPAGATION CONSTANTS ( $\mu_5, \mu_8$ ) AS FUNCTIONS OF THE PUMP AMPLITUDE ( $a' = 0.697, b' = 0.513$ ).

exponential growth since the roots are purely imaginary. The results presented and discussed thus far are independent of the sign of  $a'$  and the phase of the pump signal so that the results apply equally well to fast- or slow-wave excitations. Boundary conditions and the sign of  $a'$  will be considered while evaluating the amplitude of each of the eight waves.

The wave amplitudes are determined by inverting Eq. 6.45, which involves the inversion of the eight  $3 \times 3$  systems given in Eqs. 6.35 and I.2. This indeed becomes a cumbersome problem. Because of this it was decided to find the wave amplitudes for a limited number of cases. The cases chosen were

$$\begin{aligned} a' &= b' = 1 && \text{(fast-wave excitation)} \\ |m| &= 0.10 \\ \theta &= \text{phase of } m = \pm \frac{\pi}{2} \\ v_1(0) &= 1.0 \end{aligned}$$

The wave amplitudes for the above two cases are shown in Tables 6.1 and 6.2. In each case only two of the eight possible waves are appreciably excited. For the pump phase of  $-\pi/2$  radians, only the declining waves are excited. The two declining waves have complex conjugate amplitudes and propagation constants and can therefore be combined to give

$$\begin{aligned} v_1 &\approx 1.0511 \cos[0.124\beta_q z + 17.84^\circ] \exp[-0.0375\beta_q z] \exp\left[-j\beta_e z \left(1 - \frac{\omega_q}{\omega}\right)\right] \\ v_{11} &\approx -1.822 \sin[0.124\beta_q z] \exp[-0.0375\beta_q z] \exp\left[-j3\beta_e z \left(1 - \frac{\omega_q}{\omega}\right)\right] \end{aligned} \quad (6.46)$$

TABLE 6.1

Matrix Elements  $\epsilon$ ,  $\eta$ ,  $\tau$ ,  $\pi$   
 $m = 0.10 \exp j\theta$ ,  $a' = b' = 1$ ,  $v_1(0) = 1$

Wave No.	$\mu$	$\epsilon$	$\eta$	$\tau$	$\pi$	$\theta$
1	j6.0	-0.0000637-j0.00000187	0.0163+j1.0	0.780+j96.0	-96.0+j0.781	-90°
2	-j6.0	-0.0000637+j0.00000187	0.0163-j1.0	0.780-j96.0	-96.0-j0.781	-90°
3	j1.999	-0.000182-j0.00689	0.0376+j1.0	-0.000837+j2.27	-0.0201+j0.0021	-90°
4	-j1.999	-0.000182+j0.00689	0.0376-j1.0	-0.000837-j2.27	-0.0201-j0.0021	-90°
5	-0.0375-j0.124	0.5003-j0.161	0.0031-j0.0173	0.501-j1.66	-0.0146-j0.0139	-90°
6	0.0375-j0.124	-0.0000258-j0.0000748	19.3-j68.87	-1.25-j1.035	-123.8+j2.54	-90°
7	-0.0375+j0.124	0.5003+j0.161	0.0031+j0.0173	0.501+j1.66	-0.0146+j0.0139	-90°
8	0.0375+j0.124	-0.0000258+j0.0000748	19.3+j68.87	-1.25+j1.035	-123.8-j2.54	-90°
1	j6.0	-0.0000637+j0.00000187	-0.0163+j1.0	0.780-j96.0	96.0+j0.781	90°
2	-j6.0	-0.0000637-j0.00000187	-0.0163-j1.0	0.780+j96.0	96.0-j0.781	90°
3	j1.999	-0.000182+j0.00689	-0.0376+j1.0	-0.000837-j2.27	0.0201+j0.0021	90°
4	-j1.999	-0.000182-j0.00689	-0.0376-j1.0	-0.000837+j2.27	0.0201-j0.0021	90°
5	-0.0375-j0.124	-0.0000258+j0.0000748	-19.3-j68.87	-1.25+j1.0350	123.8+j2.54	90°
6	0.0375-j0.124	0.5003+j0.161	-0.0031-j0.0173	0.501+j1.66	0.0145-j0.0139	90°
7	-0.0375+j0.124	-0.0000258-j0.0000748	-19.3+j68.87	-1.25-j1.0350	123.8-j2.54	90°
8	0.0375+j0.124	0.5003-j0.161	-0.0031+j0.0173	0.501-j1.66	0.0145+j0.0139	90°

TABLE 6.2

Complex Wave Amplitude Coefficients

 $m = 0.10 \exp j\theta$ ,  $a' = b' = 1.0$ ,  $v_1(0) = 1$ 

Wave No.	$u_{1R}$	$u_{1I}$	$u_{11R}$	$u_{11I}$	$\theta$
1	-0.0000637-j0.00000187	0.00000083-j0.0000637	0.000130-j0.00612	0.00612+j0.0000278	-90°
2	-0.0000637+j0.00000187	0.00000083+j0.0000637	0.000130+j0.00612	0.00612-j0.0000278	-90°
3	-0.000182-j0.00689	0.00688-j0.000441	0.01564-j0.000407	0.0000040+j0.000153	-90°
4	-0.000182+j0.00689	0.00688+j0.000441	0.01564+j0.000407	0.0000040-j0.000153	-90°
5	0.5003-j0.161	-0.00124-j0.00915	-0.0166-j0.911	0.0051-j0.0093	-90°
6	-0.0000258-j0.0000748	-0.00565+j0.000334	-0.0000452+j0.0001202	0.00338+j0.00919	-90°
7	0.5003+j0.161	-0.00124+j0.00915	-0.0166+0.911	0.0051+j0.0093	-90°
8	-0.0000258+j0.0000748	-0.00565-j0.000334	-0.0000452-j0.0001202	0.00338-j0.00919	-90°
1	-0.0000637+j0.00000187	-0.00000083-j0.0000637	0.000130+j0.00612	-0.00612+j0.0000278	90°
2	-0.0000637-j0.00000187	-0.00000083+j0.0000637	0.000130-j0.00612	-0.00612-j0.0000278	90°
3	-0.000182+j0.00689	-0.00688-j0.000441	0.01564+j0.000407	-0.0000040+j0.000153	90°
4	-0.000182-j0.00689	-0.00688+j0.000441	0.01564-j0.000407	-0.0000040-j0.000153	90°
5	-0.0000258+j0.0000748	0.00565+j0.000334	-0.0000452-j0.0001202	-0.00338+j0.00919	90°
6	0.5003+j0.161	0.00124-j0.00915	-0.0166+j0.911	-0.0051-j0.0093	90°
7	-0.0000258-j0.0000748	0.00565-j0.000334	-0.0000452+j0.0001202	-0.00338-j0.00919	90°
8	0.5003-j0.161	0.00124+j0.00915	-0.0166-j0.911	-0.0051+j0.0093	90°

Similarly the growing fast waves can be excited with a pump phase of  $+\pi/2$  radians. The velocity waves in this case are

$$v_1 \approx 1.0511 \cos[0.124\beta_q z - 17.84^\circ] \exp 0.0375\beta_q z \exp\left[-j\beta_e z\left(1 - \frac{\omega_q}{\omega}\right)\right] .$$

$$v_{11} \approx 1.822 \sin 0.124\beta_q z \exp 0.0375\beta_q z \exp\left[-3j\beta_e z\left(1 - \frac{\omega_q}{\omega}\right)\right] . \quad (6.47)$$

Obviously the pump phase is a critical factor in obtaining amplification from this device, also the length must be properly chosen. The growth of the signal velocity wave at the first crest of the interference pattern ( $0.124\beta_q z - 0.311 = \pi$ ) is equivalent to a gain of 9.4 db. At this length the "gain" of the velocity of the upper sideband, that is the velocity of the upper sideband wave compared to the signal velocity at the input, is equivalent to 4.04 db. The tube length can be adjusted so that the output end is at a crest of the upper sideband velocity envelope. This would occur at  $0.124\beta_q z = \pi/2$  and the upper sideband gain would be 9.64 db while the signal gain would be - 5.5 db. The wave at the upper sideband is strongly excited and its effect on the growth constant will be discussed below. The above results will now be compared to results previously obtained by Louisell and Quate<sup>16</sup>.

In their initial work on the longitudinal-beam parametric amplifier, Louisell and Quate<sup>16</sup> considered coupling to exist only between the signal and lower sideband frequencies. As a result of this, the growth factor obtained was approximately  $0.75|m|$  for the case of  $a' = 1.0$ . This factor is twice that given above so that it can be concluded that the effect of including the upper sideband is to reduce the gain factor by one half. The results obtained by Louisell and Quate<sup>16</sup> for thicker beams indicated a threshold as mentioned above, but it was found at a lower

pump amplitude than that found by the method used in this report. The effect of the pump phase on the type of wave (growing or declining) was in agreement with the results given above.

Work by Ashkin<sup>34</sup> et al. on a longitudinal-beam parametric amplifier indicates great discrepancies between the theoretical work of Louisell and Quate<sup>16</sup> and the results obtained experimentally by Ashkin<sup>34</sup>. The signal gain for the experimental tube was found to be 13 db per plasma wavelength while the theoretical value was 40 db per wavelength. Ashkin attributed part of the error to the fact that the signal and pump velocities were not the same. The theoretical gain obtained using the upper sideband in addition to the lower sideband would be approximately 20 db. While this result is still in error it is certainly much closer to the experimental value. Therefore it can be concluded that it is essential to include at least the upper and lower sidebands in a theoretical analysis of the parametric-beam amplifier. The inclusion of more sidebands and those around the various pump harmonics would yield a still more accurate answer, however the amount of computational work would greatly increase.

6.3.2 A Description of the Mechanics of Parametric Amplification in a Longitudinal Beam. Before proceeding with a discussion of the energy exchange which produces amplification in the parametric longitudinal-beam amplifier, a brief review of the principles of power flow in longitudinal beams will be given.

L. J. Chu<sup>33</sup> introduced the kinetic power theorem in 1951. This theorem was later presented in published form by several authors<sup>29,30</sup>. The kinetic power theorem gives a picture of the energy exchange in a small-signal or linearly operating longitudinal beam device. Energy and

power are calculated using squares and cross products of the small-signal terms so that at first thought one might imagine that it is not possible to describe a linearized device in terms of energy considerations. Fortunately, Chu<sup>33</sup> resolved this problem and provided the key for the solution of many difficult and perplexing problems, among them some basic questions on noise in beam devices.

The theorem in mathematical form is<sup>30</sup>

$$\operatorname{Re} \int \left[ \frac{1}{2} E(r) \times H^*(r) + S_k(r) \right] \cdot dA = 0 ,$$

where E and H are the electromagnetic field variables and  $S_k(r)$  is a quantity called the complex power flow; A is the area enclosing volume  $\tau$ .

The complex power flow is defined as

$$S_k(r) = V(r)J^*(r) ,$$

where J(r) is the small-signal current density and V(r) is the kinetic voltage modulation defined as

$$V(r) = \frac{m}{e} u_0 v ,$$

where v is the small-signal velocity.

In words the theorem states that the sum of electromagnetic power delivered by the beam in volume  $\tau$  and the net real kinetic-power flow through the volume must be zero. This statement of energy conservation is correct within second order of the small-signal amplitudes. Both the small-signal velocity and current density are used.

In a fast space-charge wave the r-f current and velocity are 180° out of phase, while they are in phase for the slow wave. Since the convention of opposite current and electron flow is assumed, the fast wave



will have minimum velocity where electron bunches are rarefied, while the maximum velocity occurs at dense bunches. Therefore, this fast-wave beam will have a greater energy than the beam without a fast wave. The fast wave is concluded to carry positive energy. By similar reasoning the slow wave carries negative energy, which means that the beam has less energy in the presence of the slow wave than it had without the slow wave. This permits the definition of a positive kinetic voltage for the fast wave and a negative one for the slow wave.

In order to satisfy Chu's theorem, it can be seen that electromagnetic energy has to be supplied to set up the fast wave whereas it must be removed to set up the slow wave. In a klystron input resonator, where to a first-order theory the fast and slow waves are equally excited no net energy is required to excite the beam. This is consistent with the linearization.

The conventional longitudinal beam device works on the slow wave since from Chu's theorem it can be seen that to increase the electromagnetic energy it is necessary to decrease the kinetic-power flow. The decrease of the kinetic-power flow corresponds to the energy of the slow space-charge wave becoming more negative. This implies an increasing slow space-charge wave and an increase of electromagnetic energy. The increased energy in the electromagnetic field comes from a decrease of the d-c energy of the beam. It is apparent that the fast wave cannot be used to amplify a circuit wave since it can only decrease the electromagnetic energy.

Haus and Robinson<sup>32</sup> used the theorem to demonstrate that a lower limit exists on the noise in the beam of a conventional beam amplifier. The limit is dependent upon the conditions at the potential minimum.

A simple explanation for this limit is that the slow-wave noise energy is negative. In order to cancel the noise one would have to add noise energy in the correct phase and amplitude to the beam. This, of course, is impossible. The fast wave, however, has positive noise energy, therefore the noise can be completely removed by exciting waves on a circuit and dissipating the noise energy in a cool resistor. It appears that a device using a fast wave would be very attractive if the difficulties in obtaining amplification could be overcome. Circuits for removing fast-wave energy from a beam are discussed in Appendix H.

Adler<sup>52</sup> proposed using fast cyclotron waves that were pumped after the noise was removed to produce gain by parametric amplification. Louisell and Quate<sup>16</sup> proposed using the longitudinal-beam amplifier as a parametric amplifier. Haus<sup>31</sup> generalized the kinetic power theorem to cover the case of the parametric-beam amplifier. Practically noiseless parametric amplification<sup>34</sup> of space-charge waves may be accomplished by removing the fast-wave beam noise as described above, then applying a pump in the form of a fast wave. The pump then supplies energy to the sidebands which in turn interact with one another. Notice that the slow-wave noise will not take part in the interaction process and if the pump and signal are represented by discrete spectral lines the amplification will give a signal with practically no noise output. The extension of Chu's theorem for the parametric amplifier where only the upper and lower sidebands around each harmonic of the pump are considered is given as

$$\operatorname{Re} \sum_{m=-\infty}^{\infty} \oint \frac{E_{ms} XH_{ms}^* + V_{ms} J_{ms}^*}{m\omega_p + \omega_s} \cdot ds = 0 .$$

The form is closely related to the Manley-Rowe<sup>35</sup> equations.

It has been pointed out by Pierce<sup>29</sup> that the electromagnetic energy associated with the beam is much smaller than the kinetic-energy flow of the beam so that for a volume not enclosing any r-f structures, the increase of the kinetic-energy flow associated with the sidebands must be accompanied by a decrease of the kinetic energy flow of the pump.

The authors mentioned above considered coupling only between two sidebands. In the material presented in this chapter, coupling between the upper and lower sidebands and the signal were considered. This coupling was brought about by the pump. The effect of neglecting the coupling to other modes was discussed in the preceding section. The heavy excitation of the upper sideband indicates that noise will be carried at this frequency. In order to remove the noise from this device it is therefore necessary to terminate noise not only at the signal frequency but at other sideband frequencies as well.

It is interesting to consider the multimode coupling problem in the parametric amplifier investigated in this chapter. A diagrammatic representation is given in Fig. 6.5. The pump and the signal are assumed to mix in the nonlinear element which represents the beam nonlinearities. The nonlinearities then generate sideband frequencies. The sideband frequencies then can be considered as being coupled modes with the pump supplying energy. The modes are then coupled by a linear mechanism, and an analogy exists between this part of the interaction and the conventional type of coupled modes. The equations describing the linear relations between the modes were presented in Eqs. 6.28 and 6.29.

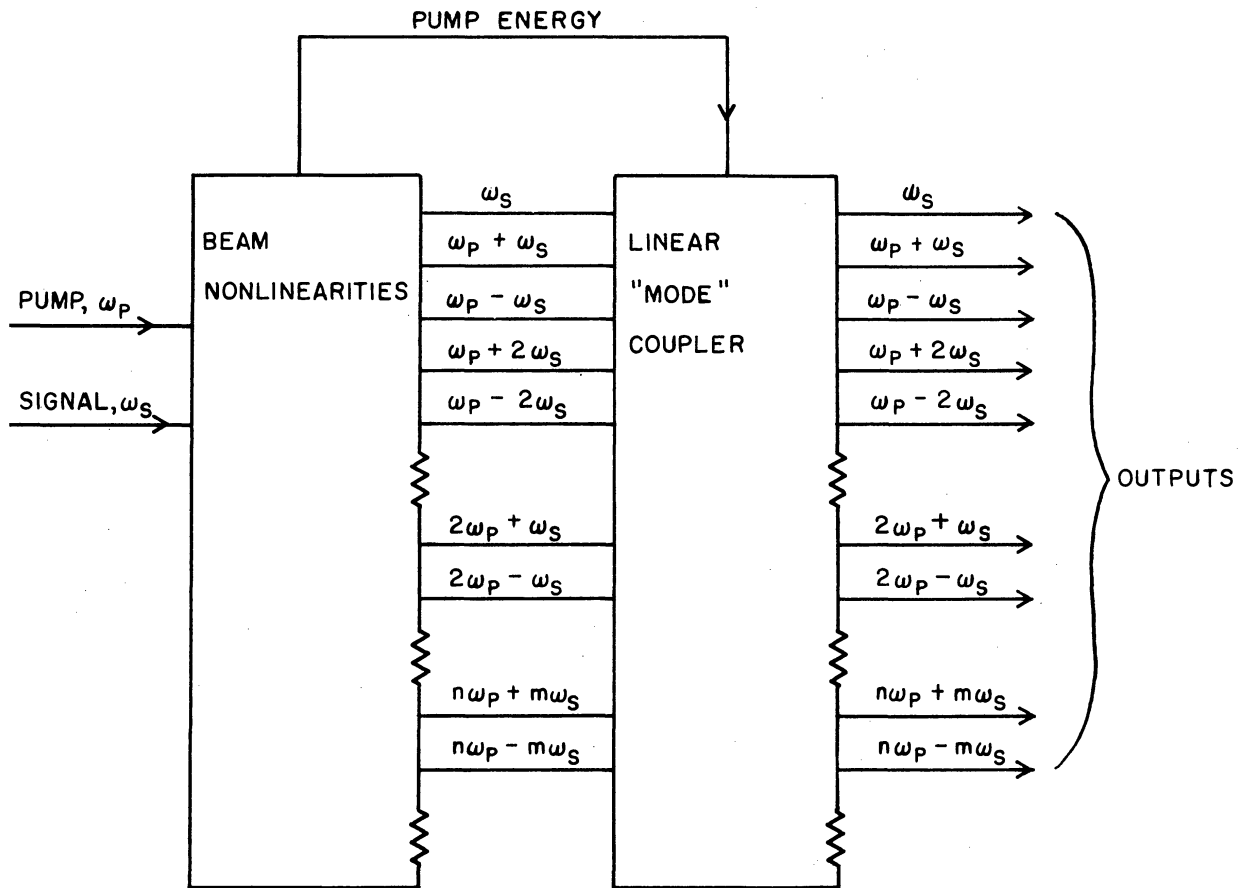


FIG. 6.5 MULTIMODE COUPLING IN THE LONGITUDINAL-BEAM PARAMETRIC AMPLIFIER.

7.1 Low-Frequency Modulation Study

A method of theoretically describing traveling-wave tubes undergoing low-frequency beam modulations by introducing the average beam current and potential as variables resulted in a more accurate description of the effects of modulation than had been previously given. The analysis was applied to both the small- and the large-signal modes of operation. In the small-signal study, loss, space-charge forces, finite values of the gain parameter  $C$ , modulation of the initial loss parameter  $A$ , and large modulation amplitudes were considered. The amplitude and phase modulation was determined by expressing the gain and phase shift as functions of a set of modulation propagation constants. The propagation constants were given in terms of the unmodulated parameters and the modulation amplitude. Good agreement was found between theoretical and experimental results. Beam modulations of large-signal traveling-wave amplifiers were similarly studied using the nonlinear ballistic equations and a Lagrangian formulation.

For both the large- and small-signal amplifiers, sets of quasi-stationary curves called the modulation device functions were presented. These functions showed the variation of phase and amplitude as functions of the beam average potential and current. The phase can be varied linearly over about a 10% range of beam potential for a  $C = 0.10$  tube while at the same time the amplitude would go through a 10 db variation. The amplitude can be varied linearly over a small range of the beam average current while the phase shift changes very little.

Saturation did not tend to change the linearity of the phase as a function of beam potential and in some instances even tended to extend

the linear range while at the same time limiting the resulting amplitude modulation. The addition of loss extended the linear range of phase modulation. Modulation effects on the initial loss parameter were shown to be of little consequence for long, low-C tubes, however they were shown to have a pronounced effect on the short high-C tubes and must be taken into account when predicting the modulation behavior during linear operation. The modulation effects on A are more important during a beam-potential modulation than during a beam-current modulation.

To obtain large phase-modulation indices it is best to use a long, low-C, lossy voltage-modulated tube. The resulting amplitude modulation can be minimized by increasing the r-f drive level until saturation sets in. To decrease the amplitude modulation further, it is necessary to resort to higher C short tubes and to use large modulation voltages.

The modulation device functions can be described as functional variations of the modulations either by fitting the curves with polynomials or by approximating the phase and gain with a truncated Taylor series. The Taylor series approach limits the results to small modulation amplitudes. Spectrum analyses were given for several common modulation wave shapes using second-degree polynomials to approximate the device functions.

The linear modulation analysis was extended to the Crestatron and the BWO at start-oscillation conditions. The Crestatron was found to be capable of producing a linear amplitude modulation with small phase modulation when the beam average potential was varied. The amplitude modulation however was limited to small indices. The start-oscillation conditions of a BWO as a function of modulation were determined using an analog computer. This appeared to be a convenient way of obtaining the

start-oscillation frequency and required starting length as a function of the beam potential variation at start-oscillation currents.

## 7.2 High-Frequency Analysis

The differential equations describing a beam carrying two signals of different frequency and passing through an arbitrary r-f structure or drift tube were derived. The signal levels were sufficient to drive the beam slightly into the nonlinear region so that a mixing interaction took place and produced many sidebands. Because of the small degree of non-linearity an Eulerian analysis was utilized. Space-charge effects as well as coupling to more sidebands than previously had been considered in similar published analyses, were taken into account. The equations were integrated for the special case of the longitudinal-beam parametric amplifier in which a large pump signal at twice the signal frequency was impressed on the beam. Both signal and pump were excited as fast space-charge waves in an effort to obtain low-noise amplification. Earlier analyses of this device took into account only coupling between the signal and lower sideband frequencies, with the result that the theoretical gain obtained was far greater than the experimental gain. The analysis presented in this dissertation considered coupling between the signal and lower and upper sideband frequencies. With this "multifrequency" coupling the gain in db was found to be one half of that obtained by a consideration of single-frequency coupling. This represented a gain figure much closer to the experimental value. The upper sideband was found to be heavily excited, indicating that in order to obtain low noise operation it is necessary to remove noise not only at the signal frequency but at other sideband frequencies as well. The threshold pump signal required to produce gain in an amplifier with a finite diameter beam was found to

be higher than the signal required in the single-sideband case.

### 7.3 Suggestions for Further Study

There appear to be several aspects of the work presented above that warrant further study. These are listed below.

7.3.1 Experiments on the Low-Frequency Beam-Modulated TWA. A traveling-wave tube to be used for modulation purposes should be designed, constructed and operated according to the recommendations listed above. It would be interesting to modulate simultaneously the average current and potential of the beam. If the phase and amplitude of the signal applied to the circuit and the grid are properly related, it appears that either phase modulation with little amplitude modulation or amplitude modulation with little phase modulation could be obtained. This idea of simultaneous modulation can be extended so that the traveling-wave tube may be used as an envelope wave-shaping device which amplifies the carrier.

7.3.2 Modulation Study of the Large-Signal BWO. A modulation study of the nonlinear BWO using the Lagrangian formulation is essential in predicting pushing and pulling characteristics of the BWO operating at currents greater than the start-oscillation current. It would also be interesting to study the effects of simultaneous modulations of the beam current and potential, both experimentally and theoretically. In this way it might be possible to obtain nearly a constant power output across the frequency band without resorting to signal equalizers.

7.3.3 High-Frequency Modulations. At present, the major drawback of the high frequency analysis is that an Eulerian analysis is used. The problem should be formulated in Lagrangian coordinates in order to take into account more accurately the nonlinear effects. At first this



could be carried out for only a minimum number of sidebands and later on applied to cases where more sidebands are considered. The Eulerian analysis given in this dissertation can be improved by considering more sidebands, especially those around the second harmonic of the pump. The analysis could be carried out using the present results and estimating the amount of second harmonic pump power either by a Lagrangian analysis or by a method similar to Pashke's<sup>38</sup>.

Some experiments should be carried out on the longitudinal-beam parametric amplifier to measure the amount of power and noise in the upper sidebands. If this amplifier is to be a low-noise device, the noise must be removed not only at the signal frequency but also the upper sideband frequency.

Additional calculations should be carried out for the longitudinal-beam parametric amplifier for different geometries and for different ratios of pump to signal frequency.

APPENDIX A. OTHER METHODS FOR MODULATING A TRAVELING-WAVE  
AMPLIFIER AT LOW FREQUENCIES

It was mentioned in Section 2.1 that a TWA may be modulated without directly perturbing the beam at modulation frequencies. Two methods in particular were mentioned and these are more fully discussed in this Appendix.

A.I. Phase Modulation by Variations in Signal Level

In Rowe's<sup>20</sup> work on the large-signal TWA, phase shift as a function of input signal was investigated. Typical results obtained by Rowe are shown in Figs. A.1 and A.2. A linear range of phase shift as a function of input is indicated. Note that for the  $C = 0.1$ , zero space-charge case, a change in input-signal level from 9 db below  $C_{o1} I_{o1} V_{o1}$  to 5 db below  $C_{o1} I_{o1} V_{o1}$ , a linear change in phase shift of 0.5 radians can be obtained. Therefore in this case a phase deviation of 0.5 radians can be obtained with an inherent AM of 4 db.

A.II. Phase Modulation by Modulation of Cold Circuit Velocity

Many of the effects produced by varying the beam velocity with respect to a fixed cold circuit velocity can be similarly produced by varying the cold circuit velocity with respect to a fixed beam velocity. It is possible to vary electronically the velocity of a circuit either by modulating the bias on a ferrite or a dielectric surrounding the circuit. Ferrites in helices and dielectrics in waveguides have been used in phase shifting devices. At present it is questionable as to whether materials exist to produce sufficient phase shift for use in traveling-wave tube modulators, but a simple analysis is included here for the sake of completeness.

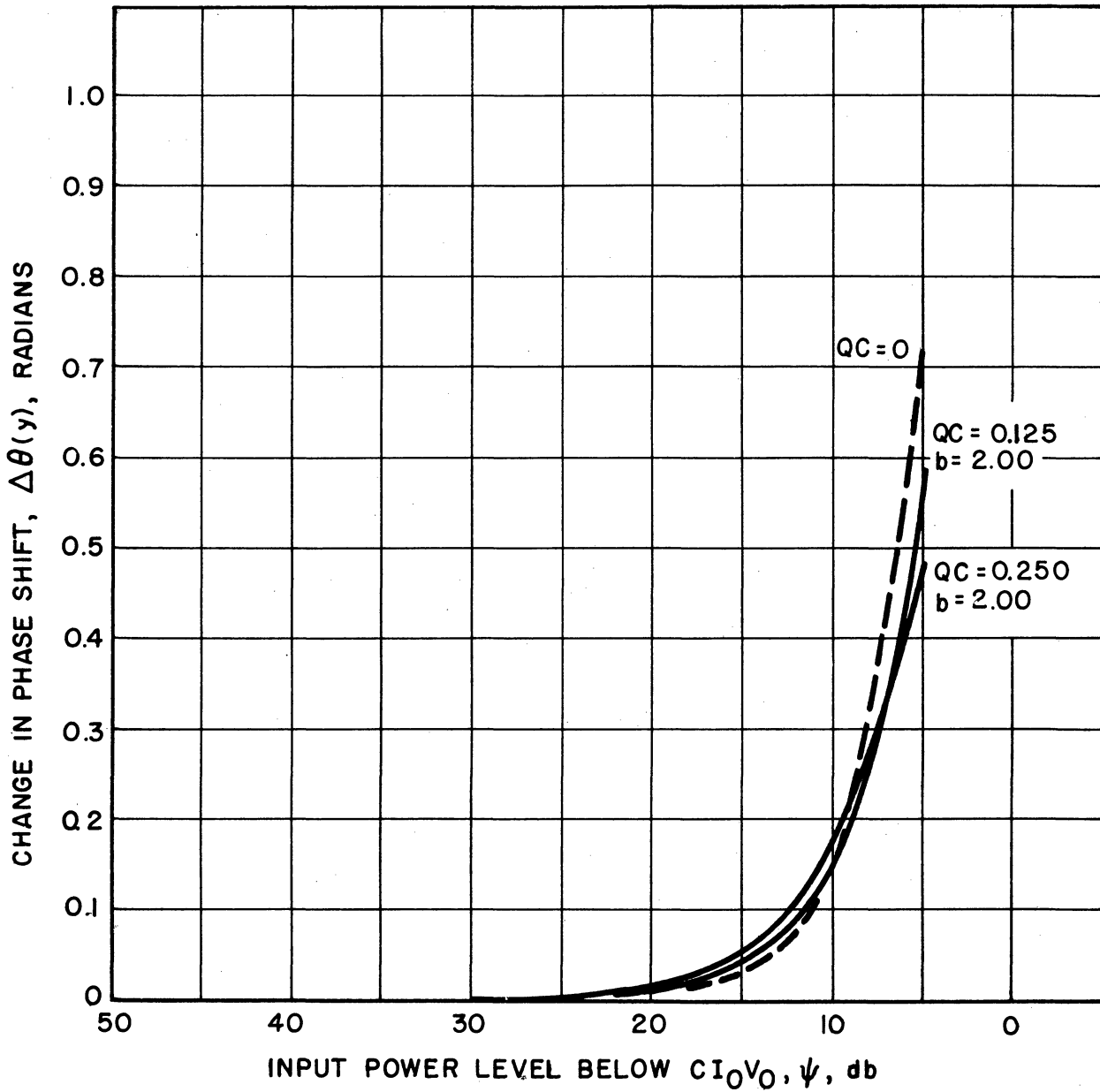


FIG. A.1 CHANGE IN PHASE SHIFT vs. INPUT POWER. ( $C=0.10$ ,  $d=0$ ,  $N_g=5.75$ ,  $B=1$ )

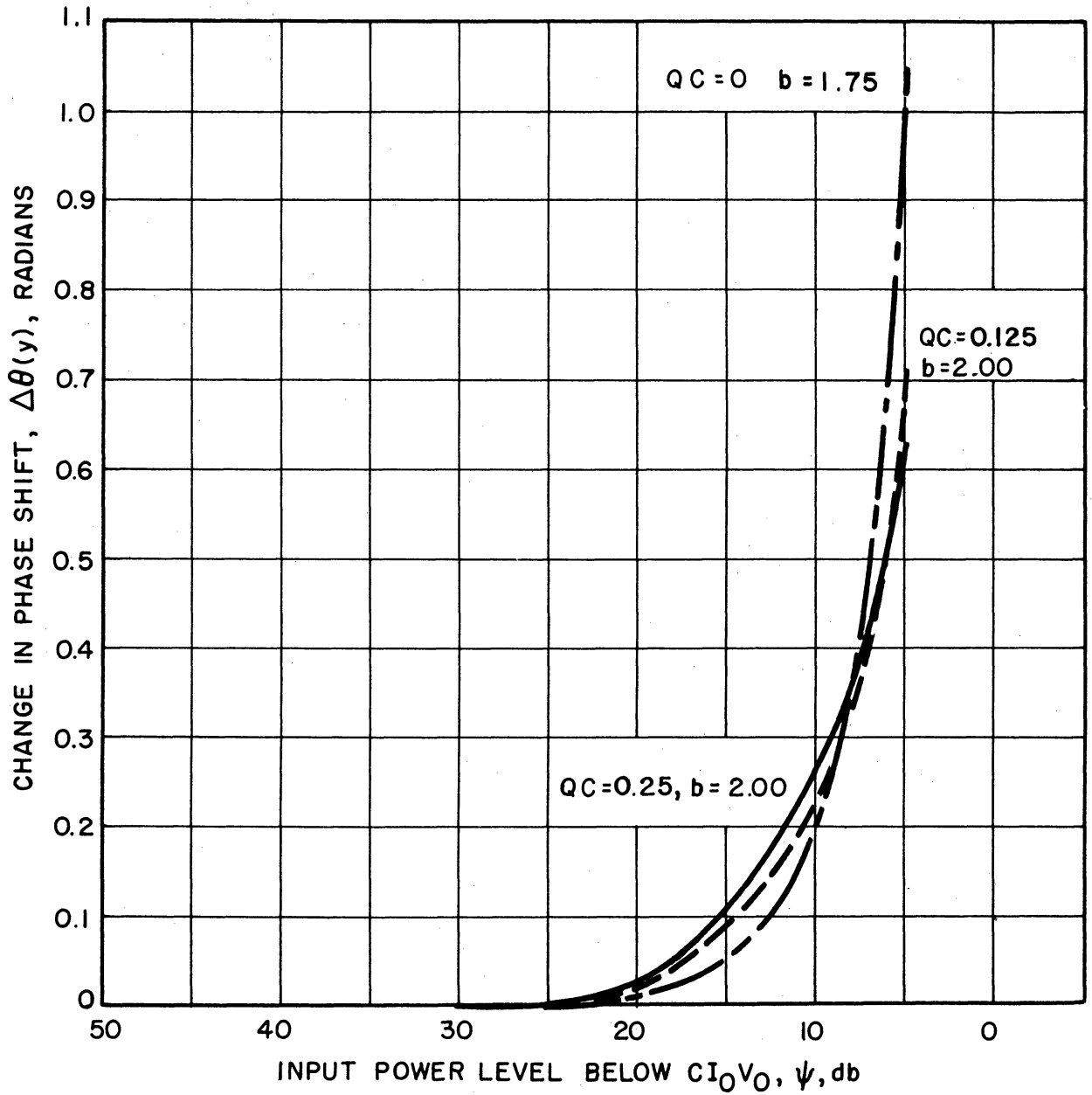


FIG. A.2 CHANGE IN PHASE SHIFT vs. INPUT POWER. ( $C=0.05$ ,  $d=0$ ,  $N_g=13$ ,  $B=1$ )

This discussion shall be only an approximate one limited to a consideration of phase variations. Any impedance changes shall be neglected. This of course is a questionable assumption in view of the fact that the impedance of most structures is dependent upon the cold phase velocity.

Approximate the phase shift through the tube as

$$\varphi \approx \beta_e L [1 - Cy_1(\xi)] \quad (\text{A.1})$$

where  $\xi$  is the particular modulation function applied to the bias of the dielectric and the ferrite. The phase shift approximated by a first-order truncated Taylor series is given as

$$\varphi \approx \varphi_0 + \left( \frac{\partial \varphi}{\partial \xi} \right)_{\xi=0} \Delta \xi \quad (\text{A.2})$$

The only variations considered will be those in  $b$ . The derivative of  $y$  with respect to  $b$  is approximately  $\partial y_1 / \partial b \approx -1/3^*$ , therefore the change in phase shift is given as

$$\Delta \varphi \approx - \frac{C_0 \varphi_0}{3} \left( \frac{\partial b}{\partial \xi} \right)_{\xi=0} \Delta \xi \quad (\text{A.3})$$

The velocity parameter  $b$  is given as

$$1 + Cb(\xi) = \frac{u_0}{v_{ph}(\xi)},$$

and the phase velocity  $v_{ph}$  is

$$v_{ph}(\xi) \approx v_{ph0} \sqrt{\frac{\mu(0)\epsilon(0)}{\epsilon(\xi)\mu(\xi)}}.$$

---

\* See Appendix C for a verification of this approximation.

Therefore Eq. A.3 becomes

$$\Delta\varphi = -\frac{\varphi_0}{6} \frac{1 + C_o b_o}{\sqrt{\mu(0)\epsilon(0)}} \left[ \epsilon(0) \left( \frac{\partial\mu}{\partial\xi} \right)_o + \mu(0) \left( \frac{\partial\epsilon}{\partial\xi} \right)_o \right] \Delta\xi \quad (A.4)$$

For the pure dielectric

$$\Delta\varphi = -\frac{\varphi_0}{6} (1 + C_o b_o) \sqrt{\frac{\mu_o}{\epsilon(0)}} \left( \frac{\partial\epsilon}{\partial\xi} \right)_o \Delta\xi \quad (A.5)$$

and for the pure ferrite

$$\Delta\varphi = -\frac{\varphi_0}{6} (1 + C_o b_o) \sqrt{\frac{\epsilon_o}{\mu(0)}} \left( \frac{\partial\mu}{\partial\xi} \right)_o \Delta\xi \quad (A.6)$$

APPENDIX B. WAVE AMPLITUDES FOR THE LOW-FREQUENCY BEAM-MODULATED  
TRAVELING-WAVE TUBE WITH A BUNCHED BEAM  
ENTERING THE INTERACTION REGION

The wave amplitudes for the low-frequency beam-modulated traveling-wave tube with an unbunched beam entering the interaction region have been presented in Eq. 2.26. There are instances when a bunched beam must be considered. These cases arise in noise analyses, r-f prebunching and, in general, considerations of discontinuities in traveling-wave tubes such as attenuator sections, drift spaces, etc. Thus in a study of the effect of discontinuities on the modulation device functions, one would have to calculate the wave amplitudes with a bunched beam at the entrance to the interaction region.

The general equation for evaluating these wave amplitudes has been given in Eq. 2.20 and is repeated below.

$$\begin{bmatrix} v(0) \\ -\frac{u_{o1} C_o v(0)}{j\eta} \\ -\frac{2V_{o1} C_o^2 i(0)}{I_{o1} \xi_2} \end{bmatrix} = \begin{bmatrix} 1 & 1 & 1 \\ \frac{1 + jC_o \delta'_1}{\delta'_1 \xi_1} & \frac{1 + jC_o \delta'_2}{\delta'_2 \xi_1} & \frac{1 + jC_o \delta'_3}{\delta'_3 \xi_1} \\ \frac{1 + jC_o \delta'_1}{\delta_1^2 \xi_1} & \frac{1 + jC_o \delta'_2}{\delta_2^2 \xi_1} & \frac{1 + jC_o \delta'_3}{\delta_3^2 \xi_1} \end{bmatrix} \begin{bmatrix} V_1 \\ V_2 \\ V_3 \end{bmatrix} \quad (2.20)$$

where  $\delta'_1 = j \frac{1 - \xi_1}{C_o} + \xi_1 \delta_1$ .

When the circuit-wave amplitudes are used, Eq. 2.20 becomes

$$\begin{bmatrix} V(0) \\ -\frac{u_{o1} C_o v(0) \xi_1}{j\eta} \\ -\frac{2V_{o1} C_o i(0) \xi_1}{I_{o1} \xi_2} \end{bmatrix} = A \begin{bmatrix} V_{c1} \frac{V_1}{V_{c1}} \\ V_{c2} \frac{V_2}{V_{c2}} \\ V_{c3} \frac{V_3}{V_{c3}} \end{bmatrix} \quad (\text{B.1})$$

where

$$A = \begin{bmatrix} 1 & 1 & 1 \\ \frac{1 + jC_o \delta'_1}{\delta'_1} & \frac{1 + jC_o \delta'_2}{\delta'_2} & \frac{1 + jC_o \delta'_3}{\delta'_3} \\ \frac{1 + jC_o \delta'_1}{\delta_1'^2} & \frac{1 + jC_o \delta'_2}{\delta_2'^2} & \frac{1 + jC_o \delta'_3}{\delta_3'^2} \end{bmatrix}$$

The ratio of the voltage at the beam to the circuit voltage is given as:

$$\frac{V_{c_i}}{V_i} = 1 + \frac{4Q C_o \xi_2}{\xi_1^2 \delta_i'^2} (1 + jC_o \delta_i')^2 \quad (\text{B.2})$$

The general expression for  $V_{c_i}$  is found by inverting Eq. B.1 and using Eq. B.2. The result is



$$\frac{V_{c_i}}{1 + \frac{4QC_o \xi_2}{\xi_1^2 \delta_i'^2} (1 + jC_o \delta_i')^2}$$

$$= \frac{V(0) + A - B}{1 + \left(\frac{\delta_{i+1}'}{\delta_i'}\right)^2 \frac{\delta_{i+2}' - \delta_i'}{\delta_{i+1}' - \delta_{i+2}'} \frac{1 + jC_o \delta_i'}{1 + jC_o \delta_{i+1}'} + \left(\frac{\delta_{i+2}'}{\delta_i'}\right)^2 \frac{\delta_{i+1}' - \delta_{i+2}'}{\delta_{i+1}' - \delta_{i+2}'} \frac{1 + jC_o \delta_i'}{1 + jC_o \delta_{i+2}'}}$$

(B.3)

where  $\delta_{i+3}' = \delta_i'$ ,

$$A = \frac{\xi_1 u_{o1} v(0)}{j\eta} \frac{\delta_{i+1}' \delta_{i+2}'}{\delta_{i+1}' - \delta_{i+2}'} \left( \frac{\delta_{i+1}'}{\delta_{i+2}'} \frac{1}{1 + jC_o \delta_{i+1}'} - \frac{\delta_{i+2}'}{\delta_{i+1}'} \frac{1}{1 + jC_o \delta_{i+2}'} \right)$$

and

$$B = \frac{-2V_{o1} C_o^2 i(0) \xi_1}{I_{o1} \xi_2} \frac{\delta_{i+1}' \delta_{i+2}'}{\delta_{i+1}' - \delta_{i+2}'} \left( \frac{\delta_{i+1}'}{1 + jC_o \delta_{i+1}'} - \frac{\delta_{i+2}'}{1 + jC_o \delta_{i+2}'} \right)$$

APPENDIX C. TAYLOR SERIES EXPANSIONS FOR THE  
MODULATION DEVICE FUNCTIONS

Taylor series expansions for the amplitude and phase modulation during a low-frequency beam modulation were given in Section 2.3. In a general form the series can be expressed as

$$\Delta = \sum_{n=1}^{\infty} \frac{1}{n!} \left( \frac{\partial^n f}{\partial I^n} \right)_{V_{01}, I_{01}} \Delta I^n + \sum_{n=1}^{\infty} \frac{1}{n!} \left( \frac{\partial^n f}{\partial V^n} \right)_{V_{01}, I_{01}} \Delta V^n + \sum_{n=1}^{\infty} \frac{1}{n!} \sum_{r=1}^n C_r^n \left( \frac{\partial^n f}{\partial V^r \partial I^{n-r}} \right)_{V_{01}, I_{01}} \Delta V^r \Delta I^{n-r} \quad (C.1)$$

For the phase modulation

$$\Delta \rightarrow \Delta S$$

and

$$f = \psi - \beta_e L (1 - C y_1) \quad , \quad (C.2)$$

while for the amplitude modulation,

$$\Delta \rightarrow \Delta a_{db}$$

$$f = 8.864 \log_{10} \left( \frac{V_1(\Delta V, \Delta I)}{V(0)} \right) + 54.6 \text{ CN}_s x_1 (\Delta V, \Delta I)$$

and

$$N_s = \frac{\beta_e L}{2\pi} \quad . \quad (C.3)$$

The small-signal propagation constants  $x_1$  and  $y_1$  can be expressed as explicit functions of the small-signal parameters,

$$\begin{aligned}x_1 &= x_1 (C, QC, b, d) \\y_1 &= y_1 (C, QC, b, d) \quad , \quad (C.4)\end{aligned}$$

and, in turn, the small-signal parameters can be expressed in terms of the beam average potential and current. The functional relations of the small-signal parameters and their derivatives with respect to the beam d-c variables are listed in the table below. All quantities are evaluated at the unmodulated point  $(I_{01}, V_{01})$ , since these are the values necessary for the Taylor expansion. The beam propagation constant  $\beta_e$  is included in Table C.1. Derivatives are listed only up to second order.

Equations C.4 and Table C.1 can be used to calculate the Taylor series coefficients in terms of the partial derivatives of the propagation constants with respect to the small-signal parameters. The second-order Taylor series for the device modulation functions are therefore

TABLE C.1  
TWA Parameters and Their Derivatives

Parameter	$\left(\frac{\partial}{\partial V}\right) \frac{I_{O1}}{V_{O1}}$	$\left(\frac{\partial^2}{\partial V^2}\right) \frac{I_{O1}}{V_{O1}}$	$\left(\frac{\partial}{\partial I}\right) \frac{I_{O1}}{V_{O1}}$	$\left(\frac{\partial^2}{\partial I^2}\right) \frac{I_{O1}}{V_{O1}}$	$\left(\frac{\partial^2}{\partial I \partial V}\right) \frac{I_{O1}}{V_{O1}}$
$C = \left(\frac{KI_0}{4V_0}\right)^{1/3}$	$-\frac{C_0}{3V_{O1}}$	$\frac{4}{9} \frac{C_0}{V_{O1}^2}$	$\frac{1}{3} \frac{C_0}{I_{O1}}$	$-\frac{2}{9} \frac{C_0}{I_{O1}^2}$	$-\frac{1}{9} \frac{C_0}{I_{O1} V_{O1}}$
$b = \frac{1}{C} \left(\frac{u_0 - v_0}{v_0}\right)$	$\frac{1}{V_{O1}} \left(\frac{5b_0}{6} + \frac{1}{2C_0}\right)$	$\frac{1}{V_{O1}^2} \left(-\frac{5b_0}{36} + \frac{1}{12C_0}\right)$	$-\frac{b_0}{3I_{O1}}$	$\frac{4}{9} \frac{b_0}{I_{O1}^2}$	$-\frac{1}{3I_{O1} V_{O1}} \left[\frac{1}{2C_0} + \frac{5b_0}{6}\right]$
$QC = \frac{C}{u_0 C_1 2K}$	$-\frac{5}{6} \frac{QC_0}{V_{O1}}$	$\frac{55}{36} \frac{QC_0}{V_{O1}^2}$	$\frac{1}{3} \frac{QC_0}{I_{O1}}$	$-\frac{2}{9} \frac{QC_0}{I_{O1}^2}$	$-\frac{5}{18} \frac{QC_0}{I_{O1} V_{O1}}$
$d = \frac{2\pi u_0}{\omega LC} \frac{0.01836 \text{ Loss (db)}}{\omega LC}$	$\frac{5}{6} \frac{d_0}{V_{O1}}$	$-\frac{5}{36} \frac{d_0}{V_{O1}^2}$	$-\frac{d_0}{3I_{O1}}$	$\frac{4}{9} \frac{d_0}{I_{O1}^2}$	$-\frac{5}{18} \frac{d_0}{I_{O1} V_{O1}}$
$\beta_e = \frac{\omega}{u_0}$	$-\frac{\beta_{e0}}{2V_{O1}}$	$\frac{\beta_{e0}}{3V_{O1}^2}$	0	0	0

$$\begin{aligned}
 \frac{\Delta S}{\beta_{eo} L} = & \left\{ \frac{I_{o1}}{\beta_{eo} L} \left( \frac{\partial \psi}{\partial I_o} \right)_{I_{o1}, V_{o1}} + \frac{y_1 C_o}{3} + I_{o1} C_o \left( \frac{\partial y_1}{\partial I_o} \right)_{I_{o1}, V_{o1}} \right\} \frac{\Delta I}{I_{o1}} \\
 & + \frac{1}{2} \left\{ \frac{I_{o1}^2}{\beta_{eo} L} \left( \frac{\partial^2 \psi}{\partial I_o^2} \right)_{I_{o1}, V_{o1}} - \frac{2y_1 C_o}{9} + \frac{2}{3} I_{o1} C_o \left( \frac{\partial y_1}{\partial I_o} \right)_{I_{o1}, V_{o1}} \right. \\
 & \left. + I_{o1}^2 \left( \frac{\partial^2 y_1}{\partial I_o^2} \right)_{I_{o1}, V_{o1}} \right\} \left( \frac{\Delta I}{I_{o1}} \right)^2 + \left\{ \frac{V_{o1}}{\beta_{eo} L} \left( \frac{\partial \psi}{\partial V_o} \right)_{I_{o1}, V_{o1}} \right. \\
 & \left. + \frac{1}{2} - \frac{5}{6} C_o y_1 + C_o V_{o1} \left( \frac{\partial y_1}{\partial V_o} \right)_{I_{o1}, V_{o1}} \right\} \frac{\Delta V}{V_{o1}} + \frac{1}{2} \left\{ \frac{V_{o1}^2}{\beta_{eo} L} \left( \frac{\partial^2 \psi}{\partial V_o^2} \right)_{I_{o1}, V_{o1}} \right. \\
 & \left. - \frac{3}{4} + \frac{55}{36} C_o y_1 - \frac{5}{3} C_o V_{o1} \left( \frac{\partial y_1}{\partial V_o} \right)_{I_{o1}, V_{o1}} \right. \\
 & \left. + V_{o1}^2 C_o \left( \frac{\partial^2 y_1}{\partial V_o^2} \right)_{I_{o1}, V_{o1}} \right\} \left( \frac{\Delta V}{V_{o1}} \right)^2 + \frac{1}{2} \left\{ \frac{V_{o1} I_{o1}}{\beta_{eo} L} \left( \frac{\partial^2 \psi}{\partial I_o \partial V_o} \right)_{I_{o1}, V_{o1}} \right. \\
 & \left. - \frac{5}{18} C_o y_1 - \frac{5}{6} I_{o1} C_o \left( \frac{\partial y_1}{\partial I_o} \right)_{I_{o1}, V_{o1}} \right. \\
 & \left. + I_{o1} V_{o1} C_o \left( \frac{\partial^2 y_1}{\partial I_o \partial V_o} \right)_{I_{o1}, V_{o1}} \right\} \left( \frac{\Delta V}{V_{o1}} \right) \left( \frac{\Delta I}{I_{o1}} \right) + \dots \quad (C.5)
 \end{aligned}$$

and

$$\begin{aligned}
 \frac{\Delta a_{db}}{8.864 \beta_{eo} C_o L} &= \left\{ \frac{V_{o1}}{8.864 \beta_{eo} C_o L} \left( \frac{\partial |A|}{\partial V_o} \right)_{V_{o1}, I_{o1}} \right. \\
 &+ V_{o1} \left( \frac{\partial x_1}{\partial V_o} \right)_{V_{o1}, I_{o1}} - \frac{5}{6} x_{10} \left. \right\} \frac{\Delta V}{V_{o1}} + \frac{1}{2} \left\{ \frac{V_{o1}^2}{8.864 \beta_{eo} C_o L} \left( \frac{\partial^2 |A|}{\partial V_o^2} \right)_{V_{o1}, I_{o1}} \right. \\
 &- \frac{5}{3} V_{o1} \left( \frac{\partial x_1}{\partial V_o} \right)_{V_{o1}, I_{o1}} + \frac{55}{36} x_{10} - V_{o1}^2 \left( \frac{\partial^2 x_1}{\partial V_o^2} \right)_{V_{o1}, I_{o1}} \left. \right\} \left( \frac{\Delta V}{V_{o1}} \right)^2 \\
 &+ \left\{ \frac{I_{o1}}{8.864 \beta_{eo} C_o L} \left( \frac{\partial |A|}{\partial I_o} \right)_{V_{o1}, I_{o1}} + \frac{x_{10}}{3} + I_{o1} \left( \frac{\partial x_{10}}{\partial I_o} \right)_{V_{o1}, I_{o1}} \right\} \frac{\Delta I}{I_{o1}} \\
 &+ \frac{1}{2} \left\{ \frac{I_{o1}^2}{8.864 \beta_{eo} C_o L} \left( \frac{\partial^2 |A|}{\partial I_o^2} \right)_{V_{o1}, I_{o1}} - \frac{2}{9} x_{10} + \frac{2}{3} I_{o1} \left( \frac{\partial x_1}{\partial I_o} \right)_{V_{o1}, I_{o1}} \right. \\
 &+ \left. I_{o1}^2 \left( \frac{\partial^2 x_1}{\partial I_o^2} \right)_{V_{o1}, I_{o1}} \right\} \left( \frac{\Delta I}{I_{o1}} \right)^2 + \frac{1}{2} \left\{ \frac{I_{o1} V_{o1}}{8.864 \beta_{eo} C_o L} \left( \frac{\partial^2 |A|}{\partial I_o \partial V_o} \right)_{V_{o1}, I_{o1}} \right. \\
 &+ \frac{V_{o1}}{3} \left( \frac{\partial x_1}{\partial V_o} \right)_{I_{o1}, V_{o1}} + I_{o1} V_{o1} \left( \frac{\partial^2 x_1}{\partial I_o \partial V_o} \right)_{I_{o1}, V_{o1}} - \frac{5}{18} x_{10} \\
 &\left. - \frac{5}{6} I_{o1} \left( \frac{\partial x_{10}}{\partial I_o} \right)_{I_{o1}, V_{o1}} \right\} \left( \frac{\Delta V}{I_{o1}} \right) \left( \frac{\Delta V}{V_{o1}} \right) + \dots, \tag{C.6}
 \end{aligned}$$

where  $|A| = 8.864 \log_{10} \left( \frac{\hat{V}_1(\Delta V, \Delta I)}{\hat{V}(0)} \right)$ , is the initial loss parameter.

The derivatives of the propagation constants with respect to the average potential and current are listed below. In the following equations  $f$  represents any of the small-signal propagation constants. Also, the zero (0) subscript refers to the derivative evaluated at  $\Delta V = \Delta I = 0$ .

$$V_{o1} \left( \frac{\partial f}{\partial V} \right)_o = -\frac{c_o}{3} \left( \frac{\partial f}{\partial C} \right)_o - \frac{5}{6} qC_o \left( \frac{\partial f}{\partial qC} \right)_o + \frac{5}{6} d_o \left( \frac{\partial f}{\partial d} \right)_o + \left( \frac{5}{6} b_o + \frac{1}{2C_o} \right) \left( \frac{\partial f}{\partial b} \right)_o \quad (C.7)$$

$$I_{o1} \left( \frac{\partial f}{\partial I} \right)_o = \frac{c_o}{3} \left( \frac{\partial f}{\partial C} \right)_o + \frac{1}{3} qC_o \left( \frac{\partial f}{\partial qC} \right)_o - \frac{d_o}{3} \left( \frac{\partial f}{\partial d} \right)_o - \frac{b_o}{3} \left( \frac{\partial f}{\partial b} \right)_o \quad (C.8)$$

$$\begin{aligned} V_{o1}^2 \left( \frac{\partial^2 f}{\partial V^2} \right)_o &= \frac{c_o^2}{9} \left( \frac{\partial^2 f}{\partial C^2} \right)_o + \frac{25}{36} qC_o^2 \left( \frac{\partial^2 f}{\partial qC^2} \right)_o + \left( \frac{5}{6} b_o + \frac{1}{2C_o} \right)^2 \left( \frac{\partial^2 f}{\partial b^2} \right)_o \\ &+ \frac{25}{36} d_o^2 \left( \frac{\partial^2 f}{\partial d^2} \right)_o + \frac{4}{9} c_o \left( \frac{\partial f}{\partial C} \right)_o + \frac{55}{36} qC_o \left( \frac{\partial f}{\partial qC} \right)_o - \frac{5d_o}{36} \left( \frac{\partial f}{\partial d} \right)_o \\ &+ \left( -\frac{5b_o}{36} + \frac{1}{12C_o} \right) \left( \frac{\partial f}{\partial b} \right)_o + \frac{5}{9} c_o qC_o \left( \frac{\partial^2 f}{\partial C \partial qC} \right)_o - \frac{5}{9} c_o d_o \left( \frac{\partial^2 f}{\partial C \partial d} \right)_o \\ &- \frac{2}{3} \left( \frac{5}{6} c_o b_o + \frac{1}{2} \right) \left( \frac{\partial^2 f}{\partial C \partial b} \right)_o - \frac{25}{18} qC_o d_o \left( \frac{\partial^2 f}{\partial qC \partial d} \right)_o \\ &- \frac{5}{3} qC_o \left( \frac{5}{6} b_o + \frac{1}{2C_o} \right) \left( \frac{\partial^2 f}{\partial qC \partial b} \right)_o + \frac{5}{3} d_o \left( \frac{5}{6} b_o + \frac{1}{2C_o} \right) \left( \frac{\partial^2 f}{\partial b \partial d} \right)_o \quad (C.9) \end{aligned}$$

$$\begin{aligned}
 I_{o1}^2 \left( \frac{\partial^2 f}{\partial I_o^2} \right) &= \frac{1}{9} c_o^2 \left( \frac{\partial^2 f}{\partial c^2} \right) + \frac{1}{9} qc_o^2 \left( \frac{\partial^2 f}{\partial qc^2} \right) + \frac{d_o^2}{9} \left( \frac{\partial^2 f}{\partial d^2} \right) + \frac{b_o^2}{9} \left( \frac{\partial^2 f}{\partial b^2} \right) \\
 &- \frac{2}{9} c_o \left( \frac{\partial f}{\partial c} \right) - \frac{2}{9} qc_o \left( \frac{\partial f}{\partial qc} \right) + \frac{4}{9} d_o \left( \frac{\partial f}{\partial d} \right) + \frac{4}{9} b_o \left( \frac{\partial f}{\partial b} \right) \\
 &+ \frac{2}{9} c_o qc_o \left( \frac{\partial^2 f}{\partial qc \partial c} \right) - \frac{2}{9} c_o d_o \left( \frac{\partial^2 f}{\partial c \partial d} \right) - \frac{2}{9} c_o b_o \left( \frac{\partial^2 f}{\partial c \partial b} \right) \\
 &- \frac{2}{9} qc_o d_o \left( \frac{\partial^2 f}{\partial qc \partial d} \right) - \frac{2}{9} qc_o b_o \left( \frac{\partial^2 f}{\partial qc \partial b} \right) + \frac{2}{9} b_o d_o \left( \frac{\partial^2 f}{\partial b \partial d} \right) . \quad (C.10)
 \end{aligned}$$

$$\begin{aligned}
 I_{o1} V_{o1} \left( \frac{\partial^2 f}{\partial I_o \partial V_o} \right) &= - \frac{c_o^2}{9} \left( \frac{\partial^2 f}{\partial c^2} \right) - \frac{5}{18} qc_o^2 \left( \frac{\partial^2 f}{\partial qc^2} \right) - \frac{5}{18} d_o^2 \left( \frac{\partial^2 f}{\partial d^2} \right) \\
 &- \frac{b_o}{3} \left( \frac{5}{6} b_o + \frac{1}{2c_o} \right) \left( \frac{\partial^2 f}{\partial b^2} \right) - \frac{c_o}{9} \left( \frac{\partial f}{\partial c} \right) - \frac{5}{18} qc_o \left( \frac{\partial f}{\partial qc} \right) - \frac{5}{18} d_o \left( \frac{\partial f}{\partial d} \right) \\
 &- \frac{1}{3} \left( \frac{1}{2c_o} + \frac{5}{6} b_o \right) \left( \frac{\partial f}{\partial b} \right) - \frac{7}{18} c_o qc_o \left( \frac{\partial^2 f}{\partial c \partial qc} \right) + \frac{7}{18} d_o c_o \left( \frac{\partial^2 f}{\partial c \partial d} \right) \\
 &+ \left( \frac{1}{6} + \frac{7}{18} c_o b_o \right) \left( \frac{\partial^2 f}{\partial c \partial b} \right) + \frac{5}{9} d_o qc_o \left( \frac{\partial^2 f}{\partial qc \partial d} \right) + \left( \frac{5}{9} qc_o b_o + \frac{qc_o}{6c_o} \right) \left( \frac{\partial^2 f}{\partial qc \partial b} \right) \\
 &- \left[ \frac{5}{9} d_o b_o + \frac{d_o}{6c_o} \right] \left( \frac{\partial^2 f}{\partial d \partial b} \right) . \quad (C.11)
 \end{aligned}$$

The evaluation of the derivatives of  $|A|$  and  $\psi$  is an extremely cumbersome task. The initial loss parameter and its phase may be evaluated at the zero modulation point by setting  $\delta' = \delta$  and  $\xi_1 = \xi_2 = 1$ . in Eq. 2.26. The required derivatives can then be evaluated from the resulting expression. This is indeed a long operation. As an approximation, use instead of Eq. 2.26



$$\frac{V_{c1}}{V(0)} \approx \frac{1}{\left(1 - \frac{\delta_3}{\delta_1}\right) \left(1 - \frac{\delta_2}{\delta_1}\right)} \approx |A| e^{j\psi} \quad (C.12)$$

This approximation is equivalent to setting  $C_0$  to a very small value and "partially" neglecting  $QC_0$ . "Partially" neglecting refers to the fact that it will be used in finding  $\delta_i$ , however it will be neglected in determining the amplitudes. The derivatives of this simplified form are once again found only after a laborious computation. The calculation actually has been carried out for one case and the results are shown in Section 3.4, however in the material following in this Appendix, variations of  $|A| e^{j\psi}$  are neglected. From Eq. C.5 it can be seen that neglecting the variations for a tube having a large  $\beta_{e0}L$  does not result in a serious error in the phase modulation. However the error in neglecting variations in  $|A|$  for the calculation of the amplitude modulation is certainly more serious since there is a  $C_0$  appearing in the denominator of the terms containing derivatives of the initial loss parameter.

There have been several presentations in the literature of the propagation constants as functions of the small-signal parameters. The derivatives may be determined graphically from Brewer and Birdsall's results<sup>21</sup> or Pierce's results<sup>1</sup>. There are also several explicit forms of the propagation constants although each has its disadvantages and limitations. The expressions that appear to be most amenable to this analysis are those given by Sensiper<sup>22</sup>. The disadvantage of Sensiper's expressions is that the results are limited to  $QC < 1/4$ , and furthermore the results are given such that each propagation constant is expressed by a long open series of the propagation constants. The

series for  $x_1$  and  $y_1$  are given below:

$$\begin{aligned}
 x_1 = & \frac{\sqrt{3}}{2} + \frac{\sqrt{3}}{12} (3c - 8qc) - \frac{d}{3} + \frac{1}{6} \left( c + \frac{8}{3} qc \right) \left( \sqrt{3} b - d \right) \\
 & - \frac{1}{9} \frac{\sqrt{3}}{2} (b^2 - d^2) - \frac{1}{9} bd + \frac{1}{3} \left( \frac{\sqrt{3}}{2} \right) \left( \frac{c^3}{8} + \frac{22}{8} c^2qc - 8cq^2c^2 \right. \\
 & \left. - \frac{64}{27} q^3c^3 \right) + \frac{1}{27} (3c^2 + 12cqc + 16q^2c^2) (\sqrt{3} b + d) \\
 & - \frac{\sqrt{3}}{81} (b^3 - 3bd^2) - \frac{1}{81} (d^3 - 3b^2d) + \frac{\sqrt{3}}{144} \left( c^4 + 128c^3qc \right. \\
 & \left. - \frac{1840}{3} c^2q^2c^2 - \frac{3584}{9} cq^3c^3 - \frac{2048}{27} q^4c^4 \right) + \frac{d}{3} \left( \frac{c^3}{4} - \frac{56}{9} c^2qc \right) \\
 & - \frac{1}{108} \left( 5c^2 + 8qcq + \frac{160}{3} q^2c^2 \right) \left[ \sqrt{3} (b^2 - d^2) - 2bd \right] + \frac{2}{81} \left( c \right. \\
 & \left. + \frac{4}{3} qc \right) \left[ \sqrt{3} (b^3 - 3bd^2) - (d^3 - 3b^2d) \right] + \dots \quad (C.13)
 \end{aligned}$$

and

$$\begin{aligned}
 y_1 = & -\frac{1}{2} + \frac{1}{12} (3c - 8qc) - \frac{b}{3} + \frac{1}{3} \left( \frac{c^2}{4} - 8cqc \right) \\
 & - \frac{1}{3} \left( c + \frac{8}{3} qc \right) \left( \frac{b}{2} + \frac{\sqrt{3}}{2} d \right) - \frac{1}{18} (b^2 - d^2) + \frac{\sqrt{3}}{9} bd - \frac{1}{6} \left( \frac{c^3}{8} \right. \\
 & + \frac{22}{3} c^2qc - 8cqc^2 - \frac{64}{27} q^3c^3 \left. \right) + \frac{1}{27} \left( 3c^2 + 12qc \right. \\
 & + 16q^2c^2 \left. \right) (b - d\sqrt{3}) - \frac{1}{81} \left[ (d^3 - 3b^2d)\sqrt{3} - (b^3 - 3bd^2) \right] \\
 & + \frac{1}{144} \left( c^4 + 128c^3qc - \frac{1840}{3} c^2q^2c^2 - \frac{3584}{9} cq^3c^3 - \frac{2048}{27} q^4c^4 \right) \\
 & + \frac{b}{3} \left( \frac{c^3}{4} - \frac{56}{9} c^2qc \right) + \frac{1}{54} \left( 5c^2 + 8cqc + \frac{160}{3} q^2c^2 \right) \left[ \frac{(b^2 - d^2)}{2} \right. \\
 & \left. + \sqrt{3} bd \right] + \frac{4}{81} \left( c + \frac{4}{3} qc \right) \left[ \frac{1}{2} (b^3 - 3bd^2) + \frac{\sqrt{3}}{2} (d^3 - 3b^2d) \right] + \dots
 \end{aligned}$$

(C.14)

Equations C.5 through C.14 can be used to determine the modulation device functions approximated by a second-order Taylor series. The results of a sample calculation are shown in Chapter III. Approximate equations for the phase are also given in Chapter III.

APPENDIX D. EXTENSION OF THE CAUCHY PRODUCT TO SERIES  
WITH INDICES RUNNING FROM  $-\infty$  TO  $+\infty$

There have been several occasions\* during the course of this dissertation when it has become necessary to multiply two infinite series with the indices running from  $-\infty$  to  $+\infty$ , therefore, it seems desirable to develop a form for this product analogous to the one for the Cauchy product. The same method as used in developing the Cauchy product will be employed.

The ordinary Cauchy product of two infinite series<sup>38</sup> is given as

$$\left( \sum_{n=0}^{\infty} c_n \right) \left( \sum_{n=0}^{\infty} d_n \right) = \sum_{n=0}^{\infty} \sum_{k=0}^n c_k d_{n-k} \quad . \quad (D.1)$$

This product is well adapted to the multiplication of power series and can be stated as

$$\left( \sum_{n=0}^{\infty} a_n x^n \right) \left( \sum_{n=0}^{\infty} b_n x^n \right) = \sum_{n=0}^{\infty} \sum_{k=0}^n a_k b_{n-k} x^n \quad . \quad (D.2)$$

Consider the product

$$\left( \sum_{n=-\infty}^{\infty} c_n \right) \left( \sum_{n=-\infty}^{\infty} d_n \right) \quad ;$$

the terms resulting from this multiplication can be written in the following array,

---

\* The products mentioned above have been used in Sections 4.1 and 6.2.



When C and d are exponentials, the product is given by

$$\left( \sum_{n=-\infty}^{\infty} A_n e^{jnx} \right) \left( \sum_{n=-\infty}^{\infty} B_n e^{jnx} \right) = \sum_{m=-\infty}^{\infty} \left( \sum_{n=-\infty}^{\infty} A_n B_{m-n} \right) e^{jmx} \quad . \quad (D.4)$$

APPENDIX E. SOLUTION OF THE BWO MODULATION EQUATIONS  
ON AN ANALOG COMPUTER

Equations describing the modulated BWO at start-oscillation conditions were presented in Section 5.3. The solution of these equations will now be discussed. The equations to be solved are

$$\xi_2 \frac{dv}{dy} + \xi_1 \frac{d\rho}{dy} + j \frac{\rho}{\epsilon_0} = 0 \quad . \quad (E.1)$$

$$\frac{1}{2} \frac{dV}{dy} + j \frac{4C_0 Q C_0}{(1 - 2C_0 \sqrt{QC_0})^2} \frac{\rho}{1 + C_0 b_0} \frac{F'}{\zeta_3} = \xi_1 \frac{dv}{dy} + j \frac{v}{C_0} \quad . \quad (E.2)$$

$$\begin{aligned} \frac{d^2V}{dy^2} + \left( \frac{1 + C_0 b_0}{C_0} \right)^2 \left( \frac{\xi_1}{\xi_3} \right)^2 V + 2j \frac{d_0}{C_0} (1 + C_0 b_0) \frac{\xi_1 \xi_2}{\xi_3} V \\ = 4C_0 (1 + C_0 b_0) \frac{\xi_1}{\xi_2 \xi_3} \rho + j \frac{8C_0^2 d_0}{\xi_3} \rho \quad . \quad (E.3) \end{aligned}$$

These above equations form a set of linear differential equations in three unknowns and can be solved by standard methods, however since oscillation conditions are to be determined, a trial and error type of solution will be used on an analog computer. In order to program this set of equations it is necessary to separate the real and imaginary parts: The variables  $V$ ,  $v$ , and  $\rho$  may be split into the real and imaginary components;

$$\begin{aligned} V &= V_R + jV_i \\ v &= v_R + jv_i \\ \rho &= \rho_R + j\rho_i \quad . \quad (E.4) \end{aligned}$$

When Eq. E.4 is substituted into Eqs. E.1 through E.3 and the real and imaginary parts separated, six equations result;

$$\xi_2 \frac{dv_R}{dy} + \xi_1 \frac{d\rho_R}{dy} - \frac{\rho_i}{C_o} = 0, \quad (E.5)$$

$$\xi_2 \frac{dv_i}{dy} + \xi_1 \frac{d\rho_i}{dy} + \frac{\rho_R}{C_o} = 0, \quad (E.6)$$

$$\frac{1}{2} \frac{dV_R}{dy} - \frac{4C_o Q C_o}{(1-2C_o \sqrt{QC_o})^2} \frac{F}{\zeta_3 (1+C_o b_o)} \rho_i = \xi_1 \frac{dv_R}{dy} - \frac{v_i}{C_o}, \quad (E.7)$$

$$\frac{1}{2} \frac{dV_i}{dy} + \frac{4C_o Q C_o}{(1-2C_o \sqrt{QC_o})^2} \frac{F}{\zeta_3 (1+C_o b_o)} \rho_R = \xi_1 \frac{dv_i}{dy} + \frac{v_R}{C_o}, \quad (E.8)$$

$$\begin{aligned} \frac{d^2V_R}{dy^2} + \left(\frac{1+C_o b_o}{C_o}\right)^2 \left(\frac{\zeta_1}{\zeta_3}\right)^2 V_R - 2 \frac{d_o}{C_o} (1+C_o b_o) \frac{\zeta_1 \zeta_2}{\zeta_3} V_i \\ = 4C_o (1+C_o b_o) \frac{\zeta_1}{\zeta_2 \zeta_3} \rho_R - \frac{8C_o^2 d_o}{\zeta_3} \rho_i, \end{aligned} \quad (E.9)$$

and

$$\begin{aligned} \frac{d^2V_i}{dy^2} + \left(\frac{1+C_o b_o}{C_o}\right)^2 \left(\frac{\zeta_1}{\zeta_3}\right)^2 V_i + 2 \frac{d_o}{C_o} (1+C_o b_o) \frac{\zeta_1 \zeta_2}{\zeta_3} V_R \\ = 4C_o (1+C_o b_o) \frac{\zeta_1}{\zeta_2 \zeta_3} \rho_i + \frac{8C_o^2 d_o}{\zeta_3} \rho_R. \end{aligned} \quad (E.10)$$

The scaling for this problem can be found by assuming an approximate variation of circuit voltage for the unmodulated BWO. The start-oscillation current of a small-C BWO can be calculated from



$$\theta_{\text{start}} \triangleq y_{\text{start}} = 2\pi C N_{\text{start}} \approx \frac{\pi^2}{5} . \quad (\text{E.11})$$

Therefore the line voltage can be approximated as

$$V \approx \cos \frac{5y}{2\pi} \exp - j \frac{y}{C_0} . \quad (\text{E.12})$$

When this value of  $V$  is substituted in Eqs. E.1 through E.3 the following approximate amplitudes of the velocity and charge are obtained,

$$|\rho| \approx \frac{0.4}{C_0^2}$$

$$|v| \approx \frac{0.625}{C_0} \quad (\text{E.13})$$

The limits shown above are normalized to a voltage amplitude of unity. A curve of the maximum values of  $|\rho|$  and  $|v|$  based on a unit voltage is shown in Fig. E.1.

A convenient time scale to use is

$$P = C_0 \frac{d}{dy} \quad (\text{E.14})$$

where  $P$  is the operator representing the time derivative in computer time. The tube analyzed in the modulation study had a gain parameter  $C_0 = 0.05$ . Figure E.1 indicates that the maximum  $|\rho|$  and  $|v|$  for unit voltage are about

$$|\rho| \approx 160$$

$$|v| \approx 12.5$$

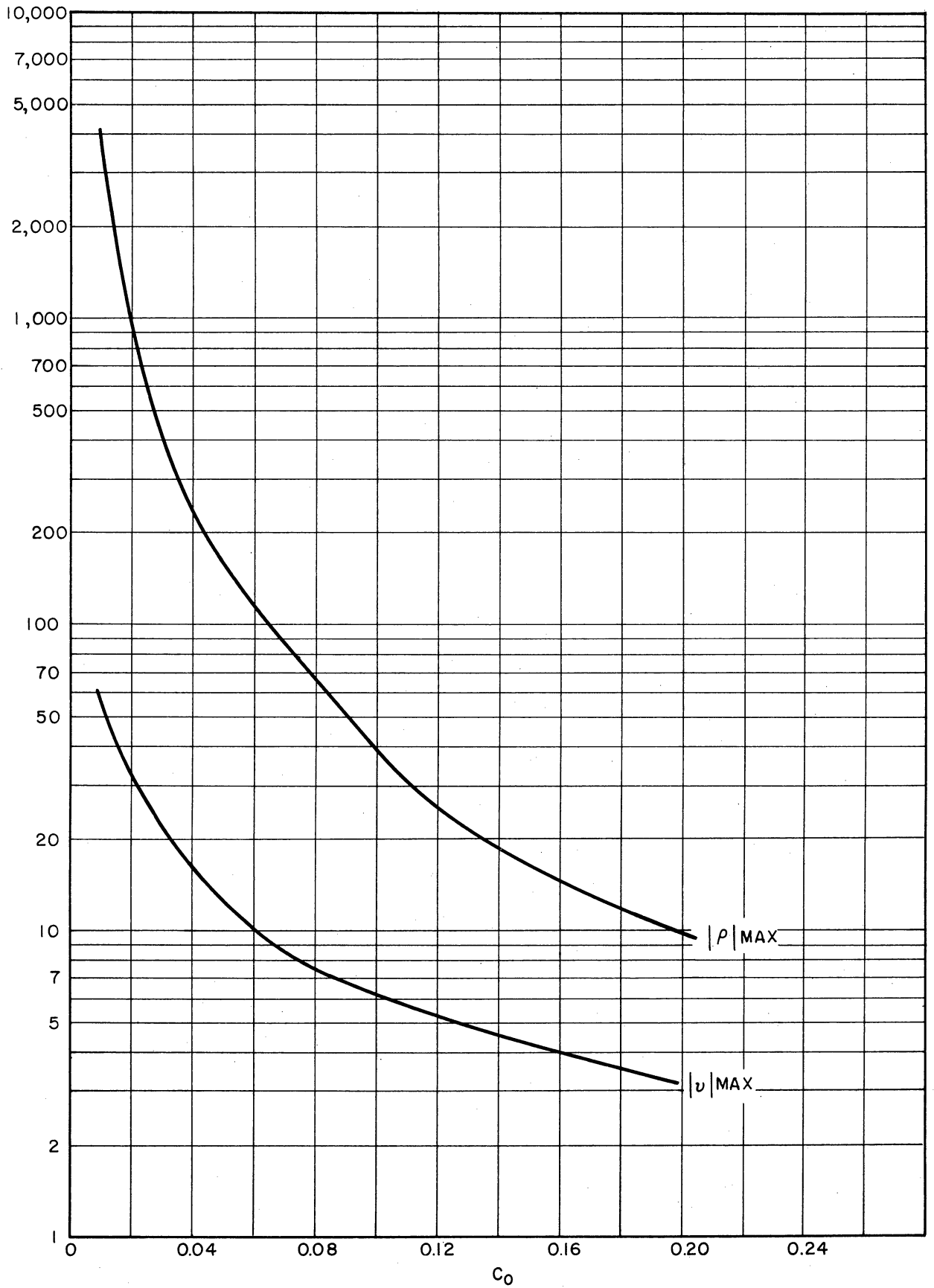


FIG. E.1 APPROXIMATE MAXIMUM VALUES OF  $|v|$  AND  $|\rho|$  BASED ON UNIT  $v_c$ .

The scaling used is 250 and 10 respectively. For a voltage maximum of 0.02 the scaling is

$$\begin{aligned} V &= 0.02 \bar{V} \\ \rho &= 5 \bar{\rho} \\ v &= 0.2 \bar{v} \quad , \end{aligned}$$

where the bar quantities represent machine variables. The time scale is chosen as

$$\frac{d}{dy} = 20 P \quad .$$

The equations to be programmed therefore are

$$\bar{\rho}_i = \xi_1 P \bar{\rho}_R + 0.04 \xi_2 P \bar{v}_R \quad . \quad (E.15)$$

$$\bar{\rho}_R = -\xi_1 P \bar{\rho}_i - 0.04 \xi_2 P \bar{v}_i \quad . \quad (E.16)$$

$$\xi_1 P \bar{v}_R = \bar{v}_i + 0.05 P \bar{v}_R - \frac{0.25 Q C_o}{(1 - 0.10 \sqrt{Q C_o})^2} \frac{F}{\xi_3 (1 + 0.05 b_o)} \bar{\rho}_i \quad . \quad (E.17)$$

$$\xi_1 P \bar{v}_i = -\bar{v}_R + 0.05 P \bar{v}_i + \frac{0.25 Q C_o}{(1 - 0.10 \sqrt{Q C_o})^2} \frac{F}{\xi_3 (1 + 0.05 b_o)} \bar{\rho}_R \quad . \quad (E.18)$$

$$- P \bar{v}_R = \left( \frac{\xi_1}{\xi_3} \right)^2 (1 + 0.05 b_o)^2 \bar{v}_R - 0.1 d_o (1 + 0.05 b_o) \frac{\xi_1 \xi_2}{\xi_3} \bar{v}_i$$

$$- 0.125 \frac{\xi_1}{\xi_2 \xi_3} (1 + 0.05 b_o) \bar{\rho}_R + \frac{0.0125 d_o}{\xi_3} \bar{\rho}_i \quad . \quad (E.19)$$

$$\begin{aligned}
 -p^2 \bar{V}_i &= \left( \frac{\zeta_1}{\zeta_3} \right)^2 (1 + 0.05b_o)^2 \bar{V}_i + 0.1d_o (1 + 0.05b_o) \frac{\zeta_1 \zeta_2}{\zeta_3} \bar{V}_R \\
 &\quad - 0.125 \frac{\zeta_1}{\zeta_2 \zeta_3} (1 + 0.05b_o) \bar{\rho}_i - \frac{0.0125d_o}{\zeta_3} \bar{\rho}_R . \quad (\text{E.20})
 \end{aligned}$$

The "roadmap" of the computer elements necessary to solve this set is shown in Fig. E.2. The potentiometer settings are given in Table E.1.

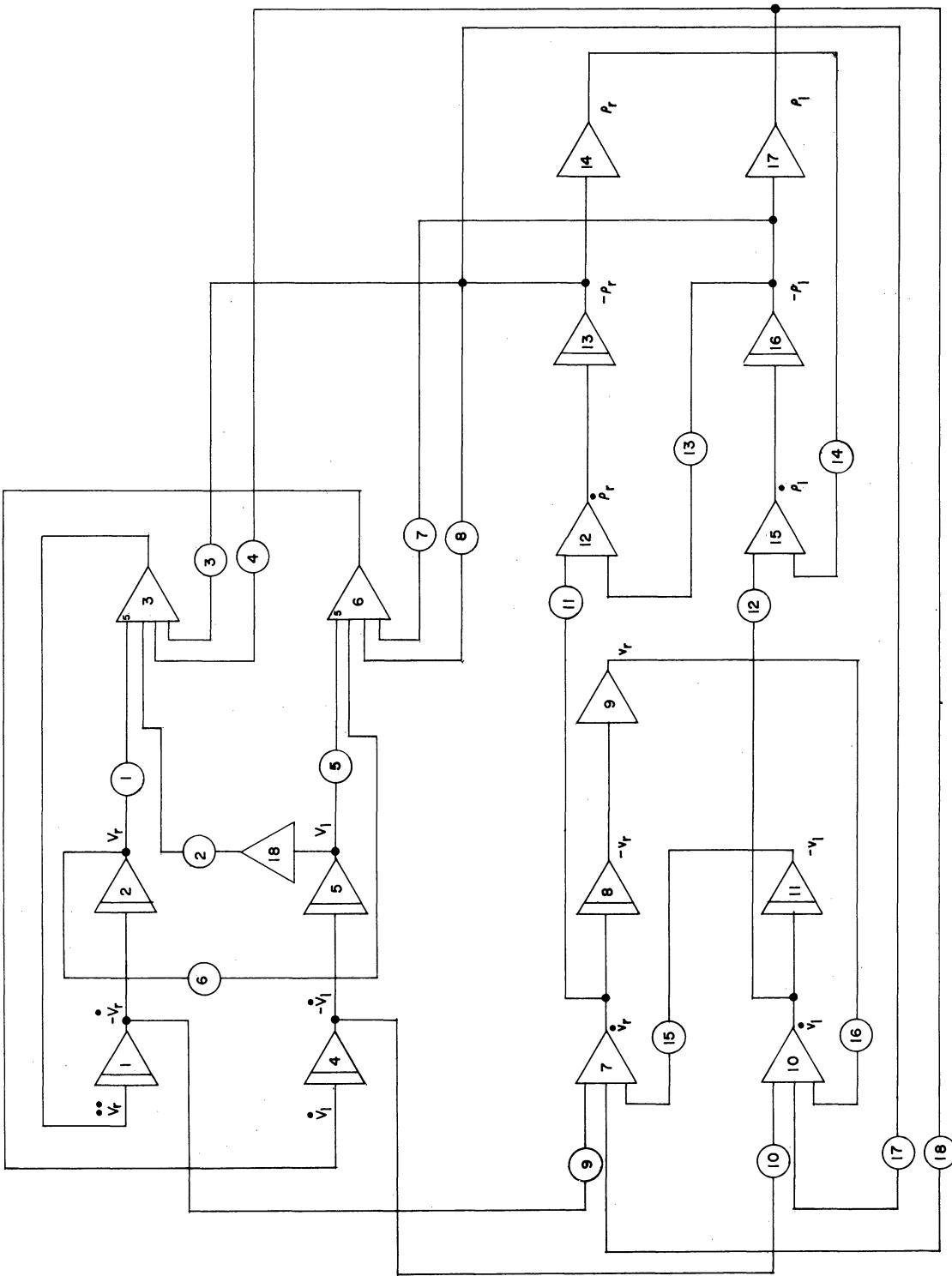


FIG.E2 "ROADMAP" OF ANALOG COMPUTER EQUIPMENT FOR FINDING START-OSCILLATION CONDITIONS OF A MODULATED BWO

TABLE E.1

Potentiometer Settings

Modulated BWO Start-Oscillation Conditions  $C_o = 0.05$

Pot No.	Setting
1, 5	$\left(\frac{\xi_1}{\xi_3}\right)^2 (1 + 0.05b_o)^2$
2, 6	$0.1d_o \frac{\xi_1 \xi_2}{\xi_3} (1 + 0.05b_o)$
3,	$0.125 (1 + 0.05b_o) \frac{\xi_1}{\xi_2 \xi_3}$
4, 8	$\frac{0.0125}{\xi_3} d_o$
9, 10	$\frac{0.05}{\xi_1}$
11, 12	$\frac{0.04\xi_2}{\xi_1}$
13 - 16	$\frac{1}{\xi_1}$
17, 18	$\frac{0.25 QC_o}{\left(1 - 0.10 \sqrt{QC_o}\right)^2} \frac{F}{\xi_3 \xi_1 (1 + 0.05b_o)}$

The scaled boundary conditions are:

$$\bar{v}_R(0) = \bar{v}_i(0) = \bar{\rho}_i(0) = \bar{\rho}_R(0) = 0 \quad . \quad (E.21)$$

$$\bar{V}(0) = \bar{V}_R(0) + j \bar{V}_i(0) \quad (\text{arbitrary}) \quad . \quad (E.22)$$

$$(P\bar{V}_R)_0 = (1 + 0.05b_0) \zeta_2 \zeta_3 \bar{V}_i(0) + 0.1d_0 \zeta_2 \zeta_3 V_R(0) \quad . \quad (E.23)$$

$$(P\bar{V}_i)_0 = - (1 + 0.05b_0) \zeta_2 \zeta_3 \bar{V}_R(0) + 0.1d_0 \zeta_2 \zeta_3 V_i(0) \quad . \quad (E.24)$$

The procedure to find an unmodulated oscillating point is to assume a value of  $C_0 (=0.05)$ ,  $QC_0$  and  $d_0$ ; set all modulation parameters equal to unity, arbitrarily choose  $V(0)$ , and then to vary  $b_0$  and plot  $V(y)$ . The total line voltage  $V(y)$  may be obtained by vectorially adding  $V_{iR}$  and  $V_{iI}$ . This can be conveniently done on the computer using a resolver. If the line voltage  $V(y)$  goes through a zero at some value of  $y$ , an oscillation condition is determined at that  $b_0$  and  $CN_s$ . The results obtained are in excellent agreement with digital computer results for start oscillation.

Once having found the unmodulated value of  $b_0$  for oscillation, modulation may be applied and the new conditions determined. The procedure for finding a modulated start-oscillation condition is to find the approximate value of  $\zeta_3$  for the particular modulation specified by  $\zeta_1$  from Fig. 5.8, then find the  $\zeta_1$ ,  $\zeta_2$  and  $F$  corresponding to this  $\zeta_3$  and integrate the equations. A second and third trial value of  $\zeta_3$  may be necessary to find the correct value of  $\zeta_3$  at which oscillations will be initiated. Typical plots at trial  $\zeta_3$  are shown in Fig. E.3.

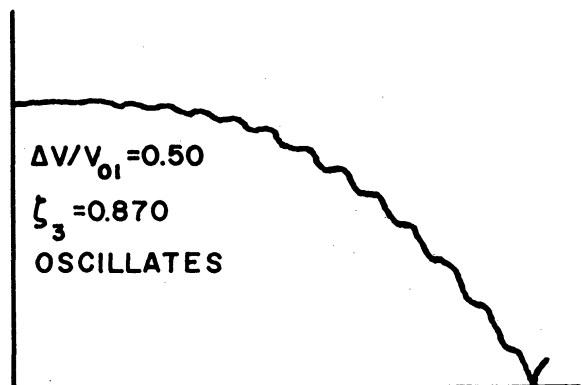
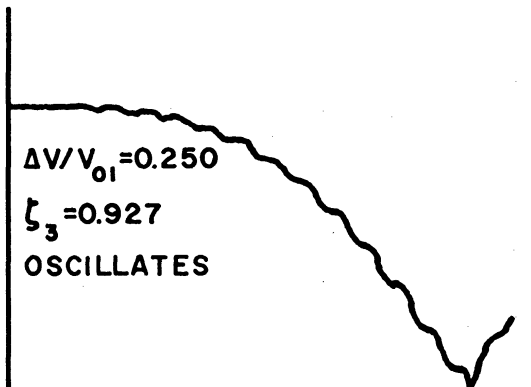
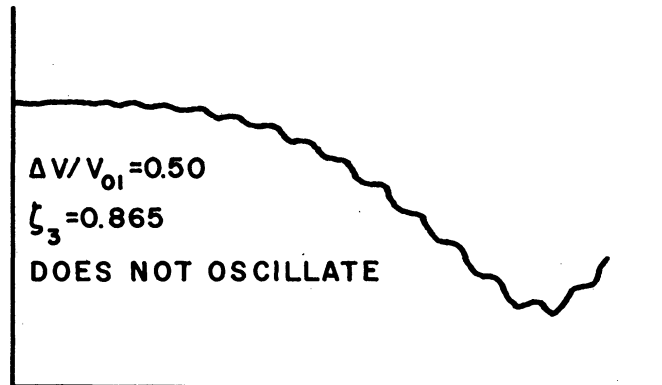
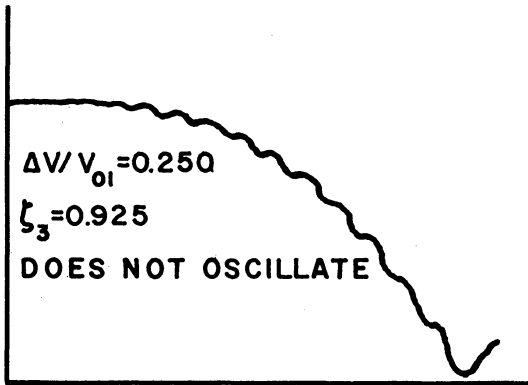
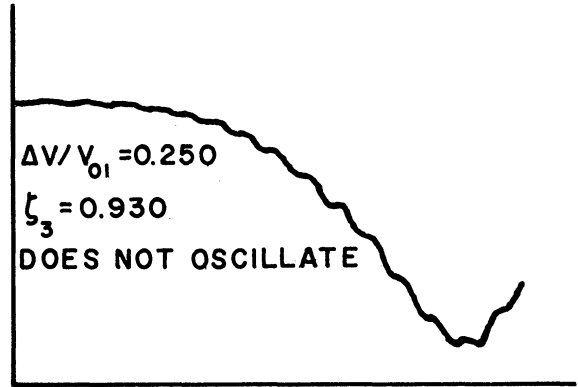
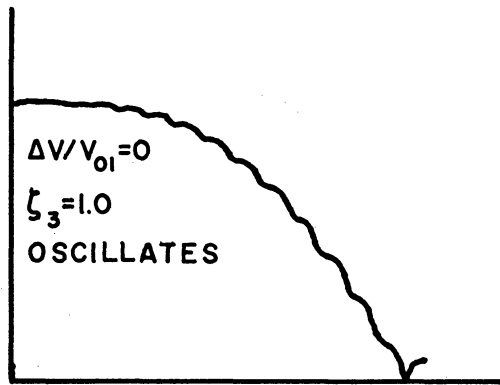


FIG. E.3 TRIAL AND ERROR PROCEDURE FOR FINDING START-OSCILLATION CONDITIONS WITH BEAM-POTENTIAL MODULATION.



APPENDIX F. CHARACTERISTIC EQUATION FOR THE LONGITUDINAL-BEAM  
PARAMETRIC AMPLIFIER

The differential equations describing the longitudinal-beam parametric amplifier were derived in Section 6.3. These are listed below:

$$\begin{aligned} \frac{d^2 u_1}{dz^2} + 2j\beta_q a' \frac{du_1}{dz} - \beta_q^2 \left[ a'^2 \left( 1 + \frac{|m|^2}{4} \right) - 1 + \frac{a'^2 |m|^2}{b'^2} \right] u_1 \\ - \beta_q^2 \frac{m}{2} \left( 1 + 2a'^2 \right) u_1^* + j\beta_q a' \frac{m^*}{2} \left[ 1 + \frac{1}{3b'^2} \right] \frac{du_{11}}{dz} \\ - \beta_q^2 \frac{m^*}{2} \left[ 1 + a'^2 \left\{ 1 + \frac{1}{b'^2} \right\} \right] u_{11} - a'^2 \beta_q^2 \frac{m^2}{4} u_{11}^* = 0 \end{aligned} \quad (F.1)$$

and

$$\begin{aligned} \frac{d^2 u_{11}}{dz^2} + 6j\beta_q a' \frac{du_{11}}{dz} - 9\beta_q^2 \left[ a'^2 (1 + b'^2) \frac{|m|^2}{4} - b'^2 \right] u_{11} \\ + j\beta_q a' \frac{3m}{2} \left[ 1 + 3b'^2 \right] \frac{du_1}{dz} - 9\beta_q^2 \frac{m}{2} \left[ a'^2 (a + b'^2) + b'^2 \right] u_1 \\ - 9a'^2 b'^2 \beta_q^2 \frac{m^2}{4} u_1^* = 0 \end{aligned} \quad (F.2)$$

To completely describe the system the complex conjugates of these above equations must be included. The complete set of equations is actually four simultaneous linear differential equations. The operator

$$\frac{d}{dz} = \beta_q \mu$$

can be introduced to describe the expected exponential solutions.

When this is done a set of homogeneous equations result;

$$\begin{bmatrix}
 \mu^2 + 2ja'\mu - A & -\frac{mE}{2} & ja'\mu D - \frac{m^*}{2} B & -\frac{a'^2 m^2}{4} \\
 -\frac{m^* E}{2} & \mu^2 - 2ja'\mu - A & -\frac{a'^2 m^* 2}{4} & -ja'\mu D - \frac{m}{2} B \\
 9b'^2 \left( ja' \frac{m}{2} \mu D - \frac{m}{2} B \right) & -9a'^2 \frac{m^2}{4} b'^2 & \mu^2 + 6ja'\mu - C & 0 \\
 -9a'^2 \frac{m^* 2}{4} b'^2 & 9b'^2 \left( -ja' \frac{m^*}{4} \mu D - \frac{m^*}{2} B \right) & 0 & \mu^2 - 6ja'\mu - C
 \end{bmatrix}
 \begin{bmatrix}
 u_1 \\
 u_1^* \\
 u_{11} \\
 u_{11}^*
 \end{bmatrix}
 = 0$$

(F.3)

where

$$A = a'^2 \left( 1 + \frac{|m|^2}{4} \right) - 1 + \left( \frac{a'}{b'} \right)^2 \frac{|m|^2}{4}$$

$$B = 1 + \left( \frac{a'}{b'} \right)^2 (1 + b'^2)$$

$$C = 9 \left[ a'^2 \left( 1 + b'^2 \frac{|m|^2}{4} \right) - b'^2 \right]$$

$$D = \frac{1 + 3b'^2}{3b'^2}$$

$$E = 1 + 2a'^2$$

Equation F.3 can be written in the simple form given in Section 6.3.

$$\begin{bmatrix} \varphi_1(\mu) & \psi_1(\mu) & \zeta_1(\mu) & \xi_1(\mu) \\ \psi_1^*(\mu) & \varphi_1^*(\mu) & \xi_1^*(\mu) & \zeta_1^*(\mu) \\ \varphi_2(\mu) & \psi_2(\mu) & \zeta_2(\mu) & \xi_2(\mu) \\ \psi_2^*(\mu) & \varphi_2^*(\mu) & \xi_2^*(\mu) & \zeta_2^*(\mu) \end{bmatrix} \begin{bmatrix} u_1 \\ u_1^* \\ u_{11} \\ u_{11}^* \end{bmatrix} = 0 \quad (F.4)$$

Equation F.3 or F.4 can only have a solution if the determinant of the coefficients vanishes. An expansion of this determinant set equal to zero defines the characteristic equation. This 4 x 4 determinant is expanded using the LaPlace expansion<sup>49</sup>. The result is:

$$\begin{aligned}
 & \begin{vmatrix} \varphi_1 & \psi_1 \\ \psi_1^* & \varphi_1^* \end{vmatrix} \times \begin{vmatrix} \zeta_2 & \xi_2 \\ \xi_2^* & \zeta_2^* \end{vmatrix} - \begin{vmatrix} \varphi_1 & \psi_1 \\ \varphi_2 & \psi_2 \end{vmatrix} \times \begin{vmatrix} \xi_1^* & \zeta_1^* \\ \xi_2^* & \zeta_2^* \end{vmatrix} \\
 + & \begin{vmatrix} \varphi_1 & \psi_1 \\ \psi_2^* & \varphi_2 \end{vmatrix} \times \begin{vmatrix} \xi_1^* & \zeta_1^* \\ \zeta_2 & \xi_2 \end{vmatrix} - \begin{vmatrix} \psi_1^* & \varphi_1^* \\ \varphi_2 & \psi_2 \end{vmatrix} \times \begin{vmatrix} \zeta_1 & \xi_1 \\ \xi_2^* & \zeta_2^* \end{vmatrix} \\
 - & \begin{vmatrix} \psi_1^* & \varphi_1^* \\ \psi_2^* & \varphi_2^* \end{vmatrix} \times \begin{vmatrix} \zeta_1 & \xi_1 \\ \zeta_2 & \xi_2 \end{vmatrix} - \begin{vmatrix} \varphi_2 & \psi_2 \\ \psi_2^* & \varphi_2^* \end{vmatrix} \times \begin{vmatrix} \zeta_1 & \xi_1 \\ \xi_1^* & \zeta_1^* \end{vmatrix} = 0 \quad .
 \end{aligned}$$

After some tedious algebraic manipulation this expansion becomes:

$$\begin{aligned}
 & \mu^8 + \left[ 40a'^2 - 2(A + C) + \frac{9}{2} |m|^2 b'^2 a'^2 D^2 \right] \mu^6 + \left[ A^2 + 4AC + C^2 - 8a'^2 C \right. \\
 & - E^2 \frac{|m|^2}{4} - 72a'^2 A + 144a'^4 + \frac{81}{16} |m|^4 b'^4 a'^4 D^4 - \frac{9}{8} |m|^4 b'^2 a'^4 \\
 & \left. - \frac{9}{2} |m|^2 b'^2 \left\{ a'^2 D^2 (C + 12a'^2 + A) - 16a'^2 BD + B^2 \right\} \right] \mu^4 \\
 & + \left[ 4a'^2 C^2 - 2CA(A + C) + 2E^2 \frac{|m|^2}{4} C + 36a'^2 A^2 - 36a'^2 \frac{|m|^2}{4} E^2 \right. \\
 & + \frac{81}{8} |m|^4 b'^4 \left( B^2 - a'^4 \frac{|m|^2}{4} \right) a'^2 D^2 - \frac{9}{4} |m|^4 b'^2 a'^2 E (B - 6a'^2 D) \\
 & - \frac{9}{8} |m|^4 b'^2 a'^4 (12a'^2 - A - C) - \frac{9}{2} |m|^2 b'^2 \left\{ 2a'^2 BD (2C + 6A) \right. \\
 & \left. - a'^2 DAC - B^2 (C + 12a'^2 + A) \right\} \right] \mu^2 + A^2 C^2 - E^2 \frac{|m|^2}{4} C^2 \\
 & + \frac{81}{16} |m|^4 b'^4 \left( B^2 - a'^4 \frac{|m|^2}{4} \right)^2 + \frac{9}{4} |m|^4 b'^2 a'^2 EBC - \frac{9}{8} |m|^4 b'^2 a'^4 AC \\
 & - \frac{9}{2} |m|^2 b'^2 ACB^2 = 0 . \tag{F.5}
 \end{aligned}$$

Equation F.5 is the general form of the characteristic equation of the longitudinal-beam amplifier. Even though it is indeed a lengthy expression, some remarks about the general nature of the waves can be made. Note that the magnitude but not the phase of the pumping signal enters into the equation; also only even powers of  $a'$  enter into the equation, therefore the waves that can propagate in such a system are independent of the phase of the pump and also of whether the pump is a slow or fast space-charge wave. The magnitudes of the waves is, of course, critically dependent upon these above factors.

It was mentioned in Section 6.3.1.1 that the same results could be obtained by using the four equations found by postulating real and imaginary parts of  $u_1$  and  $u_{11}$ , substituting these into Eqs. F.1 and F.2 and finally equating the real and imaginary parts. It can be shown that the expansion of the determinant of the matrix coefficients is identical to Eq. F.3. The resulting system has the form:

$$\begin{array}{cccc}
 \left[ \begin{array}{l} \mu^2 - \frac{|m|^2}{2} - \frac{3}{2} |m| \cos \theta \\ 2\mu - \frac{3}{2} |m| \sin \theta \\ -6\mu |m| \sin \theta \\ - \frac{27}{2} |m| \cos \theta \\ - \frac{9}{4} |m|^2 \cos 2\theta \\ 6\mu |m| \cos \theta \\ - \frac{27}{2} |m| \sin \theta \\ - \frac{9}{4} |m|^2 \sin 2\theta \end{array} \right] &
 \left[ \begin{array}{l} -2\mu - \frac{3}{2} |m| \sin \theta \\ \mu^2 - \frac{|m|^2}{2} + \frac{3}{2} |m| \cos \theta \\ -6\mu |m| \cos \theta \\ + \frac{27}{2} |m| \sin \theta \\ - \frac{9}{4} |m|^2 \sin 2\theta \\ -6\mu |m| \sin \theta \\ - \frac{27}{2} |m| \cos \theta \\ + \frac{9}{4} |m|^2 \cos 2\theta \end{array} \right] &
 \left[ \begin{array}{l} \frac{2}{3} |m| \sin \theta \mu \\ - \frac{3}{2} |m| \cos \theta \\ - \frac{|m|^2}{4} \cos 2\theta \\ \frac{2}{3} |m| \cos \theta \mu \\ + \frac{3}{2} |m| \sin \theta \\ - \frac{|m|^2}{4} \sin 2\theta \\ \mu^2 - \frac{9}{4} |m|^2 \\ 6\mu \\ \mu^2 - \frac{9}{4} |m|^2 \end{array} \right] &
 \left[ \begin{array}{l} -\frac{2}{3} |m| \cos \theta \\ - \frac{3}{2} |m| \sin \theta \\ - \frac{|m|^2}{4} \sin 2\theta \\ \frac{2}{3} |m| \sin \theta \\ - \frac{3}{2} |m| \cos \theta \\ + \frac{|m|^2}{4} \cos 2\theta \\ -6\mu \\ \mu^2 - \frac{9}{4} |m|^2 \end{array} \right] \\
 u_{1R} & & u_{1i} & & u_{1R} & & u_{1i}
 \end{array}$$

= 0

where  $m = |m|e^{j\theta}$

(F.6)

APPENDIX G. ALTERNATE DERIVATION OF THE CHARACTERISTIC EQUATION  
FOR THE LONGITUDINAL-BEAM PARAMETRIC AMPLIFIER

The characteristic equation for the longitudinal-beam parametric-amplifier was derived as a special case of the high-frequency beam modulated tube. The result is given in Section 6.3.

It is possible to derive this same result using an extension of the method given by Louisell and Quate<sup>16</sup> for coupling only to the lower sideband. The force, continuity of charge and Poisson equations can be combined into the form<sup>16</sup>

$$\frac{\partial^2 v}{\partial t^2} + \frac{\partial^2}{\partial z \partial t} \left\{ \frac{v^2}{2} \right\} = \omega_q^2 \frac{u_0}{I_0} i \quad (G.1)$$

and

$$v^2 \frac{\partial i}{\partial z} = -v \frac{\partial i}{\partial t} + i \frac{\partial v}{\partial t} \quad (G.2)$$

Assume that mixing takes place and that sidebands are generated at  $3\omega$  and  $\omega$  and also that either the fast or slow wave is excited but not both simultaneously. The notation given in Section 6.3 will be used; the current and velocity can be postulated to have the form

$$\begin{aligned}
 i = & - I_0 + \frac{m}{2} I_0 \exp \left[ - 2j\beta_e \left( 1 - \frac{a' \omega_q}{\omega} \right) z + 2j\omega t \right] \\
 & + \frac{m^*}{2} I_0 \exp \left[ + 2j\beta_e \left( 1 - \frac{a' \omega_q}{\omega} \right) z - 2j\omega t \right] \\
 & + \frac{i_1}{2} (z) \exp \left[ -j\beta_e \left( 1 - \frac{a' \omega_q}{\omega} \right) z + j\omega t \right] \\
 & + \frac{i_1^*}{2} (z) \exp \left[ + j\beta_e \left( 1 - \frac{a' \omega_q}{\omega} \right) z - j\omega t \right] \\
 & + \frac{i_{11}}{2} (z) \exp \left[ -j3\beta_e \left( 1 - \frac{a' \omega_q}{\omega} \right) z + j3\omega t \right] \\
 & + \frac{i_{11}^*}{2} (z) \exp \left[ + j3\beta_e \left( 1 - \frac{a' \omega_q}{\omega} \right) z - j3\omega t \right] \quad (G.3)
 \end{aligned}$$

and

$$\begin{aligned}
 v = & u_0 - \frac{a' \omega_q}{\omega} \frac{m}{2} u_0 \exp \left[ - 2j\beta_e \left( 1 - \frac{a' \omega_q}{\omega} \right) z + 2j\omega t \right] \\
 & - \frac{a' \omega_q}{\omega} \frac{m^*}{2} u_0 \exp \left[ + 2j\beta_e \left( 1 - \frac{a' \omega_q}{\omega} \right) z - 2j\omega t \right] \\
 & + \frac{u_1(z)}{2} \exp \left[ - j\beta_e \left( 1 - \frac{a' \omega_q}{\omega} \right) z + j\omega t \right] \\
 & + \frac{u_1^*(z)}{2} \exp \left[ + j\beta_e \left( 1 - \frac{a' \omega_q}{\omega} \right) z - j\omega t \right] \\
 & + \frac{u_{11}(z)}{2} \exp \left[ -j3\beta_e \left( 1 - \frac{a' \omega_q}{\omega} \right) z + j3\omega t \right] \\
 & + \frac{u_{11}^*(z)}{2} \exp \left[ + j3\beta_e \left( 1 - \frac{a' \omega_q}{\omega} \right) z - j3\omega t \right] \quad (G.4)
 \end{aligned}$$

When Eqs. G.3 and G.4 are substituted into Eqs. G.1 and G.2 equations with many frequency terms will result. Neglect the higher frequency



terms and make the same approximations as used in Section 6.3 and finally require that coefficients of the upper and lower sidebands independently vanish. From Eq. G.1 the lower sideband coefficient gives

$$\frac{du_1}{dz} + j\beta_q a' u_1 + j\beta_q a' \frac{m}{2} u_1^* + j\beta_q a' \frac{m^*}{2} u_{11} \approx -j \frac{\beta_q^2}{\beta_e} \frac{u_0}{I_0} i_1, \quad (G.5)$$

and the upper sideband gives

$$\frac{du_{11}}{dz} + 3j\beta_q a' u_{11} + 3j\beta_q a' \frac{m}{2} u_1 \approx -j \frac{\beta_q^2}{3\beta_e} \frac{u_0}{I_0} \left( \frac{\omega_{q11}}{\omega_q} \right)^2 i_{11}. \quad (G.6)$$

From G.2 the lower sideband gives

$$\begin{aligned} \frac{di_1}{dz} + j\beta_q a' i_1 + j\beta_q a' \frac{m}{2} i_1^* + j\beta_q a' \frac{m^*}{2} i_{11} + j\beta_e \frac{I_0}{u_0} u_1 \\ - j\beta_e \frac{I_0}{u_0} \frac{m}{2} u_1^* - j\beta_e \frac{I_0}{u_0} \frac{m^*}{2} u_{11} \approx 0, \quad (G.7) \end{aligned}$$

while the upper sideband gives

$$\frac{di_{11}}{dz} + 3j\beta_q a' i_{11} + j3\beta_e \frac{I_0}{u_0} u_{11} + j3\beta_q a' \frac{m}{2} i_1 - 3j\beta_e \frac{I_0}{u_0} \frac{m}{2} u_1 \approx 0. \quad (G.8)$$

Equations G.5 through G.8 can then be combined to give two second-order equations. The result is

$$\begin{aligned}
 & \frac{d^2 u_1}{dz^2} + 2j\beta_q a' \frac{du_1}{dz} + j\beta_q a' \frac{m^*}{2} \left[ 1 + \gamma \left( \frac{\omega_q}{\omega_{q11}} \right)^2 \right] \frac{du_{11}}{dz} \\
 & - \beta_q^2 \left[ a'^2 \left\{ 1 + \frac{|m|^2}{4} \right\} - 1 + \gamma a'^2 \left( \frac{\omega_q}{\omega_{q11}} \right)^2 \frac{|m|^2}{4} \right] u_1 \\
 & - \beta_q^2 \left[ 2a'^2 + 1 \right] \frac{m}{2} u_1^* - \beta_q^2 \frac{m^*}{2} \left[ a'^2 + \gamma a'^2 \left( \frac{\omega_q}{\omega_{q11}} \right)^2 + 1 \right] u_{11} \\
 & - \beta_q^2 a'^2 \frac{m^2}{4} u^* = 0 \quad , \tag{G.9}
 \end{aligned}$$

and

$$\begin{aligned}
 & \frac{d^2 u_{11}}{dz^2} + 6j\beta_q a' \frac{du_{11}}{dz} + j\beta_q a' \frac{m}{2} \left[ \gamma + \left( \frac{\omega_{q11}}{\omega_q} \right)^2 \right] \frac{du_1}{dz} \\
 & + \beta_q^2 \left[ \left( \frac{\omega_{q11}}{\omega_q} \right)^2 \left\{ 1 - \frac{|m|^2}{4} a'^2 \right\} - \gamma a'^2 \right] u_{11} \\
 & - \beta_q^2 \frac{m}{2} \left[ \gamma a'^2 + \left( \frac{\omega_{q11}}{\omega_q} \right)^2 a'^2 + \left( \frac{\omega_{q11}}{\omega_q} \right)^2 \right] u_1 \\
 & - \beta_q^2 a'^2 \frac{m^2}{4} \left( \frac{\omega_{q11}}{\omega_q} \right)^2 u_1^* = 0 \quad . \tag{G.10}
 \end{aligned}$$

If the definition of  $b'$  given in Eq. 6.20 is used, the above equations are identical to Eqs. 6.28 and 6.29 which were derived from the general method.

APPENDIX H. METHODS OF COUPLING TO INDIVIDUAL  
SPACE-CHARGE WAVE MODES

The derivations of Chapter VI were based on the assumption that only one space-charge wave was present. It was assumed that either the fast or the slow wave was excited, however, both were not simultaneously excited. A very simplified discussion of two possible methods of exciting one space-charge wave will now be given, one method involves a gridded resonant cavity and the other a helix as the exciting element.

Gridded Resonant Cavity

A resonant cavity with two sets of grids may be used as a directional coupler to excite one space-charge wave. Consider the cavity shown in Fig. H.1. Assume that the transit time through the grids is negligible. A low-level r-f signal is applied to the cavity to excite the initially unmodulated beam. With the usual small-signal assumptions, both the fast and slow waves will be equally excited at each set of grids. The two space-charge waves set up at the first gap will propagate to the second gap. The waves propagating past the second gap will have amplitudes determined by the vector sum of the waves excited at the second gap and those set up at the first gap. The difference in phase between the waves excited by the first and second gap is merely the transit time in radians between the gaps. For the fast wave this phase difference is,

$$(\beta_e - \beta_q) L \quad ,$$

and for the slow wave the phase difference is

$$(\beta_e + \beta_q) L \quad .$$

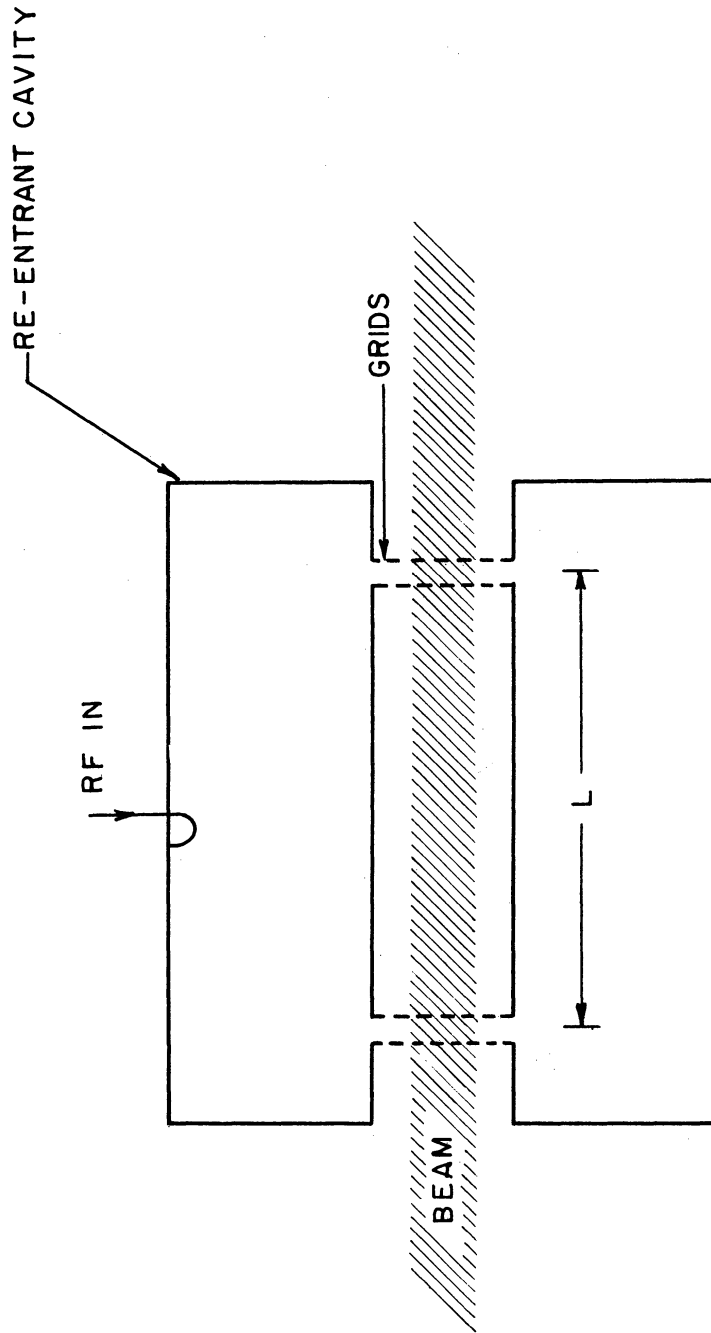


FIG. H.1 DOUBLY GRIDDED CAVITY RESONATOR FOR EXCITING A SINGLE SPACE-CHARGE WAVE.

For a fast-wave exciter, the fast waves at the second gap should be in phase, while the slow waves should be out of phase. Therefore,

$$\begin{aligned}(\beta_e - \beta_q) L &= 2n\pi \\ (\beta_e + \beta_q) L &= (2n + 1) \pi \quad ,\end{aligned}$$

which results in

$$\begin{aligned}\beta_e L &= \left(2n + \frac{1}{2}\right) \pi \\ \beta_q L &= \frac{\pi}{2} \quad .\end{aligned} \tag{H.1}$$

For a slow-wave coupler the conditions would be

$$\begin{aligned}\beta_e L &= \left(2n + \frac{1}{2}\right) \pi \quad . \\ \beta_q L &= \frac{3}{2} \pi \quad .\end{aligned} \tag{H.2}$$

It is therefore, possible to use a double gap cavity as a directional coupler to excite one wave while at the same time cancelling the other wave.

### Helix Couplers

A helix (or other slow-wave circuit) with phase velocity close to the beam velocity results in TWA interaction and a resultant growth of the slow wave. The fast wave is present but to a very small extent so that a TWA is actually a slow space-charge wave exciter.

When the TWA is operated near the Kompfner Dip Condition<sup>50</sup>, with the beam velocity much lower than the circuit phase velocity it is possible to excite only the fast wave. Consider a TWA with a large negative b value. Then for small C and in the presence of space charge,

the propagation constants are given approximately as

$$\begin{aligned}\delta_1 &\approx -2j\sqrt{QC} \\ \delta_2 &\approx 2j\sqrt{QC} \\ \delta_3 &\approx -jb \quad , \end{aligned} \tag{H.3}$$

and the waves propagate as

$$\begin{aligned} \frac{V(z)}{V_{in}} = \exp - j\beta_e z \left\{ \frac{\exp - j2\beta_e C \sqrt{QC} z}{2 \left( 1 - \frac{b}{2\sqrt{QC}} \right)} \right. \\ \left. + \frac{\exp + 2j\beta_e C \sqrt{QC} z}{2 \left( 1 + \frac{b}{2\sqrt{QC}} \right)} + \frac{\exp - j \beta_e C b z}{1 - \frac{4QC}{b^2}} \right\} . \end{aligned} \tag{H.4}$$

For large negative b values Eq. H.4 is approximated as

$$\frac{V(z)}{V_{in}} \approx \exp - j\beta_e z \left[ 1 - C|b| \right] \quad , \tag{H.5}$$

which is of course a fast wave.

APPENDIX I. EVALUATION OF MATRIX ELEMENTS FOR DETERMINING  
 WAVE AMPLITUDES IN THE LONGITUDINAL-BEAM  
 PARAMETRIC AMPLIFIER

The matrix elements  $\eta_i$ ,  $\tau_i$ , and  $\pi_i$  were introduced in Section 6.3.1.2 in order to evaluate the wave amplitudes. These elements were then found by inverting eight 3 x 3 matrices. The form of the matrices was given in Eq. 6.35 as

$$\begin{bmatrix} -\varphi_3(\mu_i) \\ -\varphi_4(\mu_i) \\ -\varphi_5(\mu_i) \end{bmatrix} = \begin{bmatrix} \psi_3(\mu_i) & \zeta_3(\mu_i) & \xi_3(\mu_i) \\ \psi_4(\mu_i) & \zeta_4(\mu_i) & \xi_4(\mu_i) \\ \psi_5(\mu_i) & \zeta_5(\mu_i) & \xi_5(\mu_i) \end{bmatrix} \begin{bmatrix} \eta_i \\ \tau_i \\ \pi_i \end{bmatrix}. \quad (\text{I.1})$$

The elements  $\varphi_3 \dots \xi_5$  may be evaluated by noting the elements in Eq. F.6.

$$\begin{aligned}
 & \left[ \begin{array}{l} -\mu_i^2 + \frac{|m|^2}{2} + \frac{3}{2} |m| \cos \theta \\ -2\mu_i + \frac{3}{2} |m| \sin \theta \end{array} \right] = \left[ \begin{array}{l} -2\mu_i - \frac{3}{2} |m| \sin \theta \\ \mu_i^2 - \frac{|m|^2}{2} + \frac{3}{2} |m| \cos \theta \end{array} \right] \\
 & \left[ \begin{array}{l} -\frac{2}{3} |m| \sin \theta \mu_i \\ -\frac{3}{2} |m| \cos \theta \\ -\frac{|m|^2}{4} \cos 2\theta \end{array} \right] = \left[ \begin{array}{l} \frac{2}{3} |m| \sin \theta \mu_i \\ \frac{2}{3} |m| \cos \theta \mu_i \\ + \frac{3}{2} |m| \sin \theta \\ -\frac{|m|^2}{4} \sin \theta \end{array} \right] \\
 & \left[ \begin{array}{l} -\frac{2}{3} |m| \cos \theta \mu_i \\ -\frac{3}{2} |m| \sin \theta \\ -\frac{|m|^2}{4} \sin 2\theta \end{array} \right] = \left[ \begin{array}{l} \frac{2}{3} |m| \sin \theta \mu_i \\ -\frac{3}{2} |m| \cos \theta \\ + \frac{|m|^2}{4} \cos 2\theta \end{array} \right] \\
 & \left[ \begin{array}{l} 6\mu_i |m| \sin \theta + \frac{27}{2} |m| \cos \theta \\ + \frac{9}{2} |m|^2 \cos 2\theta \end{array} \right] = \left[ \begin{array}{l} -6\mu_i |m| \cos \theta \\ + \frac{27}{2} |m| \sin \theta \\ -\frac{9}{4} |m|^2 \sin 2\theta \end{array} \right] \\
 & \left[ \begin{array}{l} \eta_i \\ \tau_i \\ \pi_i \end{array} \right]
 \end{aligned}$$

(I.2)



## BIBLIOGRAPHY

1. Pierce, J. R., Traveling-Wave Tubes, D. Van Nostrand, New York; 1950.
2. Hæeff, A. V., "The Electron-Wave Tube. A Novel Method of Generation and Amplification of Microwave Energy", Proc. IRE, vol. 37, No. 1, pp. 4-10; January, 1949.
3. Kompfner, R. and Williams, N. T., "Backward-Wave Tubes", Proc. IRE, vol. 41, No. 11, pp. 1602-1611; November, 1953.
4. Rowe, J. E., "Theory of the Crestatron: A Forward-Wave Amplifier", Proc. IRE, vol. 47, pp. 536-545; April, 1959.
5. Hok, G., Unpublished notes on modulation.
6. Cumming, R. C., "Frequency Translation by Modulation of Transit-Time Devices", Tech. Report No. 39, Stanford University, Applied Electronics Laboratory; August 1, 1955.
7. Learned, V., "The Klystron Mixer Applied to T-V Relaying", Proc. IRE, vol. 38, No. 9, pp. 1033-35; September, 1950.
8. Bray, W. J., "The Traveling-Wave Valve as a Microwave Phase-Modulator and Frequency Shifter", Proc. IRE, vol. 99 (Part III), pp. 15-20; January, 1952.
9. Steele, G. F., "The Modulation of Traveling-Wave Tubes", Electronics Engineering, vol. 29; September, 1957.
10. Mendel, J. T., "Grid-Modulated Traveling Wave Tube for Low-Pass Amplification", Tech. Report No. 47, Stanford University, Electronics Research Laboratory; July 31, 1952.
11. Beam, W. R., and Blattner, D. J., "Phase Angle Distortion in Traveling-Wave Tubes", RCA Review, vol. 17, pp. 86-99; March, 1956.
12. Putz, J. L., "Nonlinear Phenomena in Traveling-Wave Amplifiers", Tech. Report No. 37, Stanford University, Electronics Research Laboratory; October 15, 1951.
13. Nation, A. W. C., and Harrison, A. E., "Cross Modulation in Traveling-Wave Tube Amplifiers", Report No. 15, University of Washington, Department of Electrical Engineering; November 15, 1954.
14. DeGrasse, R. W., and Wade, G., "Microwave Mixing and Frequency Dividing", Tech. Report No. 386-1, Stanford University, Electron Tube Laboratory, Stanford Electronics Laboratories; November 12, 1957.
15. DeGrasse, R. W., "Frequency Mixing in Microwave Beam-Type Devices", Tech. Report No. 386-2, Stanford University, Electron-Devices Laboratory, Stanford Electronics Laboratories; July 28, 1958.

BIBLIOGRAPHY (cont.)

16. Louisell, W. H., and Quate, C. F., "Parametric Amplification of Space-Charge Waves", Proc. IRE, vol. 46, No. 4., pp. 707-716; April, 1958.
17. Rowe, J. E., "A Large-Signal Analysis of the Traveling-Wave Amplifier: Theory and General Results", Trans. PGED-IRE, vol. ED-3, No. 1, pp. 39-57; January, 1956.
18. Nordsieck, A. T., "Theory of the Large-Signal Behavior of Traveling Wave Amplifiers", Proc. IRE, vol. 41, No. 5, pp. 630-637; May, 1953.
19. Hahn, W. C., "Small-Signal Theory of Velocity-Modulated Electron Beams", General Electric Review, vol. 42, pp. 258-270; June, 1935.
20. Rowe, J. E., "Large-Signal Traveling-Wave Amplifiers", Tech. Report No. 20, Electron Tube Laboratory, Department of Electrical Engineering, The University of Michigan; June, 1956.
21. Brewer, G. R., and Birdsall, C. K., "Normalized Propagation Constants for a Traveling-Wave Tube for Finite Values of C", Tech. Memo No. 331, Hughes Research and Development Laboratories; October, 1953.
22. Sensiper, S., "Explicit Expressions for the Traveling-Wave Tube Propagation Constants", Memo. No. 53-16, Hughes Research and Development Laboratories; December, 1953.
23. Erdelyi, A., Higher Transcendental Functions, vol. II, Bateman Manuscript Project, California Inst. of Tech., McGraw-Hill, New York; 1953.
24. Watson, G. N., A Treatise on the Theory of Bessel Functions, Macmillan and Co., New York; 1944.
25. Goldman, S., Frequency Analysis, Modulation and Noise, McGraw-Hill Book Co., New York; 1948.
26. Janke, E., and Emde, F., Tables of Functions, Dover Publications, New York; 1945.
27. Haus, H. A., "Analysis of Signals and Noise in Longitudinal Electron Beams" Tech. Report 306, Massachusetts Institute of Technology, Research Laboratory of Electronics; August, 1955.
28. Forsyth, A. R., A Treatise on Differential Equations, Macmillan and Co., London; 1933.
29. Louisell, W. H., and Pierce, J. R., "Power Flow in Electron Beam Devices", Proc. IRE, vol. 43, No. 4, pp. 425-27; April, 1955.

BIBLIOGRAPHY (cont.)

30. Smullin, L. D., and Haus, H. A., Noise in Electron Devices, The Technology Press and John Wiley and Sons, New York; 1959.
31. Haus, H. A., "The Kinetic Power Theorem for Parametric, Longitudinal Electron-Beam Amplifiers", Trans. PGED-IRE, vol. ED-5, No. 4, pp. 225-232; October, 1958.
32. Haus, H. A., and Robinson, F. N. H., "A Minimum Noise Figure of Microwave-Beam Amplifiers", Proc. IRE, vol. 43, No. 8, pp. 981-991; August, 1955.
33. Chu, L. J., "A Kinetic Power Theorem", presented at IRE Conference of Electron Devices, Durham, N. H.; June, 1951.
34. Ashkin, A., Bridges, T. J., Louisell, W. H., Quate, C. F., "Parametric Electron-Beam Amplifiers", paper presented at IRE Wescon Meeting; August, 1958.
35. Manley, J. M., and Rowe, H. E., "Some General Properties of Nonlinear Elements-Part I", Proc. IRE, vol. 44, No. 7, pp. 904-914; July, 1956.
36. Rainville, E. D., Intermediate Course in Differential Equations, J. Wiley and Sons, New York; 1943.
37. Caldwell, J. J. and Hock, O. L., "Large Signal Behavior of High Power Traveling-Wave Amplifiers", Trans. PGED-IRE, vol. ED-3, No. 1, pp. 6-18; January, 1956.
38. Paschke, F., "On the Nonlinear Behavior of Electron-Beam Devices", RCA Review, vol. 18, pp. 221-243; June, 1957.
39. Gould, R. W., Sedin, J. W., and Sugai, I., "A Theoretical and Experimental Study of the M-Type Backward-Wave Oscillator", Electron Tube and Microwave Lab., California Inst. of Tech., Pasadena, Calif., QSR No. 12, pp. 6-13; March, 1956.
40. Rowe, J.E., "Analysis of Nonlinear O-Type Backward-Wave Oscillators", Proceedings of the Symposium on Electronic Waveguides, Microwave Research Inst. Symposia Series, vol. VIII, Polytechnic Press; 1958.
41. Heffner, H., "Analysis of the Backward-Wave Traveling-Wave Tube", Proc. IRE, vol. 42, No. 6, pp. 930-938; June, 1954.
42. Johnson, H. R., "Backward-Wave Oscillators", Proc. IRE, vol. 43, No. 6, pp. 684-698; June, 1955.
43. Grow, R. W., and Watkins, D. A., "Backward-Wave Oscillator Efficiency", Proc. IRE, vol. 43, No. 7, pp. 848-856; July, 1955.

BIBLIOGRAPHY (concl.)

44. Gewartowski, J. W., "Velocity and Current Distributions in the Spent Beam of the Backward-Wave Oscillator", Trans. PGED-IRE, vol. ED-5, No. 4, pp. 215-223; October, 1958.
45. Tien, P. K., "Bifilar Helix for Backward-Wave Oscillators", Proc. IRE, vol. 42, No. 7, pp. 1137-1144; July, 1954.
46. Watkins, D. A., and Ash, E. A., "The Helix as a Backward-Wave Circuit Structure", JAP, vol. 25, No. 6, pp. 782-790; June, 1954.
47. Rowe, J. E., "One Dimensional Traveling-Wave Tube Analyses and the Effect of Radial Field Variations", to be published in the Trans. PGED-IRE.
48. Branch, G. M., and Mihran, T. G., "Plasma Reduction Factors in Electron Beams", Trans. PGED-IRE, vol. 2, pp. 3-11; April, 1955.
49. Guillemin, E. A., The Mathematics of Circuit Analysis, The Technology Press and John Wiley and Son, New York; 1949.
50. Johnson, H. R., "Kompfner Dip Conditions", Letter to the Editor, Proc. IRE, vol. 43, No. 7, p. 874; July, 1955.
51. Bellis, D. R., and Huggins, R. A., "Phase Modulation of Traveling Wave Tubes", Engineering Note No. 7, Huggins Laboratories; March, 1957.
52. Adler, R., Hrbek, G., Wade, G., "A Low Noise Electron Beam Parametric Amplifier", Letter to the Editor, Proc. IRE, vol. 46, p. 1756; October, 1958.
53. Tien, P. K., Walker, L. R., and Wolontis, V. M., "A Large-Signal Theory of Traveling-Wave Amplifiers", Proc. IRE, vol. 43, No. 3, pp. 260-277; March, 1955.

LIST OF SYMBOLS

A	Initial loss parameter in linear TWA
$A_{nm}$	nmth sideband amplitude
$A(y)$	Amplitude of r-f potential
a	Wave amplitude defined in Eq. 2.29b
$a'$	Defined in Eq. 6.20
$a'$	Helix radius
B	Space-charge range parameter ( $\beta b'$ )
b	TWA injection velocity parameter
$b'$	Beam radius
$b'$	Defined in Eq. 6.20
C	TWA gain parameter
C	Shunt capacitance of transmission line in farads/unit length
$C_1$	Capacitance defined in Section 2.2
c	Velocity of light
d	TWA loss parameter
E	Electric field
F	Space-charge debunching force
$F(M)$	Modulated BWO factor defined in Section 5.2
$F_n$	Fourier coefficient for phase expansion
$F(\varphi' - \varphi)$	Space-charge weighting factor
f	General function
$G(\xi)$	Amplitude factor for spectrum analysis
H	Ratio of inner to outer radius of hollow beam
h	Coefficient for amplitude modulation device function expansion
$I_o$	Average beam current ( $-u_o \rho_o$ )
$I_{o1}$	Average unmodulated beam current

LIST OF SYMBOLS (contd)

$i$	Convection current
$J$	Small-signal current density
$k$	Free space radian wave number
$L$	Series inductance of transmission line in henries/unit length
$l$	Index (subscript)
$M$	Modulation parameter defined in Section 2.2
$m$	Depth of modulation of pump current
$N_s$	Stream wavelenghts
$n, m$	Index (subscript)
$P$	Power flow
$p$	Coefficient for phase modulation device function expansion
$p$	Index (subscript)
$QC$	TWA space-charge parameter
$q$	Charge in coulombs
$q$	Index (subscript)
$R$	Series loss of transmission line in ohms/unit length
$R$	Total amplitude function defined in Eq. 2.30b
$R(B)$	Plasma frequency reduction factor
$r, s$	Index (subscript)
$S$	Total phase function defined in Eq. 2.30c
$S_k$	Complex power flow
$T$	Period
$t$	Time in seconds
$u$	Velocity
$u_{01}$	Average unmodulated velocity
$u(y, \phi_i)$	Normalized velocity perturbation for large-signal analysis

LIST OF SYMBOLS (contd)

$V_c$	R-f circuit potential
$V_g$	Varying grid bias
$V_{o1}$	Average unmodulated beam potential
$x$	Real part of propagation constant
$y$	Imaginary part of propagation constant
$y$	Normalized distance ( $\beta_e Cz$ )
$Z_0$	Characteristic impedance of transmission line
$z$	Axial position
$\beta$	Phase Constant of transmission line
$\beta_e$	Radian wave number for beam ( $\omega/u_0$ )
$\Gamma$	Distance derivative operator ( $-d/dz$ )
$\Delta a$	Amplitude modulation defined in Eq. 2.33
$\Delta I$	Low-frequency beam-current modulation
$\Delta S$	Phase modulation in radians
$\Delta V$	Low-frequency beam-potential modulation
$\delta$	Propagation constant perturbation
$\epsilon_i$	Amplitude coefficient
$\zeta_1(\mu)$	Matrix element for longitudinal-beam parametric amplifier
$\zeta(M)$	Total angle defined in Eq. 2.29a
$\zeta_1, \zeta_2, \zeta_3$	Modulated BWO factors
$\eta$	Magnitude of charge-to-mass ratio of electron
$\eta_i$	Amplitude coefficient
$\theta$	Phase shift through a device
$\theta(y)$	Phase of circuit wave with respect to fictitious wave traveling at $u_{o1}$
$\mu$	Propagation constant perturbation
$\xi$	Modulating signal

LIST OF SYMBOLS (contd)

$\xi_i(\mu)$	Matrix element for longitudinal-beam parametric amplifier
$\xi_1, \xi_2$	Low frequency modulation factors defined in Section 2.2
$\pi_i$	Amplitude coefficient
$\rho$	Charge density
$\rho_{01}$	Average unmodulated beam charge density
$\sigma$	Beam cross sectional area
$\tau$	Time interval
$\tau$	Volume
$\tau_i$	Amplitude coefficient
$\phi_{oi}$	Initial phase of electron
$\phi_i(\mu)$	Matrix element for longitudinal-beam parametric amplifier
$\Phi(y, \phi_{oi})$	Phase of electron with respect to r-f wave
$\psi$	Phase of initial loss factor
$\psi_i(\mu)$	Matrix element for longitudinal-beam parametric amplifier
$\omega$	Radian frequency
$\omega_c$	Carrier frequency
$\omega_p$	Plasma frequency
$\omega_q$	Reduced plasma frequency



DISTRIBUTION LIST

<u>No. Copies</u>	<u>Agency</u>
	Commander, Rome Air Development Center, ATTN: RCLRR-3, Griffiss Air Force Base, New York
	Commander, Rome Air Development Center, ATTN: RCSST-4, Griffiss Air Force Base, New York
	Commander, Rome Air Development Center, ATTN: RCSSL-1, Griffiss Air Force Base, New York
All add. copies	Armed Services Technical Information Agency, Documents Service Center, Arlington Hall Station, Arlington 12, Virginia
1	Commander, Air Force Cambridge Research Center, ATTN: CRQSL-1, Laurence G. Hanscom Field, Bedford, Massachusetts
1	Director, Air University Library, ATTN: AUL-7736, Maxwell Air Force Base, Alabama
1	Commander, Wright Air Development Center, ATTN: WCOSI-3, Wright-Patterson Air Force Base, Ohio
1	Mr. Hans Jenny, RCA Electron Tube Division, 415 South 5th Street, Harrison, New Jersey
1	Air Force Field Representative, Naval Research Laboratory, ATTN: Code 1010, Washington 25, D. C.
2	Commander, Air Research and Development Command, ATTN: RDSFIF, Andrews AFB, Washington 25, D. C.
1	Chief, Bureau of Ships, ATTN: Code 312, Washington 25, D.C.
1	Commanding Officer, Signal Corps Engineering Laboratories, ATTN: Technical Reports Library, Fort Monmouth, New Jersey
1	Commander, Air Research and Development Command, ATTN: RDTDF, Andrews Air Force Base, Washington 25, D.C.
1	Commander, Air Research and Development Command, ATTN: RDTC, Andrews Air Force Base, Washington 25, D. C.
1	Applied Radiation Company, Walnut Creek, California, ATTN: Mr. Neil J. Norris
1	Bell Telephone Laboratories, Inc., Murray Hill Laboratory, ATTN: Dr. J. R. Pierce, Murray Hill, New Jersey

DISTRIBUTION LIST (cont.)

<u>No. Copies</u>	<u>Agency</u>
1	Director, Signal Corps Engineering Laboratories, ATTN: Thermionics Branch, Evans Signal Laboratory, Belmar, New Jersey
1	Secretariat, Advisory Group on Electron Tubes, 346 Broadway, New York 13, New York
1	Chief, European Office, Air Research and Development Command, 60 Rue Canterstein, Brussels, Belgium
1	Prof: L. M. Field, California Institute of Technology, Department of Electrical Engineering, Pasadena, California
1	Prof. J. R. Whinnery, University of California, Department of Electrical Engineering, Berkeley 4, California
1	Prof. W. G. Worcester, University of Colorado, Department of Electrical Engineering, Boulder, Colorado
1	Mr. C. Dalman, Cornell University, Department of Electrical Engineering, Ithaca, New York
1	Mr. E. D. McArthur, General Electric Company, Electron Tube Division of Research Laboratory, The Knolls, Schenectady, New York
1	Mr. S. Webber, General Electric Microwave Laboratory, 601 California Avenue, Palo Alto, California
1	Mr. L. A. Roberts, Watkins-Johnson Company, Palo Alto, California
1	Mr. T. Milek, Hughes Aircraft Company, Electron Tube Lab- oratory, Culver City, California
1	Varian Associates, 611 Hansen Way, Palo Alto, California, ATTN: Technical Library
1	Dr. Bernard Arfin, Philips Research Laboratories, Irvington on the Hudson, New York
1	Columbia Radiation Laboratory, Columbia University, 538 West 120th Street, New York 27, New York
1	University of Illinois, Department of Electrical Engineering, Electron Tube Section, Urbana, Illinois
1	University of Florida, Department of Electrical Engineering, Gainesville, Florida

DISTRIBUTION LIST (cont.)

<u>No.</u>	<u>Copies</u>	<u>Agency</u>
1		Mr. E. W. Herold, RCA Laboratories, Electron Research Laboratories, Princeton, New Jersey
1		Mrs. Margaret E. Snyder, Librarian, The Johns Hopkins University, Radiation Laboratory, Baltimore 2, Maryland
1		Sperry Rand Corporation, Sperry Electron Tube Division, Gainesville, Florida, ATTN: Mr. P. Bergman
1		Dr. M. Chodorow, Stanford University, Microwave Laboratory, Stanford, California
1		Mr. D. A. Watkins, Stanford University, Stanford Electronics Laboratory, Stanford, California
1		Mr. Skoworon, Raytheon Manufacturing Company, Tube Division, Waltham, Massachusetts
1		Mr. T. Marchese, Federal Telecommunication Laboratories, Inc., 500 Washington Avenue, Nutley, New Jersey
1		Mr. Donald Priest, Eitel-McCullough, Inc., San Bruno, California
1		Dr. Norman Moore, Litton Industries, 960 Industrial Road, San Carlos, California
1		Massachusetts Institute of Technology, Research Laboratory of Electronics, Cambridge 39, Massachusetts, ATTN: Documents Library
		Sperry Gyroscope Company, Great Neck, New York, ATTN: Engineering Library
1		Dr. D. Goodman, Sylvania Microwave Tube Laboratory, 500 Evelyn Avenue, Mountain View, California
1		Dr. G. Mouier, Polytechnic Institute of Brooklyn, Microwave Research Institute, Brooklyn 1, New York
1		Harvard University, Cruft Laboratory, Cambridge, Massachusetts, ATTN: Technical Library
1		Dr. R. G. E. Hutter, Sylvania Electric Products, Inc., Mountain View, California
1		Mr. A. E. Harrison, University of Washington, Department of Electrical Engineering, Seattle 5, Washington

DISTRIBUTION LIST (cont.)

<u>No.</u>	<u>Copies</u>	<u>Agency</u>
1		Dr. J. H. Bryant, Bendix Aviation Corporation, Research Laboratories, Northwestern Highway & 10-1/2 Mile Road, Detroit 35, Michigan
1		Mr. James B. Maher, Librarian, R & D Technical Library, Hughes Aircraft Company, Culver City, California
1		Dr. Robert T. Young, Chief, Electron Tube Branch, Diamond Ordnance Fuze Laboratories, Washington 25, D. C.
1		Bendix Aviation Corporation, Systems Planning Division, Ann Arbor, Michigan, ATTN: Technical Library
1		Mr. Gerald Klein, Manager, Microwave Tubes Section, Applied Research Department, Friendship International Airport, Box 746, Baltimore 3, Maryland
1		Department of Electrical Engineering, University of Minnesota, Minneapolis, Minnesota, ATTN: Dr. W. G. Shepherd
1		Director, Evans Signal Laboratory, Belmar, New Jersey, ATTN: Dr. Gerald E. Pokorney, Microwave Tube Branch, Electron Devices Division
1		Electronic Tube Division, Westinghouse Electric Corporation, P. O. Box 284, Elmira, New York, ATTN: Librarian
1		Power Tube Department, 1 River Road, General Electric Company, Schenectady, New York, ATTN: Dr. Bernard Hershenov
1		Microwave Electronics Corporation, 4061 Transport Street, Palo Alto, California, ATTN: Dr. S. F. Kaisel
1		Librarian, Microwave Library, Stanford University, Stanford, California
1		George Dombrowski, Microwave and Power Tube Division, Raytheon Manufacturing Company, Waltham 54, Massachusetts
1		Mr. Robert Butman, Massachusetts Institute of Technology, Lincoln Laboratory, Lexington, Massachusetts





<p>AD _____</p> <p>Univ. of Michigan, Electron Physics Lab., MODULATION CHARACTERISTICS OF O-TYPE ELECTRON-STREAM DEVICES, by H. Sobol. Nov. 1959. 246 pp. incl. illus. (Proj. 02750) (AF 30(602)-1845) Unclassified Report</p> <p>The small-signal TWA, BWO and Crestatron undergoing low-frequency beam modulation are described by sets of quasi-static functions. Modulation effects on C, Q, b and d as well as on the initial wave amplitudes are considered. The modulated TWA with a large-signal carrier is investigated using the nonlinear Lagrangian formulation. The modulation characteristics are used to determine the output spectra. Recommendations for the design of TWA's for modulation applications are given.</p> <p>The O-type device undergoing a high frequency beam modulation is investigated using a nonlinear Eulerian analysis. The analysis which includes effects of the upper sideband is applied to the longitudinal-beam parametric amplifier. The theoretical gain and noise properties are shown to give better agreement with experiments than previous analyses which neglect the upper sideband.</p>	<p>UNCLASSIFIED</p> <ol style="list-style-type: none"> <li>1. Statement of problem</li> <li>2. Low-frequency TWA device functions</li> <li>3. Numerical results for device functions</li> <li>4. Spectrum of TWA low-frequency modulations</li> <li>5. Low-frequency modulation of other device functions</li> <li>6. High-frequency modulation</li> <li>7. Summary</li> </ol> <p>I. Sobol, H. II. Rome Air Development Center</p>	<p>AD _____</p> <p>Univ. of Michigan, Electron Physics Lab., MODULATION CHARACTERISTICS OF O-TYPE ELECTRON-STREAM DEVICES, by H. Sobol. Nov. 1959. 246 pp. incl. illus. (Proj. 02750) (AF 30(602)-1845) Unclassified Report</p> <p>The small-signal TWA, BWO and Crestatron undergoing low-frequency beam modulation are described by sets of quasi-static functions. Modulation effects on C, Q, b and d as well as on the initial wave amplitudes are considered. The modulated TWA with a large-signal carrier is investigated using the nonlinear Lagrangian formulation. The modulation characteristics are used to determine the output spectra. Recommendations for the design of TWA's for modulation applications are given.</p> <p>The O-type device undergoing a high frequency beam modulation is investigated using a nonlinear Eulerian analysis. The analysis which includes effects of the upper sideband is applied to the longitudinal-beam parametric amplifier. The theoretical gain and noise properties are shown to give better agreement with experiments than previous analyses which neglect the upper sideband.</p>	<p>UNCLASSIFIED</p> <ol style="list-style-type: none"> <li>1. Statement of problem</li> <li>2. Low-frequency TWA device functions</li> <li>3. Numerical results for device functions</li> <li>4. Spectrum of TWA low-frequency modulations</li> <li>5. Low-frequency modulation of other device functions</li> <li>6. High-frequency modulation</li> <li>7. Summary</li> </ol> <p>I. Sobol, H. II. Rome Air Development Center</p>
<p>AD _____</p> <p>Univ. of Michigan, Electron Physics Lab., MODULATION CHARACTERISTICS OF O-TYPE ELECTRON-STREAM DEVICES, by H. Sobol. Nov. 1959. 246 pp. incl. illus. (Proj. 02750) (AF 30(602)-1845) Unclassified Report</p> <p>The small-signal TWA, BWO and Crestatron undergoing low-frequency beam modulation are described by sets of quasi-static functions. Modulation effects on C, Q, b and d as well as on the initial wave amplitudes are considered. The modulated TWA with a large-signal carrier is investigated using the nonlinear Lagrangian formulation. The modulation characteristics are used to determine the output spectra. Recommendations for the design of TWA's for modulation applications are given.</p> <p>The O-type device undergoing a high frequency beam modulation is investigated using a nonlinear Eulerian analysis. The analysis which includes effects of the upper sideband is applied to the longitudinal-beam parametric amplifier. The theoretical gain and noise properties are shown to give better agreement with experiments than previous analyses which neglect the upper sideband.</p>	<p>UNCLASSIFIED</p> <ol style="list-style-type: none"> <li>1. Statement of problem</li> <li>2. Low-frequency TWA device functions</li> <li>3. Numerical results for device functions</li> <li>4. Spectrum of TWA low-frequency modulations</li> <li>5. Low-frequency modulations of other device functions</li> <li>6. High-frequency modulation</li> <li>7. Summary</li> </ol> <p>I. Sobol, H. II. Rome Air Development Center</p>	<p>AD _____</p> <p>Univ. of Michigan, Electron Physics Lab., MODULATION CHARACTERISTICS OF O-TYPE ELECTRON-STREAM DEVICES, by H. Sobol. Nov. 1959. 246 pp. incl. illus. (Proj. 02750) (AF 30(602)-1845) Unclassified Report</p> <p>The small-signal TWA, BWO and Crestatron undergoing low-frequency beam modulation are described by sets of quasi-static functions. Modulation effects on C, Q, b and d as well as on the initial wave amplitudes are considered. The modulated TWA with a large-signal carrier is investigated using the nonlinear Lagrangian formulation. The modulation characteristics are used to determine the output spectra. Recommendations for the design of TWA's for modulation applications are given.</p> <p>The O-type device undergoing a high frequency beam modulation is investigated using a nonlinear Eulerian analysis. This analysis which includes effects of the upper sideband is applied to the longitudinal-beam parametric amplifier. The theoretical gain and noise properties are shown to give better agreement with experiments than previous analyses which neglect the upper sideband.</p>	<p>UNCLASSIFIED</p> <ol style="list-style-type: none"> <li>1. Statement of problem.</li> <li>2. Low frequency TWA device functions</li> <li>3. Numerical results for device functions</li> <li>4. Spectrum of TWA low-frequency modulations</li> <li>5. Low-frequency modulation of other device functions</li> <li>6. High-frequency modulation</li> <li>7. Summary</li> </ol> <p>I. Sobol, H. II. Rome Air Development Center</p>





<p>AD _____</p> <p>Univ. of Michigan, Electron Physics Lab., MODULATION CHARACTERISTICS OF O-TYPE ELECTRON-STREAM DEVICES, by H. Sobol. Nov. 1959. 246 pp. incl. illus. (Proj. 02750) (AF 30(602)-1845) Unclassified Report</p> <p>The small-signal TWA, BWO and Crestatron undergoing low-frequency beam modulation are described by sets of quasi-static functions. Modulation effects on C, Qc, b and d as well as on the initial wave amplitudes are considered. The modulated TWA with a large-signal carrier is investigated using the nonlinear Lagrangian formulation. The modulation characteristics are used to determine the output spectra. Recommendations for the design of TWA's for modulation applications are given.</p> <p>The O-type device undergoing a high frequency beam modulation is investigated using a nonlinear Eulerian analysis. The analysis which includes effects of the upper sideband is applied to the longitudinal-beam parametric amplifier. The theoretical gain and noise properties are shown to give better agreement with experiments than previous analyses which neglect the upper sideband.</p>	<p>UNCLASSIFIED</p> <ol style="list-style-type: none"> <li>1. Statement of problem</li> <li>2. Low-frequency TWA device functions</li> <li>3. Numerical results for device functions</li> <li>4. Spectrum of TWA low-frequency modulations</li> <li>5. Low-frequency modulation of other device functions</li> <li>6. High-frequency modulation</li> <li>7. Summary</li> </ol> <p>I. Sobol, H. II. Rome Air Development Center</p>	<p>AD _____</p> <p>Univ. of Michigan, Electron Physics Lab., MODULATION CHARACTERISTICS OF O-TYPE ELECTRON-STREAM DEVICES, by H. Sobol. Nov. 1959. 246 pp. incl. illus. (Proj. 02750) (AF 30(602)-1845) Unclassified Report</p> <p>The small-signal TWA, BWO and Crestatron undergoing low-frequency beam modulation are described by sets of quasi-static functions. Modulation effects on C, Qc, b and d as well as on the initial wave amplitudes are considered. The modulated TWA with a large-signal carrier is investigated using the nonlinear Lagrangian formulation. The modulation characteristics are used to determine the output spectra. Recommendations for the design of TWA's for modulation applications are given.</p> <p>The O-type device undergoing a high frequency beam modulation is investigated using a nonlinear Eulerian analysis. The analysis which includes effects of the upper sideband is applied to the longitudinal-beam parametric amplifier. The theoretical gain and noise properties are shown to give better agreement with experiments than previous analyses which neglect the upper sideband.</p>	<p>UNCLASSIFIED</p> <ol style="list-style-type: none"> <li>1. Statement of problem</li> <li>2. Low-frequency TWA device functions</li> <li>3. Numerical results for device functions</li> <li>4. Spectrum of TWA low-frequency modulations</li> <li>5. Low-frequency modulation of other device functions</li> <li>6. High-frequency modulation</li> <li>7. Summary</li> </ol> <p>I. Sobol, H. II. Rome Air Development Center</p>
<p>AD _____</p> <p>Univ. of Michigan, Electron Physics Lab., MODULATION CHARACTERISTICS OF O-TYPE ELECTRON-STREAM DEVICES, by H. Sobol. Nov. 1959. 246 pp. incl. illus. (Proj. 02750) (AF 30(602)-1845) Unclassified Report</p> <p>The small-signal TWA, BWO and Crestatron undergoing low-frequency beam modulation are described by sets of quasi-static functions. Modulation effects on C, Qc, b and d as well as on the initial wave amplitudes are considered. The modulated TWA with a large-signal carrier is investigated using the nonlinear Lagrangian formulation. The modulation characteristics are used to determine the output spectra. Recommendations for the design of TWA's for modulation applications are given.</p> <p>The O-type device undergoing a high frequency beam modulation is investigated using a nonlinear Eulerian analysis. The analysis which includes effects of the upper sideband is applied to the longitudinal-beam parametric amplifier. The theoretical gain and noise properties are shown to give better agreement with experiments than previous analyses which neglect the upper sideband.</p>	<p>UNCLASSIFIED</p> <ol style="list-style-type: none"> <li>1. Statement of problem</li> <li>2. Low-frequency TWA device functions</li> <li>3. Numerical results for device functions</li> <li>4. Spectrum of TWA low-frequency modulations</li> <li>5. Low-frequency modulations of other device functions</li> <li>6. High-frequency modulation</li> <li>7. Summary</li> </ol> <p>I. Sobol, H. II. Rome Air Development Center</p>	<p>AD _____</p> <p>Univ. of Michigan, Electron Physics Lab., MODULATION CHARACTERISTICS OF O-TYPE ELECTRON-STREAM DEVICES, by H. Sobol. Nov. 1959. 246 pp. incl. illus. (Proj. 02750) (AF 30(602)-1845) Unclassified Report</p> <p>The small-signal TWA, BWO and Crestatron undergoing low-frequency beam modulation are described by sets of quasi-static functions. Modulation effects on C, Qc, b and d as well as on the initial wave amplitudes are considered. The modulated TWA with a large-signal carrier is investigated using the nonlinear Lagrangian formulation. The modulation characteristics are used to determine the output spectra. Recommendations for the design of TWA's for modulation applications are given.</p> <p>The O-type device undergoing a high frequency beam modulation is investigated using a nonlinear Eulerian analysis. This analysis which includes effects of the upper sideband is applied to the longitudinal-beam parametric amplifier. The theoretical gain and noise properties are shown to give better agreement with experiments than previous analyses which neglect the upper sideband.</p>	<p>UNCLASSIFIED</p> <ol style="list-style-type: none"> <li>1. Statement of problem</li> <li>2. Low frequency TWA device functions</li> <li>3. Numerical results for device functions</li> <li>4. Spectrum of TWA low-frequency modulations</li> <li>5. Low-frequency modulation of other device functions</li> <li>6. High-frequency modulation</li> <li>7. Summary</li> </ol> <p>I. Sobol, H. II. Rome Air Development Center</p>

UNIVERSITY OF MICHIGAN



**3 9015 03524 5003**